A NUMERICAL INVESTIGATION OF THE DEEP WELL FREE SURFACE-SEEPAGE FACE BOUNDARY CONDITION

by

Abdulla A. Al-Thani

A dissertation submitted for the
degree of Doctor of Philosophy
at
University of Southampton

Department of Civil and
Environmental Engineering
March 2002

ABSTRACT

Modelling of groundwater flow makes an important contribution to the design of groundwater resources and groundwater control systems. When groundwater is pumped from an unconfined aquifer using deep wells, water is derived predominantly from pore-water drainage. This drainage results in a decline in water table position near the pumping wells as time progresses. The vertical surface in a pumped well, which is exposed between the free water surface in the well and the location at which the water table surface in the unconfined aquifer intersects the well, is referred to as the seepage face or seepage surface. Traditionally, seepage face has been ignored in mathematical analysis due to the difficulty of handling it in an analytical solution. In this research, the availability of numerical models enables us to investigate such flow systems to better understand flow near wells pumping from unconfined aquifers for the purpose of groundwater control and landfill remediation.

There is a long history of research dating back to 1932. This thesis revisits the previous work carried out to investigate the seepage surface in order to establish benchmarks and verify the validity of a recent numerical analysis, which permits the seepage surface to be modelled more accurately. After selecting an appropriate numerical code, various steady state and transient flow problems in unconfined aquifers with free surface-seepage face boundary conditions are analyzed. Special cases of multiple well systems, anisotropy effects, maximum well yield, and the use of wells to control leachate in landfills are also investigated.

The investigation of steady state, radial flow problems show that it is important that the impact of the seepage surface on the design of groundwater control and remediation schemes is fully appreciated. In particular caution should be used in applying a *Dupuit-Forchheimer* analysis to the design of such systems because flow velocities into a well will be overestimated, as will the shape of the free surface drawdown depth commonly known as the cone of depression. In the case of multiple well configurations, it is shown that the seepage surface is eliminated by the inter-action of the wells in the system and it appears that the seepage face surface phenomenon is not a significant factor in the performance of an array of wells.

An extended investigation of the transient seepage-face for single well configurations concludes that a fast decline of the phreatic surface takes place during the early stage of pumping due to the specific storage effect. As time progresses, the specific storage effect decreases and its effect is almost negligible after a period of time depending on the hydraulic conductivity. Intuitively, as the value of the hydraulic conductivity is increased, the faster soil tends to drain, and therefore the level of the phreatic surface is lowered more rapidly. In the case of the landfill investigation, the flow to the well appears to be taking place through the lower layers so that the yield from the well is controlled by the hydraulic conductivity in these layers.

Finally, this research provides two algebraic representations. The first gives an estimated solution for both the hydraulic limiting gradient and seepage face elevation. The second estimates the leachate elevation in a landfill after a certain period of pumping.

ACKNOWLEDGEMENTS

I would like to express my gratitude to my supervisors, Professor Jim White and Professor William Powrie, whose expertise, encouragement, patience and criticism, added considerably to my graduate experience during the past 4 years. My extended thanks go to my major supervisor Professor Jim White for his support before and after my transfer to the University of Southampton. I appreciate his vast knowledge and skill which goes beyond the field of groundwater modelling to include teaching and interaction with participants and his assistance in writing reports, papers, grant proposals and scholarship applications. Moreover for his insight, wisdom and patience with me during the thesis writing stage.

Many thanks also go to Dr. Richard Beaven and members of the Waste Management Research Group (WMRG) for the unlimited support and feedback during my research. I am also thankful to Dr. Sorab Pandy from the *HydroGeoLogic*, Inc. for his assistance and support to overcome the problems I faced when working with the MODFLOW-SURFACT code.

My deep-hearted thanks go to my parents, sisters, brothers and my close relatives especially my cousin Abdulrahman. They have been a constant source of love and support throughout my life. They have given their unconditional support, knowing that doing so contributed greatly to my absence over the last seven years. Without them, I would never have started or finished this project.

I also would like to thank my friends and especially Darryl Stephens. Darryl has changed my life over the last 4 years with his continuous support, intelligence, honesty, goodness and liveliness. Moreover, his encouragement and editing assistance contributed greatly to the completion of this project. I doubt that I will ever be able to convey my appreciation fully, but I owe him my eternal gratitude. He will always be my best friend.

In conclusion, the funding support for this research was provided by the University of Qatar and is thankfully acknowledged.

TABLE OF CONTENTS

LIST OF FIGURES

CHAPTER 1

CHAPTER 2

CHAPTER 3

CHAPTER 4

CHAPTER 5

CHAPTER 6

CHAPTER 7

LIST OF TABLES

CHAPTER 1

CHAPTER 3

CHAPTER 4

CHAPTER 5

CHAPTER 6

CHAPTER 7

COMMON NOTATIONS

μ	Viscosity of fluid	M/LT
γ	Specific weight	M/L^2T^2
ψ	Pressure head = p/γ	L
ρ	Density	M/L^3
β	Compressibility of water	LT^2/M
θ	Volumetric water content	1
ν	Kinematic viscosity = μ/ρ	L^2/T
σ_e	Effective stress	M/LT^2
α_p	Pore volume compressibility	LT^2/M
α_v	Pore volume compressibility	L^{-1}
A	Area	L^2
C	Conductance	L^2/T
g	Acceleration due to gravity	L/T^2
h	Head	L
H	Elevation of water prior to pumping	L
h_c	Height of capillary rise	L
h_s	Height of seepage face	L
h_w	Elevation of water inside the well	L
i	Hydraulic gradient	1
k	Intrinsic permeability	L^2
K	Hydraulic conductivity	L/T
K_r	Principle hydraulic conductivity along the radial axes	L/T
k_{rw}	Relative permeability	1
K_x	Principle hydraulic conductivity along the x- axes	L/T
K_y	Principle hydraulic conductivity along the y- axes	L/T
K_z	Principle hydraulic conductivity along the z- axes	L/T
n	Porosity	1
p	Pressure	M/LT^2
P_c	Capillary pressure	M/LT^2
Q	Rate of Flow	L^3/T

q	Specific flow or Darcy's velocity	L/T
r	Radial distance from the coordinate origin	L
R	Radius of influence	L
r_e	Effective well radius	L
r_w	Well radius	L
S	Storage coefficient or Storativity	1
S_s	Specific storage	L^{-1}
S_w	Saturation of porous medium	1
S_y	Specific yield or drainable porosity	1
t	Time	T
T	Transmissivity	L^2/T
v	Velocity	L/T
v_p	Pore velocity of water	L/T
V_w	Volume of water drained	L^3
w	Volumetric flux per unit volume	1/T
x	Space coordinate in x-direction	L
y	Space coordinate in y-direction	L
Z	Gravitational head measured from arbitrary datum	L
z	Space coordinate in z-direction	L

GLOSSARY

Technical terms are generally defined where they first occur in the thesis. For ease of reference a list of definitions is also set out below.

Adsorption: The attraction and adhesion of a layer of ions from an aqueous solution to the solid mineral surfaces with which it is in contact.

Anisotropy: The condition of having different properties in different directions.

Aquifer: The formation that contains sufficient saturated permeable material to yield significant quantities of water to wells and springs. This implies the ability to store and transfer water.

Baseflow: The part of the stream discharge that is not attributable to direct runoff from precipitation or melting snow; it is usually sustained by groundwater discharge.

Benchmark: Data set used to verify numerical models. See verification.

Boundary condition: A flow, constant head, or transport condition on a section of the model boundary system.

Calibration: The process of repeatedly modifying the model input data until a set of the simulated values of hydraulic heads and/or concentrations, are fitted within a chosen tolerance to a corresponding set of observed or target values.

Capillary force: The generally upward force acting on soil moisture in the unsaturated zone, attributable to molecular attraction between soil particles and water at an air/water interface.

Capillary zone or Capillary fringe: The zone in which water is held in the soil above the phreatic surface by capillary forces. It is the zone in which the pores are nearly saturated with water due to surface tension of the air-water interface and the molecular attraction of the liquid and solid phases - **capillarity**. The thickness of the capillary fringe depends on the size of the pores that form the capillary fringe. In a coarse material, for example gravel, it may be only a few mm thick. In fine-grained material, such as clay and silt, it may be several meters thick. Because of the differences in pore sizes in an area, the top of the capillary fringe is often an irregular surface.

Cauchy boundary condition: A boundary condition in which the flow or flow velocity across the boundary is calculated as a function of the calculated boundary head value. It is sometimes called a "mixed boundary condition" because it relates boundary heads to boundary flows.

Cell: Elemental sub-domain in finite-difference (FD) models.

Conceptual model: A simplified representation of a system which enables it to be investigated by analytical or numerical techniques.

Conductance (*C*): A coefficient that is usually computed using an equation similar to the following: $C = K_b A / B$, where K_b, is the hydraulic conductivity of the boundary material (L/T); A is the area of the boundary (L^2); and B is a length which may represent thickness or width of the boundary (L) (*McDonald and Harbaugh*, 1988.) It is used in the general head boundary condition to relate head to flow velocity. See Cauchy boundary condition.

Cone of depression: The cone-shaped area around a well where the groundwater level is lowered by pumping. The shape of the cone is time dependent and is influenced by the underground porosity and water yield of the well.

Confined aquifer: An aquifer bounded above and below by confining units or strata of significantly less permeability than that of the aquifer itself. Groundwater in a confined aquifer is generally under pressure greater than atmospheric.

Confining layer: A geological material through which significant quantities of water cannot move; located below unconfined aquifers, above and below confined aquifers. Also known as a confining bed.

Constitutive equations: Equations that define the intrinsic response of a system, which depends on the internal constitution of the particular materials considered. Usually constitutive equations take the form of relationships between fluxes and driving forces (*Bear*, 1972.)

Contaminant: See Pollutant.

Darcy's law: An empirical law which states that the velocity of flow through a porous medium is directly proportional to the hydraulic gradient assuming that the flow is laminar and inertia can be neglected. The constant of proportionality defines the effective hydraulic conductivity of the porous medium.

Diffusion: See Dispersion and Diffusion.

Dirichlet's condition: See Specified head boundary condition.

Dispersion and Diffusion: The phenomena by which a solute in flowing groundwater is mixed with uncontaminated water and becomes reduced in concentration. Both are proportional to solute concentration gradients. Diffusion is a molecular process, dispersion is a mechanical process and a function of seepage flow velocity.

Drain: The definition here is related directly to the MODFLOW drain that is described in the MODFLOW Package. A drain withdraws water from the aquifer when the head is above the elevation of the drain. If the head is below the elevation of the drain, the drain has no effect on the aquifer. The flow rate is $Q = C_d (h - Z_d)$ where C_d is the conductance of the material surrounding the drain; h is the head in the cell; and Z_d is the elevation of the drain. Users must specify C_d and Z_d. (*McDonald and Harbaugh*, 1988.)

Drawdown: The vertical distance the water table is lowered or the reduction of the pressure head due to the removal of water.

Effective hydraulic conductivity: The hydraulic conductivity that is used in *Darcy's* law to evaluate the velocity of flow of water through a porous medium that contains more than one fluid, such as water and air in the unsaturated zone

Effective porosity: See Specific yield.

Electrical analogy: The use of the similarity between electrical flow and groundwater flow in modelling.

Empirical model: A representation of physical or chemical processes based on observation rather than theory.

Equipotential line (or surface): Line (or surface) along which the potential head is constant.

Finite-difference method (FD): A numerical method for solving one or more constitutive equations for given boundary conditions. The constitutive equation is linearised over a small element, e.g. by expanding the equation term by term into a Taylor series, and a set of such elements is assembled to form the model space. See Finite-element method.

Finite-element method (FE): A numerical method similar to the Finite-difference method in which the constitutive equation is linearised by integration rather than differentiation over irregularly shaped elements which can be assembled to fit the model space more flexibly than the Finite-difference method. See Finite-difference method.

Galerkin method: Weighting method in finite-element (FE) models in which basic functions are chosen as weighting functions.

Gaussian elimination: A systematic application of elementary row operations to a system of linear equations in order to convert the system to upper triangular form. Once the coefficient matrix is in upper triangular form, the back substitution method is used to find a solution.

Grid: Array of blocks, in finite-difference (FD) models, or elements, in finite-element (FE) models that are used to subdivide the model area.

Head: See Hydraulic head.

Heterogeneity: A characteristic of a medium in which material properties vary from point to point.

Homogeneity: A characteristic of a medium in which material properties are identical everywhere.

Hydraulic conductivity (*K*): A coefficient of proportionality describing the volume of water that will move through a medium in a unit of time under a unit hydraulic gradient through a unit area measured perpendicular to the direction of flow. The density and the kinematic viscosity of the water influence the value of hydraulic conductivity.

Hydraulic gradient (*i*): The change in static potential head per unit of distance in a given direction. If not specified, the direction generally is understood to be that of the maximum rate of decrease in head.

Hydraulic head (*h*): The height above a datum plane (such as sea level) of the column of water that can be supported by the static hydraulic pressure at a given point in a groundwater system. For a well, the hydraulic head is equal to the distance between the water level in the well and the datum plane. Equal to the potential head.

Hydrogeologic properties: Those properties of a rock or soil that govern the entrance of water and the capacity to hold, transmit, and deliver water, such as porosity, effective porosity, permeability, and the directions of maximum and minimum permeabilities.

Hysteresis: The phenomena of a possible difference in the interfacial surface tension or wettability when a fluid-fluid interface (e.g. an air-water interface) is advancing or receding on a solid surface, during the process of saturation and desaturation.

Impermeable layer: A layer of material (clay) in an aquifer through which significant quantities of water do not pass.

Impermeable: A characteristic of some geologic material that limits its ability to transmit significant quantities of water under the head differences ordinarily found in the subsurface. See Permeability.

Initial conditions: The value of the boundary condition parameters and the pressure heads and/or concentrations within the model, at an initial time, usually at t=0.

Interflow: The component of groundwater flow in an aquifer that links surface and near surface flows to an aquifer and vice-versa. See Baseflow.

Intrinsic permeability (*k*): A property of a porous medium which when linked to the density and viscosity of the fluid gives the coefficient of *Darcy* permeability for that fluid in the medium.

Isotropy: The condition in which the property or properties of interest are the same in all directions.

Leachate: A liquid that has passed through soil, rock or waste and has extracted dissolved or suspended materials.

Leaching: The downward transport of dissolved or suspended minerals, fertilizers and other substances by water passing through a soil or other permeable material.

Leakance: The ratio of the vertical hydraulic conductivity of a confining bed or stratum to its thickness. See VCONT.

Limiting gradient: The maximum average hydraulic gradient along the cylindrical face of the well.

Mass balance model: Models that balance mass fluxes, either groundwater or solutes, over large volumes of the groundwater system.

Model: A model is a device that represents an approximation of a field situation. It can be represented as a conceptual, mathematical, or physical system. See Conceptual model.

Neumann condition: See Specified flow condition.

Newton-Raphson method: A numerical method for solving one-dimensional or multi-dimensional systems of nonlinear constitutive equations.

Nodes: Points in finite-difference and finite element models at which model parameters such as pressure head and solute concentration are evaluated.

Nonlinearity: A mathematical relationship, representing the constitutive equation, that contains terms which are not linearly related to the unknown variable, and/or has the coefficients that depend on the unknown variable is said to be non-linear.

Numerical oscillation: Occurs when the heads or concentrations that are calculated first overshoot then undershoot the solution and the calculation possibly fails to converge.

Permeability (K): The capacity of a porous medium to transmit a fluid. Sometimes used in place of the term hydraulic conductivity when applied to water seepage through rock or soil.

Phreatic surface: See Water table.

Picard method: A solution technique to solve a differential constitutive equation using the finite difference technique. In this method, the differential equation is converted into an equation involving integrals, which is called an integral equation. The integral equation is then used to obtain set of linear equations which are solved numerically.

Piezometer: A device used to measure groundwater pressure head at a point in the aquifer.

Piezometric heads: The level to which water penetrating a confined aquifer will rise.

Piezometric surface: See Potentiometric surface.

Plume: A zone of contaminated groundwater containing dissolved contaminant.

Pollutant: A solute that causes groundwater contamination.

Pollution: The process by which any substance (the pollutant), natural or synthetic, degrades water quality to such a degree that water is not suitable for a particular use.

Porosity (n): The ratio, usually expressed as a percentage, of the total volume of voids of a given porous medium to the total volume of the porous medium.

Potential head: The sum of the static pressure head and the elevation at a point.

Potentiometric surface: An imaginary surface representing the static potential head of ground water and defined by the level to which water will rise in a tightly cased well.

Pressure head (ψ): Equal p/γ, where p is the local static pressure in a fluid and γ is the specific weight of the fluid.

Pre- and post-processors (PPP): Pre-processing is assembling and preparing input data for a numerical model and post-processing is the process of reviewing and presenting the model results.

Principle of superposition: A principle in which the individual solutions of a linear constitutive equation can be added to give a solution which meets the required boundary conditions.

Relative permeability: A dimensionless term devised to adapt the *Darcy* equation to multiphase flow conditions. Relative permeability is the ratio of effective permeability of a particular fluid at a particular saturation to absolute permeability of that fluid at total saturation. If a single fluid is present in a rock, its relative permeability is 1.0. Calculation of relative permeability allows comparison of the different abilities of fluids to flow in the presence of each other, since the presence of more than one fluid generally inhibits flow.

Relaxation method: A process for obtaining steadily amended and converging approximations of the solution of a set of simultaneous algebraic difference equations.

Representative element volume (REV): A representative volume of the aquifer that is large enough to allow the simulation of the actual aquifer with a representative continuum in which macroscopic laws can be used to describe flow or transport at macroscopic scale.

Saturated zone: The portion of subsurface soil and rock where every available space is filled with water. Aquifers are located in this zone.

Saturated-unsaturated model: See Variably saturated model.

Seepage: The flow of groundwater through an aquifer.

Seepage face (h_s): A boundary between the saturated flow field and the atmosphere along which groundwater discharges. In regard to an operating well, seepage face is the vertical surface which is exposed between the free water surface in the well and the location at which the water table surface in the unconfined aquifer intersects the well.

Seepage surface: See Seepage face.

Sensitivity analysis: A set of model analyses to illustrate the model response to variations in model input data.

Slice-Successive Overrelaxation Method (SSOR): A simpler iterative scheme contained in MODFLOW. Instead of solving the entire system of unknowns at the same time, the equations are formulated for a two-dimensional vertical slice with assumptions that the heads in the adjacent two slices are known. The resulting system of equations, formulated as the change in hydraulic head, is solved by Gaussian elimination. The slice will usually contain a relatively small number of nodes because in most cases the number of model layers is small. One iteration is complete when all of the slices are processed. After a large number of iteration, the solution converges (*McDonald and Harbaugh*, 1988.)

Specific flow (q): The rate of discharge of ground water per unit area of a porous medium measured at right angles to the direction of flow. Equivalent to the *Darcy* flow velocity or *Darcy* seepage velocity.

Specific storage (S_s): The volume of water released from or taken into storage per unit volume of the porous medium per unit change in head.

Specific yield (S_y): The ratio of the volume of water which an element of porous medium after being saturated will yield by gravity drainage to the volume of the element. Sometimes described as the effective porosity.

Specified flow or velocity condition: A boundary condition in which the fluid flow or flow velocity is known. The flow can be time dependent. Also known as the Neumann condition.

Specified head boundary condition: A boundary condition in which the pressure head is known or assumed. The head can be time dependent. Also known as Dirichlet condition.

Stability: A stable numerical solution is one in which numerical errors decrease during computation and converge to a unique solution.

Stagnation point: A place in a groundwater flow field at which the groundwater is not moving. The magnitude of vectors of hydraulic head at the point are equal but opposite in direction.

Steady-state flow: A characteristic of a groundwater flow system where the magnitude and direction of specific discharge are constant in time at any point See also Unsteady flow.

Storage coefficient (S): The volume of water an aquifer releases from or takes into storage per unit surface area of the aquifer per unit change in head, virtually equal to the specific yield in an unconfined aquifer and the specific storage in a confined aquifer. See Specific yield and Specific storage.

Storativity: See Storage coefficient

Strongly Implicit Procedure (SIP): A solution approach which involves solving for the unknowns over the entire grid simultaneously (*McDonald and Harbaugh*, 1988.)

Transient: The set of instantaneous states occupied by a system prior to reaching a steady-state condition obtained by means of a time dependent solution technique. See Unsteady flow.

Transmissivity (*T*): The rate at which water of the prevailing kinematic viscosity is transmitted through a unit width of the aquifer under a unit hydraulic gradient. It is equal to an integration of the hydraulic conductivities across the saturated part of the aquifer perpendicular to the flow paths.

Truncation error: The error in numerical models due to neglecting terms in approximations of the constitutive equation. For example neglecting terms of higher order in the Taylor series expansion.

Unconfined aquifer: An aquifer in which the upper flow boundary is the water table. Because the aquifer is not under pressure the water level in an observation well will be at the same level as the water table outside the well.

Uniform flow: A characteristic of a flow system where specific flow has the same magnitude and direction at any point.

Unsaturated flow: The movement of water in a porous medium in which the pore spaces are not filled to capacity with water.

Unsaturated zone: An area, usually between the land surface and the water table, where the openings or pores in the soil contain both air and water

Unsteady flow: A characteristic of a flow system where the magnitude and/or direction of the specific discharge changes with time. Synonymous with non-steady flow. See also Steady-state flow.

Validation: A comparison of numerical model results with a data set not used in model calibration.

Van Genuchten parameter (α_v): A measure that describes the mean pore size of a porous medium.

Variability saturated model: A model in which the unsaturated/saturated zones are simulated as a continuous flow field, and in which the phreatic surface is determined as the surface of zero pressure head.

VCONT: A vertical transmission or leakage term used in MODFLOW simulations. It is calculated using the vertical hydraulic conductivity divided by the thickness from a layer to the layer below. The value for a cell is the hydraulic conductivity divided by the thickness for the material between the node in that cell and the node in the cell

below. Because there is no layer beneath the bottom later, VCONT cannot be specified for the bottom layer (*McDonald and Harbaugh*, 1988.) See Leakance.

Verification: Sometimes verification is used to describe the comparison of numerical model results with analytical or laboratory results. See Validation.

Viscosity (μ): The property of fluid describing its resistance to shear flow. Shear stresses in Newtonian fluids are proportional to velocity gradient. Viscosity is the coefficient of proportionality.

Volatilisation: The loss of a substance through evaporation.

Water table aquifer: See Unconfined aquifer.

Water table: The water level of an unconfined aquifer below which the pore spaces are generally saturated. Sometimes called phreatic surface.

Well (and Deep well): Any excavation that is drilled, cored, bored, dug, or otherwise constructed when the intended use is for the location, diversion, artificial recharge, or acquisition of groundwater. Also referred to as a deep well in order to distinguish it from shallow wells or well points which are used in shallow permeable unconfined (usually) aquifers generally less than 9m deep. In this study, the term well usually means deep wells.

Yield: The flow across the boundary of a groundwater system. In particular, the discharge flow from a well.

References:

This glossary of definitions, unless otherwise stated, has been derived by reference to the following publications *Spitz and Moreno,* 1996; *Fetter,* 1994 and *Todd*, 1980. Details may be found in the list of references starting on page 150.

Chapter (1)

Introduction

"We have made from water every living thing"
Holy Qur'an, Sûrat Al-Anbiyâ (21:30)

1.1 Background

Throughout history water has been considered to be a natural resource critical to human survival. From basic irrigation needs to modern industrial development, water has been an essential factor. The vast oceans, rivers, and lakes that cover 70 percent of the earth surface make it seem that there is plenty of water for human use. The fact is that 97 percent of all the water on the earth is salt water, which is unsuitable for drinking or growing crops. Nearly all of the remaining 3 percent is fresh water but inaccessible, effectively secured in the icecaps of Antarctica and Greenland and in deep aquifers. According to available estimates, only 0.3 percent of the total fresh water is usable for the entire human and animal populations. (*Vajpeyi*, 1998)

Readily accessible groundwater, or subsurface water, which is the term used to denote all waters found in water bearing strata beneath the surface of the ground, is therefore a subject of great importance for people and their environment. It constitutes an important component of many water resource systems, supplying water for domestic use, for industry, and for agriculture. It is an essential and vital resource.

The study of groundwater, which may be referred to as groundwater hydrology or hydrogeology, is defined as the science of the occurrence, distribution, and movement of water below the surface of the earth. Groundwater hydrology is primarily concerned

with the water that occurs beneath the water table, the saturation zone, and uses the term groundwater to denote water in this zone. An unsaturated zone may be found above the saturation zone and may extend upward to the ground surface. This water, which includes soil moisture within the root zone, is of major concern for agricultural, botanical, and soil scientists who sometimes incorporate the unsaturated zone above the water table in the term groundwater.

Groundwater is usually abstracted from aquifers using deep wells. The theory of the flow of groundwater towards wells is a special application of the more general theory of flow of fluids through porous media, which is a topic encountered in many branches of engineering and science. These branches include groundwater hydrology, reservoir engineering, soil science, soil mechanics and chemical engineering. The objective of the design of groundwater abstraction wells to meet water supply system objectives generally focuses on obtaining a high reliable yield. Increased demands for water have stimulated the development of groundwater resources. Therefore techniques for investigating the occurrence and movement of groundwater have been improved, and enhanced equipment for extracting groundwater has been developed. Concepts for resource management have also been established, and research has contributed to a better understanding of controlling groundwater processes.

A specialised activity in the area of groundwater control is to be found in the construction industry. This involves the control of groundwater in the neighbourhood of deep excavations to enable construction to take place in dry and stable conditions. The methods used for groundwater control or, as it is sometimes called, dewatering, include the installation and operation of deep wells to lower the water table or reduce pore-pressures. In contrast to the development of groundwater resources the focus of the design of a groundwater control scheme is on the drawdown achieved by the wells in the scheme rather than the yield from the wells.

The cumulative knowledge of groundwater phenomena now encompasses the understanding of the geological environments that control the occurrence of groundwater, the physical laws that describe the flow, and the chemical responses that

accompany flow. The latter includes contamination by pollutants and the role of leachate in landfills which leads on to an appreciation of the impact of human beings on the natural groundwater regime and vice versa.

In the area of contaminated land remediation, deep wells are employed to induce seepage flows through the contaminated ground in order to convey and extract groundwater contaminants to improve the ground. Similarly, in the area of landfill leachate control, deep wells are employed to induce seepage flows through the mass of solid waste in order to reduce the risk of leakage from the landfill. Future applications of deep wells are their use to improve the performance of the landfill as a waste bioreactor, and to assist with the remediation of the landfill post-closure.

The analysis of complex groundwater flow systems may be carried out using numerical modelling techniques. The objective of this research is to focus on a recent advance in the numerical modelling of a specific boundary condition flow problem encountered in groundwater flow at a deep well, the free surface-seepage face boundary condition.

The following introduction will set the stage for the later chapters by presenting an introduction to groundwater hydrology, and the methods that may be used to analyse groundwater flow, particularly numerical modelling. This introduction also draws attention to related issues currently being addressed by numerical modelling, those of groundwater control, contaminated land remediation and landfill engineering.

1.2 Groundwater in the Hydrological Cycle

The endless circulation of water between ocean, atmosphere, and land is called the hydrological cycle. Groundwater is a part of this continuous cycle as shown in the schematic diagram presented in Figure 1.1. Outflow takes place as stream flow, or runoff, and as evapotranspiration, a combination of evaporation from open bodies of water, evaporation from the soil surface, and transpiration from the soil by plants. Inflow to the hydrological cycle system arrives as precipitation, in the form of rainfall or snowmelt. Precipitation is transferred to streams both on the land surface, as overland flow to tributary channels and by subsurface flow routes, such as interflow

and baseflow following infiltration into soil forming groundwater. The subsurface processes are just as important as the surface processes. The groundwater, which flows very slowly depending on the subsurface materials, and surface water, which flows more rapidly, both move toward the oceans. Some water is used by plants, animals, and people and some is returned to the air through transpiration. The rest returns to the oceans where it once again evaporates to repeat the hydrological cycle.

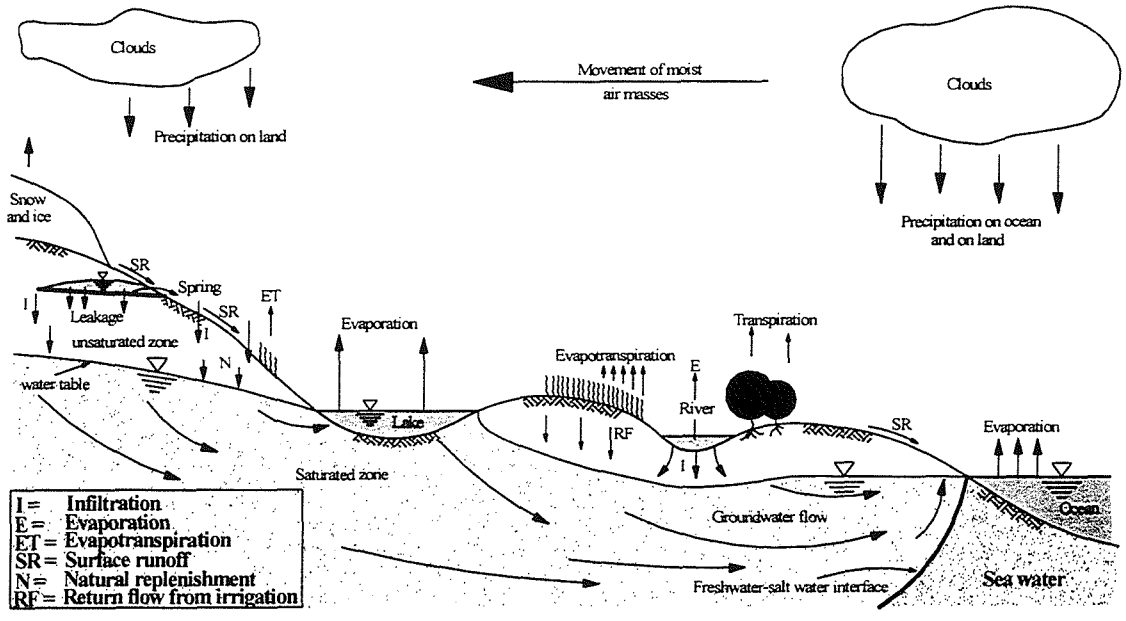

Figure 1.1 Schematic representation of the hydrologic cycle. (After *Bear* and *Verruijt*, 1987.)

1.3 Flow in Unconfined Aquifers and the Free Surface-Seepage Face

Groundwater flow takes places in aquifers which may be confined or unconfined, see Figure 1.2. Groundwater flow in unconfined aquifers is complicated by the fact that one boundary is a free surface. At this boundary, the fluid pressure is theoretically atmospheric. The complications arise from the difficulty of determining the actual position of this boundary in space. The position is required in order to obtain a numerical solution, but it cannot be confirmed without the solution itself. Therefore, an iterative solution process is required in the case of a steady-state solution. An

alternative solution procedure is to carry out a time dependent solution, which starts with a fully saturated aquifer and converges in time to the steady state solution (*Rushton and Redshaw*, 1979).

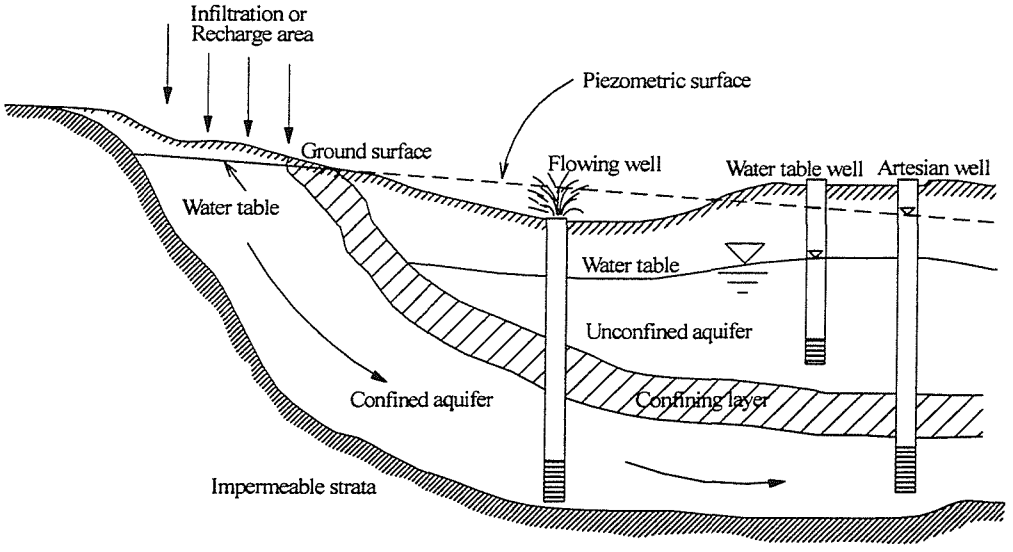

Figure 1.2 Example of groundwater occurrence. (After *Todd*, 1980.)

When groundwater is pumped from an unconfined aquifer using wells, water is derived predominantly from pore-water drainage. This drainage results in a decline in water table position near the pumping wells as time progresses. The vertical surface in a pumped well, which is exposed between the free water surface in the well and the location at which the water table surface in the unconfined aquifer intersects the well, is referred to as the seepage face or seepage surface. The reason for the occurrence of the seepage face is that the seepage flow pattern in the neighborhood of a well draining from an unconfined aquifer contains a significant vertical component of seepage velocity when the drawdown in the well is large in relation to the depth of the aquifer.

It has been pointed out by *Shamsai and Narasimhan* (1991) that the seepage face has often been ignored in analysis because of the difficulty it presents in the use of mathematical or numerical models. They also emphasise the importance of "*understanding the relationships between the free surface and the seepage face for civil engineering.*" In the field of civil engineering for example it is not known whether

or not seepage face is important when using the principle of superposition to design multiple wells acting as an array for groundwater control systems, or landfill leachate control.

The *principle of superposition* is a method in which linear combinations of elementary solutions using well-known equations describing groundwater flow toward a single well in a confined or an unconfined aquifer are used to provide additional solutions. The combined drawdown of multiple wells with drawdowns that overlap at any point within their area of the influence is assumed to be equal to the sum of the individual drawdowns from each well in a confined or unconfined aquifer. The validity of *principle of superposition* is therefore important because it is frequently used to confirm that the layout geometry and number of wells in a proposed groundwater control system will produce the required drawdown or pore pressure relief. In a recent publication, CIRIA report C515 (2000), a statement is made drawing attention to the fact that the *principle of superposition* is, in theory, not valid in unconfined aquifers. The report suggests that the method may be used with the restriction that any reduction in aquifer thickness by drawdown does not exceed about 20%. The report also points to the lack of attention given to research that deals with the estimation of individual well yields in groundwater control schemes. A similar situation is found in the field of landfill engineering where there is a requirement to design arrays of wells to flush residual contaminants out of an otherwise inert landfill site. All of these issues are addressed in more detail later in this thesis.

Commonly the seepage face has been ignored in mathematical analysis due to the difficulty of handling it in an analytical solution. At the present time the availability of numerical models enables us to investigate flow systems that were otherwise difficult to study analytically or experimentally (*Shamsai and Narasimhan*, 1991). Recent developments in numerical methods for modelling the seepage surface has led to the development of this research, Figure 1.3. The outcome of the research should result in a better understanding of the flow near wells pumping from unconfined aquifers for the purpose of groundwater supply, groundwater control and landfill remediation. In particular the research will assess the validity of the application of the principle of superposition to the design of multiple well systems, and to determine the fate of the

seepage surface on a well in an array. Furthermore, the research will contribute to the gap in the research pointed out in CIRIA report C515 (2000), page 158, by using the results from numerical models of flow near well to predict maximum yield from individual well in groundwater control scheme. Finally, the research will examine a specific case study where the assumption of negligible seepage face is generally not valid (*Rowe and Nadarajah,* 1996). The case involves the use of vertical wells as means of leachate management and control of landfills.

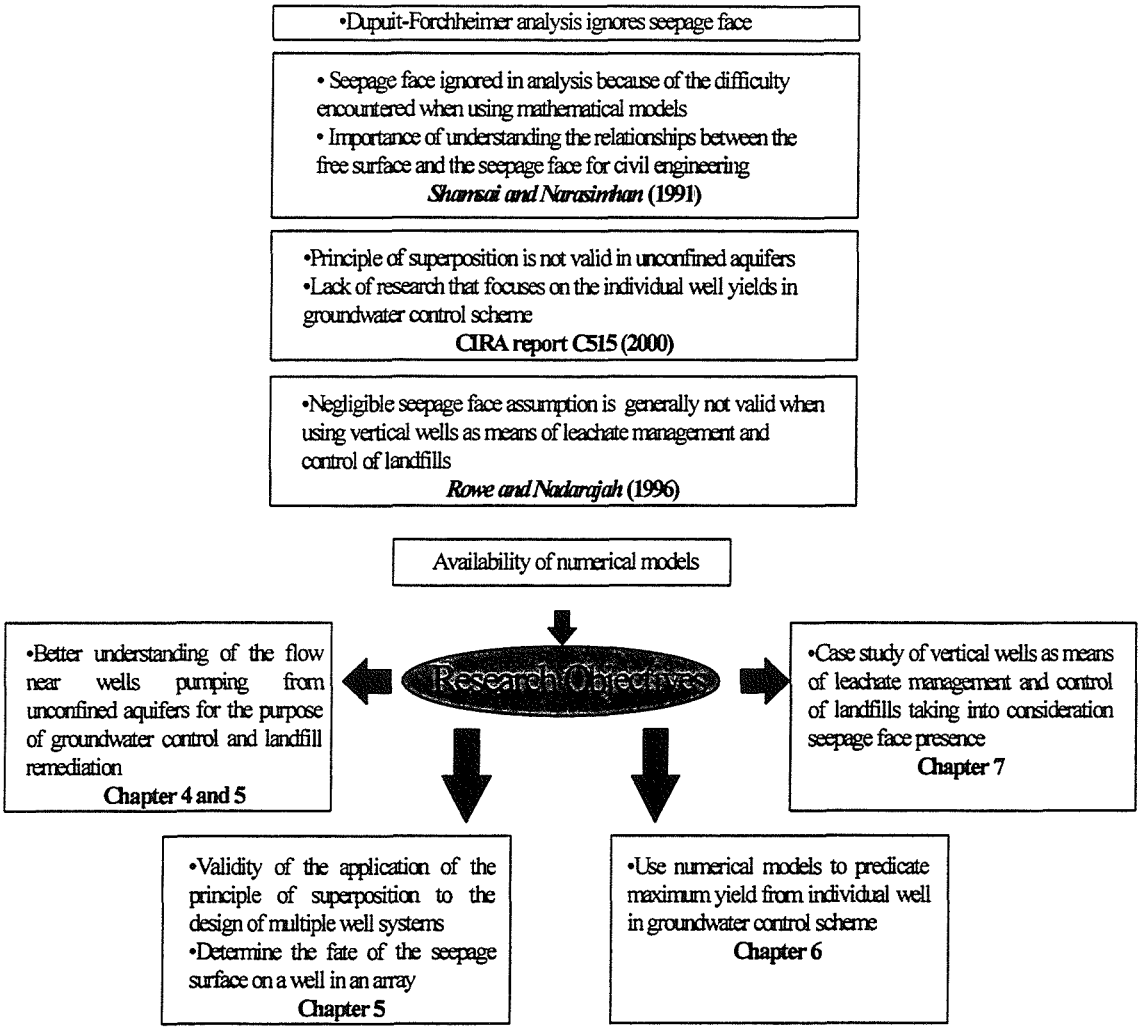

Figure 1.3 Diagram explaining the objectives of the research.

1.4 Groundwater Contamination and Remediation

In recent years, much of the emphasis in groundwater investigations in industrialized countries has shifted from quantifying groundwater supply quantities, to focus more closely on groundwater quality. The quality of groundwater in aquifers can be affected by natural and human activities, and the extent to which the quality is affected by either natural processes or human activities varies with the hydrogeologic and climatic setting. Contaminants may reach groundwater from a variety of sources as shown in Table 1.1. Some wastes are, by intentional design, discharged to the surface; examples include septic systems, spray irrigation, and land disposal of sludge. Other waste may reach groundwater unintentionally. Waste may, and generally does, migrate to groundwater from impoundment landfills, animal feedlots, leaky sewer lines, and other sources. Unprotected waste from different sources may enter groundwater systems as shown in Figure 1.4.

Table 1.1 Sources of groundwater contamination. (After *Bedient et al.*, 1994.)

Category 1	Category 2	Category 3
Sources designed to discharge substance	Sources designed to store, treat, and/or dispose of substance; discharged through unplanned release	Sources designed to retain substance during transport or transmission
Subsurface percolation (e.g. septic tanks and cesspools) Injection wells Land application	Landfills Open dumps Surface impoundments Waste tailings Waste piles Materials stockpiles Aboveground storage tanks Underground storage tanks Radioactive disposal sites	Pipelines Materials transport and transfer

Category 4	Category 5	Category 6
Sources discharging as consequence of other planned activities	Sources providing conduit or including discharge through altered flow patterns	Naturally occurring sources whose discharge is created and/or exacerbated by human activity

Irrigation practices Pesticide applications Fertilizer applications De-icing salts applications Urban runoff Percolation of atmospheric pollutants Mining and mine drainage	Production wells Other wells (nonwaste) Construction excavation	Groundwater-surface water interactions Natural leaching Saltwater intrusion, brackish water

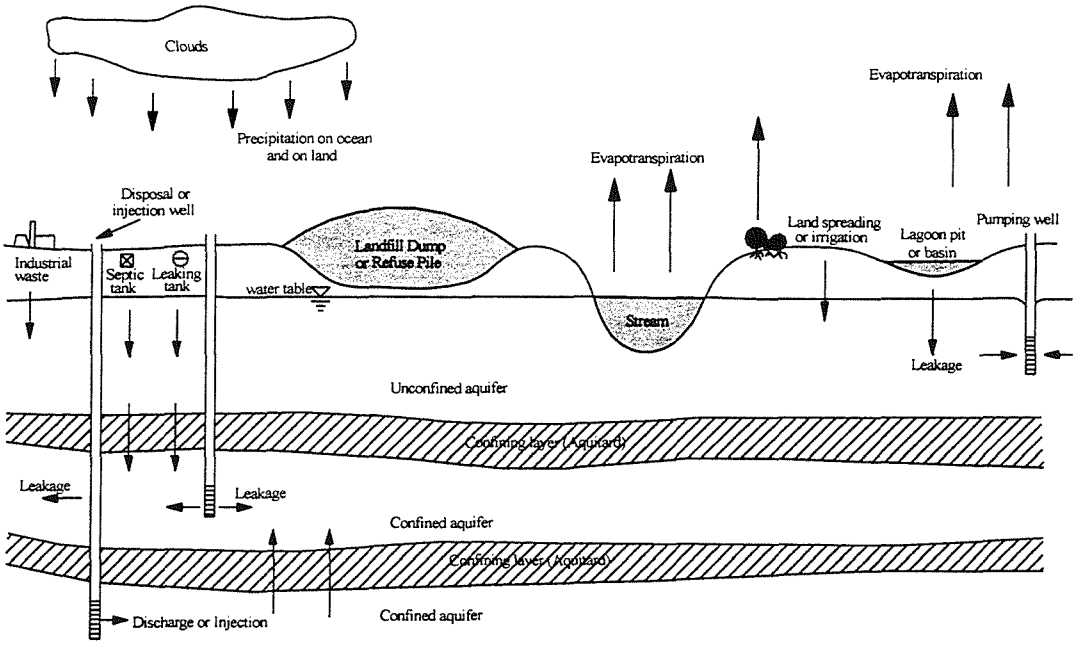

Figure 1.4 Effect of waste-disposal practices on the groundwater system. (Modified after *Bedient et al.*, 1994.)

The severity and extent of groundwater contamination is determined by the hydrogeologic setting, the nature of the contamination, and the effectiveness of regulatory action. The groundwater setting determines the potential extent of contamination. As shown in Figure 1.5, the location of the contaminant source with regard to the target may have small or large impact on the target. For example in Figure 1.5a the target is located close to the pollution source within the highest concentration part of the plume. Whereas in Figure 1.5b the target is either not in the plume path or is located away from the pollution source where the concentration of contaminants decreases due to dispersion and other attenuation effects.

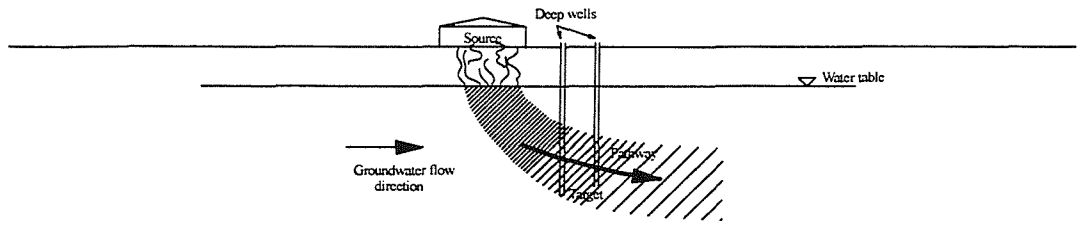

(a)

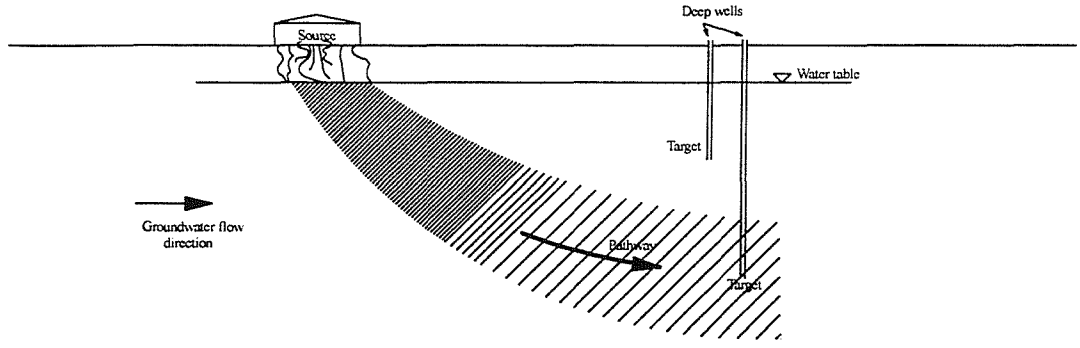

(b)

Figure 1.5 Example of the variable potential impact of contamination.

One of the important sources of groundwater contamination, as shown in Figure 1.4, is poor landfill practice. Storage in landfill is the most common means of disposing of municipal refuse: ashes, garbage, leaves, demolition debris, and sludge from municipal and industrial wastewater treatment facilities. Radioactive, toxic, and hazardous wastes have also been subjected to land burial as a means of disposal. The precipitation that infiltrates landfill can mix with the liquids present in the waste and leach compounds from the solid waste resulting in a liquid known as leachate. This leachate can move downward, through the landfill contaminant seal if it exists and is imperfect, towards the water table to mix with groundwater to form a contaminant plume that will spread in the direction of the flowing groundwater. Landfills today are built with elaborate liner systems with low leakage risk, and are located following the results of a careful hydrogeological study. However, older landfills contain no such liners or leachate collection systems and form a significant source of groundwater and soil

contamination. Landfills, along with other pollution sources, have thus led to the development of ground and groundwater remediation technology.

Groundwater contamination is not an irreversible process. There are natural conditions that act to remove contaminants known as attenuation mechanisms. This includes dilution, dispersion, mechanical filtration, volatilisation, biological activities, ion exchange and adsorption on soil particle surfaces, chemical reactions, and radioactive decay. In recent years, several techniques have developed and been accepted as alternative solutions for groundwater remediation. Some of the widely used techniques are:

1. Extraction and disposal.
2. Containment (physical barriers).
3. Pumped removal of product or contaminated water and above ground treatment (pump-and treat with activated carbon or air stripping).
4. In situ physical, biological, or chemical treatment.
5. Soil vapour extraction.

The established methods mentioned above are not the only definitive practices, in fact many new technologies are emerging. However, the above mentioned methods are the most prevalent and successful techniques currently being applied to many contaminated sites.

Pump-and-treat is one of the most widely used groundwater remediation techniques among the many mentioned previously. It may also be used to reduce the threat of old landfill sites as a source of pollution. Conventional pump-and-treat methods involve pumping contaminated water to the surface for treatment. On-site treatment facilities are usually required before water can be injected to the aquifer or released to the surface.

The pumping wells, which are used to extract water from the saturated zone, create a capture zone for migrating contaminants. Although the near-well flow pattern may be ignored in a large-scale regional groundwater resource scheme design, it becomes an

interesting problem in the context of groundwater control and remediation because of the presence of the seepage face at the pumping wells in unconfined aquifers as explained in section 1.3.

1.5 Groundwater Modelling

A groundwater model is a device that represents a simplified version of a real field situation. Models are divided into physical and mathematical. Physical models such as laboratory sand tanks simulate groundwater flow directly. On the other hand, mathematical models simulate groundwater flow indirectly by means of solving, usually numerically, a governing equation believed to give the best representation of the physical, chemical, and/or biological processes that occur in the system. A model also contains a set of equations that describe head or flow along the boundaries known as boundary conditions. Equations describing the initial condition of heads in the system are needed for time-dependent problems. Mathematical models can be solved analytically or numerically, and either type of solution may involve a computer.

The set of commands used to solve a mathematical model is presented in a computer configuration referred to as a computer program or computer code. The code is generic, whereas a model consists of a set of boundaries and initial conditions accompanied with a site-specific nodal grid, site-specific parameter values, and system controlled and uncontrolled inputs. The reader is advised to refer to *Anderson and Woessner* (1992), which is an introductory reference to modelling groundwater flow with a focus on codes such as the MODFLOW package that is used throughout this research. Other references include *Wang and Anderson*, 1982; *Huyakorn and Pinder,* 1983; *Bear and Verruijt,* 1987; *de Marsily*, 1986, and *Bedient et al.*, 1994.

Anderson and Woessner (1992) propose a modelling protocol that can be summarised as follows:

1. Establish the purpose of the model.
2. Develop a conceptual model of the system.

3. Select the governing equation and a computer code. Both the governing equation and code should be verified. Verification of the governing equation demonstrates that it accurately describes the physical, chemical, and/or biological processes occurring in the system. Code verification, which ensures that the computer program accurately solves the governing equations, is accomplished by comparing the model results to a benchmark analytical solution of a known problem.
4. Design the model. This step includes grid design, selecting time steps, setting boundary and initial conditions, and selecting model parameters that best represent aquifer parameters and system controlled and uncontrolled inputs.
5. Calibrate the model to verify that the model can reproduce field-measured heads, flows, and/or concentrations using a set of values for aquifer parameters and system inputs.
6. Establish the effect of uncertainty on the calibrated model, also known as sensitivity analysis.
7. Verify the designed and calibrated model to establish greater confidence in the model. This step involves using the set of calibrated parameter values and system inputs stresses to reproduce a second set of field data.
8. Predict results based on the calibrated model.
9. Determine the effect of uncertainty in parameter values on model predictions.
10. Present the model design and results.
11. Post audit and model redesign. As more field data is collected after the modelling study is completed, it is possible to compare the model predictions against the new field data. This may lead to changes in the conceptual model or changes in model parameters.

Panday and Huyakorn (2000) introduced an enhanced version of MODFLOW (MODFLOW-SURFACT) developed by the United State Geological Survey (USGS) overcoming a number of limitations of original MODFLOW in simulating complex field problems. One of the additions is the ability to use a component package that simulates a drain as a means of including seepage face boundary conditions. The added package has the advantage that it may be used to simulate a seepage face boundary condition by assigning the elevation of a seepage face boundary node as a boundary

condition parameter. Hence, along the boundary, no recharge is supplied until the water table builds up to the seepage face elevation. If the water table reaches the seepage face elevation, the aquifer drains to retain the seepage face elevation, that is atmospheric pressure conditions. Finally, if the water table drops below the seepage face elevation at any time during the simulation, a zero flux boundary condition is applied at the seepage face boundary. Later in the thesis, in Chapter 4, a comprehensive coverage of MODFLOW-SURFACT is given closely using the user manual MS-VMS: First Fully Integrated MODFLOW-Based Visual Modeling System with Comprehensive Flow and Transport Capability (1996), and the later document "MODFLOW: Enhancements for Robust, Reliable Simulations of Complex Environmental Flow and Contaminate Transport Situations (2000)", which was provided by the authors.

1.6 Scope and Objectives

The specific aim of this research is to verify and use the new seepage surface related numerical modelling techniques to study and investigate the influence of the seepage face on the performance capacity of deep wells in a variety of contexts. These contexts include the estimation of the yield capacity of an individual well and wells working as an array. Moreover, an evaluation is made of the potential for groundwater remediation systems enhancement, as the result of exposing a larger region of a contaminated unconfined aquifer to remediating flushing flows, due to the presence of a seepage face. The research also examines a specific case study involving the use of vertical wells as means of leachate management and control of landfills. This includes transient simulations that model dewatering of a landfill using a network of leachate abstraction wells.

1.7 Thesis Structure

This thesis presents the main outcome of the research, and presents background information where needed. Essential lengthy background information is included in the thesis appendices. References are suggested throughout the thesis for further reading

with a special focus on seepage face publications. Results are presented within the summary at the end of each chapter and are summarised at the end of the thesis along with conclusions and recommendations.

The thesis consists of eight chapters. Following this introduction, Chapter 2 presents a brief review of the previous work carried out to investigate the seepage face. Included in this chapter is a review of widely used basic laws that govern groundwater movement.

Chapter 3 presents the basic equations for three dimensional groundwater flow and the integrated form of these equations for the flow in confined and unconfined aquifers. The US Geological Survey Modular Finite-Difference Groundwater Flow Model MODFLOW, and the development of its finite difference equation is introduced. Moreover, a brief discussion on the type of numerical errors encountered when using finite difference models and the means of controlling these errors is included

Chapter 4 introduces the improved version of MODFLOW developed by *HydroGeoLogic* Inc., MODFLOW-SURFACT, and its capability to produce variably saturated models. Also discussed is the representation of an individual well, which is also known as the equivalent well block radius, in groundwater modelling and its effect on well yield predictions. The MODFLOW-SURFACT code is verified by comparing the numerical results with analytical and/or experimental solutions. The purpose of code verification is to demonstrate that the numerical solution is relatively free of round-off and truncation errors, which if uncontrolled can lead to unstable solutions, and is able to predict closely the results obtained from benchmark analytical and/or experimental solutions. An outcome of this work is the formulation of an algebraic framework that represents the historical experimental data obtained on the seepage surface. This has been used in Chapter 6 to underpin the work on maximum well yields.

Chapter 5 presents the seepage face investigations developed for single and multiple well systems under steady state and transient conditions. The investigation includes the effect of well radius, aspect ratio, and anisotropy on the well yield and the shape of the

seepage face. The opportunity has been taken to assess the validity of the application of the principle of superposition to the design of multiple well systems, and to determine the fate of the seepage surface on a well in an array.

Chapter 6 previews the limiting gradient concept and its implications for maximum well yield based on the use of numerical models taking into account the presence of seepage face. Simple analytical solutions are suggested for fast and effective limiting gradient and seepage face elevation predictions. A modification is recommended to the established method of estimating maximum well yields.

Chapter 7 discusses an important application in which the seepage face cannot be ignored. The application is the use of vertical wells as a means to control leachate level in landfills. The chapter presents transient simulations that model the dewatering of a landfill by a network of leachate abstraction wells. The results demonstrate that piezometric surface levels and base pressure heads levels differ considerably close to a well. This is an important factor in the context of assessing the performance of leachate control wells. It is also observed that the yield of landfill wells is controlled by the hydraulic conductivity of the deeper strata. Chapter 8 presents the major results of the research and a summary that outlines the main conclusions, suggestions, and recommendations for future research.

In summary, the ability of the MODFLOW-SURFACT code to model the seepage face condition using drains is the key development that has opened the door for this research investigation. Simple verification examples such as the one used in the MODFLOW-SURFACT manual (*HydroGeoLogic* Inc., 1996) have encouraged the use of the code for more complicated situations. This is the stimulus for this research.

The research is intended to help fill the gaps in the understanding of the influence of the seepage face on the performance capacity of deep wells. The inter-action between wells working as an array and the seepage face has received little attention in the past compared to its importance in groundwater control. This research will look into wells working as an array using numerical models in order to provide a comprehensive understanding of the effect on seepage face. Finally, the research examines a specific

case study where the assumption of negligible seepage face is generally not valid (*Rowe and Nadarajah,* 1996). The case involves the use of vertical wells as means of leachate management and control of landfills. This includes transient simulations that model the dewatering of a landfill using a network of leachate abstraction wells taking into account the presence of the seepage face.

Chapter (2)

Literature Review

2.1 Introduction

This chapter presents the basic laws governing the motion of groundwater in aquifers and demonstrates the way in which they maybe integrated to provide analytical models of well flow. The scale at which such equations are applicable is at the macroscopic level. Thus, for practical purposes, it is necessary to pass from the microscopic level, at which we consider what occurs at each point within a phase inside each pore, to the macroscopic level of a continuum at which only averaged phenomena are considered. This is achieved by introducing the concept of the representative elementary volume (REV) of a given porous medium (*Bear*, 1979). The main feature of the REV is that the averages of fluid and solid properties taken over it are independent of the sample size. A macroscopic value at a point within a porous medium is interpreted as the average of that variable taken over the REV centered at that point. The obvious benefit of applying the continuum approach to flow through a porous media is that it is practically impossible to describe, in any exact mathematical way, the complicated geometry of the solid surfaces that bound the moving flow. In this study, the focus is on macroscopic continuum analytical models. These models are used later to act as benchmarks for numerical models. This chapter also reviews the previous work carried out to investigate the seepage face which is also a source of benchmark data.

2.2 Darcy's Law for Saturated Flow

Henry Darcy, a French engineer, experimentally investigated the flow of water in the vertical homogenous filters for the fountains of the city of Dijon, France in 1856. From his experiments, see Figure 2.1, *Darcy* proposed the now famous formula

$$Q = KA\frac{(h_1 - h_2)}{L} \tag{2.1}$$

where Q is the rate of flow (volume of water per unit time); K is a coefficient of proportionality known as the saturated hydraulic conductivity; A is the cross-sectional area; $(h_1\text{-}h_2)$ is the hydraulic or potential head difference between the inlet and outlet; and L is the length of the sand column (Figure 2.1a). Figure 2.1b shows how equation 2.1 may be extended to flow through an inclined homogenous porous medium column. Thus,

$$h = z + \frac{p}{\gamma} \tag{2.2}$$

where z is the gravitational head or elevation measured from an arbitrary datum; p is pressure; γ is specific weight of water and $\frac{p}{\gamma}$ is the pressure head (ψ).

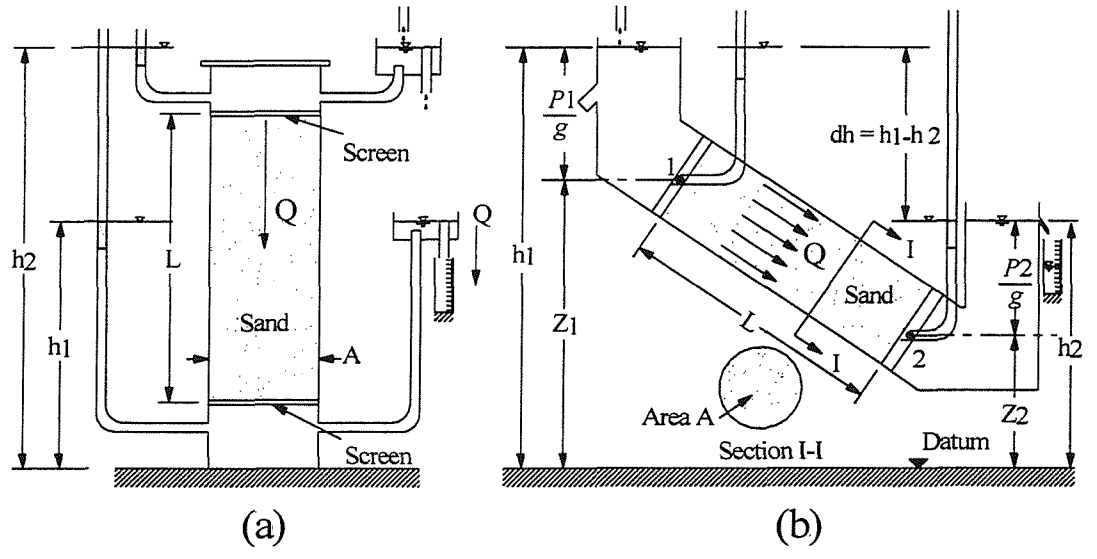

Figure 2.1 *Darcy's* experiment. (Reproduced from *Bear*, 1979.)

The hydraulic conductivity can be expressed in terms of the soil matrix and fluid properties, *Nutting* (1930). Equation 2.1 becomes

$$Q = \frac{k\rho g A(h_1 - h_2)}{\mu L} \tag{2.3}$$

where k is the intrinsic permeability of the porous matrix and its value depends entirely on the properties of the solid matrix; ρ is the density of fluid; g is the acceleration due to gravity; and μ is the viscosity of the fluid. In this form *Darcy's* law can be extended to other fluids. The value of the hydraulic conductivity will decrease if the porous medium becomes partially saturated. This is discussed further in Chapter 4.

The experimentally derived equation of motion in the form of *Darcy's* law (equation 2.1) is limited to one-dimensional flow of a homogenous incompressible fluid. The equation can be generalised for flow in three-dimensions in a vector notation as

$$q = KJ = -K\, grad\, h \tag{2.4}$$

where q is the specific flow vector with components q_x, q_y, q_z in the direction of the Cartesian xyz coordinates respectively, and J = $-grad\ h \equiv -\nabla h$ is the hydraulic or potential head gradient with components $J_x = -\partial h/\partial x$, $J_y = -\partial h/\partial y$, $J_z = -\partial h/\partial z$, in the xyz directions respectively. Although equation 2.4 represents *Darcy* fluxes q with velocity dimensions, it actually represents the macroscopic flow velocity averaged over the cross-sectional area. In saturated flow, pore velocity of water, v_p, can be expressed as

$$v_p = \frac{q}{n} \tag{2.5}$$

where n is the porosity of the soil, again a macroscopically averaged quantity. Therefore, the pore velocity represents the average rate at which the water moves between two points, and is not the individual water particle velocity within the complex pore structure. The continuum approach used to represent the actual porous medium circumvents the detailed microscopic configuration of the actual void space. At the

macroscopic level, various macroscopically averaged solid matrix coefficients, such as the porosity, and the intrinsic permeability replace the complex geometry of the void-solid interface. Thus in the macroscopic model the coefficients used are the relevant lumped effects of the microscopic void-space configuration.

2.3 The Dupuit-Forchheimer Model

The *Dupuit* approximation is one of the most powerful and simple tools available to engineers and hydrologists for dealing with unconfined groundwater flow. It is widely quoted in textbooks as the basis of most methods employed for computing unconfined flow to a well. *Dupuit* (1863) based his assumptions on the observation that in most groundwater flows, the slope of the phreatic surface is very small. Slopes of 1/1000 and 10/1000 are normally encountered. His assumptions can be summarised as: (1) the horizontal hydraulic head gradients are equal to the slope of the water table (phreatic surface) and are invariant with depth and (2) for small water table gradients, the streamlines are horizontal and the equipotential lines are vertical, see Figure 2.2.

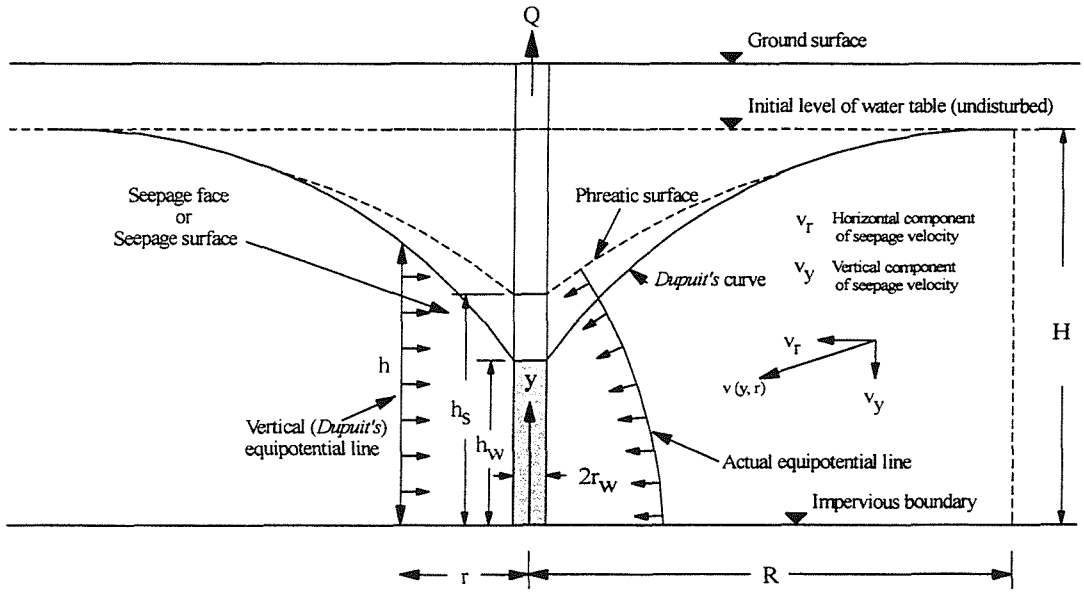

Figure 2.2 Illustration of *Dupuit's* assumptions (left) and the actual flow (right) toward a fully penetrating well in an unconfined aquifer.

The importance of *Dupuit's* equation arises from its ability to determine flow to a well accurately, despite the fact that it assumes that the drawdown at the well is equal to the drawdown inside the well and ignores the presence of the seepage face. The derivation and application of the *Dupuit-Forchheimer* model of groundwater flow toward a fully penetrating well in an unconfined aquifer will therefore be reviewed as follows.

The flow rate Q is given as the product of the cross-sectional area of flow A and the seepage velocity v shown in Figure 2.2. v is equal to $-q$, the specific flow, which is also known as *Darcy's* velocity thus,

$$Q = vA = -qA \tag{2.6}$$

The cross-sectional area of flow at distance r from the pumping well is the side of the cylinder with radius r and thickness h, which is the saturated zone thickness shown in Figure 2.3,

$$A = 2\pi rh \tag{2.7}$$

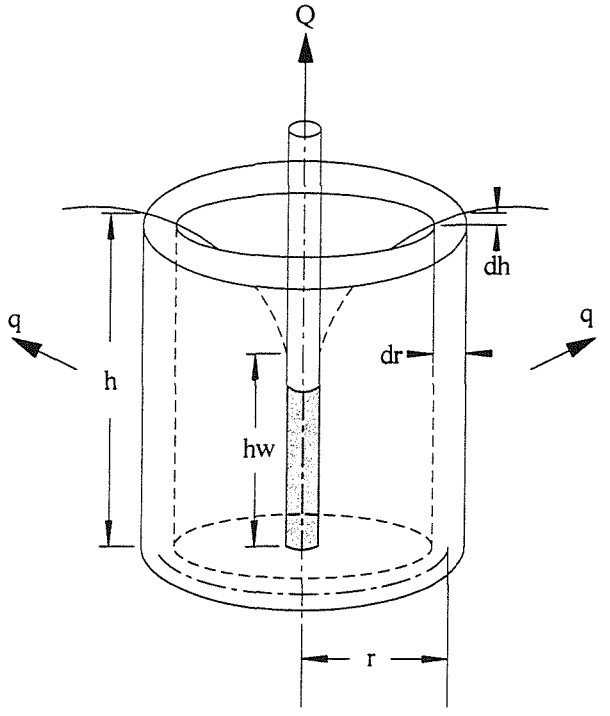

Figure 2.3 Scheme for deriving the differential equation of groundwater flow toward a fully penetrating well in an unconfined aquifer.

Darcy's velocity at distance r is given as the product of the aquifer's hydraulic conductivity K and the hydraulic gradient i, which is an infinitesimally small drop in hydraulic head dh over infinitesimally small distance dr. Applying equation 2.4,

$$q = -K\frac{dh}{dr} \tag{2.8}$$

Therefore, for flow towards a well that satisfies the *Dupuit* assumptions, the well yield Q can be expressed as

$$Q = 2\pi rKh\frac{dh}{dr} \tag{2.9}$$

Using equation 2.6, equation 2.9 may be integrated between the limits $h_1=h_w$ *at* $r_1=r_w$ *and* $h_2=h$ *at* $r_2=r$, to give

$$Q = \pi K\frac{h^2 - h_w^2}{\ln\left(\frac{r}{r_w}\right)} \tag{2.10}$$

where, h is the hydraulic head at a radial distance r from the well axis; and h_w is hydraulic head at the well radius; r_w is the well radius (Figure 2.3). If Q is known, equation 2.10 provides a way of estimating the relationship between h and r. The flow, Q, may be estimated by integrating equation 2.9 between any pair of known hydraulic heads and the corresponding radial distances from the well axis.

Equation 2.10 is known as the *Dupuit-Forchheimer* well-flow formula. Although the formula is based on the previously discussed assumptions, it predicts the value of h correctly for a given flow if r is chosen sufficiently far from the well (*Zee et al.*, 1957; *Muskat,* 1937). The applicability of *Dupuit's* equation for determing the flow to a well was investigated by *Muskat,* 1937; *Babbitt and Caldwell,* 1948; *Charnii,* 1951; *Boulton,* 1951; *Polubarinova-Kochina,* 1952; *Hantush,* 1964; *Kirkham,* 1964. The results of the investigations can be summarised as follows:

1. The flow to a fully penetrating gravity well can be estimated within 1 to 2% of those predicted by the exact solution, that is when using equation 2.10. This is valid regardless of the depth to which the water in the well is lowered. However, the capacity of the well is limited by the amount of well screen remaining below the groundwater level at the well, which accordingly must be of sufficient length, size, and capacity to admit the flow.

2. The value of h, at a distance r from the well exceeding approximately 1 to 1.5 times the height of the original water table H, will be equal to that computed from equation 2.10, reorganised as equation 2.11 below.

3. The drawdown at a distance r from the well less than 1.0 to 1.5H will be less than that computed from equation 2.11. Also, the difference between the actual drawdown and that computed from equation 2.11 will increase as the drawdown at the well increases. This is because equation 2.11 fails to describe the large vertical flow components that invalidate the *Dupuit* assumptions in this region.

2.4 The History of the Seepage-Face: Literature Review

The equation based on *Dupuit's* assumptions, that describes the position of the phreatic surface h at a distance r from the pumping well is obtained from equation 2.10 as,

$$h = \sqrt{h_w^2 + \frac{Q}{\pi K} \ln \frac{r}{r_w}} \tag{2.11}$$

This equation is known as *Dupuit's* parabola, which also can be expressed in terms of other known heads and the distances at which they are recorded. This can be done by substituting for the total flow Q (using equation 2.10 with $h = H$ and $r = R$) in equation 2.11. This is only a matter of usefulness for calculating *Dupuit's* parabola when one does not know the hydraulic conductivity K and the well flow Q. This is usually done with H being equal to the undisturbed head, in which case R is known as the radius of influence, see Figure 2.2.

$$h = \sqrt{h_w^2 + (H^2 - h_w^2)\frac{\ln\frac{r}{r_w}}{\ln\frac{R}{r_w}}} \qquad (2.12)$$

As discussed earlier the position of the total actual phreatic surface is above the *Dupuit's* parabola for distances $r < 1.5H$ from a well.

The *Dupuit-Forchheimer* theory could hardly have claimed any degree of validity without a direct empirical or rigorous analytical confirmation. In 1927, *Kozeny* published the first attempt to analyse the flow problem by direct potential-theory methods. Using *Laplace's* equation, he attempted to synthesise a solution satisfying the boundary conditions of the gravity flow system by means of elementary solutions of the type used in the problem of partially penetrating wells. Unfortunately, *Kozeny* completely neglected the discontinuity between the fluid height in the sand at the well face and the fluid level in the well. While *Kozeny's* theory cannot be considered as a satisfactory analytical solution to the problem of radial gravity flow, it provided the impelling force for the first direct empirical investigation of the problem. A more complete test of *Kozeny's* theory was carried through by *Ehrenberger* (1928). He set up an empirical correction factor to *Kozeny's* formula that evidently has no physical significance.

The next attempts to derive more satisfactory solutions to unconfined flow were two investigations by *Wenzel* (1932) and *Wyckoff et al.* (1932), which were carried out almost simultaneously. *Wenzel* was interested in determing the hydraulic conductivity of water-bearing sand by inverting the *Dupuit-Forchheimer* formula. He compared the hydraulic conductivity calculated from data collected from 80 observation wells lined up radially around two wells that were being pumped at known rates. *Wenzel* found that the hydraulic conductivity apparently increased uniformly as the distance of the second observation well increased, which led him to conclude that *Dupuit-Forchheimer* formula must need some correction, at least under his experimental conditions. However, the lack of equilibrium in the flow system is the reason for the failure to give a constant value of hydraulic conductivity rather than a fundamental error in the *Dupuit-Forchheimer* formula. (*Muskat*, 1937).

Wyckoff et al. (1932), in contrast to *Wenzel*, returned to the laboratory methods of *Kozeny* and *Ehrenberger*. The work, which was done using a sand model with 15° sector, introduced essential new features to the previous work. Manometers were connected to the bottom of the sand tank to measure the radial pressure distribution along the system bed, and a steady-state condition was maintained using continuous circulation of fluid in the tank. The results of the analysis showed that the *Dupuit-Forchheimer* formula predicted the piezometric heads along the base, but did not represent the free surface. However, because of the capillary zone the position of the free surface near the well was not determined accurately. Mention should also be made of *Kozeny's* (1933) work in which a formula was obtained for the pressure distribution at the base of a radial flow system. The formula produces a similar base pressure distribution to that found by *Wyckoff et al.* (1932).

An electrical analogy using a carbon wedge was used by *Babbitt and Caldwell* (1948) to study unconfined flow towards a well using sand and electrical models. They concluded that the shape of the free surface closely approximates the *Dupuit* curve at distances greater than H, which is the vertical distance from the bottom impermeable stratum to the free water surface at the radius of influence, from the well axis. Thus, if an observation well is located at a radial distance r, where $r > H$, the elevation of the free surface at the radius of the observation well above the impervious boundary, h, can be determined from equation 2.12

$$h^2 = \frac{H^2 - h_w^2}{\ln\left(\frac{R}{r_w}\right)} \ln\frac{r}{r_w} + h_w^2 \tag{2.13}$$

where, h_w is the elevation of the free surface at the pumping well above the impervious boundary; R is the radius of influence of the well. *Babbitt and Caldwell* also suggested an empirical expression for determining h for $r < H$

$$h = H - \frac{C_x}{H}\frac{H^2 - h_w^2}{\ln\left(\frac{R}{r_w}\right)} \ln\frac{R}{0.1H} = H - \frac{C_x}{H}\frac{Q}{\pi K}\ln\frac{R}{0.1H} \tag{2.14}$$

where C_x is a correction factor that depends on the ratio of $\frac{r}{R}$ as shown in Figure 2.4.

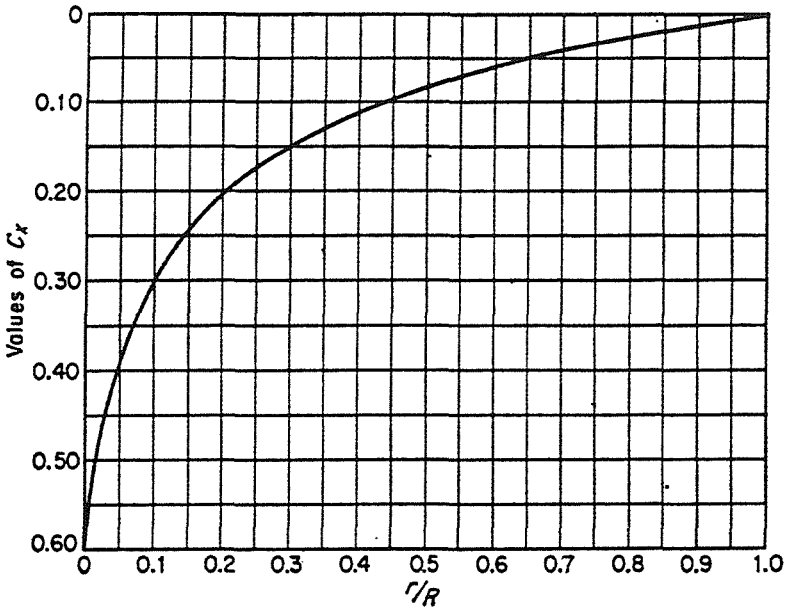

Figure 2.4 Correction factor. (After *Babbitt* and *Caldwell*, 1948.)

Numerical analysis, using relaxation methods, was applied to unconfined flow problems by *Yang* (1949), and was later used by *Zee et al.* (1957). He modified the Southwell procedure to study the seepage toward gravity wells. He applied the modified relaxation method to six cases of axially symmetrical three-dimensional flow which is typified by the problem of seepage toward a fully penetrating gravity well in a pervious stratum overlaying a horizontal impervious base. The solution, which is based on modification of the relaxation method, is a valid analytical approach to problems of seepage toward gravity wells as reported by *Hall* (1955). In 1951, *Boulton* solved four additional cases using relaxation techniques. His investigation led to the following expression for calculating h

$$h = H - \frac{Q}{2\pi KH}\left(\frac{2H}{H+h}\right)\ln\left(\frac{R}{r}\right) \tag{2.15}$$

where $\left(\frac{2H}{H+h}\right)\ln\left(\frac{R}{r}\right)$ is a factor that varies slightly from unity when Q increased from zero to its maximum value. *Boulton* suggested a value of 3.75 for wells of usual diameter and 3.5 for large wells in which $\frac{r_w}{H}$ are of the order 0.25. The relation is

similar to equation 2.14 given earlier by *Babbitt and Caldwell* (1948) who used electric-analogy tests.

Hansen (1953) clarified the nature of unconfined flow to single and multiple wells by closely studying the effect of the capillary fringe on the location of the free surface and the form of flow patterns. He established a functional relationship independent of the radius of influence relating the variables at the well, which can be applied to both single and multiple wells

$$\frac{Q}{Kr_w^2} = f_1\left(\frac{h_s}{r_w}, \frac{h_w}{r_w}\right) \tag{2.16}$$

This expression relates the depth of water, both outside and inside the well to the radius of the well, the well yield, and the hydraulic conductivity of the aquifer. *Hanson* (1953) determined a graphical solution shown in Figure 2.5 obtained using a depressed membrane under tension to simulate the free surface. This graphical solution was modified later by *Zee et al.* (1957).

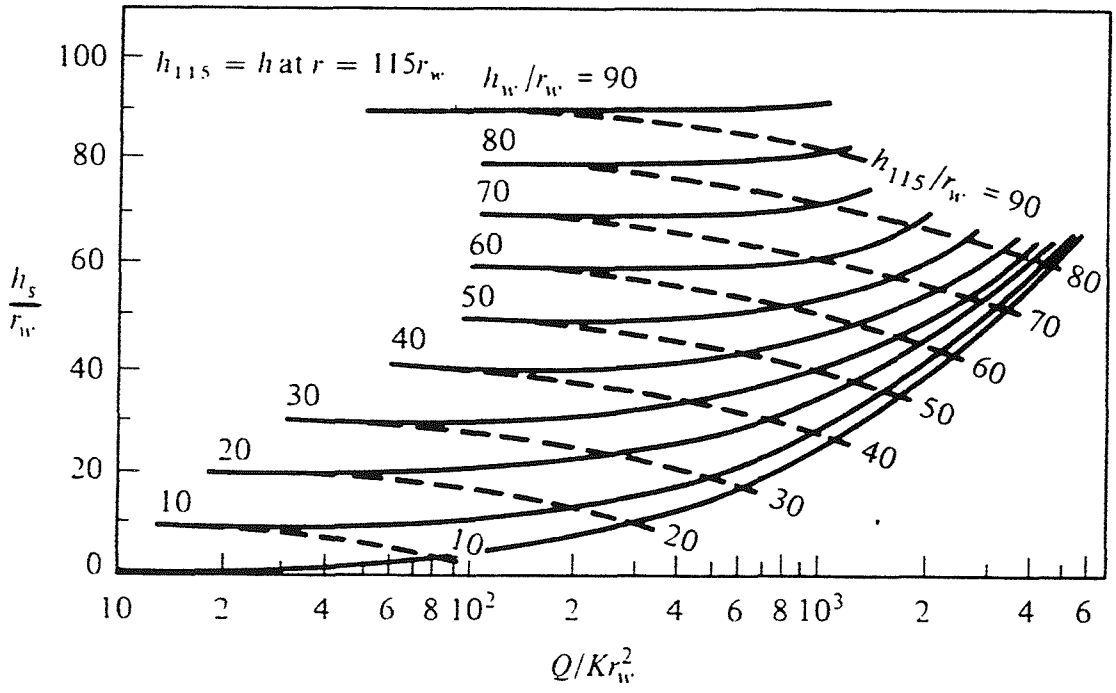

Figure 2.5 Flow rate of a well in a phreatic aquifer. (After *Hansen*, 1949.)

Kozeny (1953) described a method for predicting the maximum water table drawdown at a fully penetrating pumping well in an unconfined aquifer. He assumed that the maximum possible entrance velocity of water is equal to *K*. Based on this assumption *Kozeny* came up with a graphical solution for the height of the seepage face. There are grounds however for criticizing *Kozeny's* results and these are further discussed in Chapter 6.

Boreli (1955) studied the form of the free surface and the characteristics of flow toward partially penetrating wells using a relaxation method. He presented an empirical equation for distances less than about 1.0 to 1.5*H*. It should be noted that these equations are applicable to partially and fully penetrating gravity wells. The flow rate from any gravity well can be expressed as follows,

$$Q = \frac{\pi K\left[(H-s)^2 - t^2\right]}{\ln(R/r_w)}\left[1+\left((0.30+\frac{10r_w}{H}\right)\frac{\sin 1.8s}{H}\right] \qquad (2.17)$$

where notations are shown in Figure (2.6).

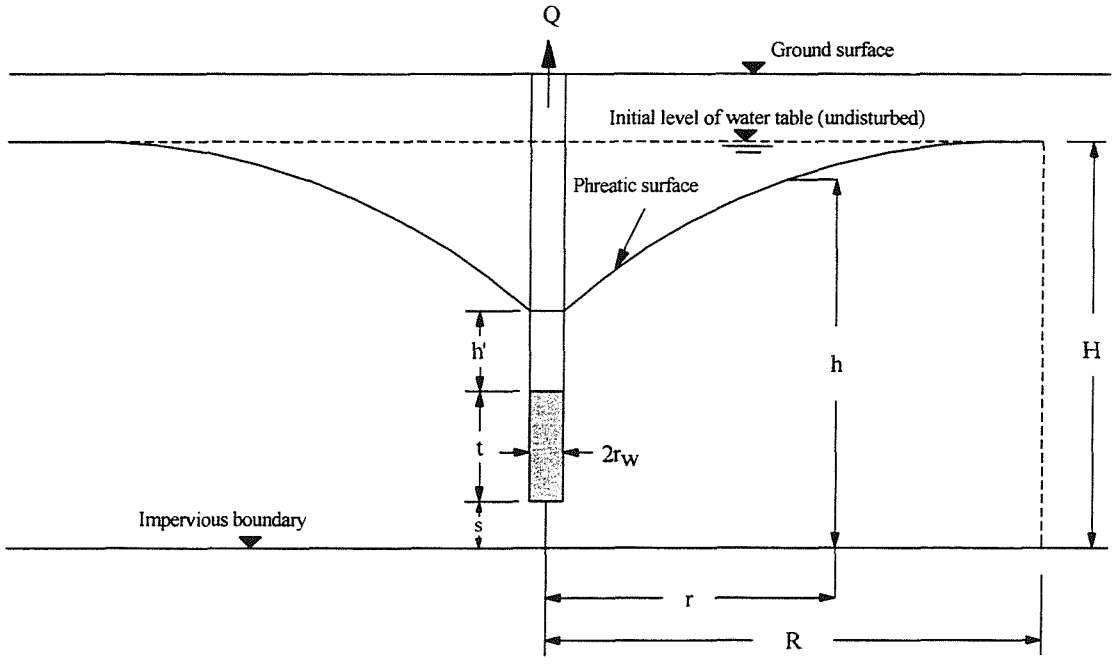

Figure 2.6 Notations for *Boreli* (1955) solution. (After *Leonards*, 1962.)

The following equations can be used to compute the drawdown after obtaining Q from equation 2.17

For $\frac{r}{h}$ greater than 1.5, the *Dupuit-Forchheimer* equation can be used

$$H^2 - h^2 = \frac{Q}{\pi K} \ln\left(\frac{R}{r}\right) \tag{2.18}$$

For $\frac{r}{h}$ less than 1.5 *Boreli* proposes,

$$H - h = \frac{Q\ P \ln\left(10\frac{R}{H}\right)}{\pi K H\left[1 - 0.8\left(\frac{s}{H}\right)^{1.5}\right]} \tag{2.19}$$

Noting that the function P depends upon the ratio $\frac{r}{h}$, *Boreli* proposed the following two equations for P depending on the value of $\frac{r}{h}$

For $0.3 < \frac{r}{h} < 1.5$,

$$P = 0.13 \ln\frac{R}{r} \tag{2.20}$$

For $\frac{r}{h}$<0.3,

$$P = \overline{C}_x + \Delta C \tag{2.21}$$

where

$$\overline{C}_x = 0.13 \ln \frac{R}{r} - 0.0123 \ln^2 \frac{R}{10r} \tag{2.22}$$

and

$$\Delta C = \frac{s}{h}\left[\left(\frac{1}{2.3}\ln\frac{R}{10r}\right)\left(1.2\frac{s}{H} - 0.48\right) + 0.113 \ln\frac{2.4H}{R}\ln\frac{R}{34r}\right] \tag{2.23}$$

Hall (1955) investigated steady-state seepage in the immediate vicinity of a fully penetrating gravity well by means of a series of large-scale tests. Beside the investigation *Hall's* purpose was to establish a satisfactory correlation between the results obtained from the model tests and those derived from theoretical analysis. His aim behind such correlation was to overcome some of the troublesome features in earlier sand models and to substantiate the results from the relaxation procedure work. Besides validating *Yang's* work involving the modification of the Southwell procedure, *Hall* developed an empirical equation to locate the phreatic line on a typical radial section through a given well. According to *Hall* the height of the seepage surface can be calculated with the following equation. Well losses are ignored.

$$h_s - h_w = \frac{(H - h_w)\left[1 - \left(\frac{h_w}{H}\right)^{2.4}\right]}{\left(1 + \frac{5}{(H / r_w)}\right)\left[1 + 0.02 \ln\left(\frac{R}{r_w}\right)\right]} \tag{2.24}$$

h_s is the height of seepage surface; h_w is the height of the water level inside the pumped well.

Another equation proposed by *Schneebeli* (1955) for determining the height of the seepage face at the well perimeter is

$$h_s - h_w = \sqrt{h_w^2 + \frac{Q}{\pi K}\left[0.4343 \ln \frac{Q}{\pi K r_w^2} - 0.4\right]} - h_w \tag{2.25}$$

or

$$h_s - h_w = \sqrt{h_w^2 + \frac{H^2 - h_w^2}{\ln \frac{R}{r_w}}\left[0.4343 \ln \frac{H^2 - h_w^2}{r_w^2 \ln \frac{R}{r_w}} - 0.4\right]} - h_w \tag{2.26}$$

The above equations should be used when $\frac{Q}{Kr_w^2} > 8$. When this parameter is less than 8, the seepage face is very small and can be ignored for practical purposes (Also see Figure 2.8)

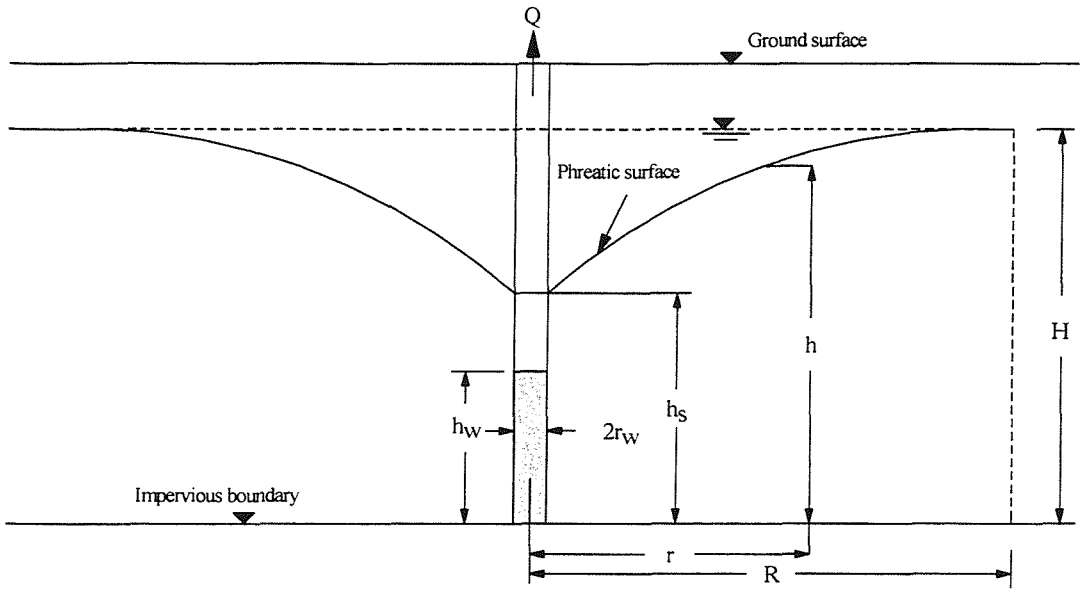

Figure 2.7 Notations for *Hall* (1955) solution. (After *Bouwer*, 1978.)

Zee et al. (1957) studied the radial unconfined flow to a well by combining the electrical analogy for hydraulic flow with the membrane analogy for a free surface. The experimental results obtained were then linked with observations of other investigators to develop empirical relationships between the flow and the geometric variables. First, *Zee et al.* obtained the data that relates h_s, h_w, and Q/Kr_w^2. Based on that, a graphical relationship between these parameters was produced (Figure 2.8) in the range of

$$10 < \frac{Q}{Kr_w^2} < 5000 \quad and \quad 10 < \frac{h_{115}}{r_w} < 90 \tag{2.27}$$

Figure 2.8 shows that the relationship between the flow variables of discharge and hydraulic conductivity with the well radius, r_w, the depth of water in the well, hw, the depth outside the well casing, hs, and the depth at a distance of 115 times the well radius, h_{115}. Figure 2.8 is also useful for predicting values of unknown variables if certain other variables are known. More about the *Zee et al.* study will be discussed later when introducing the limiting gradient concept.

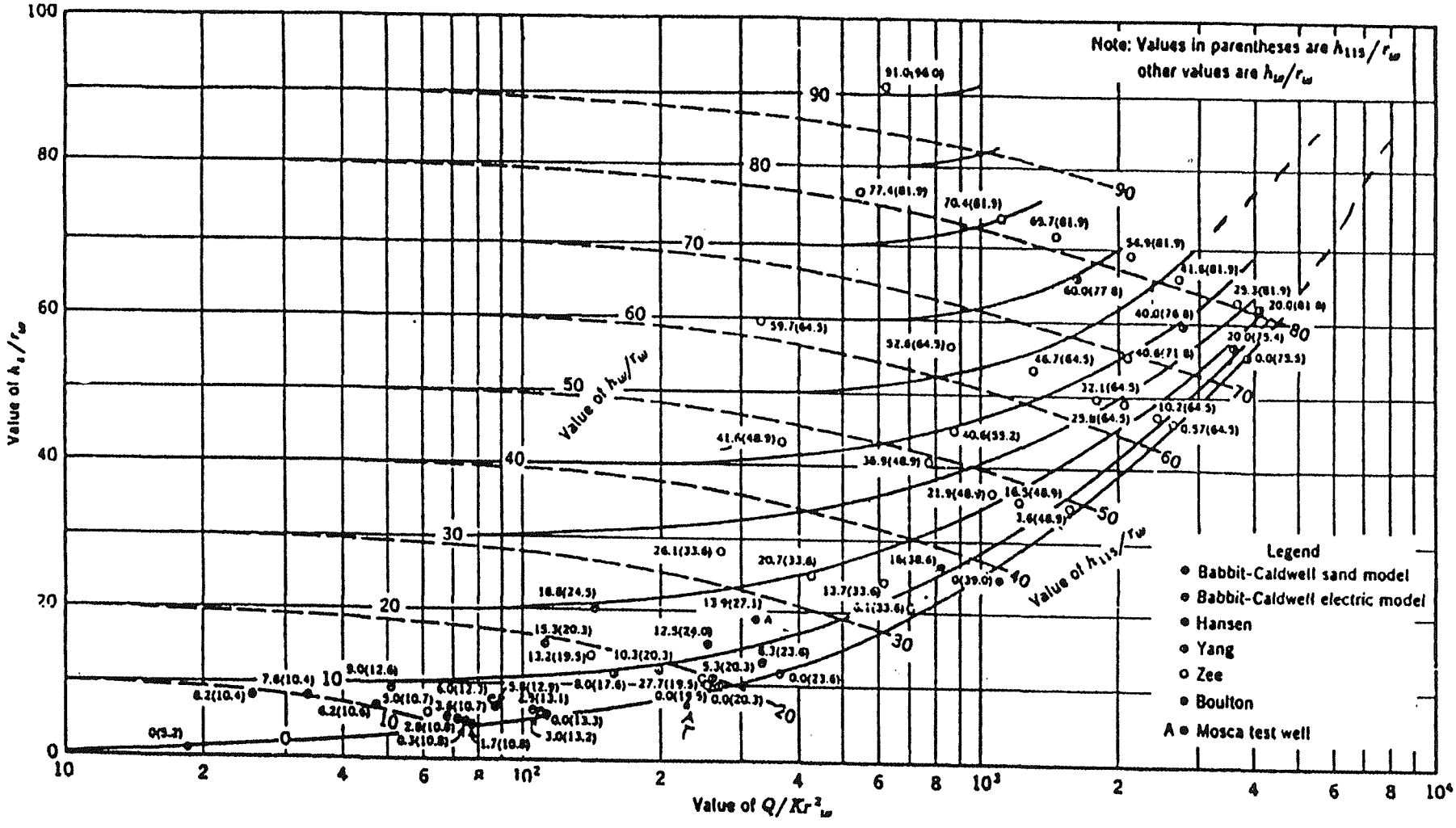

Figure 2.8 Relationship of flow rate and geometric parameters. (After *Zee et al.*, 1957.)

Kirkham (1964) developed an exact theory using an analytical solution for the height of the water table near a well penetrating to the barrier of a semiconfined aquifer. The theory begins with the development of a potential function that neglects the unsaturated zone. This zone is not neglected in the more recent studies that are reviewed later. It is also fully incorporated in the advanced MODFLOW-SURFACT code. *Kirkham* obtained the potential function by imagining that the flow medium occupies the space of the cone of depression. The height of the free surface, at any point, is then determined by the equation in which the height occurs both linearly and in terms of an infinite series of transcendental functions. The method of introducing an imaginary flow medium in the region occupied by the cone of depression seems feasible in solving the well problem. This is applicable, as *Kirkham* stated, when the free surface receives steady leakage flux and is not considered as a streamline. The solution provided by *Kirkham* is very complex because it is not obtained in an explicit form. Instead the free water surface must be calculated by some iteration process. *Kashef* (1965) eased the solution of *Kirkham* by applying some simplifying assumptions. His proposed method is based essentially on the concept of Rysenkampf's triangle of filtration. The free surface can be simply determined in one iterative cycle starting from the outer face of the percolated cylinder and moving inward toward the well. *Mahdaviani* (1967) used the work done by *Kirkham* and *Kashef* to establish a set of curves that relate the height of seepage surface of a gravity well to other geometric and physical characteristics of the surrounding aquifer.

Neuman and Witherspoon (1970) developed an iterative approach to steady seepage of groundwater with a free surface using the finite element method in a code called FREESURF. The code is applicable to heterogeneous porous media with complex geometric boundaries and arbitrary degrees of anisotropy. From around this point on the estimation of seepage surface elevations, the understanding of seepage flow near a well could be addressed using sophisticated computer methods. However it has not been possible to gain easy access to these methods until reasonably priced codes became available together with powerful but low priced computers on which to run them.

Many numerical solutions and techniques regarding the flow of water in variably saturated porous media have been published within the past three decades. *Cooley*

(1983) stated that, based on his experience, "*the need still exists for relatively simple, yet stable, techniques for solving the nonlinear matrix equation that results from numerical solution methods. The need also exists for better techniques for locating seepage faces inherent in many problems that involve a water table.*" Therefore, the literature review is extended to cover some of the most notable contributions to the numerical solution of the variably saturated flow equation described in Chapter 4. The reader is advised to look at the publications of *Clement et al.* which contain in depth a review of literature on the subject up to 1996, and which are followed closely for this part of literature review on variably saturated models.

Numerical solutions to the one-dimensional form of *Richard's* equation are generally the basis for solving variably saturated flow problems in two and three dimensions as well. However, most of the solutions are for the one-dimensional equation. The use of finite-difference approximations to solve for one-dimensional variably saturated vertical flow is extensive (e.g. *Day and Luthin*, 1956; *Whisler and Watson*, 1968; *Freeze*, 1969; *Brandt et al.*, 1971; *Haverkamp et al.*, 1977; *Dan and Mathis*, 1981; and *Haverkamp and Vauclin*, 1981). *Nielson et al.* (1986) give a comprehensive review of different types of numerical solutions to various forms of the one dimensional *Richard's* equation.

Rubin (1968) published his work on the finite-difference method for two-dimensional, variably saturated flow problems with seepage boundaries. Knowing that the position of the seepage face is initially unknown and constitutes a nonlinear boundary condition, an adjustment procedure is applied during the iterative solution. The purpose of the iterative solution is to maintained atmospheric pressure along the seepage face, negative pressures are maintained above the seepage face. A method following this approach was proposed later by *Neuman* (1973).

Narasimhan (1975) developed a variably saturated model which is reported to incorporate both seepage faces and consolidation. The model uses the integrated finite difference method. The *Narasimhan* model has an improved later version known as TRUST II, which is available in the public domain.

Cooley (1983) developed an alternative way of dealing with the seepage face problem. The difficulties in controlling the stability of nonlinear equation solvers, and determining the positions of seepage faces were dealt with in this new procedure for solving variably saturated flow problems. A subdomain finite-element method was used to solve the pressure-based form, *Richard's* equation, of the variably saturated flow equation. The method most likely offers no advantages over the more popular Galerkin formulation. It was picked simply because it evolved more naturally from the integrated finite difference approaches, and the use of a rectangular grid which is attractive because of its simplicity. The solution to the nonlinear set of equations was completed by an accelerated combination of Newton-Raphson iteration, successive approximation and *Stone's* (*Stone*, 1968) strongly implicit procedure (SIP). The iterative procedure does not use the flux concept in which nodes within the seepage face are assigned as constant heads depending on the flux direction calculated at each direction. It employs an algorithm that adjusts the location of the seepage face within the non-linear iteration process, along a specified series of nodes during each iteration. Oscillations in the solution are minimised by not allowing the seepage face height to change until the value of the head plus or minus the tolerance, indicates that this height must change. A variety of test problems was solved to demonstrate the reliability and efficiency of this approach for a wide range of problems. *Cooley* also pointed out that although the procedure used by *Neuman* based on the flux direction is necessary, it does not always ensure that the seepage face is located correctly. He asserted that he found that on occasions the seepage face was located too high using this procedure. *Neuman* (1985) later commented on *Cooley's* assertions suggesting that his method (*Neuman's*) had been wrongly interpreted.

Huyakorn et al. (1984, 1986a, and 1986b) published a sequence of three papers in which a number of finite-element models for solving two and three-dimensional water flow problems in variably saturated porous media were presented. The first paper (*Huyakorn et al.,* 1984) described an improved finite-element formulation for two-dimensional variably saturated flow problems. Included in the formulation was a technique that avoided numerical integration and was found to be computationally efficient. This paper also presents Picard and Newton-Raphson algorithms that are capable of treating field problems with severely nonlinear material properties. The formulation of an efficient and reliable mass balance computational scheme in finite-

element methods was subsequently presented in the second paper (*Huyakorn et al.*, 1986a).

In *Huyakorn et al.* (1986b) the previous two-dimensional work was extended and a finite-element model for simulating three-dimensional water flow in variably saturated porous media was developed. The Picard algorithm was enhanced and extended to accommodate highly nonlinear three-dimensional problems with seepage faces and atmospheric boundary conditions that are associated with infiltration and evaporation. The matrix solution was accomplished by a slice successive overrelaxation (SSOR) scheme. Six examples were presented to verify and demonstrate the capability of the proposed finite-element method.

Shamsai and Narasimhan (1991) used *Hall's* data to investigate the positions of the phreatic surface and seepage faces for two dimensional, steady state flow problems. The code TRUST, which can analyze transient groundwater flow in a variably saturated, deformable, heterogeneous and multidimensional system, was used to model *Hall's* data and various seepage face problems under radial and planar flow configurations. One of the conclusions from *Shamsai and Narasimhan's* study is that the flow rate estimates given by the *Dupuit* model may underestimate the flow through the system by 12 to 20%, as opposed to 1 to 2 % indicated by previous investigators (see *Hantush,* 1964 and Chapter 2). The reason for this big difference is thought by *Shamsai and Narasimhan* to be accounted for ignoring the flux through the seepage face. However *Bear* (1972, page 367) following *Hantush* clearly demonstrates that the fully-saturated model, which includes a seepage face, must agree with *Dupuit* model, as far as the flow rate is concerned. Therefore, and as shown by *Clement et al.* (1994), the deviation from *Dupuit-Forchheimer* flow is a function of soil properties and problem dimensions. Moreover, a simple sensitivity analysis for the effect of van Genuchten parameter, α_v, which is a measure that describes the mean pore size of a porous medium, showed that as the value of α_v increases the pore sizes increases; bigger pores relate to a smaller capillary fringe and therefore less extensive vadose zone available for the transmission of water. In the 10m×10m rectangular-flow domain example used in the *Clement et al.* (1996) study it is demonstrated that deviations are as high as 12% for α_v= 0.2 m^{-1} and as low as 1% for α_v = 4.0 m^{-1} which is predictable for the reason mentioned above. Furthermore, the small underestimation of the flow

rate by the *Dupuit* model is a result of ignoring flow through the unsaturated zone. (Clarke: discuss why *Shamsai and Narasimhan* differ by up to 20%) I added an explanation)

Clement et al. (1994a and b) described, from the authors point view, *Kirkland et al.* (1992) solution as the "*most successful and efficient example of a finite-difference solution to two-dimensional, variably saturated flow problems.*" The study developed a computationally simple and efficient finite-difference algorithm using a modified Picard iteration scheme presented by *Celia et al.* (1990) to handle the nonlinearity of the governing equation. *Clement et al.* (1994a) stated that "*most of the existing two dimensional finite-difference solutions to variably saturated flow problems have limitations.*" The limitations appear to be related to numerical instabilities and convergence difficulties.

Clement et al. (1996) published a comparison of modelling approaches for steady state unconfined aquifers. The comparison includes the *Dupuit-Forchheimer* analytical model, the fully saturated flow model, and the variably saturated flow model. The performances of the three models were compared for different soil properties, problem dimensions, and flow geometries. The study made two important observations; first, the numerical experiments performed clearly indicate that the deviation from *Dupuit* flow is a function of soil properties and problem dimensions. Second, the underestimation of the flow rate by the *Dupuit* model is a result of ignoring flow through the unsaturated zone.

The success of using such algorithm in simulating a variety of problems as described by they authors and presented in *Clement et al.* (1996) inspired this research since the code used in this study implements the same modified Picard algorithm presented by *Celia et al.* (1990). Furthermore, the examples used in *Clement et al.* studies are a valuable addition to the set benchmarks selected to verify the MODFLOW-SURFACT code that uses a pseudo-soil function and a drain approach to solve for seepage face. The accomplishment of such verification has allowed the research investigation to take place with the following objectives.

- A better understanding of the flow near wells pumping from unconfined aquifers for the purpose of groundwater control and landfill remediation

- Assess the validity of the application of the principle of superposition to the design of multiple well systems and to determine the fate of the seepage surface on a well in an array.

The research will also contribute to gaps in the understanding of flow near wells by two cases presented in Chapter 6 and 7:

A. The case of using numerical models to predicate maximum yield from individual well in groundwater control schemes which has received little attention in the past as stated in the CIRIA C515 report, page 158.

B. Examine the case involving the use of vertical wells as a means of leachate management and control of landfills where the assumption of negligible seepage face is generally not valid (*Rowe and Nadarajah,* 1996).

2.5 Summary

Because of the seepage face at the well and the occurrence of associated vertical-flow components in the vicinity of the well, the *Dupuit-Forchheimer* equation does not yield an accurate phreatic surface elevation near the well. However, at a radial distance of $1.5H$, the equation yields correct estimates of the phreatic surface. In addition, theoretical and experimental investigations have shown that the use of *Dupuit-Forchheimer* equation to calculate well yield gives values that are within 1 or 2 percent of the true values. These features will be used to provide benchmark data to verify the numerical modelling described in later chapters.

Babbitt and Caldwell (1948), *Boulton* (1951) and *Hansen* (1953) studied unconfined flow toward a well by means of physical models and developed different empirical relationships for the free surface near the well. Other steady-state analyses based on exact mathematical analysis and numerical techniques are presented by *Yang* (1949), *Boreli* (1955) and *Kirkham* (1964). The experimental observations of *Hall* (1955)

constitute some of the best available observational information on the relationships between free surface and seepage face in radial flow as stated by *Shamsai and Narashimhan* (1991). Although the reason for their conclusion was not discussed by *Shamsai and Narashimhan*, it is supported by the fact that *Hall's* experiment overcomes many of the troublesome features of earlier model tests and the close correlation of the results with theoretical analysis. Moreover, the intensive use of *Hall's* results for verification purposes in recent studies, *Clement et al.* (1996) and *Luther* (1998) makes it the main model database for verification in this research. The graphical work of *Zee et al.* (1957), Figure 2.8, brings together the observations of other investigations such as *Babbitt and Caldwell* (1948), *Boulton* (1951) and *Hansen* (1953), including the *Yang* (1949) study which *Hall* describes as a reliable analytical solution procedure for determining the flow pattern around a gravity well. Therefore, these have been chosen as a focus for this study and for the benchmarking of the code used. MODFLOW-SURFACT is the package that has been used here to continue the investigation of flow in the neighbourhood of a deep well. The following Chapter will introduce MODFLOW, and the development of its finite difference constitutive equations. It is evident from this literature review that there are few three-dimensional variably saturated models available, especially those that incorporate a solution that includes the seepage face boundary condition. For a comprehensive summary of a variety of numerical schemes used to solve variably saturated flow problems, refer to *Clement et al.* (1994a, 1994b, and 1996). Although the pseudo-soil function and seepage face modelling using drains (described in detail later in Chapter 4) is incorporated in MODFLOW-SURFACT, it was not previously used intensively for modelling the seepage face in a well or an array of wells pumping from unconfined aquifer.

In this research MODFLOW-SURFACT which uses the pseudo-soil function, has been used to study and investigate the influence of the seepage face on the performance capacity of deep wells in contexts that were not found in the previous studies found in the literature. These include the effect of anisotropic conditions and the effect of wells working as an array, which should contribute to the better design of groundwater control systems, Chapter 5. Moreover, an evaluation has also been made of the potential for groundwater remediation systems enhancement, as the result of exposing a

larger region of a contaminated unconfined aquifer to remediating flushing flows, due to the presence of a seepage face, Chapter 5.

The research also involve two case studies, one is the seepage face in fully drained wells which is very important in remediation systems when a pumping well is used to depress the water table in order to mobilize and recover light nonaqueous phase at or below water table (*Gefell et al.*, 1994), Chapter 6. The second case focuses on vertical wells in landfill where the assumption of negligible seepage face is generally not valid (*Rowe and Nadarajah,* 1996), Chapter 7. This involves the use of vertical wells as means of leachate management and control of landfills. It includes transient simulations that model dewatering of a landfill using a network of leachate abstraction wells taking into account the presence of a seepage face.

Chapter (3)

Numerical Modelling Using the Finite-Difference Method and MODFLOW

3.1 Introduction

Mathematical models that describe the phenomena of flow in porous media have been used since the late 1800's when a complete description of such flow was made in terms of a partial differential equation, linked with initial conditions and boundary conditions. In order to solve a given groundwater problem, this system of equations must be solved, for the particular data of that problem using analytical methods or numerical techniques. The reliability of predictions using a groundwater model depends on how well the model approximates to the field situation. Simplifying assumptions must always be made in order to build a model because the field situations are too complicated to be simulated exactly. Normally the simplifying assumptions that are necessary in order to solve a mathematical model analytically are virtually unacceptable; except for relatively simple problems that are homogeneous and isotropic. In order to deal with more practical situations, it is usually necessary to solve the mathematical model approximately using numerical techniques. Since the 1960s, numerical models have received a large impulse, to such an extent that a variety of powerful general techniques have become available to the scientific and professional community. Since high-speed digital computers have become widely available, the solution of groundwater problems by numerical models is now within the reach of most interested scientists and engineers.

The following five numerical methods are available for the analysis of groundwater systems: finite differences (FD), finite elements (FE), integrated finite differences (IFD), the boundary integral equation method, and analytic elements. The latter two methods are relatively new techniques and are not yet widely used. Integrated finite difference (IFD) techniques are closely related to the finite element method. *Narasimhan and Witherspoon* (1978) reported applications of IFD techniques for the TRUST model. Finite differences and finite elements methods are more widely used, to solve flow problems. The focus of this research centered on the finite-difference method, which is the method used in MODLFOW.

This chapter, together with Appendices A and B, presents the basic equations of groundwater motion for three-dimensional flow and the integrated equation for the flow in confined and phreatic aquifers. An introduction is also given to the US Geological Survey Modular Finite-Difference Groundwater Flow Model-MODFLOW and the development of its finite-difference equation from these basic equations. The content of this chapter is primarily descriptive, whereas the background analytical details have been reserved for the Appendices.

3.2 General Governing Equation of Groundwater Flow

Darcy's law alone is not enough to represent the groundwater flow, unless the potential head distribution within the problem domain is measured. However, the aim of groundwater modelling is to predict the head distribution under different input conditions. The head distribution, if known previously, then serves as the initial conditions in a transient groundwater study.

The differential equations applicable to the flow of groundwater are expressions of the budgetary requirement that flow volumes must be conserved in a mathematical form. The general flow equation for saturated groundwater flow is derived in many excellent textbooks such as *Bear* (1972) and *McWhorter* and *Sunada* (1991). In most analyses, the general flow equation is formulated by using the law of conservation of mass over a representative elementary volume (REV) situated inside the flow domain of an aquifer. The net inflow into the volume must equal the rate at which water is accumulating

within the volume under investigation. The general form of the governing equation, which is developed in Appendix A from first principles, is

$$\frac{\partial}{\partial x}\left(K_x \frac{\partial h}{\partial x}\right)+\frac{\partial}{\partial y}\left(K_y \frac{\partial h}{\partial y}\right)+\frac{\partial}{\partial z}\left(K_z \frac{\partial h}{\partial z}\right)-w=S_s \frac{\partial h}{\partial t} \qquad (3.1)$$

or

$$\nabla(K\nabla h)-w=S_s \frac{\partial h}{\partial t} \qquad (3.2)$$

where K_x, K_y, and K_z are values of hydraulic conductivity along the x, y, and z coordinate axes; h is the head; w is the flux term that represent sinks and/or sources of water; S_s is the specific storage; x, y, and z are coordinate directions; and t is time. Equation 3.2, is a linear partial differential equation that relates time and space distributions of piezometric head, h, in non-homogenous, anisotropic aquifers.

3.3 Initial and Boundary Conditions

Conventional mathematical models of groundwater flow are based on the solution of the previously discussed governing equation for specified boundary conditions and initial conditions. The latter describes the distribution of the values of the considered state variable at some initial time, usually taken as $t=0$, at all points within the specified domain, for example

$$h(x,y,z,t)=h(x,y,z,0)=f(x,y,z) \qquad \text{in the domain} \qquad (3.3)$$

where $f(x,y,z)$ is a known function.

Boundary conditions are mathematical statements specifying the dependent variable (head) or the derivative of the dependent variable (flux) at the problem domain boundaries. In other words, it expresses the way that the specified domain interacts with its environment. Different boundary conditions give different solutions, which

mean that the correct representation of boundary conditions is a critical step in model design. Although boundary conditions are expressed in a mathematical terms, their content clearly expresses a physical reality as viewed by the modeller.

Hydrogeologic boundaries are represented by three types of mathematical conditions presented in the following table, Table 3.1.

Table 3.1 Boundary conditions

Type no.	General name	Formal name	Remark
1	Specified head	Dirichlet	Head is given
2	Specified flux	Neumann	Derivative of head (flux) across the boundary is given. A no-flow boundary condition is set by specifying flux to be zero.
3	Head-dependent flow or mixed boundary	Cauchy	Flux across the boundary is calculated as a function of the calculated boundary head value. It is sometimes called a mixed boundary condition because it relates boundary heads to boundary flows.

There are two types of boundaries that require special attention; the phreatic surface which is also known as the water table, and the seepage face. These together form the free surface which has been discussed in section 2.3, where it was defined as the surface on which the pressure is atmospheric (conveniently taken as $p=0$). We therefore have from $h\,(x, y, z, t)= z + p(x,y,z)/\gamma$ that

$$h = h(x, y, z, t) = z \quad \text{at the phreatic surface and seepage face} \qquad (3.4)$$

Under steady state conditions the phreatic surface becomes a flow line and the flux across this part of the free-surface boundary is zero. This is not the case for the seepage surface.

3.4 The US Geological Survey Modular Finite-Difference Groundwater Flow Model- MODFLOW

MODFLOW is a three-dimensional, cell-centered, finite difference, saturated flow model developed by *McDonald and Harbaugh* (1988) of the United States Geological Survey. MODFLOW can perform both steady and transient analyses that simulate

confined, unconfined, or a combination of confined and unconfined aquifer types. Flow connected with external "stresses", such as wells, areal recharge, evapotranspiration, drains, and streams can also be simulated. The finite-difference equations are solved either using the Strongly Implicit Procedure (SIP) method or the Slice-Successive Overrelaxation (SSOR) method. Beside the easy access to the MODFLOW, the popularity of this code is attributed to four factors. First, the code proved to be a powerful and robust tool for early users who applied the code to a variety of practical problems. Second, the user's guide is very useful and extremely detailed, and provides a clear description of how the various code options are used. Third, the US Geological Survey has been very supportive to the code development and recently more specialized versions of the code have been marketed by several private companies. Finally, the success of the original code has created an extensive array of training courses and a large number of related calculation modules.

3.4.1 Derivation of the Finite-Difference Equation

The three-dimensional movement of groundwater of constant density through porous media maybe described by the partial-differential equations 3.1 or 3.2,

$$\frac{\partial}{\partial x}\left(K_x \frac{\partial h}{\partial x}\right)+\frac{\partial}{\partial y}\left(K_y \frac{\partial h}{\partial y}\right)+\frac{\partial}{\partial z}\left(K_z \frac{\partial h}{\partial z}\right)-w=S_s \frac{\partial h}{\partial t} \qquad (3.5)$$

In general, S_s, K_x, K_y, and K_z may be functions of space ($S_s = S_s(x, y, z)$, $K_x = K_x(x, y, z)$, etc.) and w may be a function of space and time $w = w(x, y, z, t)$. Equation 3.5 describes groundwater flow under non-equilibrium conditions in a non-homogenous and anisotropic medium.

Equation 3.5 along with the specification of flow and/or head conditions at the boundaries of a flow system and the specification of initial head conditions, establishes a mathematical representation of the groundwater flow system. The "solution" of a groundwater flow problem in a specified domain, with specified storage and hydraulic conductivity coefficients, means the determination of the spatial and temporal distributions of the head values that satisfy equation 3.5 at all points within the domain, as well as the specified initial and boundary conditions.

Except for very simple systems, the analytical solution of equation 3.5 is rarely possible and therefore numerical methods are generally adopted. These are more versatile and are easier to use than complex analytical solutions. One such numerical approach is the finite-difference method. In this method partial derivatives are approximated by algebraic expressions involving the values of the dependent variable at a limited number of selected points. The approximation, which results in a finite number of algebraic equations written in terms of the values of the dependent variable at the selected points, replaces the continuous system describing the problem, equation 3.5. This introduces a set of linear algebraic difference equations and their solution yields values of the head at the selected points and times. The solution may involve a large number of arithmetic operations that used to be performed manually, or by using mechanical devices. However, with the advance of technology, computer programs are now available to both set up and accomplish the solution of the system of algebraic equations. MODFLOW is described in more detail in Appendix B and the reader is also advised to refer to the reference *McDonald and Harbaugh* (1988) or visit the USGS web site at http://www.usgs.org for more information.

3.4.2 MODFLOW and Seepage Face

The phreatic surface is the most difficult boundary to define. This is because it is a feature we require as a model outcome, which means that the location of the phreatic surface boundary condition is unknown before the problem, is solved. *Anderson and Woessner* (1992) discuss the two ways to deal with the phreatic surface boundary problem:

1. Use the *Dupuit* assumptions to model flow in the top layer of the model, which is the approach used in MODFLOW. Some errors are introduced in MODFLOW simulations since it is a requirement to specify fixed values for the vertical transmission or leakage term known as VCONT at the beginning of the simulation.

2. Use a variably saturated model to solve the problem, which means that the unsaturated/saturated zones are simulated as a continuous flow field, and that the phreatic surface is determined as the surface of zero pressure head.

The seepage face, which is always present when the phreatic surface ends at the downstream external boundary of the flow domain or when it intersects a pumping well casing in an unconfined aquifer, requires the same mathematical condition as that required for phreatic surface ($p=0$). The boundary conditions along the seepage face is $h= z$. The seepage face is neglected in most modelling applications because it is small when compared to the scale of the problem. Nevertheless, representation of the seepage face can be important for other groundwater problems and some engineering applications as will be pointed out throughout this study.

The attempt to simulate seepage face is described in the Drain Package in MODFLOW. The drain ceases to flow when the water table falls below the drain. Hence, drain nodes can be specified for the general area where seepage is likely to occur; the drain nodes will be activated only if the water table rises up to the level of the drain. In this way, locations of seeps are distinguished during the simulation as the drain nodes become activated. Beside the fact that this method of simulating a seepage face can be very tedious when each grid cell has a different elevation, it is not rigorous in that the standard MODFLOW model uses *Dupuit* assumptions, (*Anderson and Woessner*, 1992). Another complication in the original MODFLOW is the drying cell problem. When the head in a cell falls below the bottom of the cell elevation, the cell becomes dry and is assigned with zero hydraulic conductivity and creates impermeable barriers in the model. By default, nodes that become isolated because the surrounding cells "go dry" are assigned a head of 999 so as to identify them in the output. This condition may occur during the iteration process and may not have physical significance. Once this occurs, the situation will never change unless the re-wetting option is employed in the BCF package, which is the case in the newer versions of MODFLOW. Figure 3.1 shows a typical head elevation output for the different model layers from MODFLOW. The result is unsatisfactory with dry cells replaced with high elevation values.

Re-wetting packages have been introduced by many authors such as *McDonald et al.* (1991) and *Goode* and *Appel* (1992) to reconvert no-flow cells into variable head cells to allow resaturation of the cells using transmissivity averaging schemes. These packages are not a solution for model input problems because it forces the model to converge by using unrealistic solver parameters. *Arnold* (1988) suggested that for a

multi-layer model, making a few cells adjacent to the well inactive in the upper few layers of the model can solve the problem, which means that prior knowledge of the position of phreatic surface is required. The re-wetting packages will be discussed more in Chapter 4.

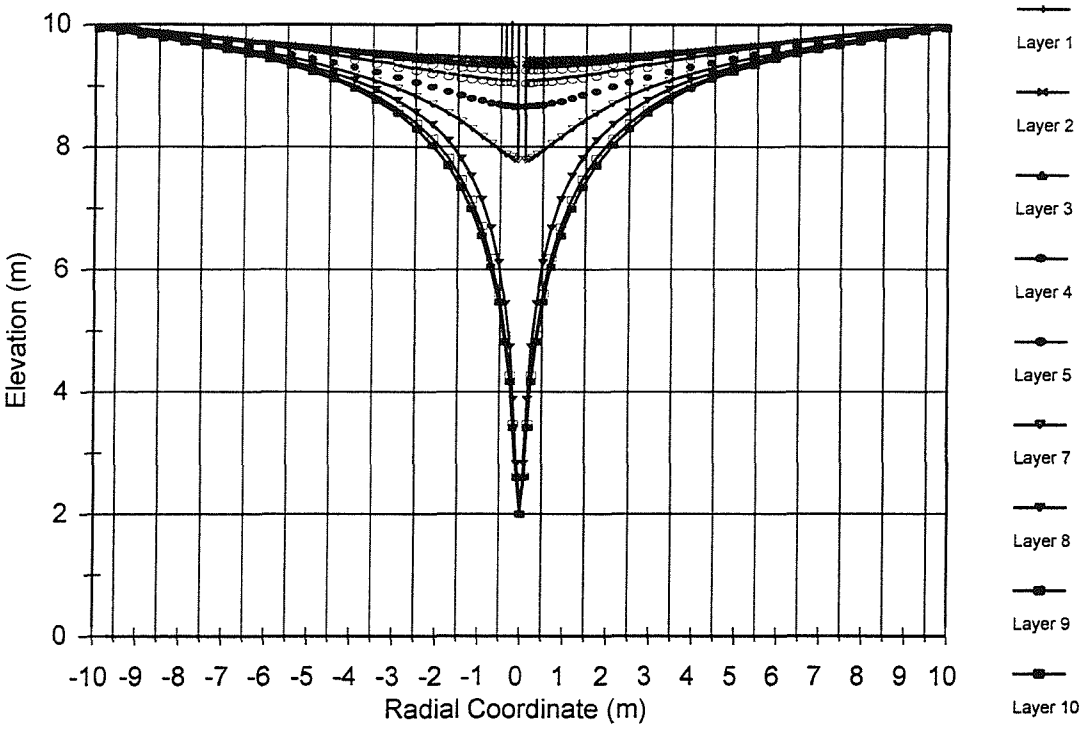

Figure 3.1 Typical output from MODFLOW showing unsatisfactory solution.

3.4.3 MODFLOW Using Pre- and Post-Processors (PPP)

The explosion in the early 1990's of Personal Computer (PC) capabilities and the availability of graphical tools resulted in the development of sophisticated input and output data managers, which are commonly referred to as pre- and post-processors (PPP). *Zheng and Bennert* (1995) define pre-processing as assembling and preparing input data for a numerical model and post-processing as the process of reviewing and presenting modelling results. Recent pre- and post-processors provide modelers with WINDOWS based or WINDOWS-like interfaces that accelerate and simplify data input, translating this information into files that can be used by the numerical code, and then translate the model output into graphical representations.

An interesting recent study, based on experienced teachers, that was carried out by *Woessner and Anderson* (1998) using a survey questionnaire, showed a general agreement that PPP eased the teaching and use of MODFLOW. Moreover, most experimental MODFLOW users also expressed approval, with reservations, that PPP is a useful tool for new users of MODFLOW provided they have a complete understanding of the code structure and its operation, and how the hydrogeological parameters and conditions are treated by MODFLOW. Although the use of PPP as a tool for studying MODLFOW was thought to have some disadvantages, it is believed that its use saves time and provides excellent visualisation. In this research, the use of PPP proved to be effective for data input and output analysis, knowing that the user is experienced with the use of the original MODFLOW and well aware of the solving processes.

Groundwater Vistas (GV) is the package that is used throughout this study as the PPP for running MODFLOW. It is a groundwater-modelling environment for Microsoft Windows that couples a powerful model design system with comprehensive graphical analysis tools. GV is designed to be a model-independent system, which means a wide range of groundwater models can be used. This is an advantage for this study since this study will move on to using a modified version of MODFLOW which is supported by GV. Readers may refer to the User's Manual for more details (*McDonald and Harbaugh*, 1988 and *GV Manual*).

3.5 Numerical Errors in Finite-Difference Models

The finite-difference model discretizes the continuua of space and time into discrete intervals. All values such as hydraulic conductivity are represented as average values over these intervals. Discretization and averaging together with approximate solution procedures cause numerical errors to occur. Understanding the errors associated with the use of the finite-difference method are essential. A review of error types and solutions is the focus of the following section

3.5.1 Type of Numerical Errors

Modelling is subject to many types of errors; errors in model conceptualization, errors in data collection and input, errors in calibration, and errors in presentation of model results. *Spitz and Moreno* (1996) discussed numerical errors for both flow and transport models, and since we are focusing on flow modelling, the discussion will only cover the errors associated with flow models. Numerical errors as pointed out by *Spitz and Moreno* (1996) are:

- *Truncation error. Truncation errors are created when expressing a complicated function such as the potentiometric head distribution as a series of piecewise simpler functions. The error is embedded in numerical theory.*
- *Roundoff error. Roundoff error is always present and is due to the limitation of the computer to represent digits. Roundoff errors may invoke numerical errors that increase in time. Cumulative roundoff errors will eventually cause numerical instability. Most models apply double precision arithmetic to improve accuracy.*
- *Instability. The stability or, respectively, instability of a numerical model is of considerable practical importance. Instability is the result of a feedback process in which errors grow as each succeeding step is taken to obtain the solution. The growth of errors is often exponential and oscillatory. The numerical solution fails to converge to the exact one. Stability is a necessary condition for convergence. Convergence implies stability. In almost all situations, an unstable solution is easy to distinguish from a stable one. The model user must understand however that stability and convergence does not automatically imply convergence to the correct solution. Hence, consistency must be tested before an approximate solution is accepted.*
- *Iteration residual error. The iteration residual error is involved in iterative solution procedures. When iteration is involved, the model user specifies a convergence criterion such as a specified error tolerance. Iteration is stopped if the numerical solution is within the specified error tolerance. The choice of the convergence criterion determines the size of the iteration residual error.*

The following observations summarise other typical problems encountered in model application:

- Making the model excessively detailed, and forgetting that models are always a simplification of reality.
- Poor conceptualization such as coarse space discretization in areas where large responses are expected, in areas where aquifer properties change abruptly, or in areas where boundary conditions change rapidly.
- Input errors due to typing or over optimistic faith in pre-processors, where the input differs sometimes from that which the modeler sees on the computer.
- Not understanding boundary conditions.

3.5.2 Controlling Numerical Errors

Spitz and Moreno (1996) suggests a list of practical controls in order to reduce numerical errors:

- *Orientating the discretization grid along the main flow direction.*
- *Ensuring gradual variation in time and space discretization.*
- *Keeping prescribed potentiometric surface numbers as small as possible to reduce roundoff errors. This can be done by subtracting the datum. Decreasing real numbers in numerical operations results in reducing loss of significant digits.*
- *Keeping the cell aspect ratio within at least one order of magnitude.*
- *Decreasing the time step to improve stability. Unstable numerical effects depend on the time step. If two solutions obtained with two significantly different and reasonably small time steps are essentially the same, then the numerical solution is probably stable.*
- *Concentrating fine discretization on areas with large changes in aquifer properties or expected aquifer responses.*
- *Choosing the right boundary condition that best describes the real situation.*

3.6 Summary

The equation of continuity combined with *Darcy's* law produces the general form of the governing equation of groundwater flow in three dimensions. The derivation of the numerical form of this governing equation for the USGS MODFLOW code has been introduced, in this chapter and appendices A and B along with the packages that make

up the code. Investigation of the use of MODFLOW in determining the seepage surface confirms that the common problem of the finite-difference cells drying up is an obstacle. The re-wetting package in MODFLOW is not a solution to this problem because it forces the model to converge by using unrealistic solver parameters as described in detail in Chapter 4. The conclusion is that the standard version of MODFLOW does not adequately accommodate and represent the water table surface in unconfined aquifers. Therefore further investigation is needed in order to find an effective code to carry out the investigation. The next chapter will examine the variably saturated code, MODFLOW-SURFACT as an alternative code. Introduction to the literature supporting the model and verification of the code will be the focus of the following chapter. The verification procedure is an important step which ensures the code reliability so it can be used to achieve research objectives. This procedure requires benchmark data and this has been obtained by developing an algebraic framework to contain the historical seepage face data reviewed in Chapter 2.

Chapter (4)

Verification of the Variably-Saturated Code MODFLOW-SURFACT

4.1 Introduction

This chapter presents a brief background to *Darcy's* law for variably saturated flow. As discussed in Chapter 3, the USGS MODFLOW and MODFLOW-96 encounter difficulties or conceptual restrictions in the simulation of unconfined systems and in the handling of wells. MODFLOW-SURFACT contains the functionality to model seepage surfaces and has been introduced by *HydroGeoLogic*, Inc. as an alternative to overcome these difficulties. In this variably-saturated groundwater code, MODFLOW-SURFACT, the unsaturated/saturated zones are simulated as a continuous flow field, and the phreatic surface is determined as the surface of zero pressure head. In this Chapter, the performance of MODFLOW-SURFACT is verified against previously published experimental data and against the analytical model reviewed in Chapter 2. Representation of individual wells in groundwater modelling is also reviewed and the results are used throughout the remainder of the study to improve model predictions. The purpose of doing this work has been to underwrite the later use of MODFLOW-SURFACT in studies investigating more complex systems, and is an original contribution to the subject area.

4.2 Darcy's Law for Variably-Saturated Flow

The governing equation for water flow in variably saturated soils can be obtained by combining a special form *Darcy's* law and the continuity equation written for the water phase. *Richards* (1931) extended *Darcy's* law to describe flow in unsaturated soils. Water is retained under tension due to capillary forces and the values of pore pressure heads become less than atmospheric. The relative permeability of an unsaturated medium is a function of the volumetric water content, θ, which in turn is a function of the pressure head, ψ, which in this case is the capillary pressure head denoted as $h_c = \frac{P_c}{\rho g}$. The relationship between the volumetric water content of the soil and the pressure is determined experimentally for a given soil. The results are graphed as a soil-water retention curve (function), Figure 4.1, which characterizes the ability of the porous medium to retain water when it is being displaced (e.g., during drainage or drying). For a given soil, the water retention function follows two distinct curves during a drying and wetting cycle, called drying and wetting scanning curves. Therefore, the relationship between capillary pressure and saturation, S_w, (expressed by the retention curve) also depends on the wetting-drying history of the soil sample under consideration, the phenomenon known as hysteresis. The combination of the soil-water retention function and the relative permeability function defines unsaturated zone hydraulics properties (*Bear*, 1987, *Chapter 5*). *Richards* (1931) proposed that the water content and the hydraulic conductivity of unsaturated soils might be expressed as functions of the capillary pressure head, and modified *Darcy's* law to give the following pressure-based expression

$$q = -K\, k_{rw}(\theta)\, \nabla\left[\frac{P}{\gamma} + z\right] = -K\, k_{rw}(\theta)\, \nabla[\psi + z] \qquad (4.1)$$

where $k_{rw}(\theta)$, is the relative permeability function; θ, is the volumetric water content; and ψ is the pressure head. Volumetric water content and saturation are related to each other by $\theta = nS_w$, where n is the porosity.

4.3 HydroGeoLogic, Inc. Version of MODFLOW

MODFLOW-SURFACT is a new flow and transport model that is based on the USGS MODFLOW code. MODFLOW, however, has certain limitations in simulating complex field problems and additional computational modules have recently been incorporated to enhance the simulation capabilities and robustness. The new flow packages which complement/supplement the original MODFLOW are referred to as SURF packages, whereas the ACT modules provide the capability to perform single-species and multi-component transport analyses. Three of the main features added are (1) the ability to readily accommodate conditions of desaturation /resaturation of aquifer systems, (2) the ability to simulate prescribed ponding, recharge, and seepage-face boundary conditions, and (3) the ability to perform axi-symmetric analysis. The enhanced model is called MODFLOW-SURFACT, which runs under DOS, but can be executed from the data pre-processing and post-processing interface Groundwater Vistas (GV). The conceptual model can be created with the GV interface and then run using MODFLOW-SURFACT (*HydroGeoLogic,* Inc. MODFLOW version) rather than MODFLOW (USGS version) in order to take advantage of the new features to investigate the seepage face. Two of the added packages, which are significant in solving seepage face problems, are described next in order to allow the reader understand the solution concept. The next three sections (4.3.1, 4.3.2, and 4.3.3) follow closely the manual (*HydroGeoLogic,* Inc., 1996) and (*Pandy and Huyakorn*, 2000), which was provided by the authors, to review the important additions to the original MODFLOW that enabled this study to take place.

Table 4.1 A summary of the added packages in MODFLOW-SURFACT Ver. 1.2 and used in this study (*HydroGeoLogic*, Inc.).

Package Name	Package Description
Block-Centered Flow (BCF4)	Incorporates the new variably saturated flow formulation and includes axi-symmetric simulation option.
Recharge Seepage Face Boundary (RSF4)	Accommodates unconfined recharge option and allows simulation of seepage face boundary conditions.

4.3.1 The Block-Centered Flow (BCF) Package

The MODFLOW code uses a block-centered finite-difference approach to solve the groundwater flow equation. The flow domain is discretized into rows, columns, and layers to represent a rectangular block of porous media, which is referred to as a cell. A node, which is assumed to be located at the center of the finite-difference grid represents either a no-flow, variable-head, or constant-head cell, and any hydraulic property associated with a cell is specified with respect to the corresponding node.

The original BCF package in the MODFLOW code (*McDonald and Harbaugh*, 1988), which is also known as BCF1, converts a desaturated variable-head cell into a no-flow cell. This has the effect of eliminating parts of the flow domain from the model simulation. "*The inability of MODFLOW to return these cells to variable-head cells in case of any recovery of potentiometric levels may cause the code to show misleading or erroneous simulation results*". An option that allows cells to convert from no-flow to variable-head was made by *McDonald et al.* (1991). The rewetting scheme was implemented in the BCF2 package. Based on head in surrounding cells, the new rewetting option attempts to wet cells that are dry. Unsuccessfully, the BCF2 rewetting option is not a solution for all model input and is prone to convergence and stability problems during rewetting or when withdrawals dry up the respective cells. This is because the added procedure that used to reactivate dry cells can seriously disturb flow mass conservation principles, see *McDonald et al.* (1991) for the BCF2 limitations. Moreover, the harmonic transmissivity-averaging scheme that is used in the code becomes physically inappropriate when the head-dependent transmissivity at a neighboring cell reduces to zero.

Goode and Appel (1992) documented problems associated with the BCF2 rewetting package. Furthermore, they added the BCF3 package to MODFLOW, which provides an alternative procedure for averaging transmissivites. *HydroGeoLogic*, Inc., then developed a new approach that satisfies flow continuity requirements of the whole domain and allows free movement of the water table in unconfined layers without any forced conversion of cells to no-flow cells. The package uses a three-dimensional variably saturated flow formulation with pseudo-soil water retention functions automatically generated to reduce the unsaturated flow problem to one seeking the

water table level, that is the elevation where pressure head is zero or atmospheric. The design was aimed at providing an accurate representation of the water table and at capturing the delayed response of an unconfined system to pumping and recharge. This is done without changing data requirements for the simulation since the pseudo-soil relations are used instead of the real soils, Figure 4.1. Using the finite-difference method, the variably saturated formulation with pseudo-soil functions is programmed into the existing BCF3 package for MODFLOW and the new version in MODFLOW-SURFACT is referred to as the BCF4 package. The interblock conductance in the new package is calculated as a product of the weighted harmonic mean of the block hydraulic conductivities, relative permeability, and mean flow area. The original MODFLOW BCF1 and BCF2 packages use the harmonic mean of the effective transmissivites of adjacent blocks to calculate the interblock transmissivity. For unconfined systems, the effective transmissivity of a block is computed as the effective hydraulic conductivity multiplied by the saturated block thickness.

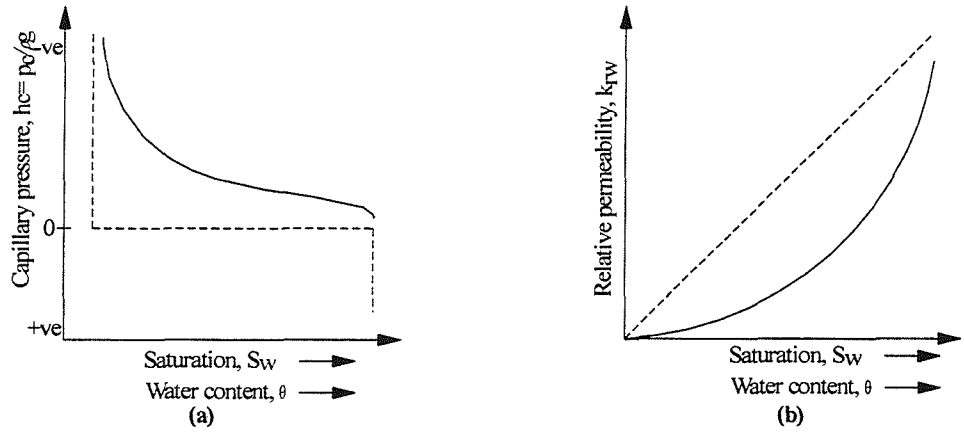

Figure 4.1 (a) A typical moisture content curve in soil during drainage and **(b)** A typical relative permeability curve, solid line represents real-soil and dashed line represents the pseudo soil. (Modified after *Panday and Huyakorn*, 2000.)

As shown in the MODFLOW-SURFACT manual, harmonic averaging of interblock transmissivites can cause misrepresentations in an aquifer systems, as explained by the extreme example represented in Figure 4.2.

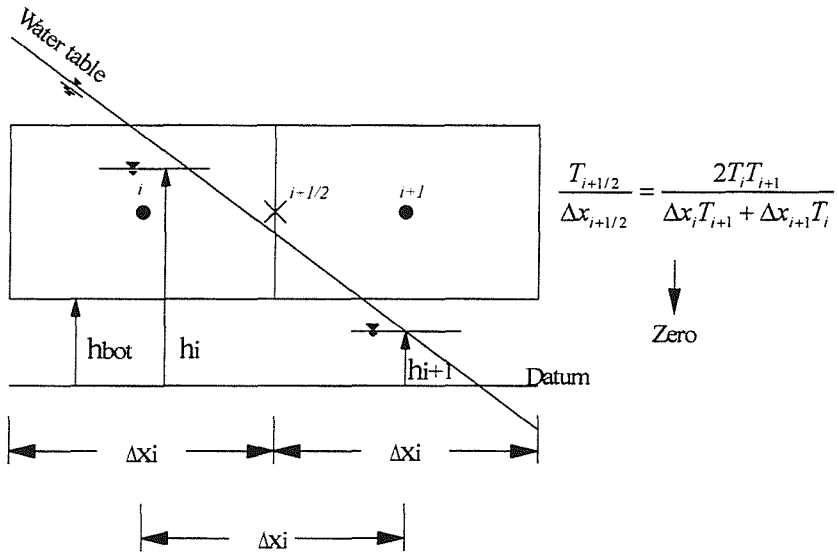

Figure 4.2 A case of adjacent grid blocks where harmonic averaging of head-dependent transmissivites is inadequate. (After *HydroGeoLogic, Inc.*, 1996.)

Consider i and $i+1$ to be adjacent grid blocks in an unconfined aquifer being flooded from left. The situation at a given instant is such that grid block i has an average water-table elevation of h_i which is above the bottom of the layer, and block $i+1$ has an average water-table elevation of h_{i+1}, below the bottom of the layer. The transmissivity of grid-block i is some positive value since h_i is above the bottom, and zero for grid block $i+1$ since its saturated thickness is zero.. The harmonic mean transmissivity is therefore computed as zero, and grid-block $i+1$ never saturates, contrary to what is physically expected. A more suitable and physically consistent procedure is to use the harmonic mean of the saturated hydraulic conductivities (or fully saturated transmissivites), with midpoint (or upstream) weighting on the relative permeabilities. The relative permeabilities are then related to the saturated grid-block thickness by the pseudo-soil functions for variably saturated scheme implementation, Figure 4.2. *Romeu* and *Noetinger* (1995) noted that the harmonic mean of block conductivities leads to an underestimation of the equivalent conductivity, and refined grids maybe used to overcome this problem. However, comparison examples between the use of the original BCF package included in the MODFLOW-SURFACT manual shows that harmonic averaging of head-dependent transmissivites leads to a further underestimation of the aquifer transmissivites property when compared with the use of BCF4. Moreover, this problem may not be overcome by grid refinement as suggested by *Romeu* and *Noetinger*. (*HydroGeoLogic,* Inc., 1996)

In summary, there are two main advantages of the new package BCF4 that is based on pseudo-soil function and used in MODFLOW-SURFACT. First, a new approach to the unconfined flow problem that treats desaturation and resaturation as an integral part of the governing equation and does not require soil water retention data. Second, the use of harmonic averaging of saturated hydraulic conductivities is more appropriate than harmonic averaging of effective (head-dependent) transmissivites. The MODFLOW-SURFACT version used throughout this research contains the BCF4 package and therefore uses the pseudo soil function shown in Figure 4.1, which produces very good results when compared with the results from more rigorous model that uses *Richard's* equation for the unsaturated zone as will be shown in section 5.2. The latest version of MODFLOW-SURFACT, which was released during the last stage of this research, contains a new BCF package that is extended for rigorous unsaturated zone water flow modeling using *Richard's* equation with options for modelling relative permeability functions of the form shown by the dotted-line curves in Figure 4.1and based *on van Genuchten* (1980) and/or *Brooks-Corey* (1966) models.

4.3.2 Formulation of the Unconfined Flow Equation using a Variably-Saturated Flow

The three-dimensional formulation for the movement of water in a variably saturated system used by MODFLOW-SURFACT is expressed by using the *Huyakorn et al.* (1986) solution.

$$\frac{\partial}{\partial x}\left(K_x k_{rw}\frac{\partial h}{\partial x}\right)+\frac{\partial}{\partial y}\left(K_y k_{rw}\frac{\partial h}{\partial y}\right)+\frac{\partial}{\partial z}\left(K_z k_{rw}\frac{\partial h}{\partial z}\right)-w=n\frac{\partial S_w}{\partial t}+S_w S_s\frac{\partial h}{\partial t} \qquad (4.2)$$

where x, y, and z are Cartesian coordinates (L); K_x, K_y, and K_z are the principle components of hydraulic conductivity along the x, y, and z coordinate axes, respectively (LT^{-1}); k_{rw} is the relative permeability, which is a function of water saturation; h is the hydraulic head (L); w is a volumetric flux per unit volume and represents sources and/or sinks of water (T^{-1}); n is the drainable porosity taken to be equal to the specific yield, S_y; S_w is the degree of saturation of water, which is a function of the pressure head; S_s is the specific storage of the porous medium (L^{-1}); and t is time (T). Pseudo-soil relations are used to define the functional relationships; S_w =

S_w (ψ) and $k_{rw} = k_{rw}$ (S_w), where ψ is the pressure head defined as $\psi = h - z$, with z being positive in the vertically upward direction.

Equation 4.2 is reduced to the basic groundwater flow equation, equation 4.3, used in the development of MODFLOW for a fully-saturated medium (i.e., K_{rw} =1.0 and S_w =1.0). (*McDonald and Harbaugh,* 1988)

$$\frac{\partial}{\partial x}\left(K_x \frac{\partial h}{\partial x}\right)+\frac{\partial}{\partial y}\left(K_y \frac{\partial h}{\partial y}\right)+\frac{\partial}{\partial z}\left(K_z \frac{\partial h}{\partial z}\right)-w = S_s \frac{\partial h}{\partial t} \tag{4.3}$$

Equation 4.3 contains interblock hydraulic conductivities that are obtained as a weighted harmonic mean of nodal values of the participating cells. The modeling option for the BCF4 package is that the user specifies horizontal saturated hydraulic conductivities (K_x, K_z and K_y) and the top and bottom elevations of the cell. Interblock effective hydraulic conductivities are then determined by multiplying the interblock saturated hydraulic conductivities by the relative permeability. A Picard approximation (*Celia et al.*, 1990) is used to linearise the resulting nonlinearity of the variably saturated flow equation. Finally, as in previous BCF packages, the user inputs the dimensionless primary storage coefficient, which when divided by the block thickness yields the specific storage, S_s, used in equation 4.2.

The BCF4 package also provides the option to perform an axi-symmetric analysis using an axially symmetric cylindrical coordinate system. This option saves time by avoiding the use of fully three-dimensional Cartesian (x, y, z) coordinates. The BCF4 package uses the following form of the saturated groundwater flow equation

$$\frac{1}{r}\frac{\partial}{\partial r}\left(rk_r \frac{\partial h}{\partial r}\right)+\frac{\partial}{\partial z}\left(k_z \frac{\partial h}{\partial z}\right) = S_s \frac{\partial h}{\partial t} \tag{4.4}$$

where r and z are the radial and vertical coordinates of the axi-symmetric cylindrical coordinate system, and K_r and K_z are the principle hydraulic conductivities along the radial and vertical axes, respectively. (*HydroGeoLogic*, Inc., 1996)

4.3.3 The Recharge-Seepage Face Boundary Condition (RSF4) Package

The new BCF package with its variable saturation capabilities enabled another new package to be added to the *HydroGeoLogic*, Inc. version of MODFLOW. This overcomes certain limitations in using the Recharge package (RCH1) in the original MODFLOW. In unconfined aquifer situations, the capacity of the aquifer to absorb the supplied recharge may reduce to the extent that excess water is shed as surface runoff. The RCH1 package is incapable of handling such situations and provides the aquifer with continuous recharge with heads continually rising above the ground surface. The RSF4 package of MODFLOW-SURFACT is designed to eliminate this unrealistic physical condition by allowing recharge into groundwater system only if the water table is below a user prescribed pool (ponding) elevation. When the pool elevation matches the groundwater surface elevation there is no ponding. While the water table elevation of a cell remains below the pool elevation, the entire recharge rate is applied to the boundary. During a simulation, if the water table level exceeds the pool level, the latter is maintained and the recharge to the system is reduced to the maximum recharge rate acceptable by the system under pool elevation conditions. On the other hand, if the water table later falls below the prescribed pool elevation, the full recharge rate is again applied to the system. Again, a modified Picard method (*Celia et al.*, 1990) is used for adding the extra volume of ponded water to the storage term when the pool elevation is above the land surface. (*HydroGeoLogic*, Inc., 1996)

"*In addition to modelling surface recharge-drainage conditions, the RSF4 package has the advantage that it may be used to simulate a seepage face boundary condition by assigning the elevation of a seepage face boundary node. Hence, along the boundary, no recharge is provided until the water table builds up to the seepage face elevation. If the water table reaches the seepage face elevation, the aquifer drains to maintain seepage face elevation, i.e. the atmospheric pressure conditions. Finally, if the water table drops below the seepage face elevation conditions at anytime during the simulation, a zero flux boundary condition is applied at the seepage face boundary.*" (*HydroGeoLogic*, Inc., 1996) This ability of the code to model the seepage face condition is this key development in the MODFLOW-SURFACT code that has enabled this investigation to take place.

Figure 4.3 shows a simple example of phreatic surface prediction using MODFLOW-SURFACT. The figure shows the correct position of the phreatic surface and the cells that otherwise would be dry (inactive) when using the original MODFLOW. Therefore, the standard version of MODFLOW does not adequately allow for the water table surface in unconfined aquifers, and hence the enhanced MODFLOW version developed by *HydroGeoLogic*, Inc. is considered as an alternative.

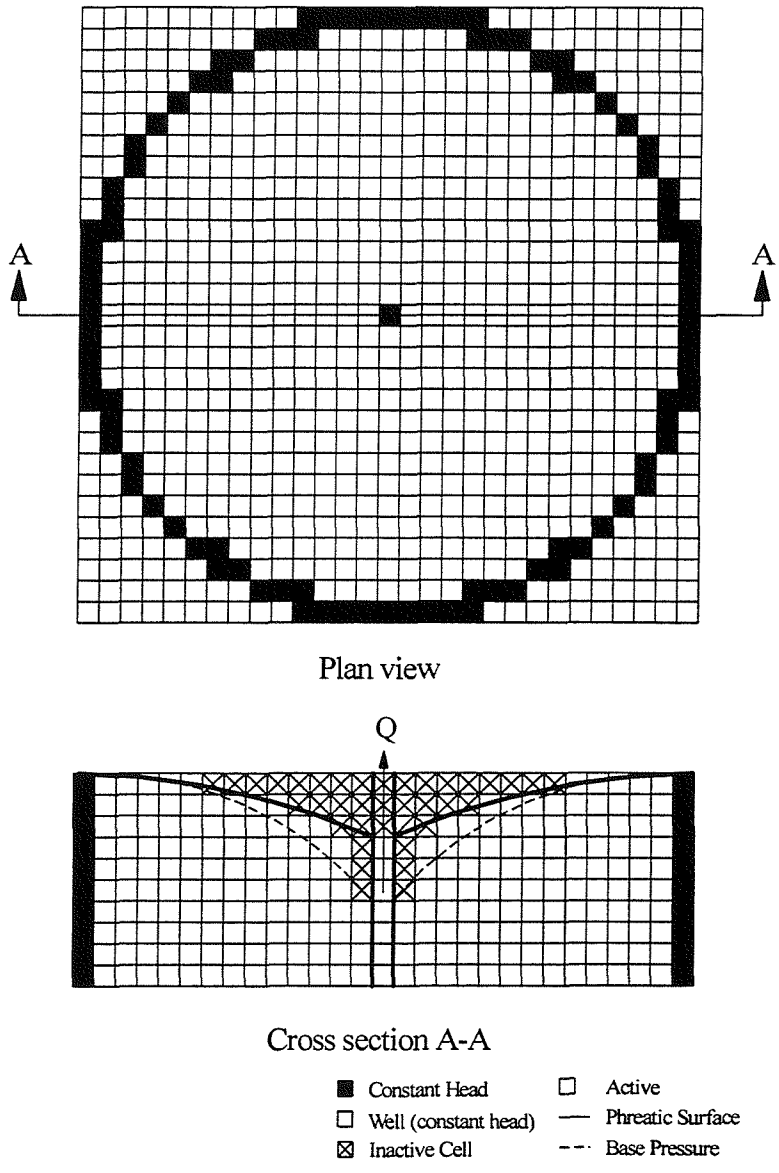

Figure 4.3 Example of the drying cell problem encountered in the original MODFLOW.

4.4 Representation of Individual Wells (Equivalent Well Block Radius)

MODFLOW uses a block-centered discretization formulation, which means that the head in a well is calculated at the node in the centre of the well block (that is the block containing a well) based on the finite-difference form of the continuity equation for flows. The computed hydraulic head in the well block is a representation of the average head for the block and not the head in a specific well. Analytical methods for computing the nodal correction use the equivalent well block radius, which is defined as the radius at which the steady-state hydraulic head in the aquifer is equal to the numerically calculated head of the well block. Localised refinement of the mesh can be used by introducing more columns and rows to improve near well zone modelling when using numerical methods. The accurate computation of hydraulic head in a well is important for both flow and transport modelling, therefore an investigation was carried out to study the problem of representing individual wells in groundwater modelling.

According to *Beljin* (1988), *Herbert and Rushton* (1966), *Prickett* (1967) and *Prickett* and *Lonnquist* (1971) were the first in the hydrological literature to point out the need for corrections in modelling the true radius of a well. For a square mesh of sides Δx and constant transmissivity T (Figure 4.4) the standard finite-difference equation with a pumping well at the node (i, j) has the form

$$h_{i-1,j} + h_{i+1,j} + h_{i,j-1} + h_{1,j+1} - 4h_{ij} = \frac{Q}{T} \tag{4.5}$$

The equation for the confined radial flow that takes place from an outer circle, radius Δx, to an inner circle, radius r_e, is derived as shown in section 2.3 and equation 2.9 for confined aquifer is

$$Q = 2\pi r b K \frac{dh}{dr} \qquad \Rightarrow \qquad \frac{Q}{T} = \frac{2\pi(h^* - h_{ij})}{\ln\left(\frac{\Delta x}{r_e}\right)} \tag{4.6}$$

taking h^* to be the average of $h_{i-1,j}$, $h_{i+1,j}$, $h_{i,j-1}$, and $h_{i,j+1}$. By combining equation 4.5 and 4.6, *Prickett* and *Lonnquist* (1971) has derived the following expression

$$\ln\left(\frac{\Delta x}{r_e}\right)=\frac{\pi}{2} \tag{4.7}$$

or

$$r_e=\left(e^{\frac{-\pi}{2}}\right)\Delta x \approx 0.208\Delta x \tag{4.8}$$

Equation 4.8 can also be derived by combining the radial flow equation, Figure 4.4b, and *Darcy's* law, Figure 4.4c. *Van Poollen et al.* (1970), who assumed that the computed head of the well block equals the areal average head, proposed another expression

$$r_e = 0.342\Delta x \tag{4.9}$$

Finally, *Peaceman* (1978, 1983) solved the problem numerically and derived the following equation

$$r_e = 0.198\Delta x \tag{4.10}$$

Furthermore, he showed that equation 4.9 is incorrect and that equation 4.8 is a good approximation. In other words, increasing Δx in the model to five times the real well radius a way to reach the same flow rate calculated by *Dupuit-Forchheimer* equation, which earlier proved to give accurate flow rate regardless of not taking account of seepage face.

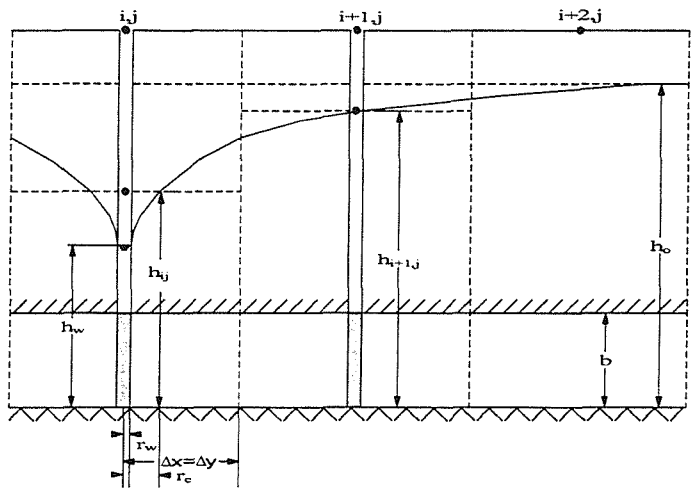

(a)

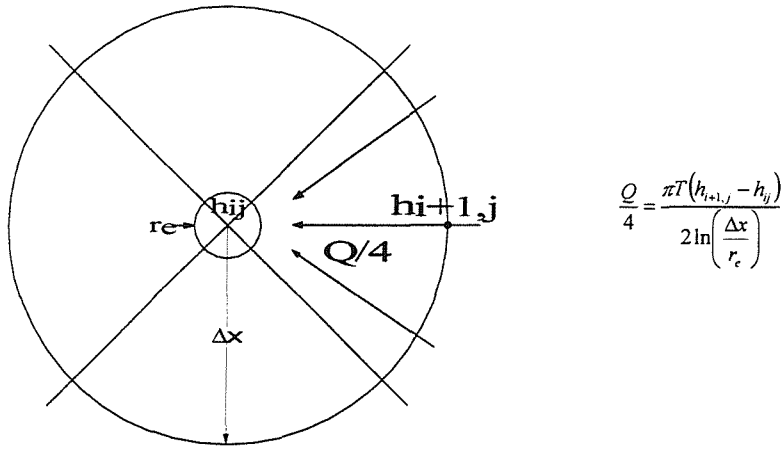

(b)

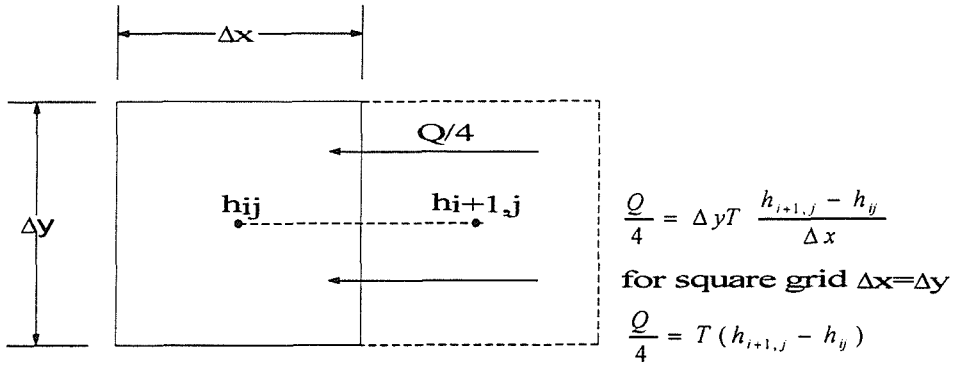

(c)

Figure 4.4 Flow from node $(i+1, j)$ to node (i, j). **(a)** cross sectional; **(b)** equivalent radial flow; and **(c)** finite-difference representation. (Reproduced from *Beljin, 1988.*)

4.5 MODFLOW-SURFACT Code Verification

Codes for groundwater flow are verified by comparing the numerical results with one or more analytical and/or experimental solutions. The purpose of code verification is to confirm that the numerical solution is relatively free of round-off and truncation errors, which, if uncontrolled, can lead to an unstable solution. The comparison with numerical results will also depend on the choice of error criterion, grid spacing, and time step. MODFLOW, which is the basis of MODFLOW-SURFACT, has been verified and produces numerically stable solutions. A water balance calculation, which is included in MODFLOW-SURFACT, is another assurance that the code correctly and accurately solves the mathematical model.

Throughout this study, a square constant head is used for the outer boundary for simplicity as shown in Figure 4.5. A comparison study was carried out to ensure that the errors resulting from this simplified design are small when compared to the more accurate representation shown in Figure 4.5a. Consider a radial flow toward a well pumping in a finite unconfined aquifer. The radius of the flow domain (radius of influence) is 10m, the elevation of the domain is 10m and the radius of the well is 0.1m. The saturated hydraulic conductivity of the soil is set to 1.0m/day and the pumping level is 2m. The steady state, radial-flow problem is solved using two different grid designs shown in Figure 4.5. As shown in Figure 4.6 and Figure 4.7, the phreatic surface for both cases show a reasonable agreement and the flow rate difference is less than 2%. Therefore, the simple representation is used throughout the research for faster model design.

The selection of the nodal spacing size is an important step in grid design. "*The size of the nodal spacing in the horizontal dimension is a function of the expected curvature in the water table or potentiometric surface. Finer nodal spacing will be required to define highly curved surfaces. Similarly, the change in head in the vertical direction will influence the selection of the vertical nodal spacing* (*Anderson and Woessner*, 1992)". Throughout the study a special care was directed to the grid design step and a sufficient spacing size near wells is considered. Moreover, more layers are introduced whenever there is a significant vertical head gradient. The grid designs for the models used in this study were only considered correct if refining the grids or adding more

layers make no changes to the model outcome. Finally, the successful grid design for the models used for verification later in the study, shows confidence in the criteria set throughout the study for grid design.

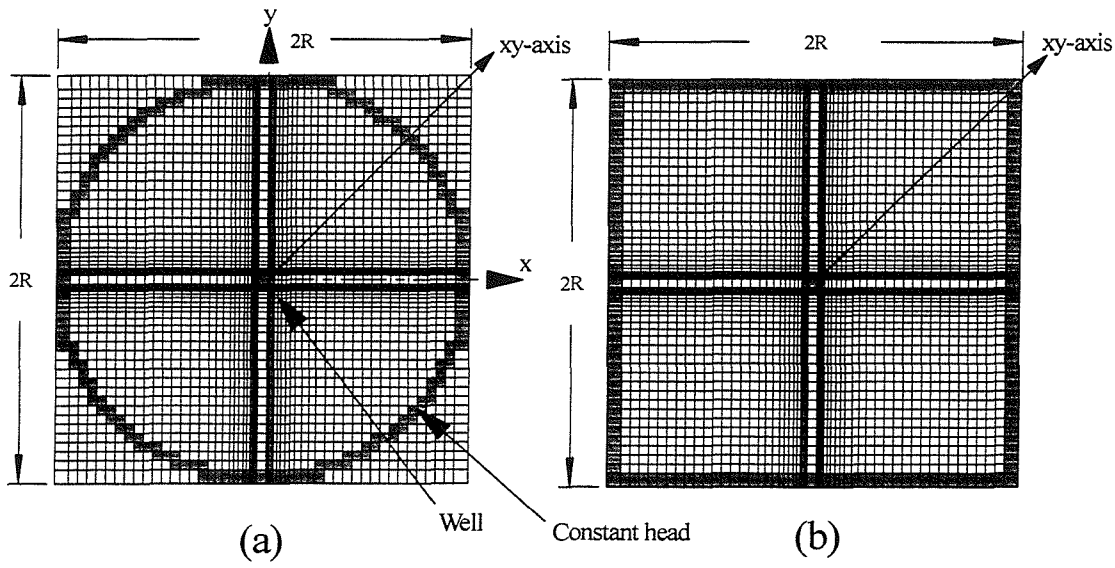

Figure 4.5 Different grid design. **(a)** circular constant head and **(b)** square constant head at the outer boundary.

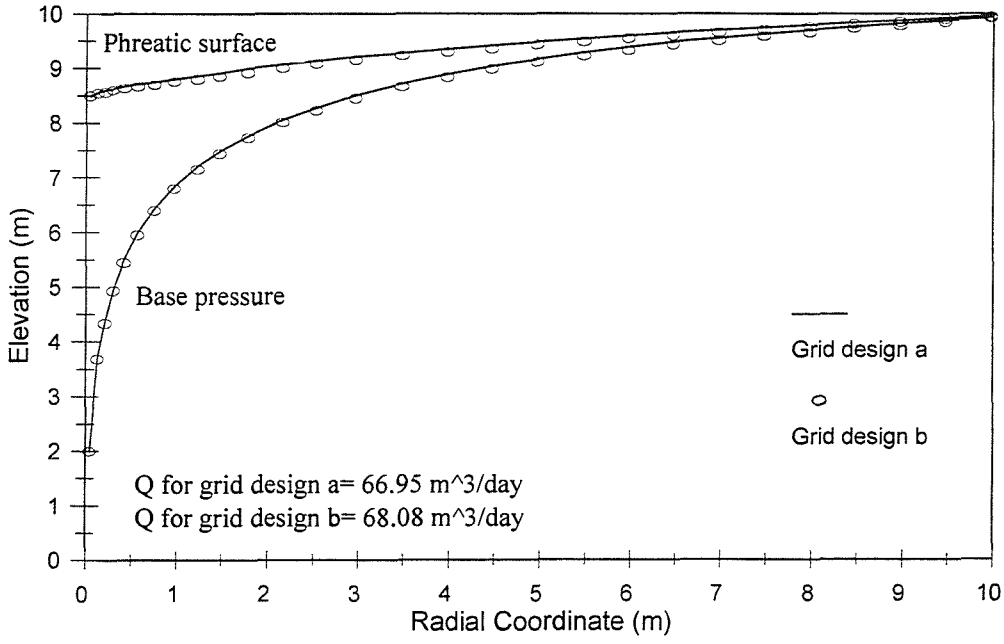

Figure 4.6 Phreatic surface and base pressure from the well edge along the *x*-axis for the two different grid designs shown in Figure 4.5.

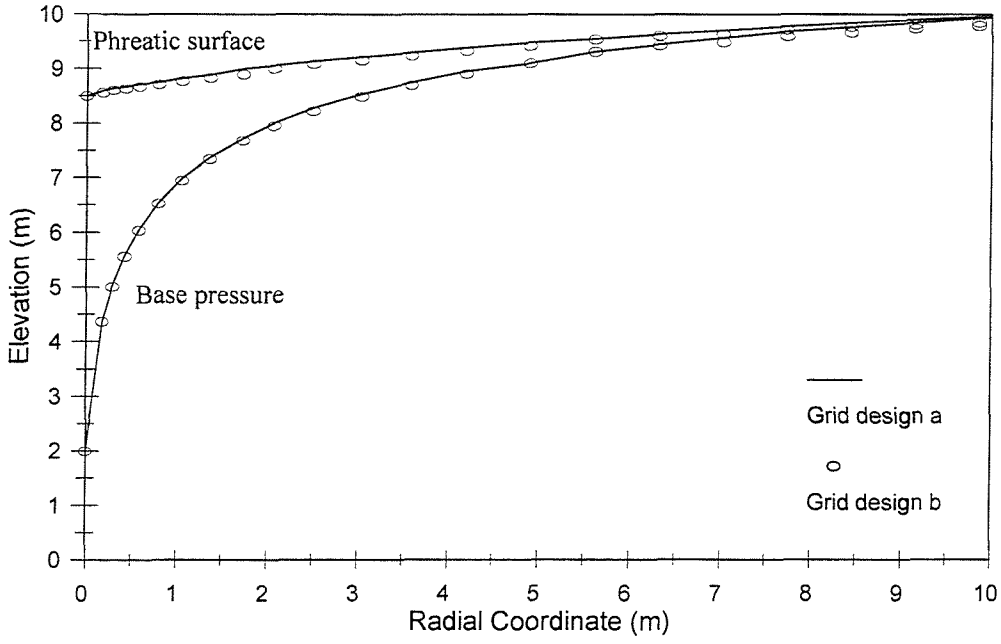

Figure 4.7 Phreatic surface and base pressure from the well edge along the *xy*-axis for the two different grid designs shown in Figure 4.5.

4.5.1 Hall (1955) Study

The experimental observations of *Hall* (1955) produced some of the best available observational information on the relationships between the free surface, seepage face and well geometry in radial flow. This data has been chosen as the basis for this numerical model verification. The physical model as explained earlier consisted of a 15° sector of the region surrounding a fully penetrating well. The surface ABCD in Figure 4.8a represents a plan view of the underlying horizontal impervious base. The radius of the well was r_w = 0.122m, and the distance from the well center to the outer boundary of the radial system was R = 1.951 m. Thus the ratio R/r_w was 16 to1.

The same model dimensions were used in our numerical model investigation. A single cell (in plan view) is used to represent the pumped well in this discretization scheme shown in Figure 4.8b. The dimensions of the cell (x and y-coordinates) are set to the diameter of the well. The (column and row) dimensions of the cells adjacent to the well are set to a small fraction of the well diameter. Cell dimensions radially increase with increasing distance from the well. The expansion factor, α, which relates the cell

dimensions of any two adjacent cells is generally given a value not more than 1.5. By having very small cell widths near the well cell, errors associated with finite differencing of small distance between nodes are small. The domain is discretized into 26 layers of thickness 0.05 m and 31 rows and columns. The initial head value, for all cells and the outer boundary constant head values, were set at 1.22 m. The value of the hydraulic conductivity in *Hall's* experiments was 0.0041 m/sec and the same value was used for the numerical model.

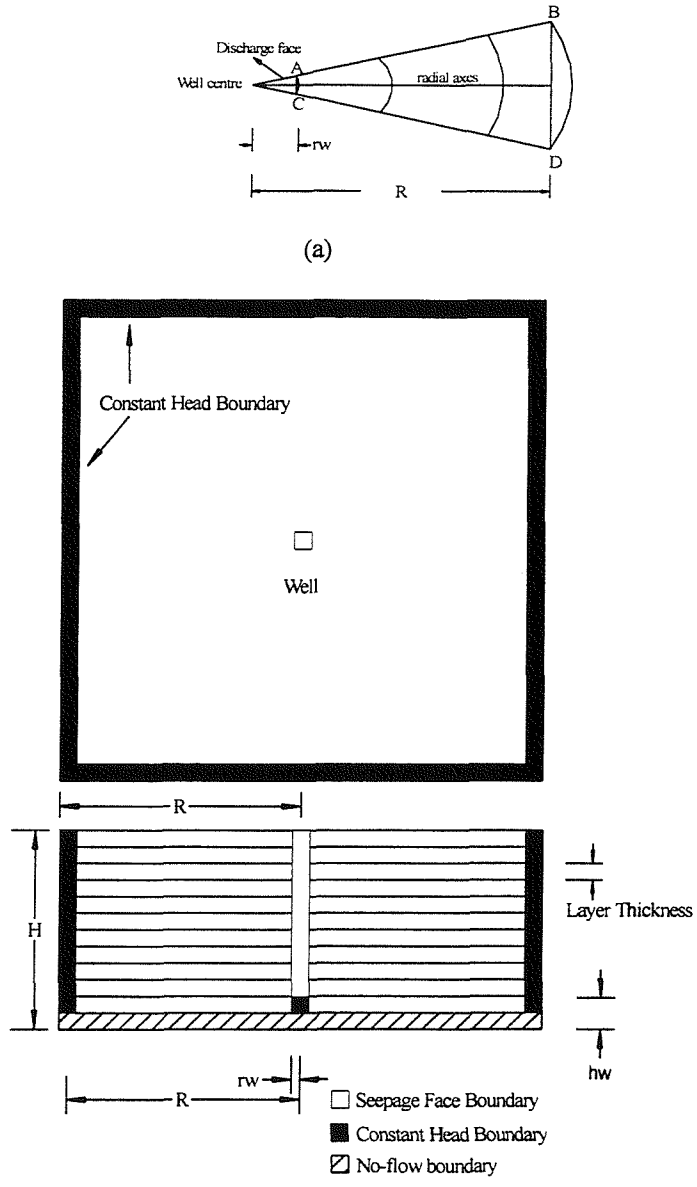

Figure 4.8 Representations of *Hall's* sand tank model. **(a)** plan view of the radial flow system and **(b)** discretization of the flow region for *Hall's* sand tank model.

Eight cases corresponding to *Hall's* (1955) experiment were simulated using different head values at the well cell. Numerical results predicted by MODFLOW-SURFACT are compared to *Hall's* results in Table 4.2 and Figure 4.9. These demonstrate that there is good agreement between the phreatic surface predicted by MODFLOW-SURFACT and that observed by *Hall*. The maximum difference between the flow rates predicted by MODFLOW-SURFACT, providing a radius correction for the well as suggested by *Beljin* (see section 4.5), and that calculated using *Dupuit-Forchheimer* equation is 3.96% as shown in Table 4.2a. This error is reduced significantly when *Hall* results are compared with the numerical model results. The maximum error when the levels of the seepage face compared is 0.54%, Table 4.2b. This indicates that the numerical computation of free surface is reliable. Moreover, Figure 4.9 shows that *Dupuit-Forchheimer* free surface calculated using equation 2.11 agrees with the computed hydraulic head at the base. The results presented above show that MODFLOW-SURFACT model, which will be used throughout the study, is an acceptable tool for analyzing unconfined flow problems.

Table 4.2a Computed and analytical quantities of flow.

		Flow rates (m^3/day)				
Test	**h_w (m)**	***Hall* (1955)** **A**	***Dupuit* Model** **B**	**MODFLOW-SURFACT** **C**	**Error (%)** **B vs. C**	**Error (%)** **A vs. C**
A	0.000	-	597.533	615.064	2.93	-
B	0.152	612.842	588.257	604.031	2.68	1.44
C	0.304	577.679	560.431	577.532	3.05	0.03
D	0.456	534.144	514.055	534.410	3.96	0.05
E	0.608	463.818	449.127	465.204	3.58	0.30
F	0.760	380.096	365.649	376.514	2.97	0.94
G	0.912	269.584	263.621	268.237	1.75	0.50
H	1.064	138.980	143.042	143.191	0.14	2.90

Table 4.2b Computed and observed extents of seepage face.

		Seepage Face (m)		
Test	**h_w (m)**	***Hall* (1955)**	**MODFLOW-SURFACT**	**Error (%)**
A	0.000	0.833	0.829	0.45
B	0.152	0.833	0.831	0.25
C	0.304	0.848	0.849	0.06
D	0.456	0.864	0.862	0.25
E	0.608	0.902	0.898	0.40
F	0.760	0.945	0.940	0.54
G	0.912	1.043	1.038	0.46
H	1.064	1.107	1.100	0.66

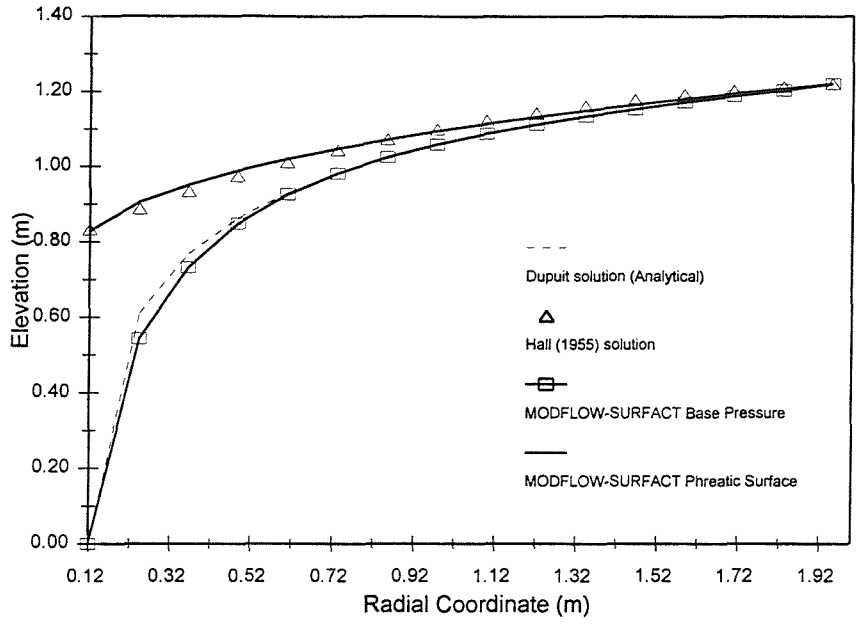

(a)

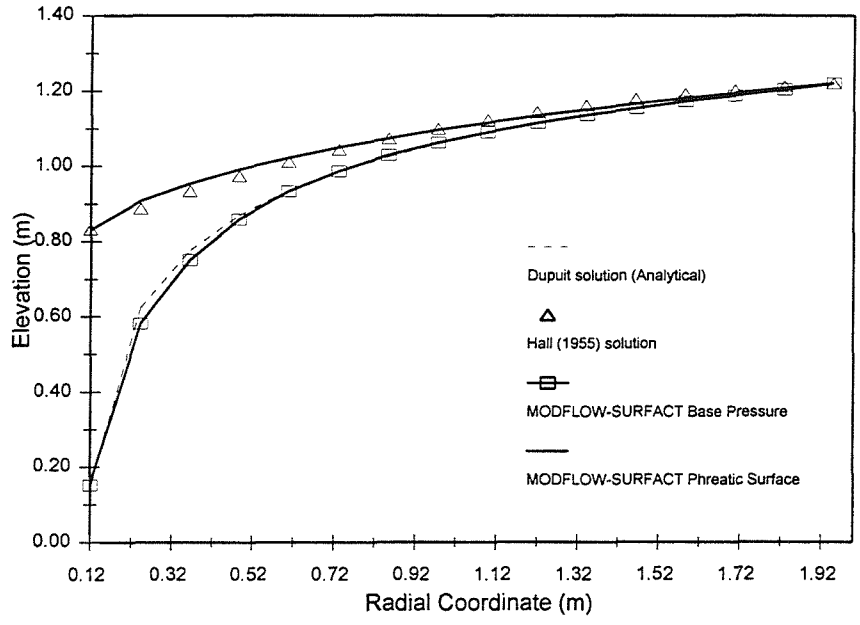

(b)

Figure 4.9 **(a)** and **(b)** Comparison of *Dupuit-Forchheimer* model, *Hall* (1955) observations, and MODFLOW-SURFACT code results for h_w= 0m and 0.152m respectively.

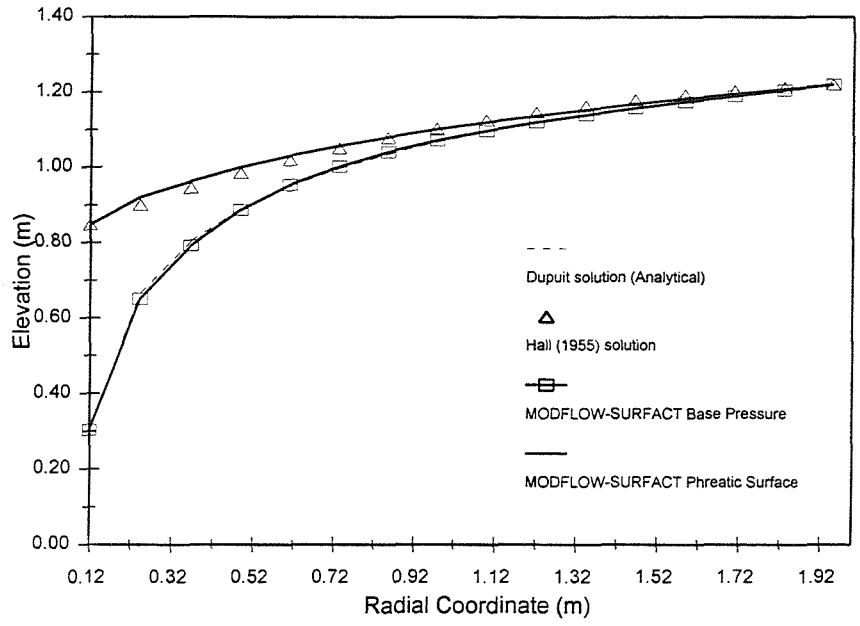

(c)

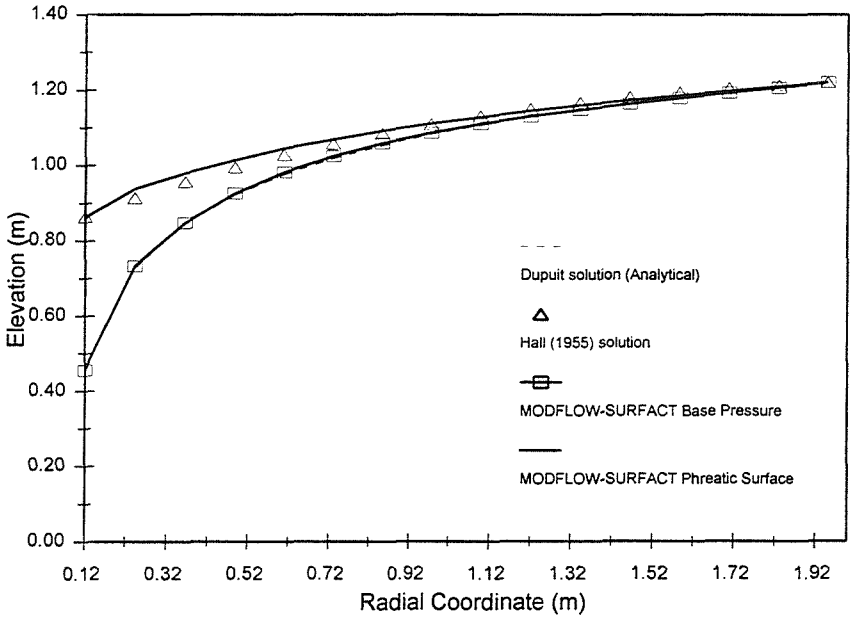

(d)

Figure 4.9 (c) and **(d)** Comparison of *Dupuit-Forchheimer* model, *Hall* (1955) observations, and MODFLOW-SURFACT code results for h_w= 0.304m and 0.456m respectively.

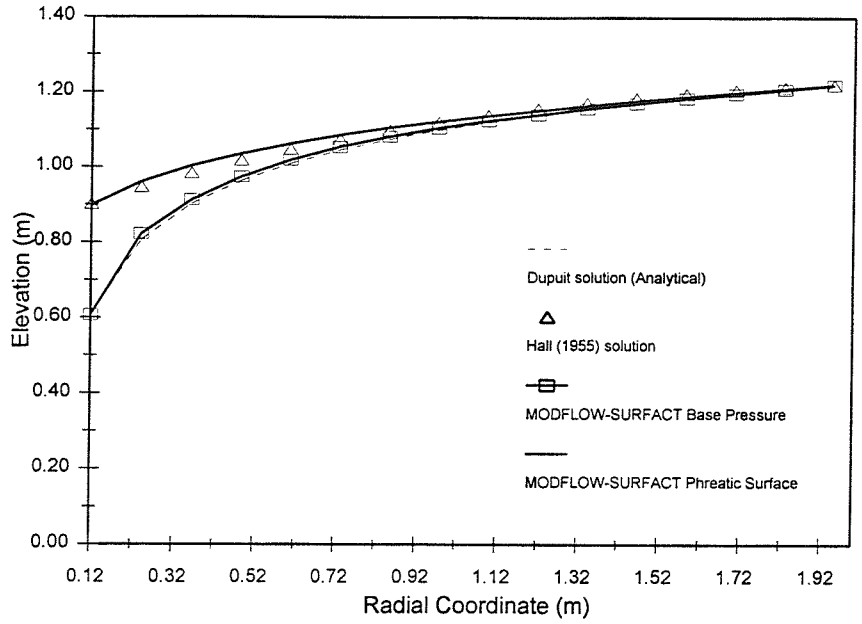

(e)

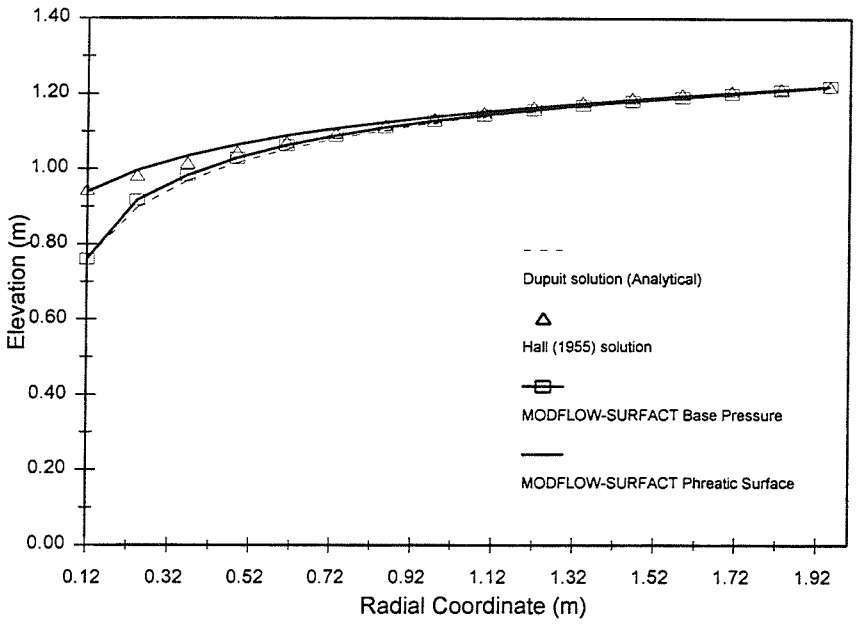

(f)

Figure 4.9 **(e)** and **(f)** Comparison of *Dupuit-Forchheimer* model, *Hall* (1955) observations, and MODFLOW-SURFACT code results for h_w= 0.608m and 0.760m respectively.

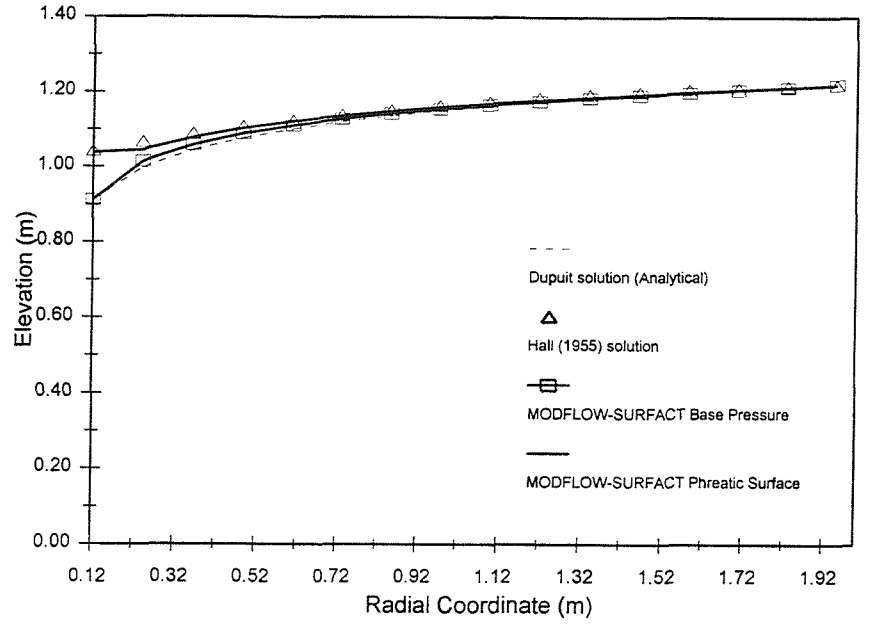

(g)

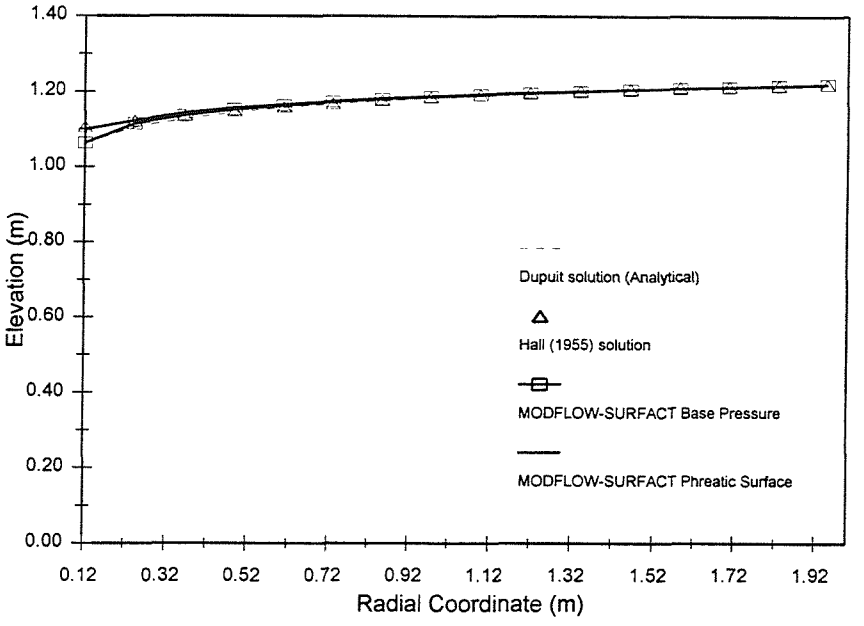

(h)

Figure 4.9 **(g)** and **(h)** Comparison of *Dupuit-Forchheimer* model, *Hall* (1955) observations, and MODFLOW-SURFACT code results for h_w= 0.912m and 1.064m respectively.

4.5.2 Zee et al (1957) Study

The work of *Zee et al.* (1957) is particularly interesting in that it contains a large quantity of data collected from tests on a single well carried out by a number of authors. Based on the experimental results and the data from others, $\frac{h_s}{r_w}$, $\frac{h_w}{r_w}$ and $\frac{Q}{Kr_w^2}$, *Zee et al.* (1957) produced a graphical relationship between the parameters shown as in Figure 2.8. The data gathered by *Zee et al.* is extracted and shown in Table 4.3 and Figure 4.10.

Table 4.3 *Zee et al.* (1957) gathered data and the calculated results based on the algebraic fit.

Data number	*Zee et al.* gathered data			$\frac{Q}{Kr_w^2}$ based on the algebraic fit to *Zee et al.* Data
	$\frac{h_s}{r_w}$	$\frac{h_w}{r_w}$	$\frac{Q}{Kr_w^2}$	
1	1.5	0	18	14.6
2	8.3	8.2	26	19.2
3	8	7.6	33	38.6
4	7	6.2	48	48.8
5	9.5	9	50	51.6
6	6	5	60	47.1
7	5.5	2.8	69	73.1
8	5.6	3.6	72	63.5
9	4.5	2.3	74	53.7
10	4.5	1.7	78	61
11	7.5	6	85	73
12	7.4	5.8	86	74.5
13	6.5	3	105	99.1
14	6.4	2.9	106	97.6
15	6.2	0	107	128
16	16	15.3	107	104
17	14.5	13.2	140	130.8
18	20	18.8	142	172.9
19	11.2	8	160	162.9
20	12	10.3	200	124.8
21	10	0	245	266
22	10	0	255	266
23	10.5	5.3	250	197.5
24	16	12.5	250	244
25	28.5	26.1	270	355.8
26	12	0	360	351.6
27	13.5	6.3	310	301.7

28	18.5	13.9	308	326.1
29	43	41.6	370	403.4
30	25	20.7	406	425.2
31	24	13.7	603	648.5
32	20.05	6.1	702	636.2
33	40.5	36.9	780	626.9
34	27	16	802	755.4
35	46	40.6	890	882.7
36	35.5	16.5	1080	1326.8
37	35	3.6	1500	1707.3
38	50	32.1	1750	1810.7
39	54	46.7	1100	1215.7
40	66	60	1600	1339.1
41	71	65.7	1450	1348.9
42	49.5	25.8	2010	2080.1
43	47.5	10.2	2150	2538.5
44	46.5	0.57	2250	2774.8
45	55.5	40.6	2020	1823.7
46	59.9	40	2800	2294.5
47	69.5	54.9	2030	2259.2
48	66.5	41.6	2800	2868.6
49	57	20	3400	3033.1
50	56	0	3900	3711.9
51	64	25.3	3450	3487.7
52	62.5	20	4020	3579.3

A fresh analysis of the data has been used to obtain an algebraic representation. Starting with the hypothesis that the hydraulic gradient at the well is related algebraically to the difference in the seepage surface and well surface elevations by a simple power law the following equation gives the best fit to the data, see Figure 4.10.

$$i = 1.25\left(\frac{h_s}{r_w} - \frac{h_w}{r_w}\right)^{0.53} \tag{4.11}$$

where; i is the effective hydraulic gradient; h_s is the depth of water outside the well (L); h_w is the depth of water in the well (L) and r_w is the radius of the well (L).

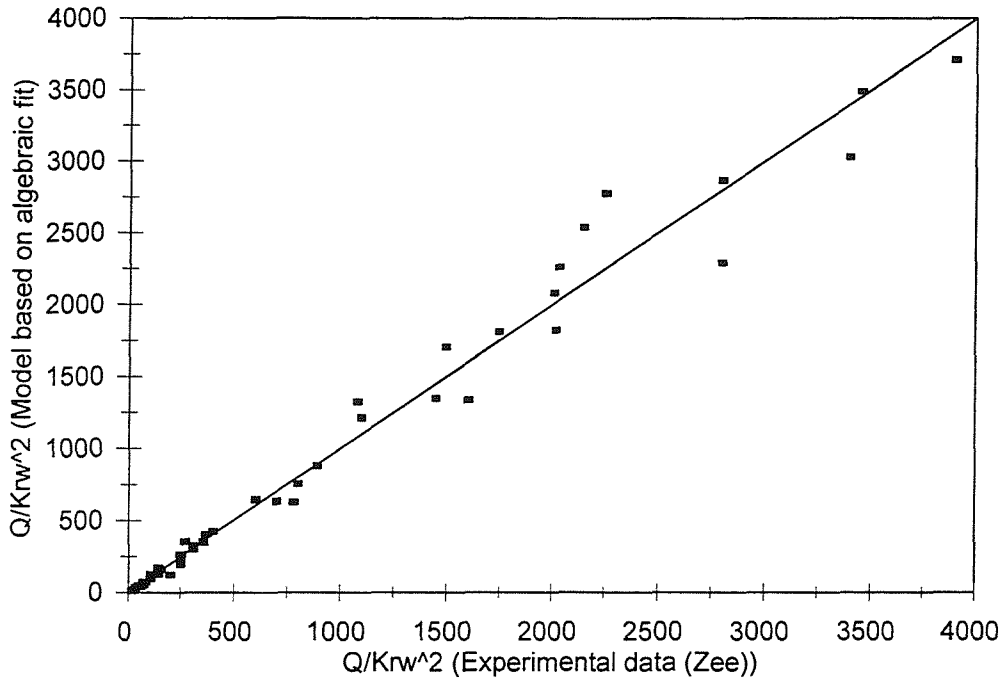

Figure 4.10 Comparison between *Zee et al.* (1957) gathered data and that predicted based on the algebraic fit.

Applying *Darcy's* law to the boundary of individual well, $Q = KiA$, gives

$$\frac{Q}{Kr_w^2} = 2.5\pi \frac{h_s}{r_w}\left(\frac{h_s}{r_w} - \frac{h_w}{r_w}\right)^{0.53} \tag{4.12}$$

where; Q is the flow rates from the well (L^3/T); K is the hydraulic conductivity (L/T)and

$$10 < \frac{Q}{Kr_w^2} < 5000 \qquad 0 < \frac{h_s}{r_w} < 90 \tag{4.13}$$

The discretization scheme for this application follows the same concept described earlier for *Hall's* experiment. With such discretization, the MODFLOW-SURFACT model has been used to model the seepage surface for a single well over a range of parameters extending the range of *Zee et al.* to

$$0 < \frac{Q}{Kr_w^2} < 65000 \qquad 10 < \frac{h_s}{r_w} < 350 \qquad (4.14)$$

The results are compared in Figure 4.11. It can be seen that MODFLOW-SURFACT results are confirmed by the experimental/analytical results assembled by *Zee et al.* In addition, it appears that equation 4.12, based on the *Zee et al.* results, may be used to extrapolate over a much greater range of parameters. The well radius correction plays an important role in order for MODFLOW-SURFACT to predicted accurate flow rate values. As shown in Figure 4.11 there is a better agreement after the well radius correction.

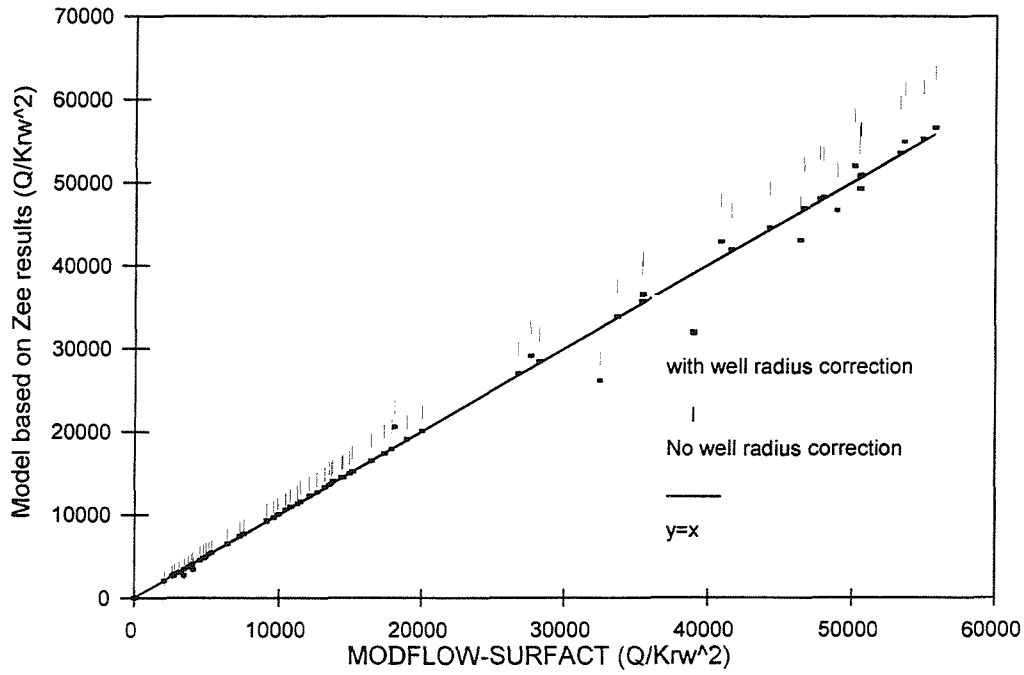

Figure 4.11 Comparison between MODFLOW-SURFACT numerical results and the model based on *Zee et al.* (1957) experimental results.

Figure 4.12 shows two examples comparing the MODFLOW-SURFACT results with the prediction of the seepage face based on *Zee et al.* data. The Figure illustrates that there is a good agreement between the seepage face predicted by the model and that based on *Zee et al.* data. Moreover, and as a matter of interest, the seepage face based on *Zee et al.* data compared with the model for a fully drained well is show in Figure 4.13. This result is very important and will be extended later in Chapter 6, when the limiting gradient concept is investigated.

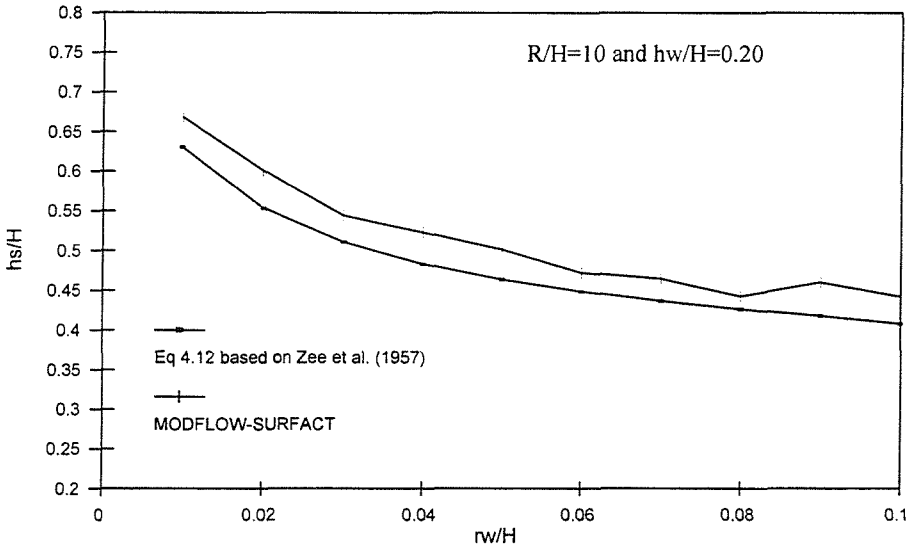

Figure 4.12 Comparison between MODFLOW-SURFACT numerical results and *Zee et al.* (1957) experimental results for R/H=10 and h_w/H=0.20.

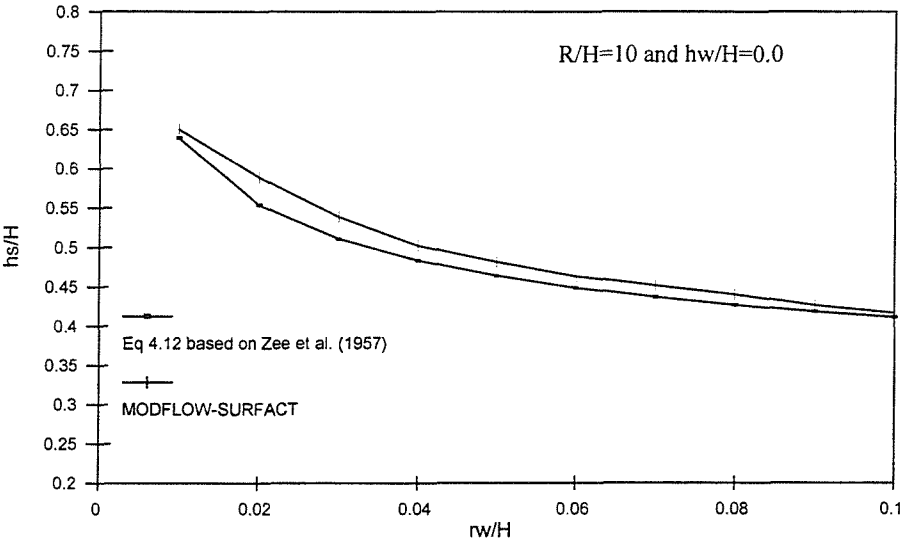

Figure 4.13 Comparison between MODFLOW-SURFACT numerical results and *Zee et al.* (1957) experimental results for R/H=10 and h_w/H=0.0.

4.6 Summary

The code MODFLOW-SURFACT has been introduced as a means of modelling variably saturated flow through porous media. The code performance has been verified against the experimental work of *Hall* and the large range of data collected and presented by *Zee et al.* The code is demonstrated to work well for the determination of seepage faces and phreatic surfaces. Moreover, the pseudo-soil water retention functions that are automatically generated to reduce the unsaturated flow problem to one of seeking the potential head in a cell appear to be very effective. The near-well zone needs to be modeled carefully and the well radius correction should be made to the grid representing individual wells in MODFLOW in order to predict well yields correctly. The work represents an original contribution to the subject area.

The verification of the code in using these examples gives confidence to its application for problems which are unsupported by experimental data. This code has therefore been used to study a range of steady state and transient flow problems with seepage face boundaries for single and multiple well configurations. The next chapter presents a study of the seepage face for a single well and multiple well configurations for both steady-state and transient flow conditions.

Chapter (5)

Seepage Face Numerical Investigations

5.1 Introduction

As discussed in Chapter 1, in order to design and operate deep well systems for remediation unconfined aquifers or landfills, information about the characteristics of induced seepage flows is important. Estimating the position of the free surface and seepage face is also of importance in the context of groundwater control. In Chapter 4, findings indicate that MODFLOW-SURFACT solutions are consistent with other experimental and analytical models for determining the seepage surface. Therefore, it should be possible to use the package to evaluate the effect of the seepage face, and three-dimensional effects in general, in the neighbourhood of a single well and of a circular array of multiple deep wells. This will be relevant to the design of groundwater remediation systems in that it will demonstrate the potential for the system enhancement when accounting for seepage face. That is it will allow the evaluation of the impact of exposing a larger region of a contaminated unconfined aquifer to remediating flushing flows as discussed in Chapter 1. The work described in this chapter goes beyond the assumptions made in most theoretical and physical models and investigates more general flow conditions that include the effect of anisotropy conditions and the geometry of the flow domain.

5.2 Single Well Investigation – Steady-State Flow

The investigation here will follow the work of *Clement et al* (1996) and then extend it to investigate the influence of anisotropy. The same example used by *Clement et al.* (1996) is adopted in this study, for steady-state and transient flow. The purpose of following such an example to begin with is to compare the code used in this study, which uses the pseudo-soil moisture content/pore pressure function, with the more accurate representation given by *Van Genuchten*, (*Van Genuchten*, 1980), and used by *Clement et al.* (1996).

A quasi-radial flow toward a pumping well in a finite, unconfined, rectangular square domain is investigated. The dimensions of the quasi-radial flow problems considered are as follows; the 'radius' of the flow domain, the distance of influence to one side of the square is, 10m, the height of the domain is 10m, the radius of the well is 0.1 m and the pumping level varies between 2m and 8m. The saturated hydraulic conductivity of the soil is set to 1 m/day. (Figure 5.1)

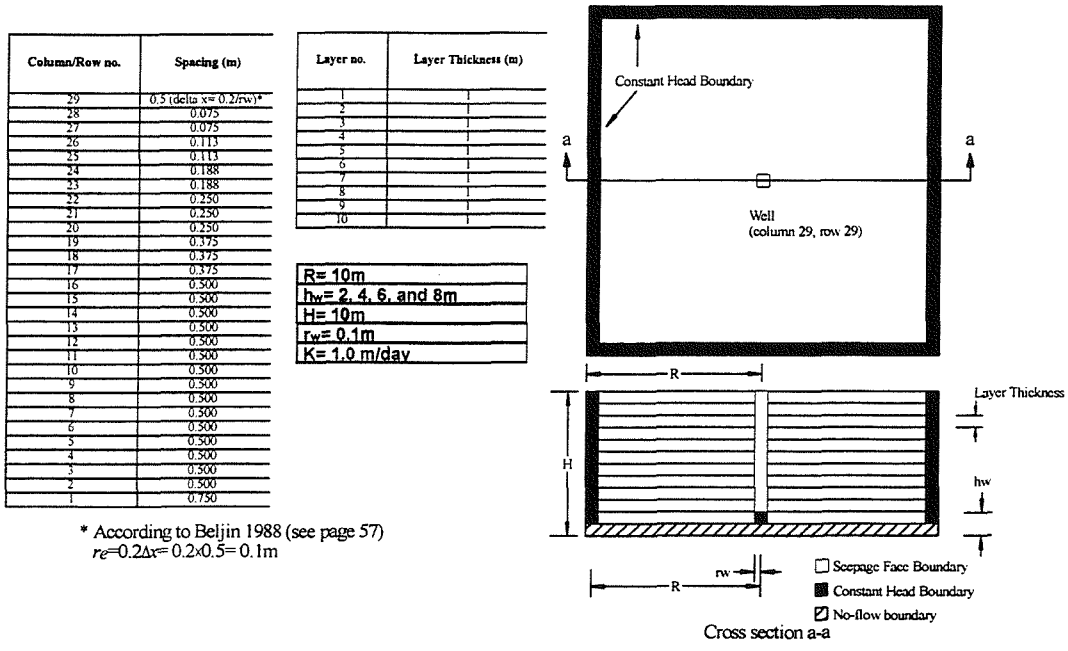

Figure 5.1 Model for a single well problem in an unconfined aquifer.

The radius of influence in this section set to 10m as a length of the flow domain, which will be changed later to examine seepage face sensitivity to the different aspect ratios. In general the radius of influence is too far from the well to influence the seepage surface other than indirectly by influencing the discharge, Q.

The steady state problem for a single pumping well has been solved using MODFLOW-SURFACT and the results are shown in Figure 5.2. The location of the phreatic surface predicted by MODFLOW-SURFACT, when the pumped level at the well is 2m, is in a good agreement with the results of *Clement et al.* (1996). Moreover, *Clement et al.* (1996), suggested that the effect of transport through the vadose zone is relatively small in radial flow. This conclusion is based on the reasonable agreement between the position of the phreatic surface computed by the fully saturated flow model and the variably saturated flow model. This can also be concluded when the flow rate estimates computed by the model, (65.70 m^3/day) are compared with fully saturated flow rate estimates computed using *Dupuit-Forchheimer* equation (65.50 m^3/day, for H=10m, h_w=2m, R=10m, r_w=0.1m and K=1m/day). It should be noted that the model prediction matches the *Dupuit-Forchheimer* analytical solution only when a grid correction is made, r_e=0.2Δx= 0.2×0.5= 0.1m, as suggested by *Beljian* (1988) (see page 57). Figure 5.2 also compares the pressure-head distribution at the bottom of the flow domain (base-pressure head) predicted by *Dupuit's* model and MODFLOW-SURFACT model. The results show a good agreement between both models for base-pressure head distribution. The difference between this distribution and the phreatic surface location is created by the seepage surface effect.

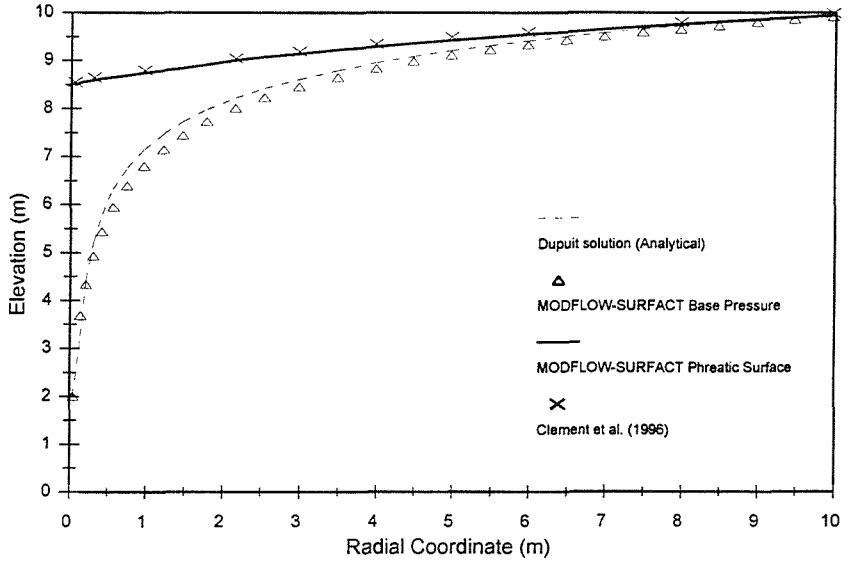

Figure 5.2 Comparison between *Dupuit* model and MODFLOW-SURFACT model results.

Inflow and outflow horizontal (normal) velocity distributions obtained from the MODFLOW-SURFACT results are shown in Figure 5.3. The inflow horizontal velocities are relatively unchanged with respect to vertical position. The outflow velocities increase considerably with depth and approach their maximum value near the elevation of the downstream open-water level. The outflow velocities then decrease rapidly and approach a constant value below the downstream open-water-level. Vertical and horizontal flow components at the well are show in Table 5.1. Both *Clement et al.* (1996), using a numerical modeling approach, and *Peterson* (1957) using experimental work, noticed this type of outflow velocity distribution.

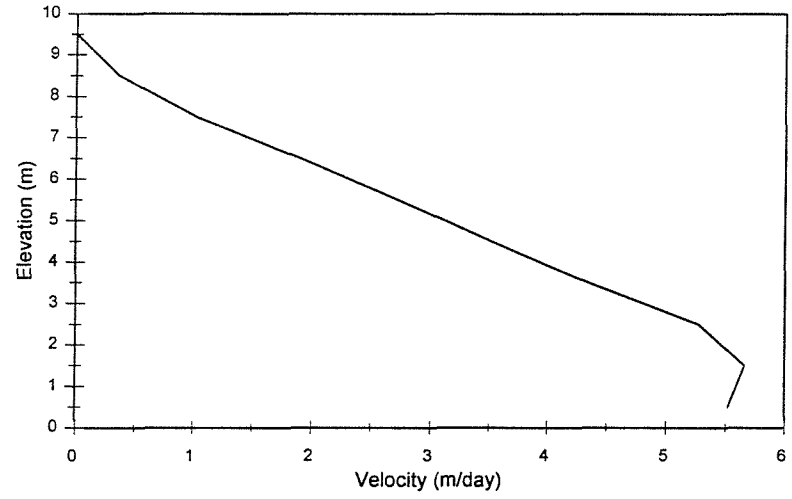

Figure 5.3a Outflow horizontal velocities.

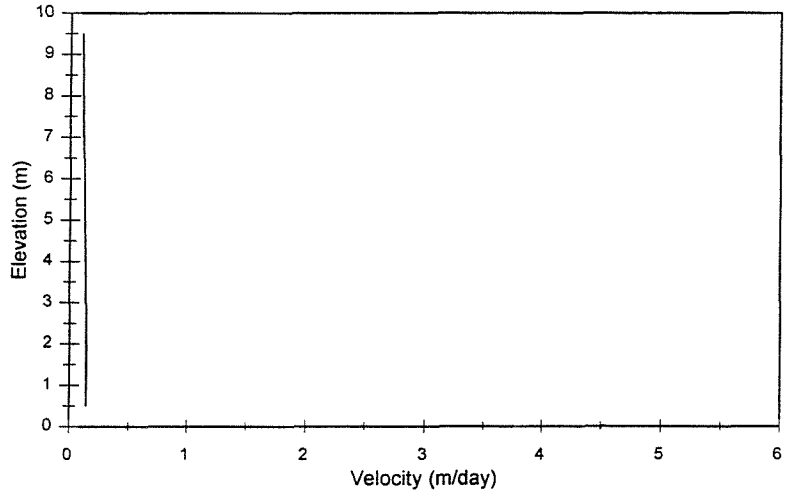

Figure 5.3b Inflow horizontal velocities.

Table 5.1 Horizontal and vertical flow components.

Elevation (m)	V_x (m/day)	V_z (m/day)
9.5	3.638E-06	-1.65E-05
8.5	0.3642032	-0.305312
7.5	1.029323	-0.805238
6.5	1.907307	-0.805238
5.5	2.727838	-0.999898
4.5	3.530345	-0.999897
3.5	4.353519	-0.999886
2.5	5.274706	-0.750274
1.5	5.661536	-0.250336
0.5	5.522883	0

The cone of depression predicted by MODFLOW-SURFACT is much smaller than that predicted by the *Dupuit-Forchheimer* model because of the numerical calculation taking account of three-dimensional effects and the presence of the seepage face. The piezometric head at the base of the model aquifer coincided with *Dupuit-Forchheimer*, as did the flow predictions, provided that the correction for well radius proposed by *Beljian* (1988), $0.2\Delta x$, was applied. This finding about the cone of depression plays an important role when designing remediation systems for contaminated aquifers using pump-and-treat systems. Moreover, it confirms the *Clement et al.* (1991) statement about the advantage of a seepage face presence:

"*Seepage faces and associated rises in phreatic surfaces are usually beneficial to pump-and-treat schemes since they expose a larger volume of soil to flushing flows, which will ease the removal of contaminants during clean-up efforts. Furthermore, at higher pumping rates the water level inside a well decrease, but the volume exposed to the flow remains relatively unchanged over a significant variation of drawdown due to the seepage face effect. This is very important since the remediation wells are usually installed in the most contaminated parts of the site.*"

5.2.1 Influence of Aspect Ratio

The sensitivity of the phreatic surface position predicted using MODFLOW-SURFACT to variations in the aspect ratio of the radial-flow problem has been investigated. Three flow domains with dimensions of 10m×10m, 20m×10m,

50m×10m, 100m×10m, 500m×10m, and 1000m×10m are considered. The length-to-height (radius of influence-to-aquifer depth) ratios of the problems considered are thus unity, two, five, ten, fifty, and one hundred respectively. The simulation is repeated four times using different pumping levels 2m, 4m, 6m, and 8m, respectively. The results from these simulations are summarized in Figures 5.4, respectively. The figures show that seepage faces are dominant and persistent in radial flow problems (as observed by *Shamasi and Narasimhan* (1991) and *Clement et al.* (1996). In Figure 5.4a, which shows results for the aspect ratio of unity, changes in the pumping level have a minor influence on the phreatic surface. The influence of the seepage face remains significant for problems with aspect ratio more than unity, hence, the *Dupuit-Forchheimer* model continues to be a poor approximation, especially near the well. Moreover and as stated in most groundwater textbooks, after a distance of 1.0 to 1.5H away from the well, the *Dupuit-Forchheimer* equation gives a fair but not accurate representation of the phreatic surface. Thus from our observations based on numerical modelling, a distance of ≥1.5H is more appropriate for using *Dupuit-Forchheimer* equation.

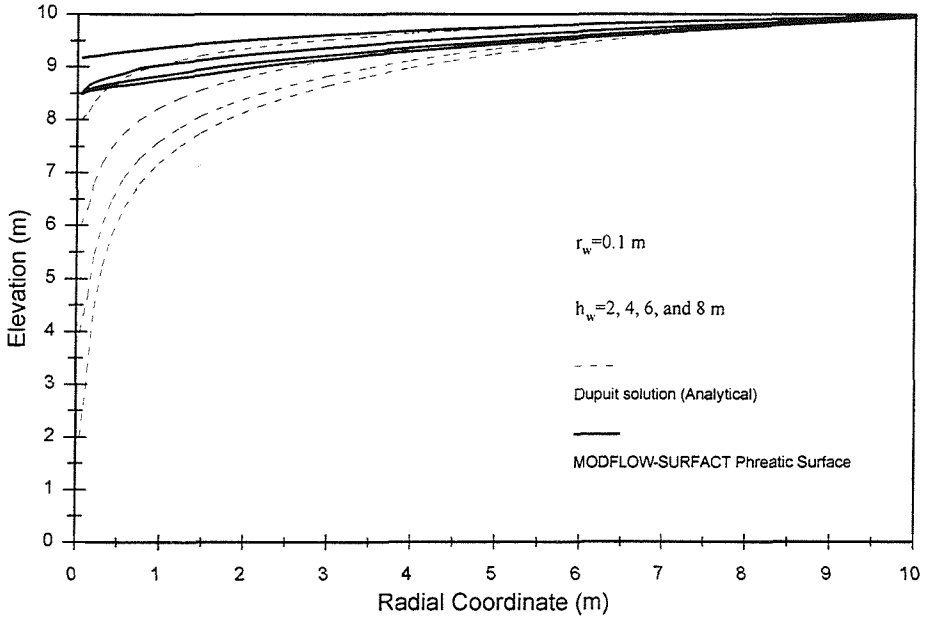

Figure 5.4a Phreatic surface variations to different pumping levels for the 10m×10m radial-flow problem.

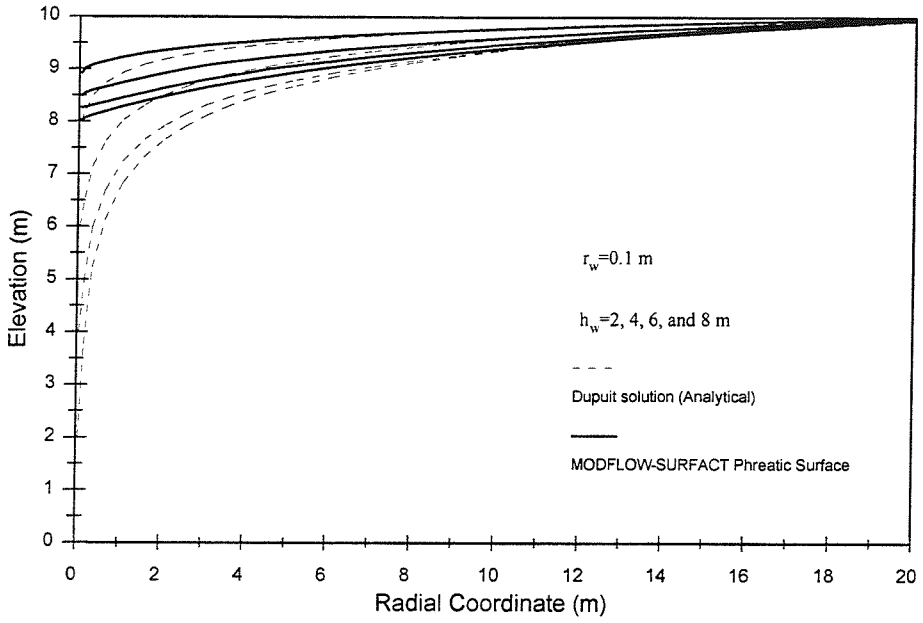

Figure 5.4b Phreatic surface variations to different pumping levels for the 20m×10m radial-flow problem.

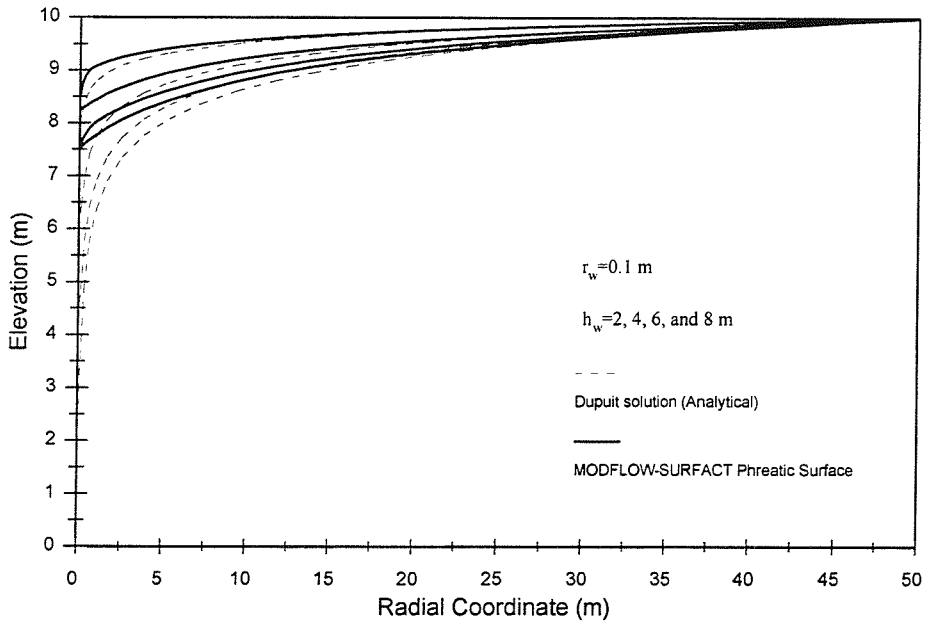

Figure 5.4c Phreatic surface variations to different pumping levels for the 50m×10m radial-flow problem

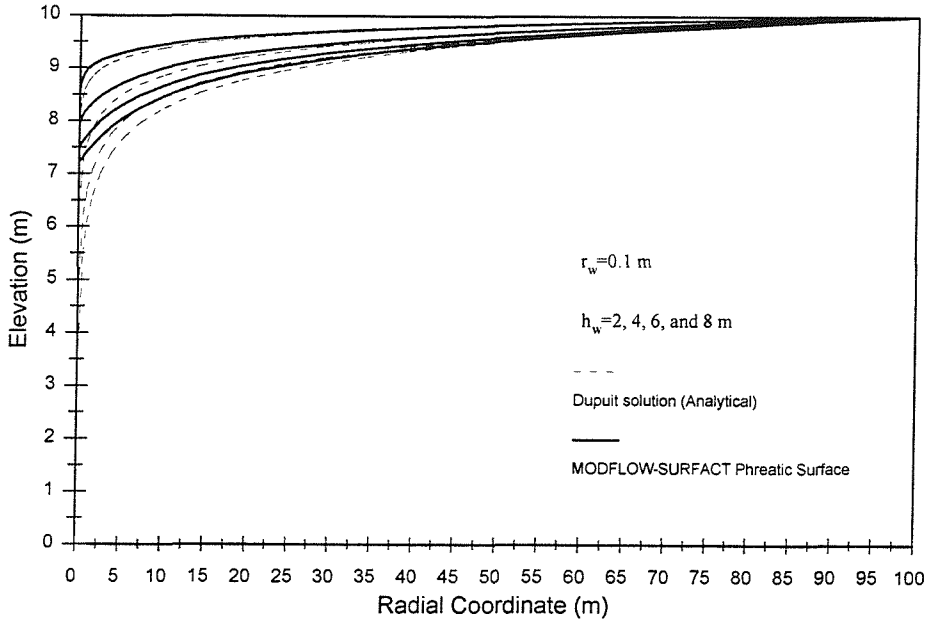

Figure 5.4d Phreatic surface variations to different pumping levels for the 100m×10m radial-flow problem.

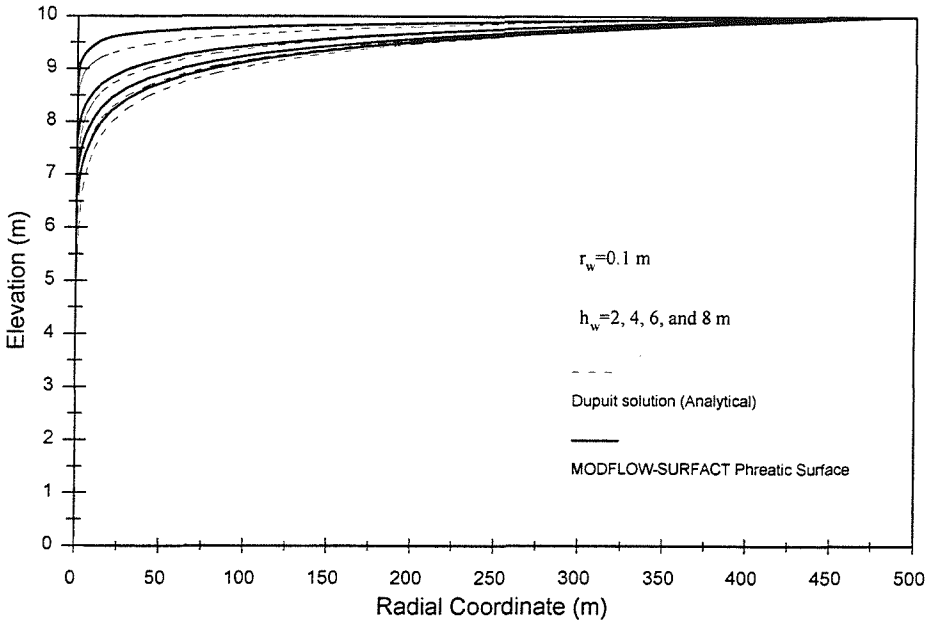

Figure 5.4e Phreatic surface variations to different pumping levels for the 500m×10m radial-flow problem.

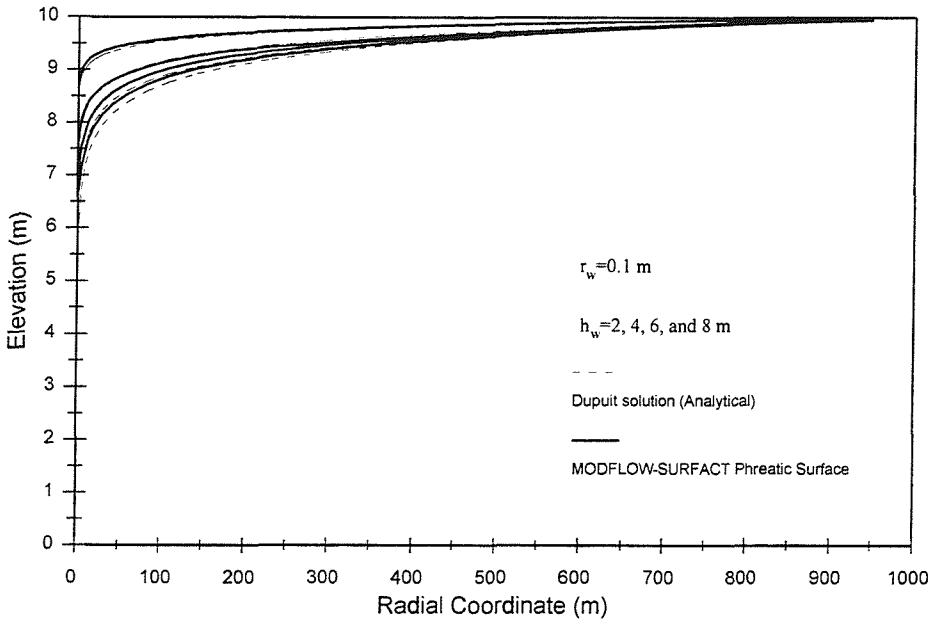

Figure 5.4f Phreatic surface variations to different pumping levels for the 1000m×10m radial-flow problem.

5.2.2 Sensitivity to Well Radius

The sensitivities of the seepage-face and the phreatic-surface positions to changes in the well radius are not so obvious. The phreatic-surface positions decrease as the well radius increases and therefore the seepage-faces decrease (Figure 5.5a and Figure 5.5b). This matches the results predicted by *Clement et al.* (1996), who also observed that variably saturated, radial flow problems seem to be relatively more sensitive to the well radius than to the soil properties. This relative insensitivity reported by *Clement et al.* (1996) was said to be "*one reason why, in spite of using different types of soil characteristics, several workers, including Shamasi and Narasimhan (1991), Cooley (1983) and Taylor and Luthin (1969), were able to model Hall's (1955) experimental (radial flow toward a gravity well in a sand-filled, wedge-shaped box) phreatic-surface data reasonably well, despite the fact that Hall did not report any capillary properties of his soil.*"

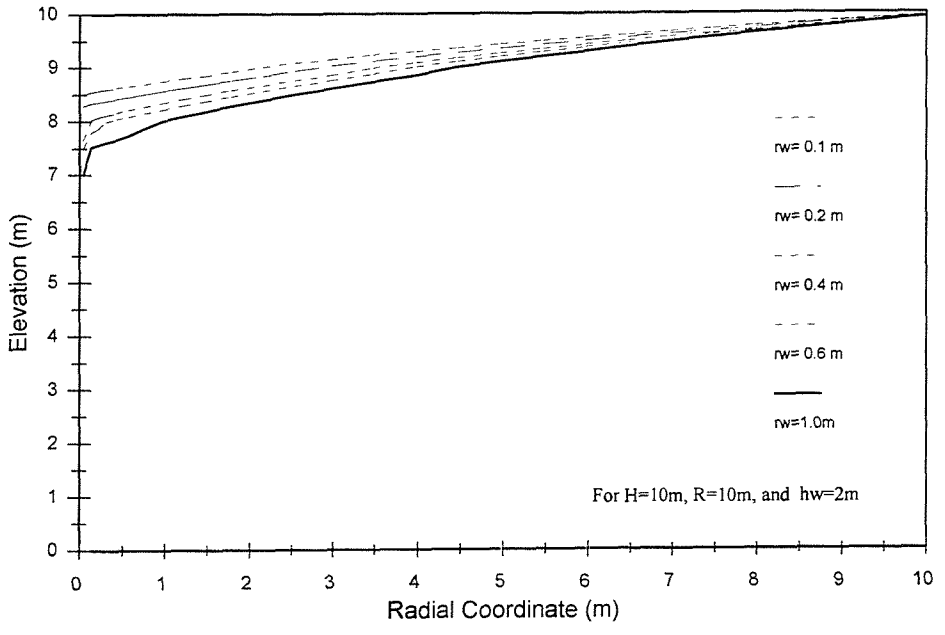

Figure 5.5a Phreatic-surface elevation variation with changing well radius.

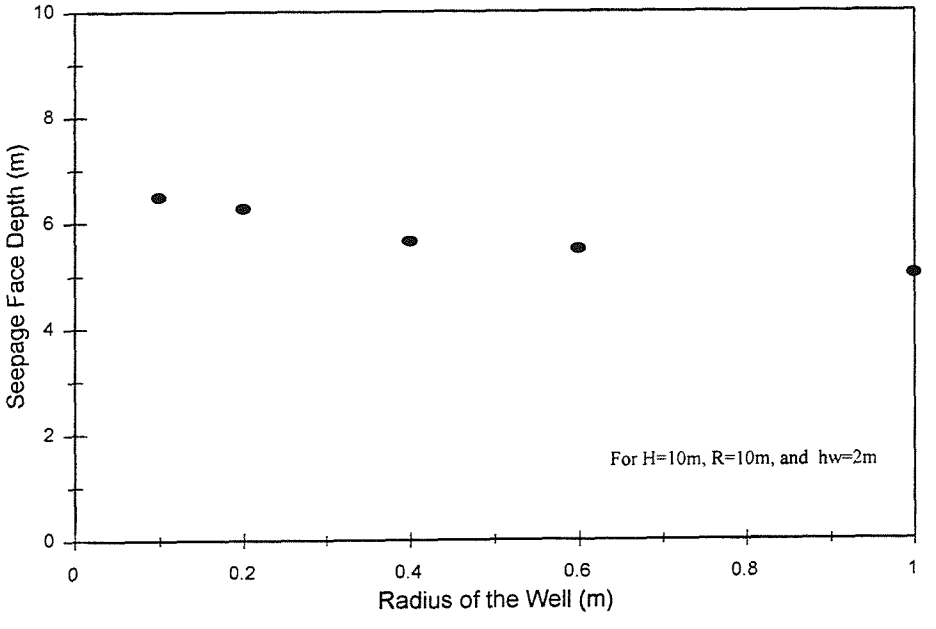

Figure 5.5b Seepage-face depth variation with changing well radius (Seepage-face depth = Phreatic-surface elevation – 2m.)

5.2.3 Influence of Anisotropy

Figure 5.6 shows the effect of soil anisotropy on the phreatic-surfaces and seepage-faces. As the vertical hydraulic conductivity, K_z, decreases the height of the seepage face increases. Figure 5.6 shows the change in seepage-face and phreatic-surface positions between K_h/K_z=1, 5 and 10.

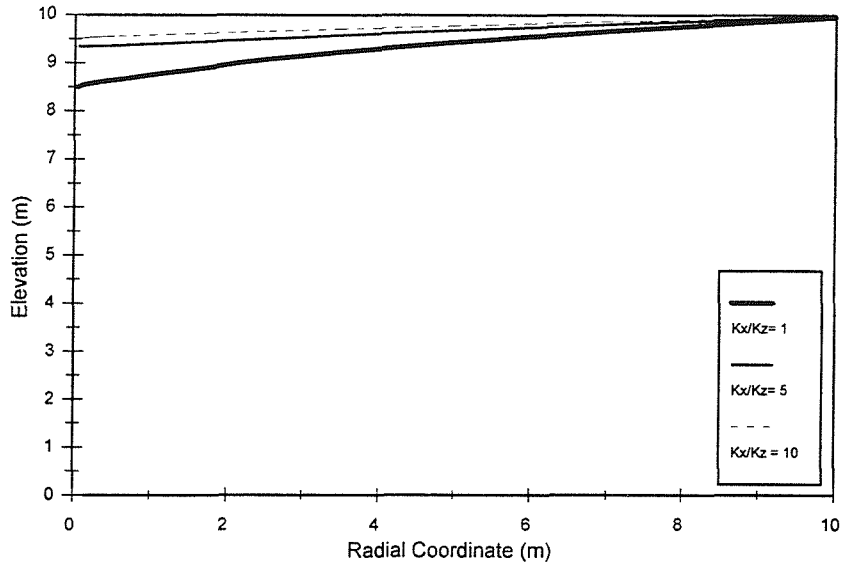

Figure 5.6 Phreatic-surface and seepage-face variation with anisotropy.

5.3 Single Well Investigation- Transient Flow

In spite of the fact that many steady-state seepage face studies have been performed, few have actually covered seepage face in transient flow problems. Many of the transient water table drainage problems are limited to a one-dimensional analysis (*Youngs* and *Aggelides,* 1976; *Sisson et al.*, 1980; and *Watson and Awadalla,* 1985). A few studies have used variably saturated models to investigate two-dimensional ditch drainage processes during a surface infiltration event (*Rubin,* 1968; *Vauclin et al.,* 1979; and *Ahmed et al.,* 1993). According to *Vauclin et al.* (1979), a water table aquifer can be solved correctly only by considering the flows in the entire saturated-unsaturated domain, and that the classical saturated flow approach is unable to determine the transfer time for water in the unsaturated zone.

Vauclin et al. (1975) presented results from both experimental and numerical investigations of transient seepage-face and phreatic-surface behaviour in a two-dimensional Cartesian flow problem. The experimental model of a saturated porous medium was allowed to drain after an immediate drop in the external water table. This sudden drop problem was investigated by measuring the water content and pressure head distribution during the drainage phase. The variably-saturated flow algorithm developed by *Clement et al.* (1996) correctly simulated *Vauclin et al.* (1975) experimental results.

Liggett and Liu (1983) developed a boundary-integral-equation method for solving the two-dimensional, saturated flow equation in homogenous porous media accompanied with transient phreatic-surface and seepage-face boundaries. The method estimates the phreatic surface and the extent of the seepage face based in a two-dimensional saturated flow analysis. Therefore, it ignores the existence of the unsaturated zone.

Clement et al. (1994b) numerically investigated a two-dimensional, transient-drainage, Cartesian-flow problem using fully and variably-saturated flow models. The results for the transient water-table drainage problem shows that the location of the phreatic surface and the height of the seepage face are greatly influenced by the unsaturated zone. Moreover, sensitivity analysis of the soil properties suggested that variations in *van Genuchten's* parameters have a significant influence on the location of the transient phreatic-surface and seepage-face boundaries.

Our objective is to use the variably saturated code, MODFLOW-SURFACT, to investigate the transient flow to a single well pumping from an unconfined aquifer. The investigation will show how the phreatic surface responds to pumping with time and the sensitivity of this to the hydraulic conductivity (K).

5.3.1 Problem Description

As mentioned before, the example from the *Clement et al.* (1996) study was adopted here. A schematic of the problem used in our investigation is shown in Figure 5.7. The dimensions of the quasi-radial flow problems considered in this study are similar to the steady-state flow problem discussed earlier. The top and the base of the flow domain

has no-flow boundaries, and the porous medium is assumed to be homogenous and isotropic with a saturated hydraulic conductivity of K= 1 m/day, specific storage S_s= 0.01m^{-1}, and a porosity of n= 0.40. The water table is initially at the top of the domain and the flow system is at static equilibrium. The water table on the right boundary is maintained at a constant level of H= 10m and the radius of the flow domain that is the distance of influence to one side of the square is 10m. The radius of the well is 0.1m and the external water table at the left face of the domain (in the well) is lowered instantaneously at time t= 0 from z= 10m to z= 2m and maintained at that elevation.

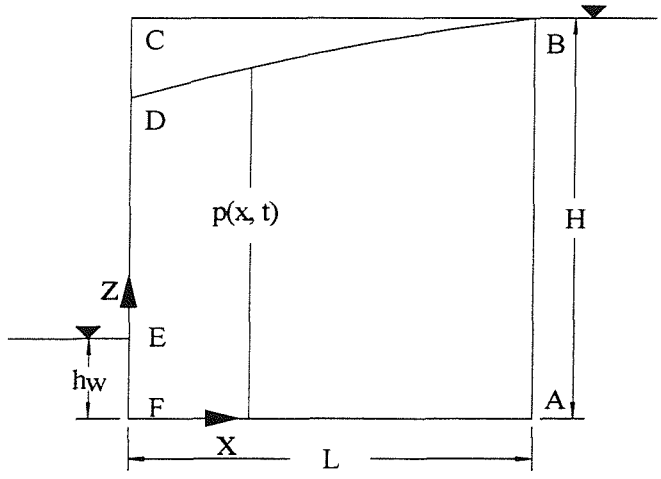

Figure 5.7 Schematic of the flow domain used in all simulations presented in this section (Modified after *Clement et al.*, 1996.)

5.3.2 Flow Model

The governing equation for water seepage in a three-dimensional, variably-saturated porous medium modeled by MODFLOW-SURFACT is as described earlier (equation 4.2). The initial and boundary conditions in general for a variably-saturated, two-dimensional flow problem, shown in Figure 5.7 are as follow

$h = H$ all point (x, z) at $t \leq 0$ (initial condition; hydrostatic equilibrium), (5.1)

$h = H$ along AB, (constant-head boundary), (5.2)

$\frac{\partial h}{\partial z} = 0$ along BC, (no-flow boundary), (5.3)

$h = z$ along CD, (Seepage face boundary), (5.4)

$h = z$ along DE, (seepage-face boundary), (5.5)

$h = h_w$ along EF, (constant-head boundary), and (5.6)

$\frac{\partial h}{\partial z} = 0$ along AF, (no-flow boundary), (5.7)

The nodal spacing in the x, y, and z directions are shown in Figure 5.1. The selection of time step, Δt, is critical step beside the construction of the grid. This is because the values of the space and time discretization strongly influence the numerical results. In general, it is good to use small time steps so that partial differential equation is better approximated. This step is should always be followed by sensitivity analysis. It is recommended to use small time steps at the beginning of the simulation when a stress such as pumping exist, and increases as the simulation progresses. Usually, a multiplier of $\sqrt{2}$ is a good selection to increase the time step as stated by *de Marsily* (1986, page 399). In this research, several trail runs of the model were made using different Δt and the largest possible Δt that does not significantly change the solution selected for the output runs. A simulation time of 10 days was used in our investigations with a variable time step Δt, ranging from 0.0000002 day to 2.3 day (i.e. 100 time steps with 1.2 multiplier.)

5.3.3 Analysis and Results

The instantaneous drop in the external water level (at the well) results in a fast drop in the pressure along the left edge of the domain (well), resulting in the development of large pressure gradients. The effect of this pressure change results in a rapid decline of the phreatic surface at an early stage and a slower decline thereafter. Figure 5.9b shows that specific storage effects are important, especially at early times at which the specific storage accommodates the fast pressure variations within the porous medium. As a result there is a rapid decline in phreatic surface. As *Clement et al.* (1994b) reported, no experimental data has been found in the literature addressing this type of problem. This is possibly because of the great difficulty in carrying out such experiments (transient ones). Although *Liggett and Liu* (1983) analyzed a similar problem using numerical techniques, the approach used ignores transport of water

through the vadose zone and assumes that the phreatic surface acts as the upper (no-flow) boundary of the flow domain.

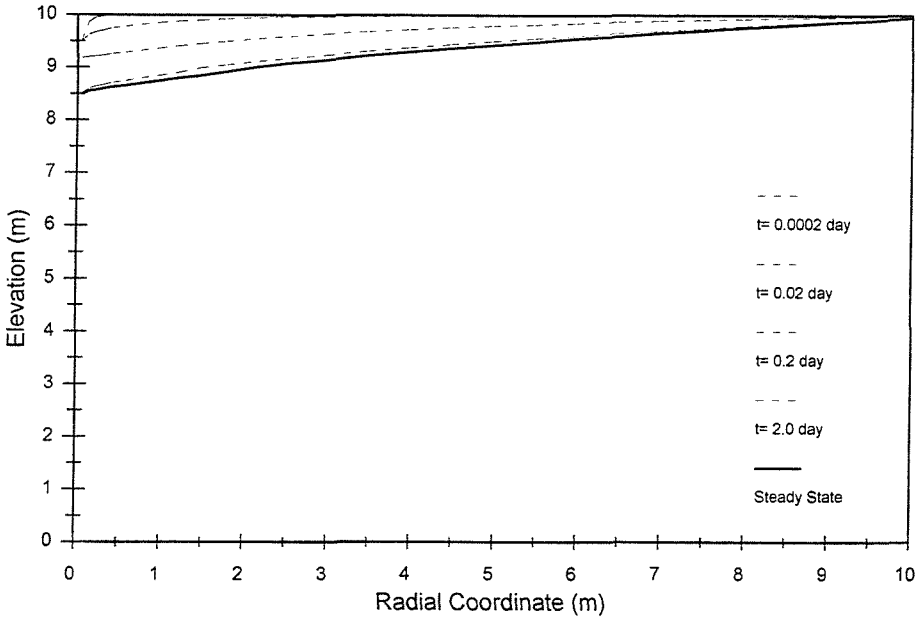

Figure 5.8 Phreatic-surface transient profiles.

Figure 5.8 shows transient profiles of the phreatic surface predicted by MODFLOW-SURFACT. As shown in the figure, the decline of the phreatic surface is quite fast during the early stage, after dropping the water level in the well to 2m. The flow rates vs. time behaviour distributions of the various processes are shown in Figure 5.9a. The figure demonstrates that the early storage is controlled by the specific storage effect which contains the quick pressure variations within the porous medium and the resulting fast decline in the phreatic surface. Nevertheless, as time progresses, the specific storage effect decreases rapidly and its effect is almost negligible after 8.0day. It can be seen from Figure 5.9b, which is plotted to a different scale that, as the time progresses, the outflow rate decreases and the inflow rate increases and come closer to each other to reach a constant steady-state value.

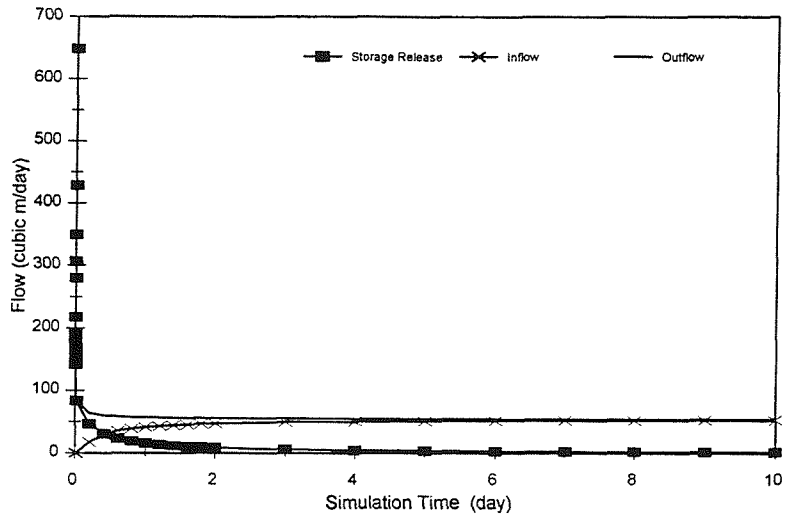

Figure 5.9a Flow corresponding to different processes.

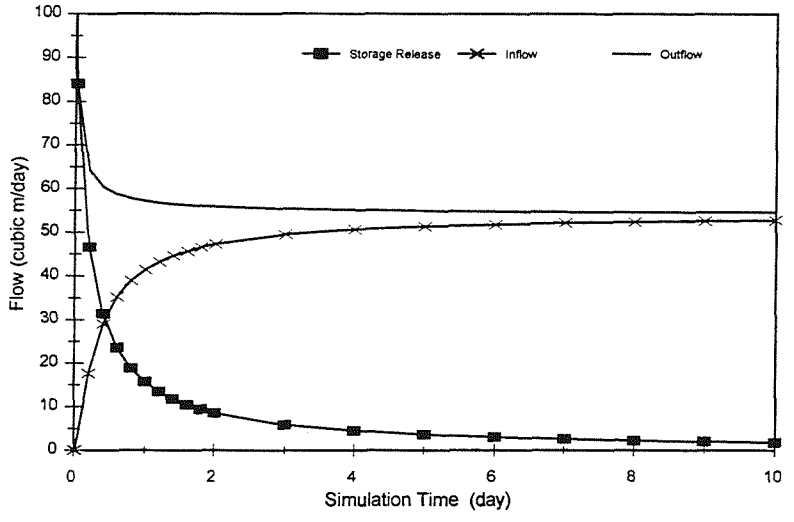

Figure 5.9b Flow corresponding to different processes-different scale.

5.3.4 Sensitivity to Hydraulic Conductivity (*K*)

Figure 5.10 shows the locations of the transient phreatic surface at time t= 0.02day, for values of hydraulic conductivity K= 0.1, 1.0, 10 and 20 m/day, respectively. The figure shows that as the value of the hydraulic conductivity is increased, the faster the soil tends to drain, and therefore, the location of the phreatic surface is lowered more rapidly. This result, using the pseudo-soil moisture content/pore pressure function, agrees with that predicted by *Clement et al.* (1994b).

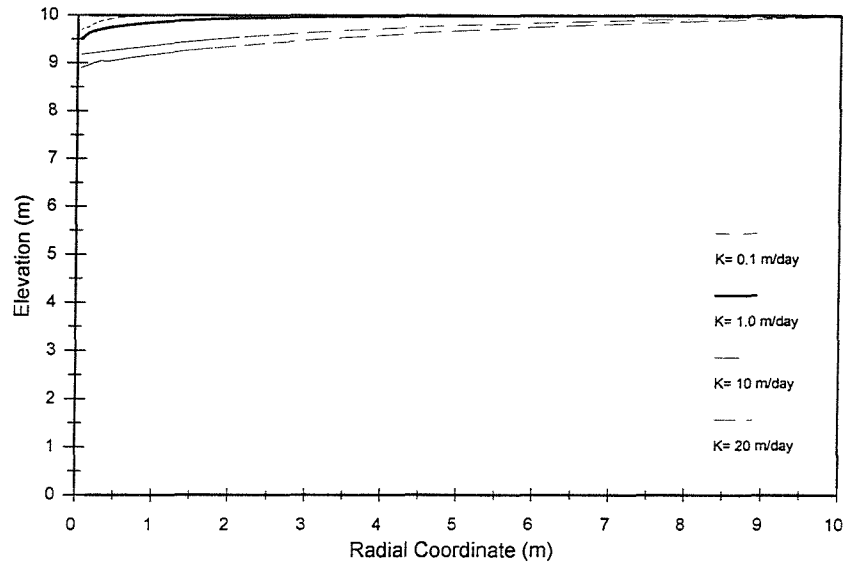

Figure 5.10a Phreatic-surface variation at t= 0.02day related with changes in hydraulic conductivity (K).

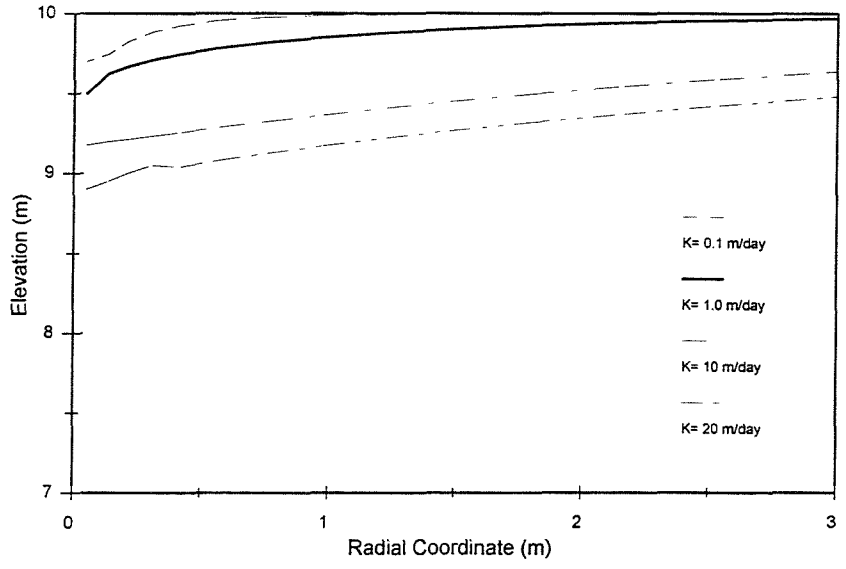

Figure 5.10b Phreatic-surface variation at t= 0.02day related with changes in hydraulic conductivity (K) (enlarged scale).

5.4 Multiple-Well Investigation – Steady-State Flow

When wells are spaced at distances smaller than the radius of influence R, they affect each other's drawdown and flow rate. The drawdown at any point in a confined aquifer affected by a simultaneous pumping of two or more wells may be estimated from the algebraic sum of drawdowns caused by each well. This is known as the principle of

superposition, which is valid for linear, homogenous, partial differential equations and greatly expands the range of problems for which analytical solutions can be obtained in confined aquifers. The principle of superposition can be used in unconfined aquifer with some error, as long as the water table drawdown is small compared to the aquifer as stated by *Bouwer* (1978, page 205):

"*Superposition is technically correct only for confined aquifers, where T is not affected by the height of the piezometric surface. For unconfined aquifers, T varies directly with H, which introduce an error when superimposing several individual flow systems because T in the composite system will then differ from T in the individual systems. As long as the water-table drawdowns are small compared to the height of the aquifer, however, the error will be small.*"

In steady-state flow in a phreatic aquifer, employing the *Dupuit's* assumptions, the partial differential equation (3.34) with $\partial h/\partial t = 0$ is linear in h^2, therefore principle of superposition is applied to h^2 (see next section). It will be interesting to examine the superposition numerically in this research beside the effect of multiple wells system acting as an array on seepage face.

In hydrogeological practice, it is far more common to analyze situations with more than one well operating. One important practical application is dewatering systems for groundwater control. These consist of a number of wells that are pumped to provide reduction of groundwater levels. One of the major problems in designing such systems is to determine the number and spacing of wells required to reduce the groundwater level to the desired levels. Therefore, it is important to determine the relationship between drawdown caused by a group of wells and the flow from such systems. However, the drawdown distance curve based on *Dupuit-Forchheimer* needs to be modified to take account of the seepage face effect.

5.4.1 Drawdown Calculation: Analytical Solution

The methods most commonly used for the design of dewatering systems are basically those presented by *Mansur* and *Kaufman* (1962). When n wells are pumping in a phreatic aquifer with a horizontal bottom, and the *Dupuit* assumptions are used to

determine the drawdown for steady state flow in an observation well. The principle of superposition with respect to h^2 leads to

$$H^2 - h^2 = \frac{1}{\pi K} \sum_{i=1}^{i=n_w} Q_{wi} \ln \frac{R_i}{r_i} \tag{5.8}$$

where Q_{wi} is the flow rate from the i^{th} well; R_i is the radius of influence for i^{th} well; r_i is the distance from the i^{th} well to the point at which drawdown is computed; and n_w is the number of the wells in the system. (see Figure 5.11).

The head h_{wj} at any well, for example, well j, in a system of n_w wells can be determined from the following equation

$$H^2 - h_{wj}^2 = \frac{1}{\pi K} \left(Q_{wj} \ln \frac{R_j}{r_{wj}} + \sum_{i=1}^{i=n_w-1} Q_{wi} \ln \frac{R_i}{r_{i,j}} \right) \tag{5.9}$$

where Q_{wj} is the flow rate from the j^{th} well; R_j is the radius of influence of well j; r_{wj} is the effective well radius of well j; and $r_{i,j}$ is the distance from each well to well j. Q_{wi} and R_i are as defined previously.

Using equation 5.9 the head at the centre of a circular array of equally spaced wells, h_c, with equal flow ratess, Q_w, assuming that the wells fully-penetrate the aquifer, may be expressed as

$$H^2 - h_c^2 = \frac{F_c}{\pi K} \quad \text{and} \quad F_c = n_w Q_w \ln \frac{R}{r_c} \tag{5.10}$$

Equation 5.9 may also be used to determine the head at the well. *Leonards* (1962, page 303) gives the following expression for computing the head at the well

$$H^2 - h_w^2 = \frac{F_w}{\pi K} \quad \text{and} \quad F_w = Q_w \ln \frac{R^{n_w}}{n_w r_w r_c^{(n_w - 1)}} \tag{5.11}$$

where n_w is number of wells ; Q_w is the flow per well; F_c and F_w are factors which depend upon the flow from and position of each well in the system and r_c is the circular array radius. (Note some simple algebra suggests that n_w should be omitted from equation 5.11).

5.4.2 Drawdown Calculation: Numerical Solution

The flow towards a circular array of wells pumping from an ideal unconfined aquifer has been investigated numerically using MODFLOW-SURFACT. The following assumptions are made

- The aquifer is homogenous and isotropic.
- The aquifer lies on a horizontal impermeable stratum.
- The aquifer is saturated below the phreatic surface and the phreatic surface is uniform prior to pumping throughout the aquifer.
- Capillary effects are negligible and water is released by decline in piezometric head.
- Steady-state conditions are reached and the pumping rate is constant.
- There is no rainfall recharge or evaporation.
- The wells penetrate the entire aquifer.

The flow domain and aquifer parameters for the circular array model are shown in Figure 5.11. The wells are placed in a circular array with an appropriate radius, r_c, so that the drawdown effect due to pumping appears at the other neighbouring wells. The water level in the wells has been drawn down to a small level compared to the aquifer depth so that we can observe a large seepage face height.

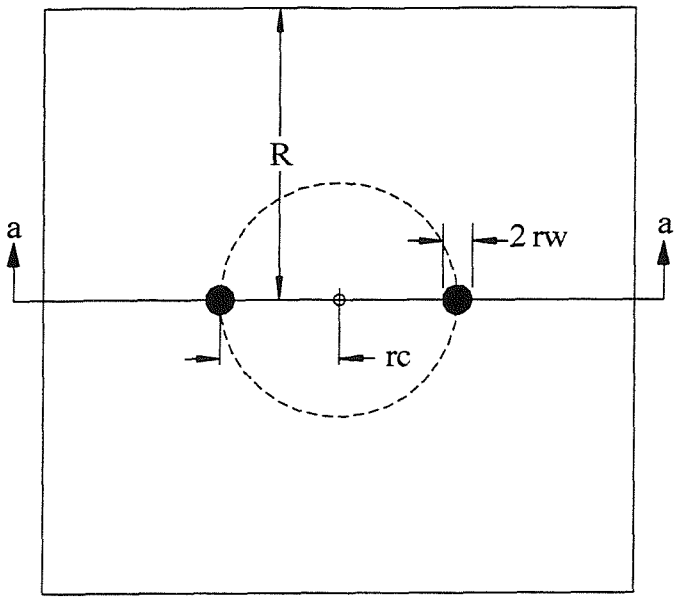

Plan view of the circular array (*Note: the example used is for 2 wells*)

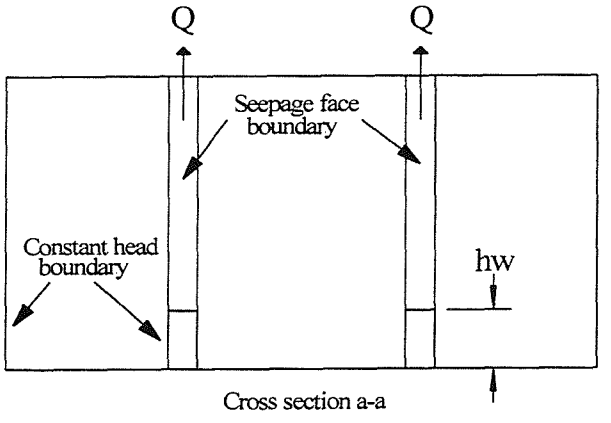

R= 1000m
H= 20m
K= 1.0 m/day

hw= 2, 4, 6, and 8 m
rc = 10m
rw = 0.1m

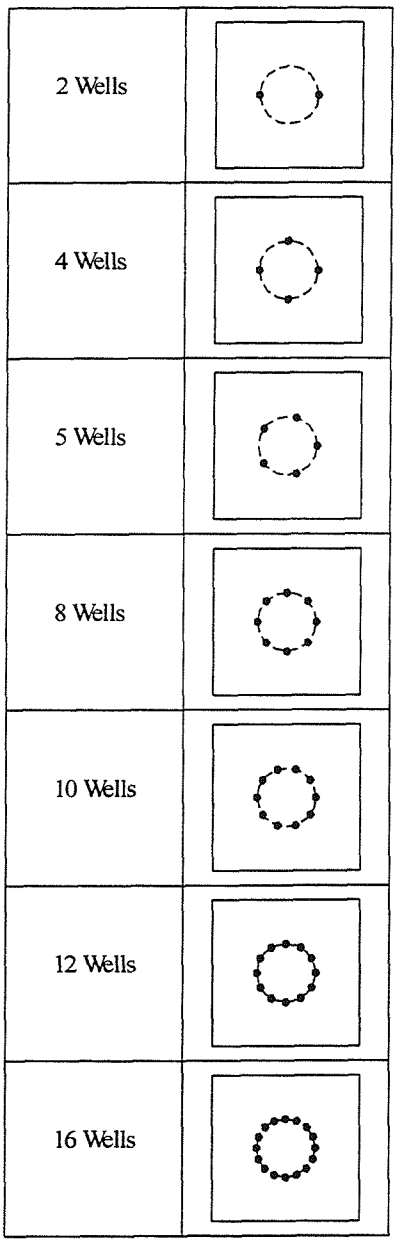

Figure 5.11 The flow domain and aquifer parameters for the circular array model.

The unconfined aquifer domain consists of 20 layers with 1m thickness and a radius of influence at 1000m. A circular array of deep wells with a radius of 10m is located at the domain center. The number of wells is increased for each case as shown in Figure 5.11 and Table 5.2. In each case, all wells have the same flow rate. This is done by fixing the head in the wells to the same level. Boundary conditions include a constant head of 20m, which is the initial water table level and constant heads representing

pumping levels in the well. Moreover, seepage-face boundary conditions are applied to the well cells above the pumping level in order to capture the seepage surface.

The problems described have been solved using the analytical solution, which is based on *Dupuit-Forchheimer* assumptions and ignores the seepage face, and by using the code MODFLOW-SURFACT. The phreatic surfaces computed using MODFLOW-SURFACT with different pumping levels are shown in Figure 5.12. Table 5.2 shows a summary of the results using analytical and numerical methods.

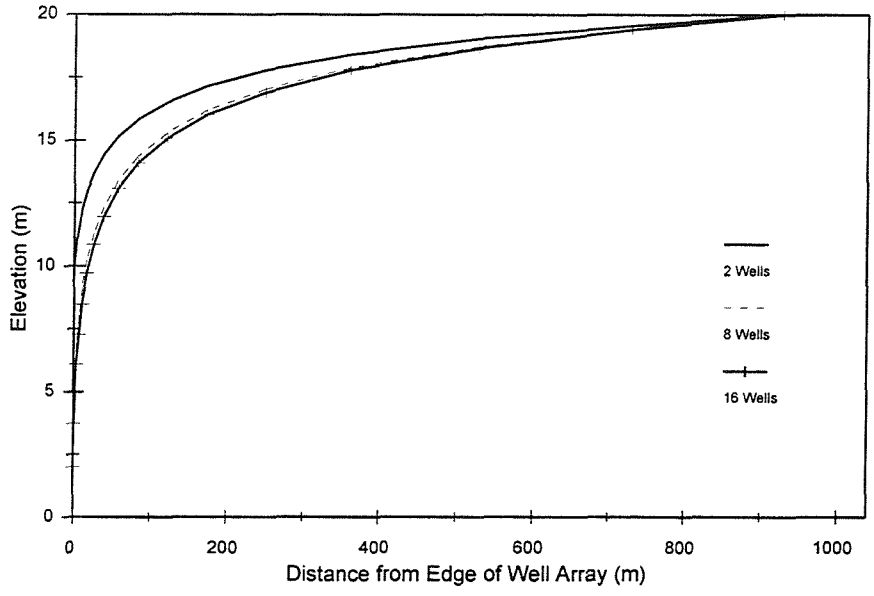

Figure 5.12 The phreatic surfaces computed using MODFLOW-SURFACT for an array of wells consisting of 2, 8, and 16 wells along cross section a-a shown in Figure 5.11.

Table 5.2 Analytical and numerical results summary (*Ana.* =Analytical and *Num.*= Numerical).

Pumping level at the wells is 2m										
n_w	r_c	h_c (m)			Q_{total} (m^3/day)		Q_w (m^3/day)		**Error (%) Q_{total}**	**Error (%) h_c**
		Ana.	*Num.*		*Ana.*	*Num.*	*Ana.*	*Num.*		
			Upper	*bottom*						
2	10	10.32	10.53	10.28	200.18	201.39	100.09	100.70	0.60	2.00
4	10	7.19	7.35	7.25	237.57	240.37	59.39	60.09	1.18	2.22
5	10	6.32	6.45	6.39	245.59	248.31	49.12	49.66	1.11	2.01
8	10	4.77	4.90	4.87	257.35	260.82	32.17	32.60	1.35	2.64
10	10	4.17	4.30	4.29	261.02	263.44	26.10	26.34	0.93	3.26
12	10	3.74	3.92	3.92	263.35	269.47	21.95	22.46	2.33	4.94
16	10	3.17	3.31	3.31	266.03	269.47	16.63	16.84	1.29	4.62

Pumping level at the wells is 4m										
n_w	r_c	h_c (m)			Q_{total} (m^3/day)		Q_w (m^3/day)		**Error (%) Q_{total}**	**Error (%) h_c**
		Ana.	*Num.*		*Ana.*	*Num.*	*Ana.*	*Num.*		
			Upper	*bottom*						
2	10	10.74	10.92	10.70	194.12	195.34	97.06	97.67	0.63	1.62
4	10	7.89	7.99	7.90	230.37	232.47	57.59	58.12	0.91	1.28
5	10	7.14	7.27	7.20	238.15	240.72	47.63	48.14	1.08	1.95
8	10	5.85	5.91	5.88	249.55	252.59	31.19	31.57	1.22	1.02
10	10	5.38	5.44	5.42	253.11	255.43	25.31	25.54	0.91	1.03
12	10	5.07	5.17	5.16	255.37	259.48	21.28	21.62	1.61	2.12
16	10	4.67	4.78	4.77	257.97	260.46	16.12	16.28	0.96	2.34
Pumping level at the wells is 6m										
n_w	r_c	h_c (m)			Q_{total} (m^3/day)		Q_w (m^3/day)		**Error (%) Q_{total}**	**Error (%) h_c**
		Ana.	*Num.*		*Ana.*	*Num.*	*Ana.*	*Num.*		
			Upper	*bottom*						
2	10	11.41	11.57	11.38	184.01	184.82	92.00	92.41	0.81	1.36
4	10	8.94	9.06	8.97	218.37	220.03	54.59	55.01	1.66	1.38
5	10	8.31	8.39	8.33	225.74	228.38	45.15	45.68	2.64	0.95
8	10	7.30	7.37	7.34	236.55	238.79	29.57	29.85	2.24	1.07
10	10	6.95	7.03	6.99	239.93	241.15	23.99	24.12	1.22	1.13
12	10	6.72	6.83	6.80	242.07	245.61	20.17	20.47	3.54	1.62
16	10	6.45	6.54	6.52	244.53	246.08	15.28	15.38	1.55	1.50
Pumping level at the wells is 8m										
n_w	r_c	h_c (m)			Q_{total} (m^3/day)		Q_w (m^3/day)		**Error (%) Q_{total}**	**Error (%) h_c**
		Ana.	*Num.*		*Ana.*	*Num.*	*Ana.*	*Num.*		
			Upper	*bottom*						
2	10	12.29	12.43	12.28	169.85	170.74	84.93	85.37	0.89	1.16
4	10	10.22	10.31	10.23	201.58	205.32	50.39	51.33	3.74	0.82
5	10	9.72	9.81	9.75	208.38	210.71	41.68	42.14	2.33	0.90
8	10	8.94	9.03	8.98	218.35	220.98	27.29	27.62	2.63	1.01
10	10	8.68	8.76	8.71	221.48	222.41	22.15	22.24	0.93	0.91
12	10	8.51	8.60	8.56	223.44	227.18	18.62	18.93	3.74	1.00
16	10	8.31	8.36	8.34	225.72	227.54	14.11	14.22	1.82	0.56

The phreatic surface predicted by MODFLOW-SURFACT, at the well array center, is larger than that predicted by the *Dupuit-Forchheimer* model as the result of the model calculation taking accurate account of three-dimensional effects. It was found that the piezometric head at the bottom of the model aquifer coincided with the conventional method of superposition, *Mansur* and *Kaufman* (1962), that is based on *Dupuit-Forchheimer model.* The results are shown in Table 4.2 for the well array center. The flow predictions matched that calculated with the *Dupuit-Forchheimer model* provided

that the correction for well radius proposed by *Beljian* (1988), $0.2\Delta x$, was applied (see page 65). The conventional method of superposition gave results that agreed with the model head calculations at the aquifer base as shown in section 5.2. However, these needed to be elevated by a correction as in Figure 5.13 to match the level of the free surface. The additional flow computed by the variably saturated flow model may be attributed to water transport through the vadose zone.

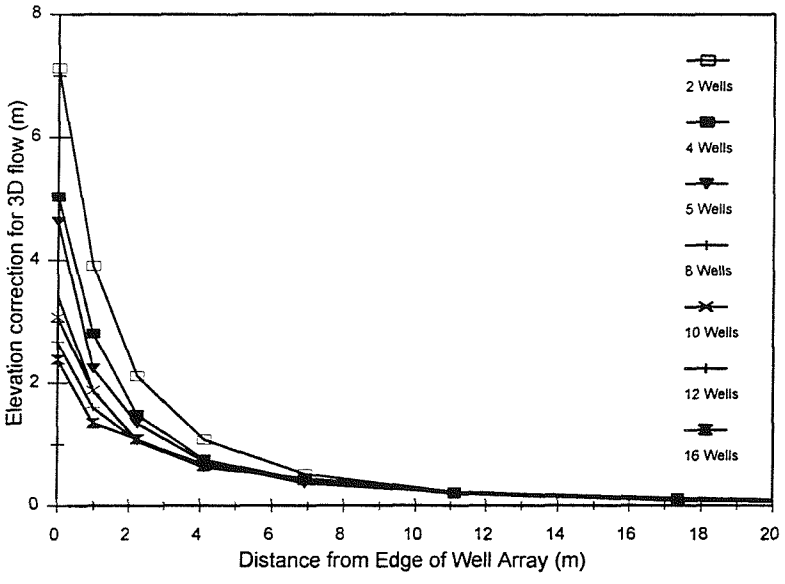

Figure 5.13a Correction needed to the conventional method of superposition (equation 5.9) when h_w=2m.

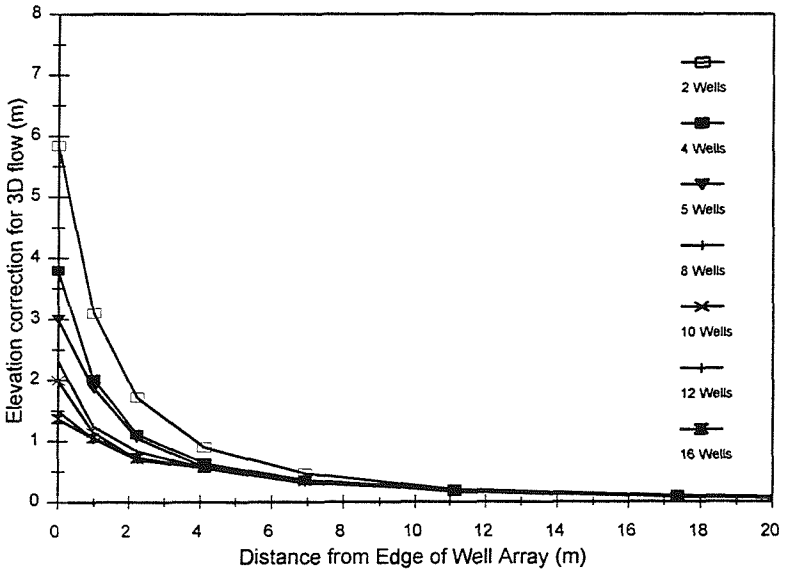

Figure 5.13b Correction needed to the conventional method of superposition (equation 5.9) when h_w=4m.

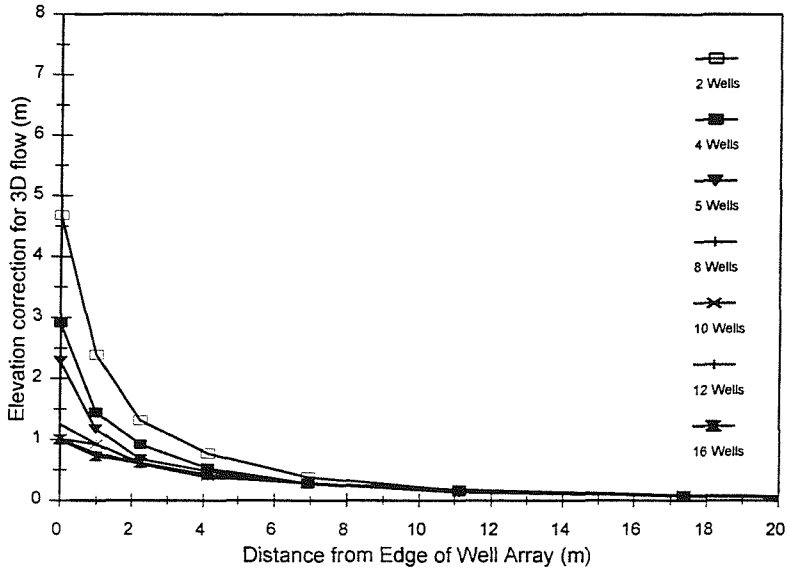

Figure 5.13c Correction needed to the conventional method of superposition (equation 5.9) when h_w=6m.

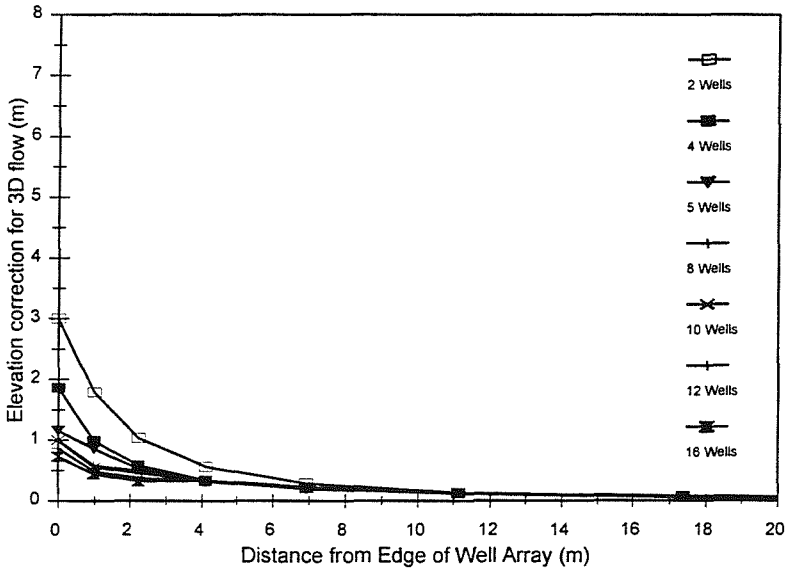

Figure 5.13d Correction needed to the conventional method of superposition (equation 5.9) when h_w=8m.

Figure 5.13 shows that as the number of wells increases the elevation correction for the *Dupuit-Forchheimer* solution decreases. This means that, the seepage surface is eliminated by the inter-action of the wells in the systems and it thus appears that the seepage face surface phenomenon is not a significant factor in the performance of an array of wells (*Al-Thani* and *White*, 2000).

5.5 Summary

The set of modules that has been developed and incorporated into the USGS groundwater flow simulation code, MODFLOW, by *HydroGeoLogic*, Inc. have proved to be useful. The enhancement of the capability of modelling an unconfined aquifer using the governing equations for the variably-saturated flow in a porous medium system to overcome MODFLOW's difficulties with drying and rewetting of cells is particularly valuable. The success of MODFLOW-SURFACT in simulating a variety of problems gives confidence to its application for modeling multiple well arrays.

The investigation of a steady-state, radial-flow problem show that the cone of depression predicted by MODFLOW-SURFACT is much smaller than that predicted by the *Dupuit-Forchheimer* model as the result of the calculation taking accurate account of three-dimensional effects. It was found that the piezometric head at the base of the model aquifer, in the case of a single well, coincided with *Dupuit-Forchheimer* analytical model, as did the flow predictions, provided that the correction for well radius proposed by *Beljian* (1988), 0.2 Δx, was applied. However, piezometric heads needed to be elevated by a correction to obtain a match with the level of the free surface. This correction, presented by an example in section 5.4, plays an important role when designing remediation systems for contaminated aquifers using pump-and-treat systems as concluded by *Clement et al.* (1996):

"*Seepage faces and associated rises in phreatic surfaces are usually beneficial to pump-and-treat schemes since they expose a larger volume of soil to flushing flows, which will ease the removal of contaminants during clean-up efforts. Furthermore, at higher pumping rates the water level inside a well decrease, but the volume exposed to the flow remains relatively unchanged over a significant variation of drawdown due to the seepage face effect. This is very important since the remediation wells are usually installed in the most contaminated parts of the site.*"

Because the transient seepage-face plays an important role in the transport of water near groundwater-surface water boundaries, the investigation was extended to cover transient flow. The results show that a contribution from the storage release is dominant only for a short duration in early time steps and decreases rapidly afterward.

The investigation of multiple well systems shows similar results to those found with a single well configuration. The conventional method of superposition gave results that agreed with the model head calculations at the aquifer base. However, these needed to be elevated by a correction height to match the level of the free surface in the models. The additional flow computed by the variably saturated flow model may be attributed to water transport through the unsaturated zone. The major conclusion from using multiple well configurations is that as the number of wells increases the elevation correction for *Dupuit-Forchheimer* solution decreases. Proven numerically as shown in Figure 5.13 the seepage surface is eliminated by the inter-action of the wells in the systems and it appears that the seepage face surface phenomenon is not a significant factor in the performance of an array of wells. Therefore, the advantage of exposing larger volume of soil to flushing flows found in single well remediation systems is not applicable for multiple well systems.

This numerical investigation has indicated that MODFLOW-SURFACT may be applied with some confidence to unconfined aquifers pumped by multiple deep wells such as those used for pump-and-treat systems. The work indicates that design predictions can be made using simple conventional algebraic models supported by correction schemes derived from numerical studies.

The results of the study of individual (using pseudo soil) and multiple well systems are an original contribution to the subject area. The next chapter will review a concept related to the seepage face, the limiting gradient concept, for estimating maximum well yields and its implication. Numerical investigations will be carried out to present results of three-dimensional analyses that will give support to the approach.

Chapter (6)

Application to Well Yield Estimation

6.1 Introduction

Deep wells are used in groundwater control systems to prevent an excavation below the water table from flooding. When water is taken from a homogeneous soil using a deep well, the water table is lowered in a circular area. For a fully penetrating well in an unconfined aquifer, the maximum possible pumping rate is accomplished by maintaining the water level inside the well at the bottom, see equation 2.10. This will create a seepage face along the pumping well, which will affect the drawdown of the water table in the aquifer. Moreover, the presence of the seepage face (or an upper limit of drawdown around a well) is related to the yield or flow from the well through the hydraulic gradient at the entrance along the cylindrical face of the well, see equation 4.11. The prediction of the maximum individual well yield is of great importance in the design of groundwater control systems, but has received relatively little research attention. Understanding the characteristic of the field of groundwater flow near a fully drained well in an unconfined aquifer is vital when designing and operating dewatering systems. Besides the height of seepage-face, or the maximum possible drawdown of a gravity well, the form of the entire free surface is often of great interest. This chapter will explore the implications of equation 2.10 and 4.11 in order to review the limiting gradient concept and its implications for estimating maximum well yields. The review is supported by numerical modelling using MODFLOW-SURFACT.

6.2 Background

In the German literature, the existence of a seepage-face, and thus of an upper limit to the drawdown around a well is often referred to as a limiting gradient. The limiting gradient may be defined as a certain maximum average hydraulic gradient of entrance along the cylindrical face of the well. *Sichardt* (1928) identified the possibility of the existence a limiting gradient, i, and thought that it might be related to hydraulic conductivity, K. His results, Figure 6.1, appear to be based on field data from multiple well groundwater systems combined with laboratory model tests on a single well. There are only nine data supporting the results and the range of the hydraulic conductivity is limited to 5.3×10^{-3} to 10^{-4} m/sec.

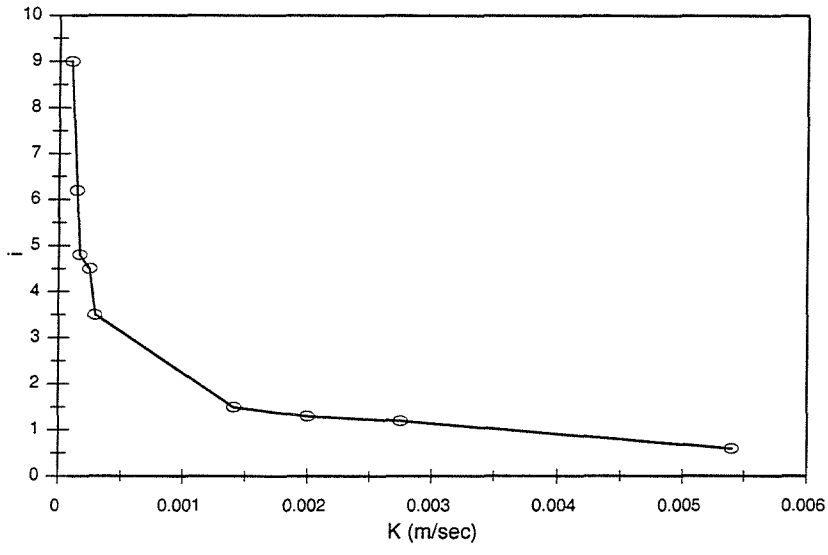

Figure 6.1 Relation between the slope at which the groundwater approaches the well face and the hydraulic conductivity as presented by *Sichardt* (1928).

Several authors, such as *Powers* (1992) and *Hausmann* (1990), quote *Sichardt's* algebraic relationship which is based on the data in Figure 6.1 for estimating the maximum average hydraulic gradient at entry into a well,

$$i_{max} = \frac{1}{15\sqrt{K}} \qquad (6.1)$$

Darcy's law can be applied to the boundary of an individual well to give

$$Q_{\max} = AKi_{\max} \tag{6.2}$$

where Q_{max} is the individual well yield; A is the area of the seepage face, or wetted cylinder of aquifer material remaining at the screen; and i_{max} is the maximum hydraulic gradient of entrance along the cylindrical face of the well. Thus, the yield from an individual well Q_{max} proposed by *Sichardt* (1928) may be expressed as

$$Q_{\max} = 2\pi r_w h_s K i_{\max} = 2\pi r_w h_s K \frac{1}{15\sqrt{K}} = 0.133\pi r_w h_s \sqrt{K} \tag{6.3}$$

Application of this formula is the basis of the design chart, Figure 6.2, used in CIRIA 113 report (*Somerville*, 1986, Design Chart 5). Moreover, equation 6.3 gives similar results to the limiting screen entrance velocity approach advocated in the water supply industry for well design in aquifers of hydraulic conductivity 2.3×10^{-4} to 2.8×10^{-3} m/sec (*Howsam et al.*, 1995.)

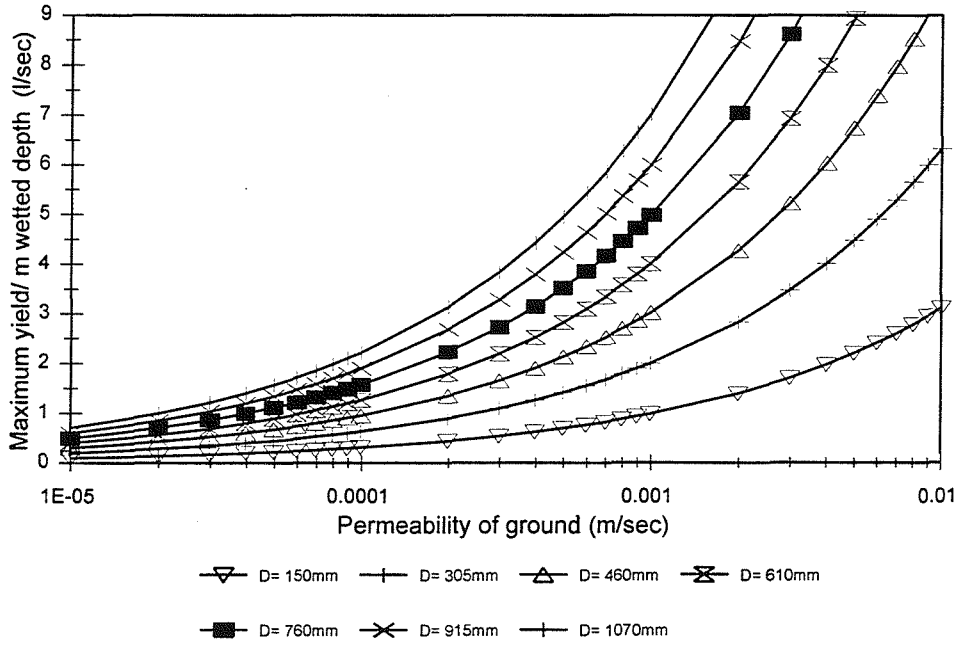

Figure 6.2 Design chart for maximum well yields, D = Diameter of well. (Reproduced after *Somerville*, 1986, CIRIA 133.)

Zee et al. (1957), as introduced in the literature review (see Chapters 2 and 4), collected a large quantity of data from laboratory tests on a single well. These were carried out to investigate the magnitude of the seepage surface. Based on the experimental results and the data from others, which relates h_s to h_w and Q/Kr_w^2, *Zee et al.* (1957) produced a graphical relationship between these parameters shown in Figure 2.8. As shown in Chapter 4 (equation 4.11), the fresh analysis of the data, gives approximately

$$i = 1.25\left(\frac{h_s - h_w}{r_w}\right)^{0.53} \tag{6.4}$$

Equation 6.4 has been further verified by work reported in this thesis (see section 4.6.2). For a fully drained well h_w will be zero and thus equation 6.4 may be rewritten as

$$i_{\max} = 1.25\left(\frac{h_s}{r_w}\right)^{0.53} \tag{6.5}$$

Assuming i_{max} occurs when h_w=0. Therefore, the maximum yield from an individual well, Q, implied by the work of *Zee et al.* (1957) is

$$Q_{\max} = 2.50\pi r_w h_s K\left(\frac{h_s}{r_w}\right)^{0.53} \tag{6.6}$$

Brauns (1981) studied the problem of assessing the maximum possible drawdown of a fully drained gravity well that penetrates a homogenous soil layer of a finite depth, using a finite-element program to perform systematic numerical analysis. The *Brauns result*, which depends on the geometrical boundary conditions, shows that the height of the seepage face may vary in a wide range. Thus, the "lump values which are given in the literature, e.g. h_s/H=0.5, are unfound and indefensible". Table 6.1 summarizes the available solutions for the maximum drawdown as reviewed by *Brauns*.

Table 6.1 Summary of the available solutions for the maximum drawdown (After *Brauns,* 1981.)

Author	Method	Solution	Eq.
Brauns (1981)	Combining the maximum gradient of entrance after *Sichardt* (equation 6.1) with *Dupuit's* formula for well yield	$\frac{h_s}{H}=\sqrt{\left(\frac{1}{15\sqrt{K}}\frac{r_w}{R}\frac{R}{H}\ln\left(\frac{R}{r_w}\right)\right)^2+1}-\frac{1}{15\sqrt{K}}\frac{r_w}{R}\frac{R}{H}\ln\left(\frac{R}{r_w}\right)$	6.7
Boulton (1951)	Relaxation method	$\frac{h_s}{H}=1-\frac{\xi_0}{2\ln\frac{R}{r_w}}$ where ξ_0 is a factor depending on ratio r_w/H to some extent, for common geometrical conditions ξ_0 is approximately 3.75. * *Babbitt and Caldwell* (1948) gave similar relation using electric-analogy tests.	6.8
Kozeny (1953)	Using the assumption that the maximum possible entrance velocity of the water is equal to K	$\frac{h_s}{H}=\frac{r_w}{R}\frac{R}{H}\ln\left(\frac{R}{r_w}\right)\left[\sqrt{1+\left(\frac{H}{R}\frac{R}{r_w}\frac{1}{\ln\left(\frac{R}{r_w}\right)}\right)^2}-1\right]$	6.9
Boreli (1955)	Relaxation method	$\frac{h_s}{H}=1-\frac{\ln\left(\frac{R}{H}\right)+2.3}{\ln\left(\frac{R}{r_w}\right)}\left[0.13\ln\left(\frac{R}{r_w}\right)-0.0123\left(\ln\left(\frac{R}{r_w}\right)-2.3\right)^2\right]$	6.10
Hall (1955)	Relaxation method and sand tanks	$\frac{h_s}{H}=\frac{1}{\left(1+0.02\ln\left(\frac{R}{r_w}\right)\right)\left(1+5\frac{r_w}{R}\frac{R}{H}\right)}$	6.11
Heinrich (1964)	Approximative analytical solution in the explicit form	$\frac{h_s}{H}=\frac{\ln\left[\frac{1}{2}\left(\frac{R}{r_w}+1\right)\right]}{\ln\left[\frac{1}{2}\frac{R}{r_w}\left(\frac{R}{r_w}+1\right)\right]}$	6.12

Roberts (1988) produced the funnel diagram as a tool for the design of groundwater control systems, Figure 6.3. The boundary of demarcation between ejectors and wells , is supported by a one-dimensional theory that is based on the concept of the limiting gradient. This procedure shifts the design emphasis away from the body of the aquifer to the conditions near the well. The limits in Figure 6.3, are found to depend primarily on the sub-strata hydraulic conductivity and the drawdown of the water table required. Apart from the economic limits on the effective range of application for dewatering

equipment, physical effects also become significant as the limits are approached. For soils with low hydraulic conductivity, surface tension effects may adversely affect drawdowns. On the other hand, turbulence may lead to excessive formation losses, thus restricting drawdown in soils with high hydraulic conductivity. *Roberts* concluded that the limiting gradient concept provides a simple and effective model for estimating the behaviour of dewatering systems in both idealised homogenous and inhomogeneous anisotropic conditions.

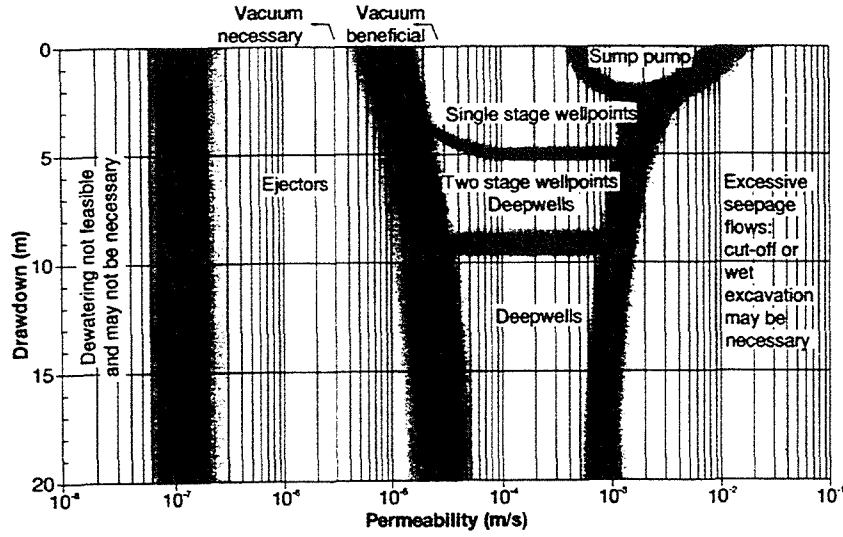

Figure 6.3 Range of application of dewatering techniques related to hydraulic conductivity and drawdown. (*Preene et al.*, 2000.)

Gefell et al. (1994) described *Kozeny's* (1953) method for predicting the maximum water table drawdown at a fully penetrating pumping well in an unconfined aquifer. The method was confirmed by using a physical model designed to constrain the three geometric parameters that control the maximum water-table drawdown; (1) the effective radius of the well; (2) the initial saturated thickness of the aquifer; and (3) the radius of influence. According to *Gefell et al.*, *Kozeny* (1953) theorised that the water table adjacent to the borehole immediately outside the well would decline to a predictable fraction of the initial saturated thickness. Furthermore, achieving a water table drawdown greater than approximately 30-35 percent of the initial aquifer thickness may be physically impossible for a typical constructed well.

Based on *Kozenys's* analysis, *Gefell et al.* (1994) suggested that a unit (i.e. 1/1) hydraulic gradient represented gravity drainage in an unconfined aquifer along the seepage face. Thus, the maximum potential flow to the well can be expressed by substituting unity for i_{max} in equation 6.2

$$Q_{\max} = AK = 2\pi r_w h_s K \tag{6.13}$$

This assumption of a constant hydraulic gradient throughout the seepage face is incorrect, because the horizontal hydraulic gradient at the seepage face in neither uniform nor limited by a maximum of unity. Only the vertical head gradient in an unconfined aquifer cannot exceed unity.

Theoretically, the free surface enters the seepage face tangentially (*Boulton*, 1951), and since the free surface is a flowline in steady state, the horizontal hydraulic gradient at the top of the seepage face is zero. The horizontal hydraulic gradient increases with depth to reach a maximum that can be, and often is, notably greater than unity. Consider an example where $H > (R-r_w)$ and $h_w=0$, in this case the average horizontal head gradient along the base of the aquifer is greater than unity. Moreover, since the head gradient increases when r decreases, it is certainly greater than unity when entering the well, (*Kawecki*, 1994). *Gefell et al.* (1994) also presented *Kozeny's* graphical technique, with additions to a derived mathematical expression for convenience, to estimate the maximum water table drawdown at a steady-state flow rate into a gravity well. The validation of *Kozeny's* solution is questioned by *Kawecki* (1994) and *Clement et al (1994b).*

Preene et al. (1992) gathered data from arrays of wells indicating that a range of gradient values were possible, Figure 6.4. Based on this data, *Preene et al.* stated that the outcome equation of combining *Darcy's* law with *Sichardt's* formula (equation 6.3) gives a reasonable first estimate for the yield from wells in aquifers with hydraulic conductivity above about 10^{-4} m/sec. For aquifers with high hydraulic conductivity, $K>10^{-3}$m/sec, the potential well yields may be so large that flowrates are controlled by the capacity of the pump rather than the well. For aquifers with hydraulic conductivity

below about 10^{-4} m/sec, equation 6.1 appears to give unrealistically high values of hydraulic gradient and hence well yield. *Powrie and Preene* (1992) found that measured individual wells yields can vary by a factor of more than 100 at a given site. This was concluded following analysis of data from a number of case studies where vacuum based pore water pressure control systems were used in soils of hydraulic conductivity 5×10^{-4} to 10^{-6} m/sec. Although the range can vary significantly, consistency was found by considering average hydraulic gradients and it was shown that i_{max} was approximately 10 for sealed ejector wells and 4 for vacuum wellpoints.

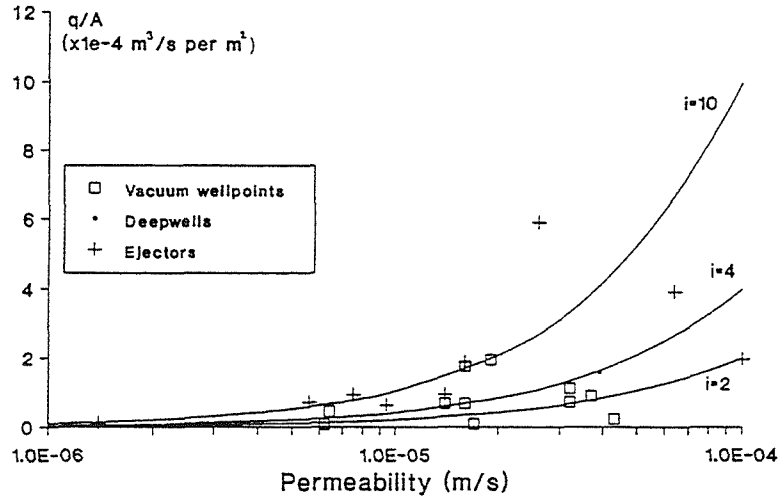

Figure 6.4 Hydraulic gradients mobilized at the face of the well vs. hydraulic conductivity. (After *Preene* , 1992.)

6.3 Dupuit-Forchheimer Well Yield

The flow towards a single well or to the equivalent well formed by an array of wells in a groundwater control scheme may be assumed to be given by the *Dupuit-Forchheimer* equation as mentioned previously. This was shown in a rigorous mathematical proof by *Charnii* (1951), (or *Czarny* or *Charny*), as reported by *Polubarinova-Kochina* (1962). In addition to the theoretical proof, experimental work by many researchers using different techniques have shown that the *Dupuit-Forchheimer* equation gives the correct flow rate within the limits of experimental accuracy. Several examples are listed by *Polubarinova-Kochina* (1962) and *Hantush* (1964).

The values of the yield obtained using numerical models are a good fit to the theoretical line predicted using the *Dupuit-Forchheimer* equation throughout $0 \leq h \leq H$, and are thus independent of the development of a seepage face (see Figure 6.5). The example used here is for R=10m, r_w= 0.10m to 0.8m, h_w= 0, and K in the range from 1E-6 m/sec to 1 m/sec. The slight differences in Figure 6.5 are possibly because the code we are using is based on variably saturated theory.

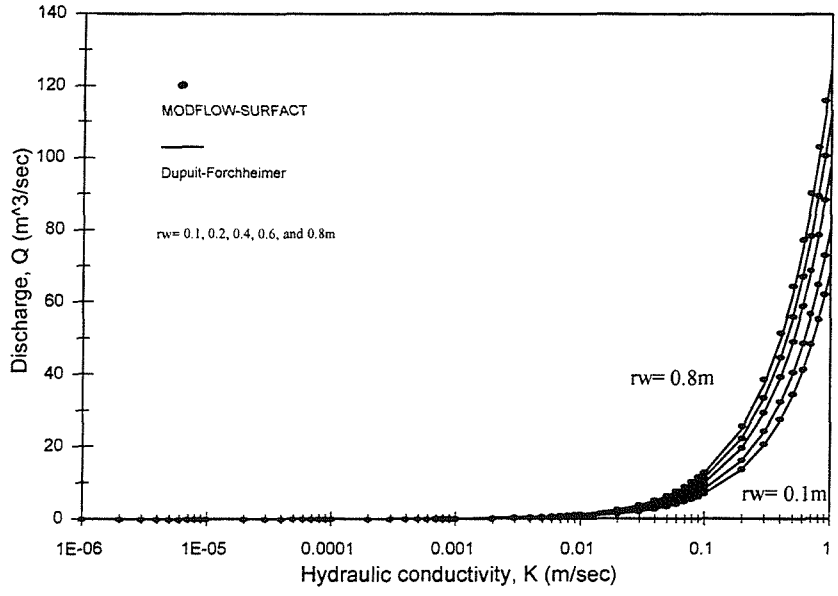

Figure 6.5 Comparison between the well yield predicted by MODFLOW-SURFACT and *Dupuit-Forchheimer.*

6.4 Single Well Investigation

A seepage analysis is generally used to estimate the total extraction flow for a groundwater control system. An important constraint on the design of such a system is that the required drawdown will be reached within a reasonable time. In order to estimate the number of dewatering wells required, flowrates to individual wells need to be assessed. *Preene et al.* (2000) listed the factors affect the yield of a well:

- Hydraulic characteristics of the aquifer, e.g. hydraulic conductivity (K).
- Wetted length of well screen (h_s).
- Effective radius of well.
- Screen filter specification.

- Correct well development.

In order to provide more understanding about the maximum possible drawdown of a fully penetrating gravity well, systematic numerical analyses have been performed using MODFLOW-SURFACT. In view of the results reported in Section 4.3, Other variably saturated codes, such as those discussed by *Cooley* (1983) and *Shamasi* and *Narasimhan* (1991), should also yield equivalent results to MODFLOW-SURFACT when used for a single well.

The domain of the problem, which is shown in Figure 6.6, is cylindrical with 10m in height and 10m in radial extent. The saturated hydraulic conductivity of the domain varies between 1×10^{-6} to 0.001 m/sec. The radius of the well, axially centered in the domain, varies between 0.1 to 1.0m. A constant head of 10m is maintained at the radial boundary of the domain, H= 10m at R= 10m. Inside the well, water level is maintained at the bottom, h_w= 0. The calculations and analysis presented in this section assume the following conditions: (1) fully penetrating, fully screened well; (2) homogenous and isotropic water-table aquifer; (3) steady-state drawdown; (4) steady-state, laminar flow; (5) no recharge due to infiltration; and (6) variably-saturated model based on a pseudo-soil function. (see Chapter 4.)

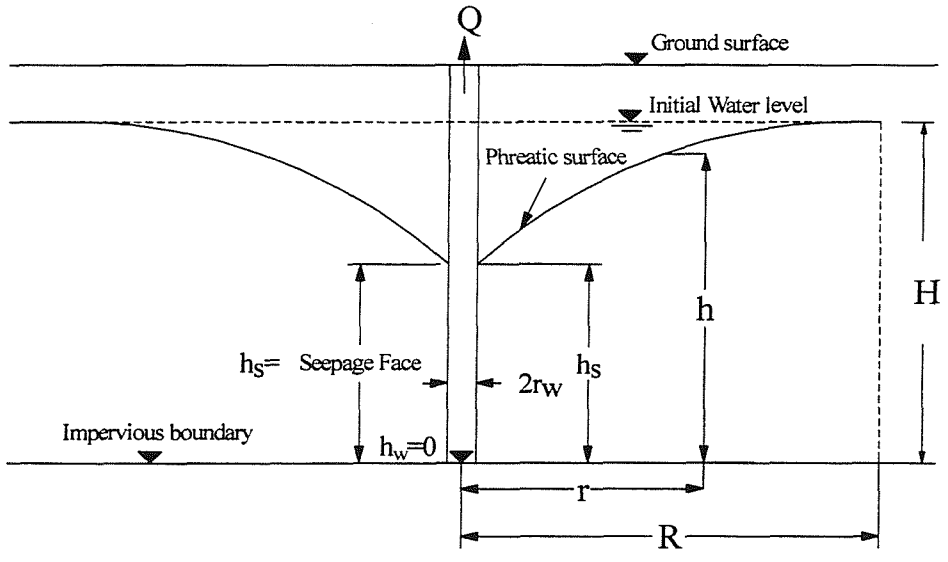

Figure 6.6 Fully drained single well model.

The results compared to other solutions presented in Section 6.2 are shown in Figure 6.7. This figure shows the relationship between the aquifer hydraulic conductivity and well yield per unit length of wetted screen per unit effective radius. The figure can be used to provide a first estimate of average individual well yields. Moreover, i_{max} appears to be very sensitive to changes in well radius and shows that although the *Preene et al.* (2000) assumption of i_{max} equal 6 is good, MODFLOW-SURFACT results predicte i_{max} equal 6 when r_w equal 0.3m. Again, Figure 6.7b shows a comparison between the available analytical solutions for the maximum well yield and MODFLOW-SURFACT results. *Kozeny's* and *Sichardt's* solutions for $K>10^{-4}$ m/sec appear to be the only two that do not give adequate predictions. *Boulton* (1951), *Boreli* (1955), *Hall* (1955), and *Heinrich* (1964) give very close results to that predicted using MODFLOW-SURFACT.

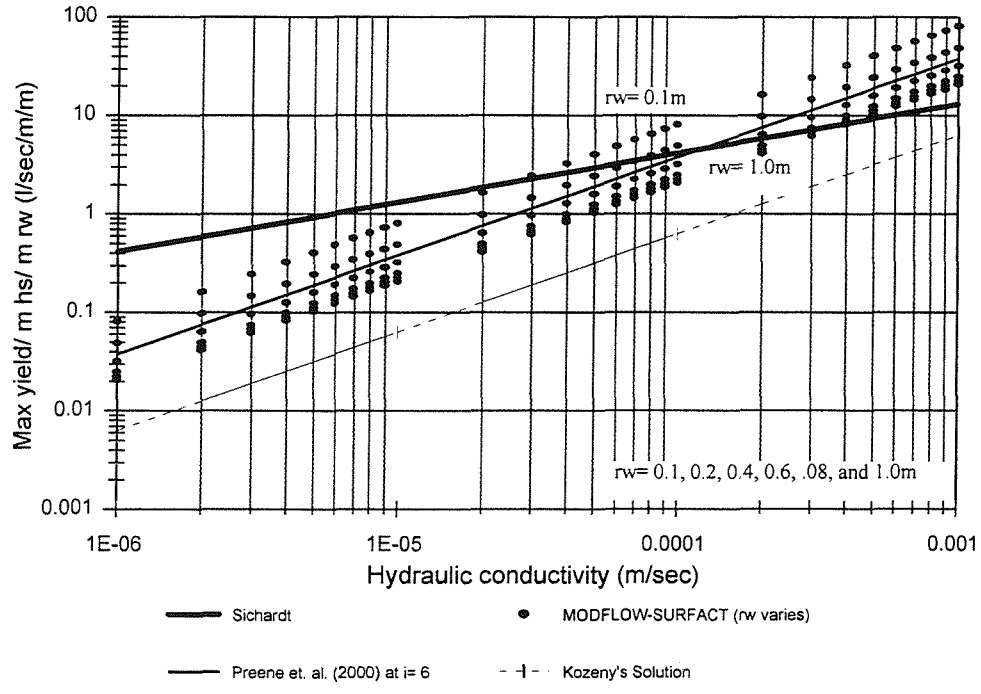

Figure 6.7a Maximum well yield.

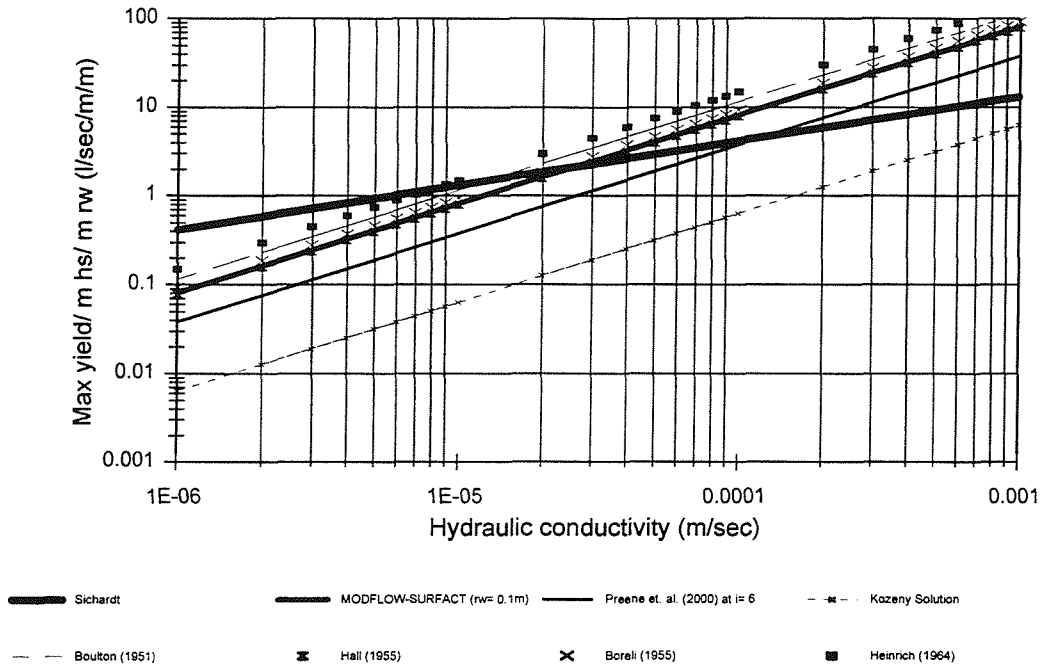

Figure 6.7b Comparison between the available analytical solutions for the maximum well yield (Eq.6.7-6.12) and MODFLOW-SURFACT results.

Since these results are limited to the case of R=10m and H=10m, an attempt has been made in the following section to use the results described in Section 4.6.2 and 6.2 to obtain a more general statement. This is done by using models with a different range of the geometric parameters that control the maximum well yield stated by *Gefell et al.* (1994):

(1) The effective radius of the well (the range used in the following section is r_w= 0.1m →1.0m).

(2) The initial saturated thickness of the aquifer (the range used in the following section is H= 10m →100m).

(3) The radius of influence (the range used in the following section is R= 10m →500m).

According to *Gefell et al.* (1994) *"the effective radius of the pumping well has far the greatest effect on the maximum potential water-table drawdown. The steady-state radius of influence, which has the least effect on the maximum water-table drawdown, can be judiciously estimated in actual pumping situations without introducing serious error to the results."*

6.5 Algebraic Representation

A combination of the fresh analysis of *Zee et al.* (1957) data shown in equation 6.4, along with the *Dupuit-Forchheimer* equation, and the numerical data that has been generated, are now used to establish a simple algebraic representation that might be applied to Figure 6.7. The equation will be used to calculate both the hydraulic limiting gradient and the seepage face elevation, as well as the maximum yield/m h_s/m r_w.

Starting with equation 6.6 and knowing that it must yield the same flow, Q, when using the *Dupuit-Forchheimer* equation when h_w= 0, *Hantush* (1964), the outcome is

$$2.50\pi r_w h_s K\left(\frac{h_s}{r_w}\right)^{0.53} = \pi K \frac{H^2}{\ln\frac{R}{r_w}} \tag{6.14}$$

Rewriting the equation for h_s gives,

$$h_s = \left(\frac{H^2}{2.5\ln\frac{R}{r_w}}\, r_w^{-0.47}\right)^{\frac{1}{1.53}} \tag{6.15}$$

or

$$\frac{h_s}{r_w} = \left(\frac{\left(\frac{H}{r_w}\right)^2}{2.5\ln\frac{R}{r_w}}\right)^{0.654} = 0.549C^{0.654} \tag{6.16}$$

Where $C = \dfrac{1}{\left(\dfrac{r_w}{H}\right)^2 \ln\dfrac{R}{r_w}}$

Substituting for h_s in equation 6.5 also gives

$$i_{\max} = \frac{1.25}{r_w^{0.53}}\left(\frac{H^2}{2.5\ln\dfrac{R}{r_w}}\, r_w^{-0.47}\right)^{\frac{0.53}{1.53}} \tag{6.17}$$

or

$$i_{\max} = \frac{0.91}{\left[\left(\dfrac{r_w}{H}\right)^2 \ln\left(\dfrac{R}{r_w}\right)\right]^{0.346}} = 0.91C^{0.346} \tag{6.18}$$

These algebraic representations predict very good results when compared with data gathered from the literature as shown in Table 6.2, and the indication is that they may be applicable to aquifers with a range of geometries.

Table 6.2 Analytical solution evaluation.

Author	Method	Geometry	*K*	Solution			
				From the literature		Equations 6.16 and 6.18	
				i_{max}	h_s	i_{max}	h_s
Kawecki (1994)	Finite difference	R= 61cm r_w= 2.55cm H= 31cm	0.086 cm/sec	3.30	17.90cm	3.44	17.26cm
Kawecki (1994)	Finite difference	R= 61cm r_w= 5.08cm H= 31cm	0.086 cm/sec	2.477	15.60cm	2.32	16.38cm
Clement et al. (1994)	Finite difference	R= 10m r_w= 0.1m H= 10m	1.0 m/day	13.03	8.60m	12.99	8.35m

Also from equation 6.6 and 6.16,

$$\frac{Q_{\max}}{h_s r_w} = 2.5\pi K\left(\frac{h_s}{r_w}\right)^{.0.53} = 5.72KC^{0.346} \tag{6.19}$$

Values of Q_{max}, i, and h_s as a function of C have been obtained using MODFLOW-SURFACT for r_w= 0.1, 0.2, 0.4, 0.6, 0.8 and 1.0m as before, see Section 6.4, H=10, 20, and 100m, and R=10, 20, 50, 100 and 500m. The results are plotted in Figures 6.8, 6.9 and 6.10. Throughout, K was kept constant at 1.0 m/day.

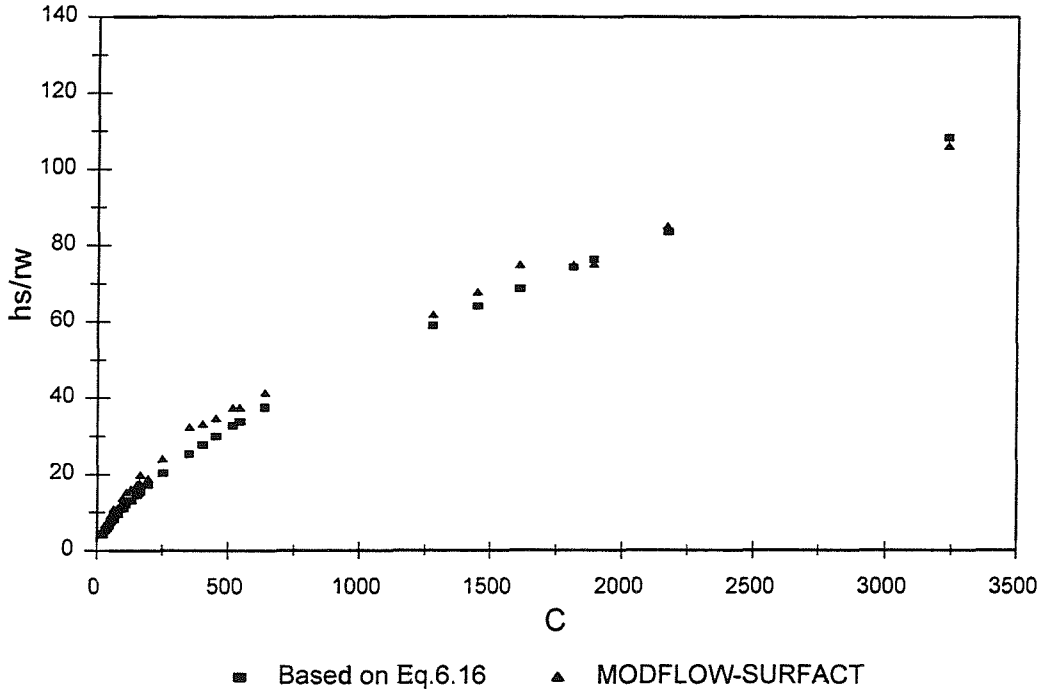

Figure 6.8 Comparison between the new algebraic solutions (equation 6.16) and MODFLOW-SURFACT results.

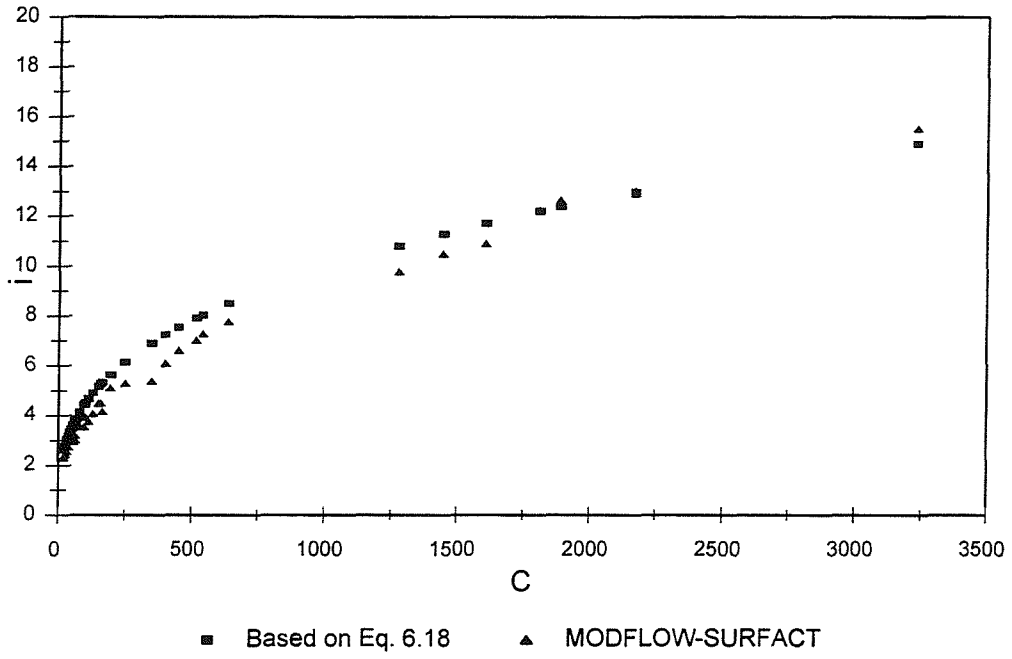

Figure 6.9 Comparison between the new algebraic solutions (equation 6.18) and MODFLOW-SURFACT results.

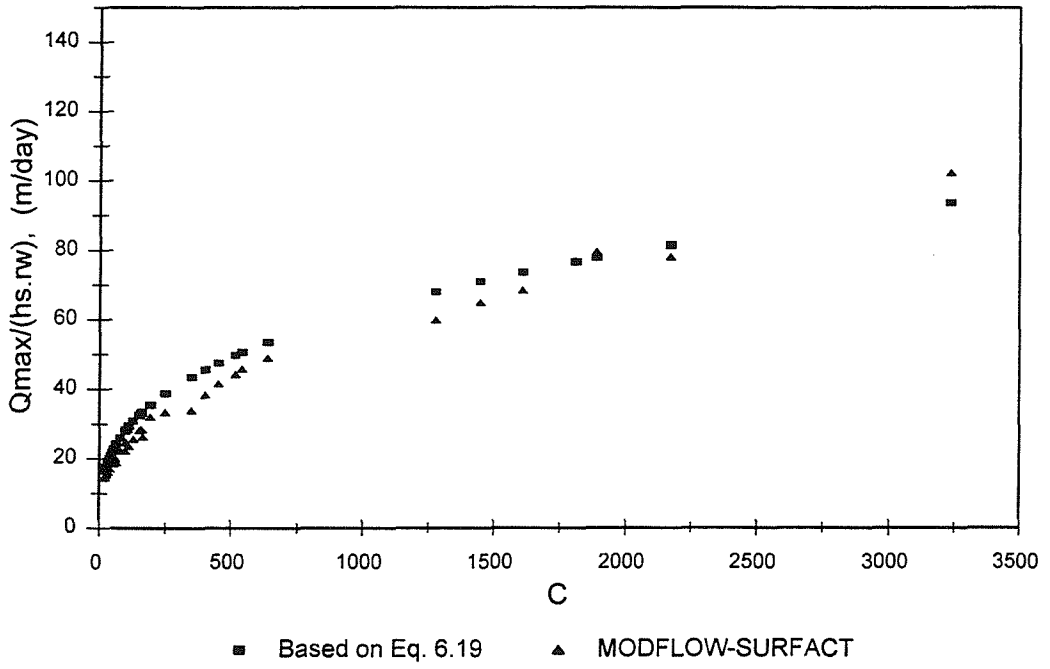

Figure 6.10 Comparison between the new algebraic solutions (equation 6.19) and MODFLOW-SURFACT results.

Figure 6.8, 6.9, 6.10 show a good agreement between the numerical results and the relatively simple algebraic solutions that are based on the geometry of the well and aquifer.

6.6 Summary

The code MODFLOW-SURFACT has further been used to estimate individual well yields in order to examine *Sichardt's* formula for estimating the maximum hydraulic gradient at entry into the well. A modified figure giving the well yield per unit length of wetted screen per unit effective radius is provided. This figure can be used to provide a first estimate of the a maximum yield of individual wells. The maximum hydraulic gradient appears to be very sensitive to changes in well radius. Although the *Preene et al.* (1997) assumption of a maximum hydraulic gradient equal to 6 is good, the MODFLOW-SURFACT results predict a maximum hydraulic gradient equal to 6 when the radius of the well is equal 0.3m.

A combination of our fresh analysis of the *Zee et al.* (1957) data along with the *Dupuit-Forchheimer* equation and the numerical data generated by MODFLOW-SURFACT has been used to establish a simple algebraic representation. This important and original outcome is based on the geometry of the well and aquifer and can be used to estimate both the hydraulic limiting gradient and seepage face elevation. Verification of the analytical solution with the available data from the literature shows that it is effective as an initial estimate. The next chapter presents another application of the code related to transient dewatering of a landfill and the possible effects of seepage faces in the dewatering of a landfill by a grid of pumped leachate wells.

Chapter (7)

Application to Leachate Control in Landfills

7.1 Introduction

Vertical wells are frequently used as a means of controlling leachate levels in landfills. They are often the only available dewatering option for both old landfills without any basal leachate collection layer and for newer sites where the installed drainage infrastructure has failed. When the well is pumped, a seepage face develops at the entry into the well so that the drawdown in the surrounding waste will not be as great as might be expected. Landfill operators' experiences of using leachate wells to control leachate levels are varied. It is common for the yield of leachate wells to be relatively small (often <1 m^3/day) and for the monitored drawdown around the well to be limited. The low yield of wells can often be related to the low hydraulic conductivity of the surrounding waste and may also be due to poor well design or badly developed wells. However, it is also possible that the apparent limited drawdown may in part be explained in terms of the development of a seepage face at the well. Seepage faces are caused by vertical components of flow in the vicinity of a pumped well where the drawdown in the well is a large proportion of the saturated thickness (*Al-Thani and White*, 2000 and p.308 *Bear*, 1979). Previous studies have considered the effect of seepage faces on pumped leachate wells (*Rowe and Nadarajah*, 1996) but results were only presented for steady state conditions. A method of analysis was required that could investigate the transient response to pumping, based on independently measured

values of hydraulic conductivity, K, and specific yield, S_y, in a landfill. In this chapter, the numerical groundwater flow code, MODFLOW-SURFACT, has been used to investigate the transient dewatering of a landfill and the possible effects of seepage faces in the dewatering of a landfill by a grid of pumped leachate wells.

7.2 Problem Description

Figure 7.1 shows a schematic view of a 30m deep landfill with a 20m deep saturated zone with a grid of leachate pumping wells at a spacing of 10m. This spacing was to some extent arbitrary, but probably represents the closest well spacing (at 100 wells per hectare) likely to be installed on most landfills. The wells are assumed to penetrate the landfill fully, and have a fixed radius of 0.15m. The wells are pumped at rate that maintains fully drawn down conditions inside the well.

A single cell (in plan view) is used to represent the pumped well in this discretization scheme. The dimensions of the cell (x- and y-coordinates) are set to the diameter of the well after the correction, 0.75 m (r_e=0.2Δx= 0.2×0.75= 0.15m, see page 65). The (column and row) dimensions of the cells adjacent to the well are set to a small fraction of the well diameter. Cell dimensions gradually increase with increasing distance from the well. The expansion factor, α, which relates the cell dimensions of any two adjacent cells is generally not more than 1.5. The boundaries to the model were set as no flow boundaries at a distance of 5m from the well in the x and y directions. The model was divided vertically into 21 layers as shown in Figure 7.1. The thickness of Layer 1 was set at 10m (representing the unsaturated zone) and the remaining layers at 1m.

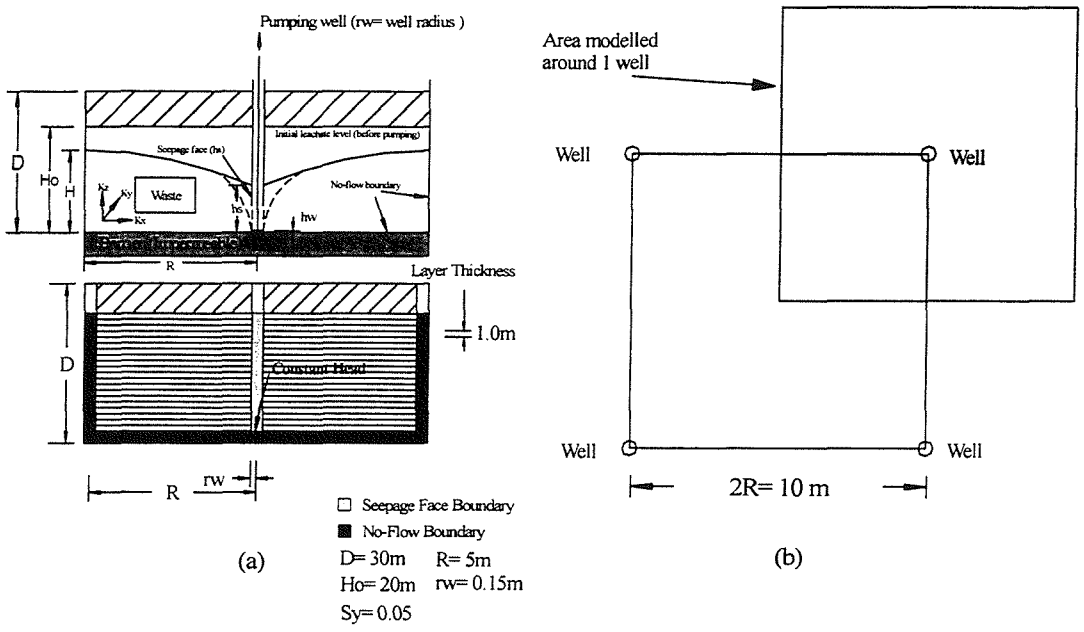

Figure 7.1 Schematic view of the landfill model **(a)** cross section **(b)** plan view of a grid.

Table 7.1 Upper bound (Case A) and Lower bound (Case B) hydraulic conductivities.

Depth (m)	Case A (m/sec)	Case B (m/sec)	Depth (m)	Case B (m/sec)	Case B (m/sec)
10.5	3.12×10^{-6}	1.66×10^{-6}	20.5	6.55×10^{-7}	2.54×10^{-7}
11.5	2.57×10^{-6}	1.31×10^{-6}	21.5	5.80×10^{-7}	2.19×10^{-7}
12.5	2.14×10^{-6}	1.05×10^{-6}	22.5	5.16×10^{-7}	1.90×10^{-7}
13.5	1.80×10^{-6}	8.53×10^{-7}	23.5	4.61×10^{-7}	1.66×10^{-7}
14.5	1.52×10^{-6}	7.00×10^{-7}	24.5	4.13×10^{-7}	1.46×10^{-7}
15.5	1.30×10^{-6}	5.79×10^{-7}	25.5	3.72×10^{-7}	1.28×10^{-7}
16.5	1.12×10^{-6}	4.84×10^{-7}	26.5	3.36×10^{-7}	1.14×10^{-7}
17.5	9.72×10^{-7}	4.07×10^{-7}	27.5	3.04×10^{-7}	1.01×10^{-7}
18.5	8.47×10^{-7}	3.46×10^{-7}	28.5	2.76×10^{-7}	8.98×10^{-8}
19.5	7.43×10^{-7}	2.95×10^{-7}	29.5	2.52×10^{-7}	8.03×10^{-8}

The initial saturated leachate level was set at 20m. A specific yield of 0.05 (5%) is used in this study, based on research into the hydrogeological properties of waste (*Hudson et al.*, 1999). The variations in hydraulic conductivity with depth are based on relationships between hydraulic conductivity, K, and effective stress, σ_e, determined experimentally by *Beaven* (2000). Two scenarios using the Upper bound K's (Case A) and Lower bound K's (Case B) of the experimental data are used in this study, Table 7.1. The operation of the well was replicated by applying a combination of a constant

head and drains to the cells representing the well. A constant head cell (with a head of zero) was allocated to the cell in the bottom layer of the model (i.e. the well is fully dewatered) and drain cells to each layer above. Drain cells operate by removing water from the model if the head in the model is above the level set for the drain. Each drain cell was allocated a head equivalent to the elevation head of the cell. This has the effect of applying seepage face boundary conditions at the well.

7.3 Results of Numerical Investigation

The MODFLOW-SURFACT code was used to solve the described problem for both hydraulic conductivity scenarios in Table 7.1 over a period of 200 days. Figure 7.2 shows the location of piezometric head after 50 days, 100 days and 200 days of pumping.

The solid lines represent the elevation of the phreatic surface, i.e. the location at which leachate would be encountered if an observation well was drilled from the surface. These lines are relatively flat. The dashed lines represent the piezometric levels at the base of the site. The leachate levels drop faster in the Case A scenario of hydraulic conductivity. This is an expected result, because higher hydraulic conductivity values lead to higher well discharges as shown in Table 7.2.

The equation for steady state flow to a pumped well in an unconfined aquifer is, see Chapter 2,

$$Q = \frac{\pi K (h_2^2 - h_1^2)}{\ln(r_2 / r_1)} \tag{7.1}$$

This equation is based on the *Dupuit-Forchheimer* assumptions that flow is horizontal and uniformly distributed with depth throughout an isotropic formation underlain by an impermeable stratum. As discussed in Chapter 2, the equation neglects the seepage face at the well and the applicability of the equation for determining flow to a well has been investigated by *Hantush* (1964) who found that equation 7.1 gives an exact result despite the presence of the seepage face. However, because it does not take account of

the existence of the seepage face, equation 7.1 does not give an accurate shape curve for the phreatic surface. Moreover, the *Dupuit-Forchheimer* assumptions imply that an overall average value for hydraulic conductivity is assumed hence anisotropy of the hydraulic conductivity as will be found in a solid waste landfill is not taken into account in equation 7.1. Nevertheless it is possible to use equation 7.1 to define an overall instantaneous effective isotropic hydraulic conductivity for a matrix in which the permeability is anisotropic. The result is simply a guide to the relative changes in hydraulic conductivity which is helpful in interpreting the results. Thus, the results from the numerical analysis have been substituted into equation 7.1 to determine an overall average hydraulic conductivity for each time step. In this case, $h_2 = H$ (=20m at time zero and changes with time) and $h_1 = 0$. R the radius of influence =5.00m. Following *Beljian* (1988), r_w the radius of the well was taken to be the effective well radius equal to 0.20 times the size of the grid representing the well, in this case 0.2×0.75=0.15m.

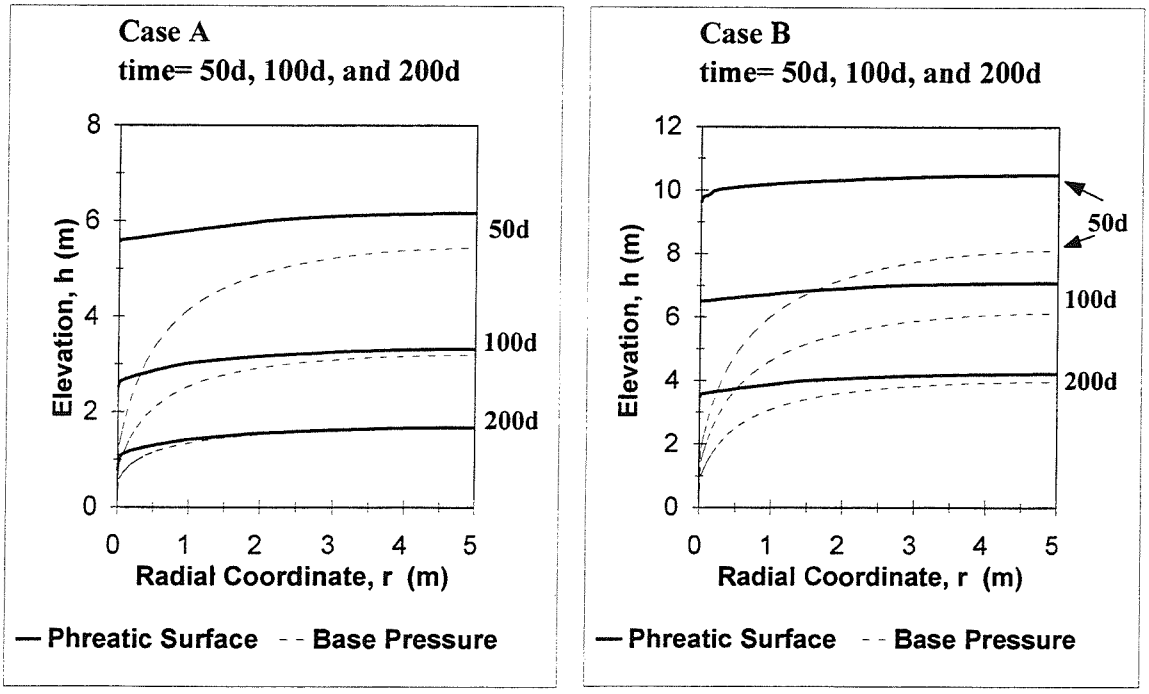

Figure 7.2 Spatial variation of leachate heads during pumping **(a)** Case A and **(b)** Case B.

Table 7.2 Discharge values for both scenarios versus time.

Time	Case A				Case B			
	Q	H	h_s	Mass Bal' Error	Q	H	h_s	Mass Bal' Error
(day)	(m^3/day)	(m)	(m)	%	(m^3/day)	(m)	(m)	%
10	4.389	15.02	14.62	1.74	2.789	15.88	13.24	2.25
50	0.681	6.17	5.57	2.47	0.704	10.49	9.61	3.27
100	0.207	3.33	2.51	3.23	0.326	7.09	6.5	6.37
150	0.095	2.25	1.50	4.21	0.176	5.28	4.51	6.40
200	0.057	1.68	0.77	6.00	0.111	4.23	3.50	7.40
250	-	-	-	-	0.078	3.49	2.50	3.83

Table 7.3 Calculation of hydraulic conductivity from model results and equation 7.1.

Q (m^3/day)	Model run	H (m)	K (m/sec)	Equivalent infiltration over $100m^2$ (m/year)
4.389	Case A	15.02	2.513E-07	16.02
0.681	Case A	6.17	2.311E-07	2.49
0.207	Case A	3.33	2.411E-07	0.76
0.095	Case A	2.25	2.424E-07	0.35
0.057	Case A	1.68	2.609E-07	0.21
2.789	Case B	15.88	1.429E-07	10.18
0.704	Case B	10.49	8.264E-08	2.57
0.326	Case B	7.09	8.377E-08	1.19
0.176	Case B	5.28	8.155E-08	0.64
0.111	Case B	4.23	8.013E-08	0.41
0.078	Case B	3.49	8.272E-08	0.28

The results are recorded in Table 7.3. A comparison of the calculated hydraulic conductivities with Table 7.1 indicates that it is the hydraulic conductivity in the lower layers that appears to control flow rates. This is concluded because average hydraulic conductivities calculated in Table 7.3 is closer to the values of the experimentally determined hydraulic conductivities in lower layers. Table 7.3 also contains a calculation of the infiltration rate Q/A corresponding to the flow rate Q. These values indicate that the average flow rate could approach typical annual infiltration rates into uncapped landfills in the UK. Where this occurred reductions in leachate levels would be difficult to progress, and may indeed reverse, and an increase in the density of the well array would be require to continue dewatering.

The numerical simulation also provided data on flow rates into the well from each 1 metre thick layer in the model. Figure 7.3 shows that the maximum flow into the well, Q, generally occurred at the very base of the model, despite this corresponding with the

layer with the lowest hydraulic conductivity. The explanation for this is that hydraulic gradients within the seepage face in the waste adjacent to the well are predominantly vertical. This drives leachate downwards towards the base of the model (rather than into the well) until the lower impermeable barrier is reached.

The exception to this is during the early stages of dewatering, before the vertical hydraulic gradients associated with the seepage face have become established and when flow is predominantly horizontal into the well. At this stage there is a closer relationship between the vertical distribution of flow rates into the well and the variation in hydraulic conductivity with depth. This is seen mainly in the simulation using the worst case hydraulic conductivity at times earlier than 20 days. It is also evident within the data set for the best-fit hydraulic conductivity model at a time of 5 days. As dewatering progresses more rapidly with the higher hydraulic conductivities, data for times earlier than 5 days for the best fit hydraulic conductivity model would produce similar curves to those produced for worst case hydraulic conductivity model prior to 20 days.

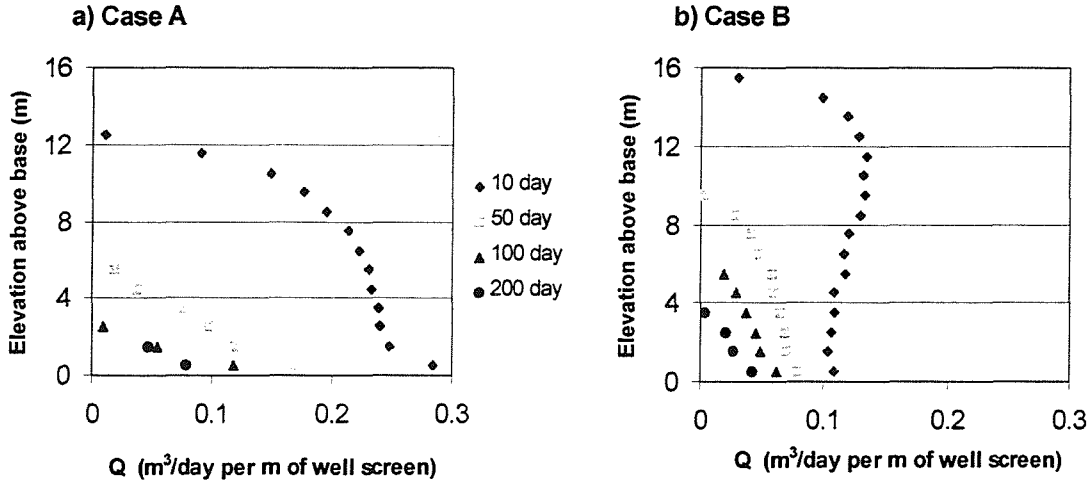

Figure 7.3 Flow from seepage face into well screen at varying elevations for **(a)** Case A and **(b)** Case B.

7.4 Algebraic Representation

The numerical investigation indicates that the drop of the leachate elevation is almost flat. This observation can be used to develop a simple algebraic representation of the

data which may be used to extrapolate the results so that they can be applied to similar systems with different dimensions and hydrogeological parameters.

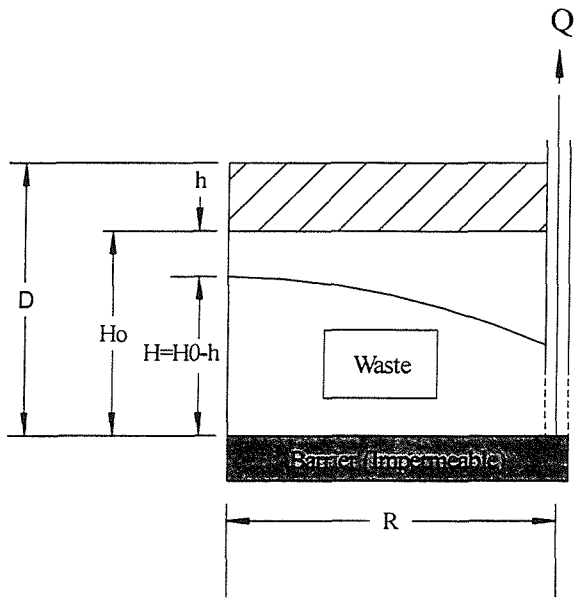

Figure 7.4 Parameter definition diagram for theoretical representation.

Assuming that the piezometric surface is effectively horizontal, the flow Q at any time t may be equated to the rate of change of the drained volume above the surface. This volume is equal to $An(H_0 - H)$ where A is the plan area and n is porosity (see Figure 7.4). Thus,

$$Q = -An\frac{dH}{dt} \tag{7.2}$$

However Q may be calculated using *Dupuit-Forchheimer* equation so that

$$Q = \frac{\pi K}{\ln\frac{R}{r_w}} H^2 = -An\frac{dH}{dt} \tag{7.3}$$

Rearranging and integrating we have,

$$\int_0^t \frac{\pi K}{An \ln \frac{R}{r_w}} dt = \int_{H_0}^{H} \frac{dH}{H^2} \tag{7.4}$$

or $$D = \frac{1}{H} - \frac{1}{H_0} \tag{7.5}$$

where $$D = \frac{\pi K t}{An \ln \frac{R}{r_w}} \tag{7.6}$$

The data in Table 7.2 have been plotted, $1/H$ against time, for both cases. The outcome of the linear fit of both plots are shown in Figure 7.5a and b.

$$0.00026t = \frac{1}{H} - \frac{1}{H_0} \qquad \text{Case A} \tag{7.7}$$

$$0.0009t = \frac{1}{H} - \frac{1}{H_0} \qquad \text{Case B} \tag{7.8}$$

Calculations for D based on the theory, equation 7.5, using the hydraulic conductivity in the lower layer and corrected r_w, yield,

$$\frac{\pi K t}{An \ln \frac{R}{r_w}} = 0.00301t \qquad \text{Case A} \tag{7.9}$$

$$\frac{\pi Kt}{An\ln\frac{R}{r_w}} = 0.00096t \qquad \text{Case B} \qquad (7.10)$$

When relating the model calculated results to that calculated using theory, equation 7.5, an average factor of 0.9 is required to make equation 7.5 fit the calculated data. This leads to equation 7.12, which is a conventional algebraic model that can be used to extrapolate the results to systems with similar geometry at different scales.

$$0.9D = \frac{0.9\pi Kt}{An\ln\frac{R}{r_w}} = \frac{1}{H} - \frac{1}{H_0} \qquad (7.12)$$

where K is the hydraulic conductivity in the lower layer; A is the area of landfill element; n is the porosity; R is the radius of influence based on $\sqrt{\frac{A}{\pi}}$ and r_w is the radius of the well.

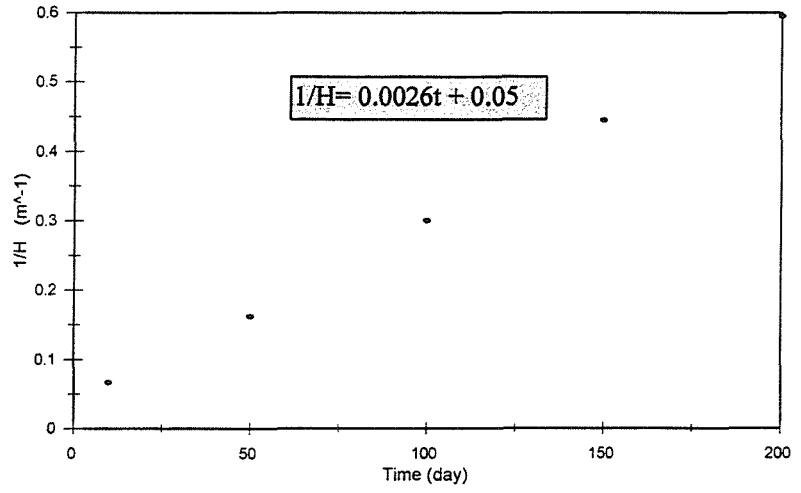

Figure 7.5a The data in Table 7.2 plotted to obtain equation 7.12. Case A.

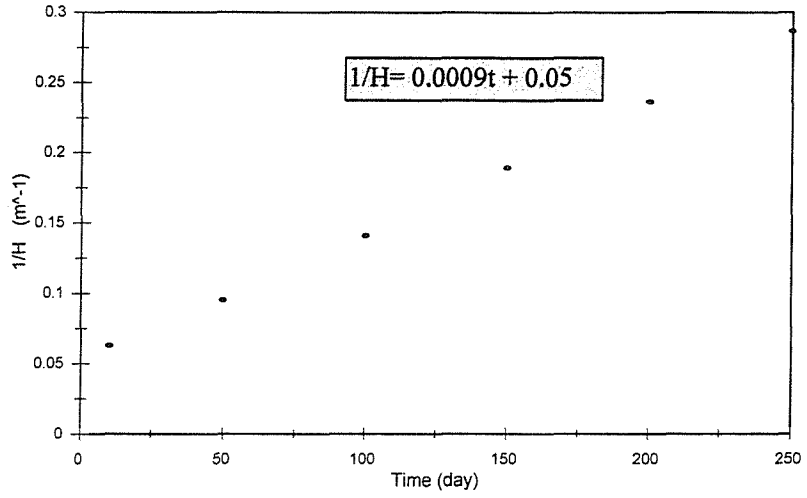

Figure 7.5b The data in Table 7.2 plotted to obtain equation 7.12. Case B.

7.5 Summary

The impact of the development of a seepage face at a vertical well has been demonstrated in the context of landfill dewatering. Strong vertical seepage velocities are set up resulting in pore pressures in the upper part of the landfill being higher than at the base producing an almost horizontal phreatic surface. Care therefore needs to be taken when carrying out field investigations to assess the pore pressures on the base of a landfill: only piezometers with a well defined and limited response zone should be used for this purpose. Fully screened observation wells in close proximity to a pumped well will give ambiguous if not meaningless results.

When a well is initially pumped, and before seepage faces have developed, hydraulic gradients are predominantly horizontal. Consequently, the vertical distribution of flow rates into the well is related to the vertical variation in hydraulic conductivity with depth. In the cases analysed, where the hydraulic conductivity of the waste reduces with depth, flow rates into the well are greatest in the upper saturated layers and reduce with depth.

With continuous pumping over time, a seepage face develops as hydraulic gradients in the immediate vicinity of the well change from being predominantly horizontal to predominantly vertical. The vertical distribution of flow rates into the well also changes and becomes greatest at the base of the well even though this corresponded to the lowest hydraulic conductivity layer in the simulations. The overall yield from the well appears to be controlled by the hydraulic conductivity in these lowest layers. The *Dupuit-Forchheimer* equation for steady state flow to a pumped well can be used to predict discharge rates with a reasonable degree of accuracy if the hydraulic conductivity at the base of the site is used in the equation.

The flow to the well appears to be taking place through the lower layers so that the yield from the well is controlled by the hydraulic conductivity in these layers. For the case of a 30m deep landfill, the predicted yield from pumped wells becomes very low when leachate levels are drawn down below approximately 1.5 to 3m (for a grid of pumped wells at 10m spacing). Rates of dewatering become slow and could even stop if the pumped rate falls below the equivalent annual rainfall infiltration rate. The data obtained for the case of a model with specific dimensions has been used to calibrate a conventional algebraic model. This outcome, which can be used to extrapolate the results to systems with similar geometry at different scales, is another original contribution adding greatly to the modelling of wells in landfills.

Chapter (8)

Conclusions and Recommendations

8.1 Introduction

This Thesis describes a comprehensive numerical investigation into the influence of the vertical component of seepage on the capacity and drawdown characteristics of deep wells pumping from unconfined aquifers. The early stages of the research include an intensive literature review of previous work carried out to investigate the seepage face. The second stage of the research focused on finding the appropriate code available to achieve the goal of investigating the influence of the vertical component of seepage on the capacity and drawdown characteristics of deep wells. Once this was accomplished, the code was used to analyse various steady state and transient flow problems in unconfined aquifers with free surface-seepage face boundary conditions. The final stage of the research, which contributes most to the understanding of the problem, focuses on the special cases of multiple well systems, anisotropy effects, maximum well yield, and the use of vertical wells in landfills. This chapter sums up the major contributions of the research adding some recommendations for useful future research.

8.2 Conclusions

The problem of cells drying up in the USGS model MODFLOW is a major obstacle to using this package to determine the seepage surface. The re-wetting package in MODFLOW is not a solution to this problem because it forces the model to converge by using unrealistic solver parameters. The standard version of MODFLOW, which is a

fully saturated code, does not therefore adequately represent the water table surface in unconfined aquifers. The improved version of MODFLOW developed by *HydroGeoLogic* Inc. MODFLOW-SURFACT, which contains the functionality to model seepage surfaces, has been used to determine the seepage surface for a number of problems described in the published literature for validation. The pseudo-soil water retention functions in MODFLOW-SURFACT that are automatically generated to reduce the unsaturated flow problem to one of seeking the potential head in a cell proved to be very effective.

Code validation

The validity of the code was demonstrated by comparing the code performance against the experimental work of *Hall* (1955), the large range of data collected and presented by *Zee et al.* (1957), and the numerical model by *Clement et al.* (1996). The results of the comparison are as follow:

- The numerical results predicted by MODFLOW-SURFACT are compared to *Hall's* results, Table 4.2 and Figure 4.9. These results demonstrate that there is good agreement between the phreatic surface predicted by MODFLOW-SURFACT and that observed by *Hall*. The maximum difference between the flow rates predicted by MODFLOW-SURFACT, providing a radius correction for the well as suggested by *Beljin*, section 4.5, and that calculated using *Dupuit-Forchheimer* equation is 4%, Table 4.2a. This error is reduced significantly when *Hall* results are compared with the numerical model results. The maximum error when the levels of the seepage face compared is 0.54%, Table 4.2b. This indicates that the numerical computation of the free surface is reliable.

- The hydraulic head calculated using *Dupuit-Forchheimer* equation, equation 2.11, agrees with the MODFLOW-SURFACT computed hydraulic head at the base, Figure 4.9.

- MODFLOW-SURFACT results are further confirmed by the experimental/analytical results assembled by *Zee et al.*, Figure 4.11 and equation

4.12. The MODFLOW-SURFACT results indicate that equation 4.12 may be used to extrapolate the *Zee et al* results over a much greater range of parameters.

- MODFLOW-SURFACT results compared well to the numerical study conducted by *Clement et al.* (1996), which uses the pseudo-soil moisture content/pore pressure function, with more accurate representation given by *Van Genuchten*, (*Van Genuchten*, 1980). The comparison, Figure 5.2, confirmed the reliability of the code, MODFLOW-SURFACT, used in this research.

The verification of the code in using these examples gives confidence to its application for problems which are unsupported by experimental data. This code has therefore been used to study the following problems; 1. a range of steady state and transient flow problems with seepage face boundaries for single and multiple wells configurations, 2. the investigation of maximum well yield from individual well in groundwater scheme, and 3. the case of using of vertical wells as means of leachate management and control of landfills where the assumption of negligible seepage face is generally not valid (*Rowe and Nadarajah,* 1996). The following summarises the major contributions of these studies:

Single well study

- The near-well zone needs to be modelled carefully and the well radius correction should be made to the grid representing individual wells in MODFLOW as proposed by *Beljian* (1988), $0.2\Delta x$, in order to predict well yields correctly.

- The numerical investigation in this research contradicts the following result concluded by *Shamsai and Narasimhan* (1991): " *The Dupuit formula may not provide accurate estimates of discharge when the presence of a seepage face cannot be ignored. In general, Dupuit assumptions will tend to under estimate discharge because the flux through the seepage face is ignored. Considering the results obtained with the physical and numerical models, Dupuit equation under estimates the well discharge by 12 to 10%. This deviation is noticeably more than 1 to 2% deviation indicated by previous investigators (Muskat, 1937; Babbitt and Caldwell, 1948; Boulton, 1951).*" The results from the numerical investigations

conducted as part of this research clearly show that discharges in all of the examples used throughout the study coincided with that calculated using *Dupuit* formula, provided that the correction for well radius proposed by *Beljian* (1988), $0.2\Delta x$, was applied. This result confirms the applicability of *Dupuit's* equation for determing the flow indicated by *Muskat,* 1937*; Babbitt and Caldwell,* 1948*; Boulton,* 1951*; Hantush,* 1964; and *Clement et al.* (1996).

- The cone of depression predicted by MODFLOW-SURFACT is much smaller than that predicted by the *Dupuit-Forchheimer* model as a result of the numerical calculation taking account of three-dimensional effects. It was found that the piezometric head at the base of the model aquifer, in the case of a single well, coincided with *Dupuit-Forchheimer*, as did the flow predictions, provided that the correction for well radius proposed by *Beljian* (1988), $0.2\Delta x$, was applied. However it was found that these *Dupuit-Forchheimer* heads needed to be elevated to match the level of the free surface computed by MODFLOW-SURFACT. This correction, presented by an example in section 5.2, plays an important role when designing remediation systems for contaminated aquifers using pump-and-treat systems as concluded by *Clement et al.* (1996): "*Seepage faces and associated rises in phreatic surfaces are usually beneficial to pump-and-treat schemes since they expose a larger volume of soil to flushing flows, which will ease the removal of contaminants during clean-up efforts. Furthermore, at higher pumping rates the water level inside a well decrease, but the volume exposed to the flow remains relatively unchanged over a significant variation of drawdown due to the seepage face effect. This is very important since the remediation wells are usually installed in the most contaminated parts of the site.*"

- Increasing the length of the flow domain results in a decrease in the extent of the seepage face for the same drawdown, Figure 5.4. However this decrease is not particularly sensitive to the length of the flow domain and indicates that the seepage face behaviour determined more by conditions close to the well.

- As the vertical hydraulic conductivity, K_z, decreases the height of the seepage face increases. This effect of anisotropy on the phreatic-surfaces and seepage-faces is shown in Figure 5.6.

- In the case of the transient seepage-face investigation for single well configurations, the research confirmed the *Clement et al.* (1994b) results that a fast decline of the phreatic surface takes place during the early stages of pumping due to the specific storage effect. Nevertheless, as time progresses, the specific storage effect decreases and its effect is almost negligible after a period of time depending on the hydraulic conductivity, Figure 5.9. Intuitively, as the value of the hydraulic conductivity is increased, the faster a soil tends to drain, and therefore the level of the phreatic surface is lowered more rapidly, Figure 5.10.

Multiple well Study

- The investigation of multiple well systems shows similar results to those found with a single well configuration. The conventional method of superposition gave results that agreed with the model head calculations at the aquifer base. However, these needed to be elevated by a correction height to match the level of the free surface in the models. The additional flow computed by the variably saturated flow model might be attributed to water transport through the unsaturated zone.

- The major conclusion from using multiple well configurations is that as the number of wells increases the elevation correction for *Dupuit-Forchheimer* solution decreases. Proven numerically, Figure 5.13, the seepage surface is eliminated by the inter-action of the wells in the systems and it appears that the seepage face surface phenomenon is not a significant factor in the performance of an array of wells. Therefore, the advantage of exposing larger volume of soil to flushing flows found in single well remediation systems is not applicable for multiple well systems.

Individual well yields

- MODFLOW-SURFACT has been used to estimate individual well yields in order to examine the validity of using *Sichardt's* formula for estimating the maximum hydraulic gradient at entry into the well. A modified relationship between the aquifer hydraulic conductivity and the well yield per unit length of wetted screen per unit effective radius, has been obtained, Figure 6.7. This relationship can be used to provide a first estimate of average individual well yields.

- The maximum hydraulic gradient appears to be very sensitive to changes in well radius and shows that although the *Preene et al.* (1997) assumption of maximum hydraulic gradient equal to 6 is good, the MODFLOW-SURFACT results predict a maximum hydraulic gradient equal to 6 when the radius of the well is equal 0.3m.

- A combination of the fresh analysis of the *Zee et al.* (1957) data along with the *Dupuit-Forchheimer* equation and the numerical data generated by MODFLOW-SURFACT has been used to establish simple analytical solutions, section 6.5. This important research outcome, is based on the geometry of the well and aquifer and can be used to estimate both the hydraulic limiting gradient and seepage face elevation.

Leachate control in landfills

- Care needs to be taken when carrying out field investigations to assess the pore pressures on the base of a landfill, only piezometers with a well defined and limited response zone should be used for this purpose. Fully screened observation wells in close proximity to a pumped well will give ambiguous if not meaningless results. This is because strong vertical seepage velocities are set up resulting in pore pressures in the upper part of the landfill being higher than at the base producing an almost horizontal phreatic surface, Figure 7.2 and Figure 7.3.

- Rates of dewatering become slow and could even stop if the pumped rate falls below the equivalent annual rainfall infiltration rate.

- When a well is initially pumped, and before seepage faces have developed, hydraulic gradients are predominantly horizontal. Consequently, the vertical distribution of flow rates into the well is related to the vertical variation in hydraulic conductivity with depth. In the cases analysed, Chapter 7, where the hydraulic conductivity of the waste reduces with depth, flow rates into the well are greatest in the upper saturated layers and reduce with depth.

- With continuous pumping over time seepage face develops as hydraulic gradients in the immediate vicinity of the well change from being predominantly horizontal to predominantly vertical. The vertical distribution of flow rates into the well also changes and becomes greatest at the base of the well even though this corresponded to the lowest hydraulic conductivity layer in the simulations. The overall yield from the well appears to be controlled by the hydraulic conductivity in these lowest layers. The *Dupuit-Forchheimer* equation for steady state flow to a pumped well can be used to predict discharge rates with a reasonable degree of accuracy if the hydraulic conductivity at the base of the site is used in the equation.

- The data obtained for the case of a model with specific dimensions has been used to calibrate a conventional algebraic model, which can be used to extrapolate the results to systems with similar geometry at different scales, section 7.4.

8.3 Recommendations for Future Research

This research has investigated the influence of the seepage face on the capacity and drawdown characteristics of deep wells pumping from unconfined aquifers using numerical models. There are relatively few studies that are based on variably saturated flow models that investigate in detail the flow processes within the cone of depression near deep pumping wells. In fact at the time of publication, no published study has been found that examines the relationship between the principle of superposition of drawdown and seepage face. Studies of such a nature will improve the design methods of wells and flushing systems.

The research reported in this thesis has fallen under the headings of code validation, single wells, multiple wells, well yields, and leachate control in landfills. Each element of the study has revealed areas where further research would be beneficial. The following topics are suggestions by the author for future work.

Code validation

The new MODFLOW-SURFACT code component that provides the seepage surface boundary condition has been validated using steady state benchmarks. It has been assumed that the original benchmarking (*HydroGeoLogic*, Inc., 1996) of the main body of the code for transient conditions is still valid. This assumption needs to be confirmed by comparing the performance of the code with an independent calculation of an example that involves transient changes in the position of the seepage surface.

An improved version of MODFLOW-SURFACT, MODFLOW-SURFACT 99, was released during the final stages of this research project. This latest version contains a new BCF package that is extended for rigorous unsaturated zone water flow modelling using *Richard's* equation with options for modelling relative permeability based on the *van Genuchten* (1980) or *Brooks-Corey* (1966) models.

These relative permeability models are more realistic than the pseudo-soil model, but they require certain parametric values to be identified. A useful first step in progressing their use would therefore be to relate the parametric values to the variably saturated permeability characteristics of real soils. This could be readily done using existing soils data in this area. The next step would be to use the benchmark data identified in this thesis to repeat the validation of the code, but using the new models. This would add confidence to the use of the models in applications such as those investigated in this project and in other areas where the variably saturated component of groundwater flow is significant.

Single wells

The work described in the thesis has confirmed that it is possible to model satisfactorily the significant zone of unsaturated groundwater flow that exists in the vicinity of deep

wells above the phreatic surface. It is possible that such modelling could be extended to investigate the effectiveness of using deep wells to remove contaminants from this unsaturated zone. The importance of this is the fact that common groundwater contaminants, such as petroleum hydrocarbons, are less dense than water and primarily reside as residual LNAPLs (Light Non-Aqueous Phase Liquid) at or above the phreatic water surface.

In order to model the transport of contaminants in unsaturated conditions it would first be necessary to obtain experimental data that would link contaminant transport to seepage velocity in variably saturated conditions. A literature study would be required to identify existing data and the areas in which this was inadequate. A supporting experimental study would then need to be specified and carried out. Subsequent modelling studies would then be aimed at broadening the understanding of seepage face dynamics and would enable the quantification of the transport capacities in this area.

Multiple wells

This research has indicated that the seepage surface is removed from wells that are operating as part of a closely spaced array. Many such arrays are installed regularly and are closely monitored as part of groundwater control systems in the construction industry. The existence of these data-bases offers the opportunity to confirm or otherwise, the current numerical investigation conclusion of seepage face elimination due to the inter-action of the wells in array systems.

Well yields

The work on relating seepage surface to maximum well yield has resulted in an algebraic representation linking well yield to other key parameters of the well and aquifer properties. This algebraic representation arose by developing the work involved in preparing data for the validation of the numerical code. Whilst this representation is very helpful in that it reinforces the basis for presenting the data on maximum well yields, it is limited by the assumption that the aquifer has a uniformly distributed hydraulic conductivity.

It was demonstrated in Chapter 5 that the vertical hydraulic conductivity of the aquifer is likely to have an influence on the extent of the seepage surface and thus on the maximum well yield. It would therefore be sensible to try to extend the data on well yields to include the effects of anisotropy. This could most readily be achieved by means of a numerical model study using the methodology established by the research reported in this thesis.

Leachate control in landfills

The modelling study carried out in the context of leachate control in landfills has indicated that the performance of deep wells in unconfined conditions is likely to be controlled by the hydraulic conductivity of the deeper layers in the aquifer at the lower end of the well screen. This is a significant result, particularly if it is extended to pumping from natural aquifers, because it has a strong influence on the selection of the correct hydraulic conductivity for design purposes.

Thus a priority for future work appears to be further modelling, and the collection of existing and new field data, aimed at studying flow to vertical wells in unconfined aquifers or landfills, in circumstances where there is a major change in hydraulic conductivity with elevation. This would help to verify the numerical modelling used in this research and guide future studies aimed at modifying such models if necessary. In the case of landfills this might require the consideration of other factors that are likely to have an impact on the hydrogeological properties such as effective stress, biodegradation, and gas production.

The generalisation of the results obtained to date has been through the development of a simple algebraic representation that assumes that the steady state *Dupuit-Forchheimer* equation may be applied under transient conditions. Although this appears to give an acceptable outcome it would be more satisfactory if a more realistic theoretical model could be developed to act as a framework for extrapolating the results reported on this thesis.

8.4 Summary of Outcomes

A comprehensive numerical investigation into the influence of the vertical component of seepage on the capacity and drawdown characteristics of deep wells pumping from unconfined aquifers has been carried out and has produced new results.

The MODFLOW-SURFACT seepage face boundary condition component of code has been validated using a wide range of experimental and analytical data. This has not been done before.

The validation process produced an algebraic model that extrapolates seepage surface results beyond those available to date.

This model has also been developed further so that it can be used to estimate the maximum yield from wells in unconfined aquifers. This supports and refines the currently available guidance on this subject

The code has been used to analyse multiple well systems and produce for the first time correction factors for the results obtained by the method of superposition.

The code has been used to investigate the performance of vertical wells in landfills. This work also produced an algebraic representation of the results which enables them to be extrapolated to different scales. The work indicated that flow to a vertical well is strongly influenced by the hydraulic conductivity of layers near the base of the well. This observation has not been made before.

References

Al-Thani, A.A. and J.K. White, 1999, The impact of the seepage surface on the design of pump-and-treat remediation systems for contaminated aquifers-based on single well, Workshop on Ground Water Pollution, Protection and Remediation, November 7-10, Qatar.

Al-Thani, A.A. and J.K. White, 2000, The impact of the seepage surface on the design of pump-and-treat remediation systems for contaminated aquifers-based on multiple wells, *Groundwater 2000*, Proceedings of the International Conference on Groundwater Research, June 6-8, Copenhagen-Denmark, A.A. Balkema, Rotterdam.

Anderson, M.P., and W.W. Woessner, 1992, *Applied Groundwater Modeling: Simulation of Flow and Advective Transport*, Academic Press, Inc., New York, N.Y., 381 p.

Arnold, F.D., 1998, 5,000 Phone calls- the user support perspective on modeling education issues, Proceedings of MODFLOW'98, Volume 1, October 4-8, Golden, Colorado, pp. 481-488.

Babbitt, H.E., D.H. Caldwell, 1948, The free surface around, and interface, gravity wells, University of Illinois Engineering Experiment Station Bulletin, 374, 60 pp.

Bear, J., 1972, *Dynamics of Fluids in Porous Media*, American Elsevier, New York, N.Y., 764 p.

Bear, J., and A. Verruijt, 1987, *Modeling Groundwater Flow and Pollution*, D. Reidel Publishing Co., 414 p.

Bear, J., 1979, *Hydraulics of Groundwater*, McGraw-Hill Inc., New York, N.Y., 569 p.

Beaven, R.P., 2000, *The Hydrogeological and Geotechnical Properties of Household Waste in Relation to Sustainable Landfilling*, PhD Dissertation, University of London.

Bedient. P.B., H.S. Rifai, and CC.J. Newell, 1994, *Groundwater Contamination: Transport and Remediation*, Prentice Hall Inc., Englewood Cliffs, N.J., 541 p.

Beljian, M.S., 1988, Representation of individual wells in two-dimensional groundwater water modeling, Proceedings of Solving Ground Water Problems with models, February 10-12, Denver, Colorado, pp. 350-351.

Boreli, M., 1955, Free-surface flow toward partially penetrating wells, Transactions. American Geophysical Union, 36(4) pp. 664-672.

Boulton, N.S., 1951, The flow pattern near a gravity well in a uniform water bearing medium, Journal of Institution of Civil Engineers (London), 36(10), pp. 534-550.

Boreli, M., 1955, Free-surface flow toward partially penetrating wells, Transactions. American Geophysical Union, 36(4) pp. 664-672.

Bouwer, H., 1978, *Groundwater Hydrology*, McGraw-Hill Inc., New York, N.Y., 480 p.

Brandt, A., E. Bresler, N. Diner, L. Ben-Asher, J. Heller, and D. Goldman, 1971, Infiltration from a trickle source: 1. Mathematical models, Proceedings of the American Society of Soil Science, 35, pp. 675-689.

Brauns, J., 1981, Drawdown capacity of groundwater wells, Proceedings of the Xth International Conference of Soil Mechanics of Foundation Engineering, pp. 391-396.

Brooks, R.H. and A.T. Corey, 1966, Properties of porous media affecting fluid flow, Journal of Irrigation and Drainage Division, ASCE, 92(IR2), pp. 61-68.

Celia, M.A., E.T. Bouloutas, and R.L. Zarba, 1990, A general mass-conservative numerical solution of the unsaturated flow equation. Water Resources Research, 26(7), pp. 1483-1496.

Charnii, I.A., 1951, A rigorous derivation of Dupuit's formula for unconfined seepage with seepage surface, Dokl. Akad. Nauk. U.S.S.R. (in Russian), Moscow, 79(6). (see Bear (1979) page 311)

Clement, T.P., R.W. Wise, and F.J. Molz, 1994a, A physically based, two-dimensional, finite-difference algorithm for modeling variably saturated flow, Journal of Hydrology, 161, pp. 71-90.

Clement, T.P., R.W. Wise, and F.J. Molz, 1994b, A physically based, two-dimensional, finite-difference algorithm for modeling variably saturated flow, Journal of Hydrology, 161, pp. 91-108.

Clement, T.P., R.W. Wise, F.J. Molz, and M. Wen, 1996, A comparison of modeling approaches for steady-state unconfined flow, Journal of Hydrology, 181, pp. 189-209.

Cooley, R.L., 1983, Some new procedure for numerical solution of variably saturated flow Problems, Water Resources Research, 19(5), pp. 1271-1285.

Dane, J.H., and F.H. Mathis, 1981, An adaptive finite difference scheme for the one-dimensional water flow equation, Proceedings of the American Society of Soil Science, 45, pp. 1048-1054.

Darcy, H., 1856, *Les Fontaines Publiques de la Ville de Dijon*, Victor Dalmont, Paris, 647 p. (see Bear (1979) page 60)

Day, P.R., and J.N. Luthin, 1956, A numerical solution of the differential equation of flow for a vertical drainage problem, Proceedings of the American Society of Soil Science, 20, pp. 443-446.

de Marsily, G., 1986, *Quantitative Hydrogeology*, Academic Press, London, 440 p.

Domenico, P.A., and F.W. Schwartz, 1990, *Physical and Chemical Hydrogeology*, John Wiley and Sons, New York, N.Y., 506 p.

Dupuit, J., 1863, *Etudes Theoriques et Pratigues sur le Mouvement des Eaux dans les Canuax de Couverts et a Travers les Terrains Permeables*, 2nd edition, Dunod, Paris, 304 p. (see Bear (1979) page 76)

Ehrenberger, R., 1928. (see Muskat (1937) page 367).

Environmental Simulations, Inc., 1997, *Guide to Using Groundwater Vistas*, Environmental Simulations, Inc., Herndon, VA.

Environmental Simulations, Inc., 1998, *Guide to Using Groundwater Vistas*, version 2.0, Environmental Simulations, Inc., Herndon, VA.

Ferris, J.G., D.B. Knowles, R.H. Browne, and R. W. Stallman, 1962, Theory of aquifer test, U.S. Geological Survey Water-Supply Paper 1536-E.

Fetter, C.W., 1994, *Applied Hydrogeology*, Prentice Hall, Upper Saddle River, N.J., 691 p.

Forchheimer, P., Wasserbewegung durch Bodem, Z. Ver. Deutsch, Ing., 45, 1782-1788, 1901. (see Bear (1979) page 78)

Freeze, R.A, 1969, The mechanism of natural groundwater recharge and discharge: 1. One-dimensional, vertical, unsteady, unsaturated flow above a recharging and discharging groundwater flow system, Water Resources Research, 5(1), pp. 153-171.

Freeze, R.A., and J.A. Cherry, 1979, *Groundwater*, Prentice Hall, Englewood Cliffs, N.J., 604 p.

Gefell, M.J., G.M. Thomas, and S.J. Rossello, 1994, Maximum water-table drawdown at fully penetrating pumping well, Ground Water, 32(3), pp. 411-419.

Goode, D.J. and C.A. Appel, 1992, Finite-difference interblock transmissivity for unconfined aquifers and for aquifers having smoothly varying transmissivity: U.S. Geological Survey Water-Resources Report 92-4124.

Hall, H.P., 1955, An investigation of steady flow toward a gravity well, La Houille Blanche, 10, pp. 8-35.

Hansen, V.E., 1949, *Evaluation of Unconfined groundwater flow to multiple wells by Membrane Analogy*, Thesis, Iowa state University.

Hansen, V.E., 1953, Unconfined groundwater flow to multiple wells, Transactions. American Society of Civil Engineers, N.Y., 118, pp. 1098-1130.

Hantush, M.S., 1964, Hydraulics of Wells in V.T. Chow, *Advances in Hydroscience*, Vol. 1, Academic Press Inc., San Diego, CA, pp. 281-432.

Harr, M.E., 1991, *Groundwater and Seepage*, Dover Publications Inc., Mineola, N.Y., 315 p.

Hausmann, M.R., 1990, *Engineering Principles of Ground Modification*, McGraw-Hill Inc., New York, N.Y., pp. 200-203.

Haverkamp, R., and M. Vauclin, 1981, A Comparative study of three forms of Richards' equation used for predicting one-dimensional infiltration in unsaturated soil, Proceedings of the American Society of Soil Science, 45, pp. 13-20.

Haverkamp, R., M. Vauclin, J. Touma, P.J. Wierenga, and G. Vachaud, 1977, Comparison of Numerical simulation models for one-dimensional infiltration, Proceedings of the American Society of Soil Science, 41, pp. 285-294.

Heinrich, G., 1964, Eine Näherung für die freie Spiegelfläche beim vollkommenen Brunnen, Österreichische Wasserwirtschaft, 16(12), pp. 15-20. (see Brauns (1981))

Herbert, R., and K.R. Rushton, 1996, Ground water flow studies by resistance networks, Géotechnique, 16, pp. 53-75.

Hill, M.C., 1990, Preconditioned conjugate-gradient 2 (PCG2), A computer program for solving ground-water flow model using nonlinear regression, USGS, Water-Resources Investigations Report 90-4048, 43p.

Howsam, P., B. Misstear and C. Jones, 1995, *Monitoring Maintenance and Rehabilitation of Water Supply Boreholes*, CIRIA report no. 113, 137 p.

Hudson, A.P., R.P. Beaven, and W. Powrie, 1999, Measurement of the hydraulic conductivity of household waste in a large scale compression cell, *Sardinia 99*, Proceedings of the Seventh International Waste Management and Landfill Symposium, S. Margherita di Pula, Cagliari, Italy; October 4-8, Vol III, pp 461-468.

Hunt, B.W., 1970, Exact flow rates from Dupuit's approximation, Journal of the Hydraulics Division, Proceedings of the ASCE, N.Y., 96(HY 3), pp. 633-641.

Huyakorn, P.S., G.F. Pinder, 1983, *Computational Methods in Subsurface Flow*, Academic Press, Inc., London, 473 p.

Huyakorn, P.S., S.D. Thomas, and B.M. Thompson, 1984, Techniques for making finite elements competitive in modelling flow in variably saturated porous media, Water Resources Research, 20(8), pp. 1099-1115.

Huyakorn, P.S., B.G. Jones, and P.E. Anderson, 1986a, Finite-element algorithms for simulating three-dimensional groundwater flow and solute transport in multilayer systems, Water Resources Research, 22(3), pp. 361-374.

Huyakorn, P.S., E.P. Springer, V. Guvanasen, and T.D. Wadsworth, 1986b, A three-dimensional finite-element model for simulating water flow in variably saturated porous media, Water Resources Research, 22(13), pp. 1790-1808.

HydroGeoLogic, Inc., 1996, *MS-VMS Software Version 1.2 and Documentation*, HydroGeoLogic, Inc., Herndon, Virginia.

Kashef, A.I., 1965, Exact free surface of gravity wells, Journal of the Hydraulics Division, Proceedings of the ASCE, N.Y., 91(HY4), pp. 167-184.

Kashef, A.I., 1986, *Groundwater Engineering*, McGraw-Hill Inc., New York, N.Y., 512 p.

Kawecki, M.W., 1994, Discussion on Maximum water-table drawdown at fully penetrating pumping well, Ground Water, 33(3), pp. 498-499.

Kirkham, D., 1964, Exact theory for the shape of the free surface about a well in a semiconfined aquifer, Journal of Geophysical Research, 69(12), pp. 2537-2549.

Kirkland, M.R., R.G. Hills, and P.J. Wierenga, 1992, Algorithms for solving Richards' equation for variably saturated soils. Water Resources Research, 28, pp. 2049-2058.

Kozeny, J., 1927, Über kapillare Leitung des Wassers im Boden, Wasserkraft uns Wassenwirtschaft, 22, 120. (see Muskat (1937) page 365).

Kozeny, J., 1933, Theorie und berechnung der brunnen, Wasserkraft uns Wassenwirtschaft, 28, 88-92, 101-105, 113-116. (see Muskat (1937) page 367).

Kozeny, J., 1953, *Hydraulik: Ihre Grundlagen und Praktische Anwendung, Springer-Verlag, Vienna.* (see Gefell, M.J., G.M. Thomas, and S.J. Rossello (1994)).

Kresic, N., 1997, *Quantitative Solutions in Hydrogeology and Groundwater Modeling*, CRC Lewis Publishers, Boca Raton, FL, 461 p.

Leonards, G.A., 1962, *Foundation Engineering*, McGraw-Hill Inc., New York, N.Y., 1136 p.

Liggett, J.A., and P.L-F. Liu, 1983, *The Boundary Integral Method for Porous Media Flow*, George Allen and Unwin, London, UK, 255 p.

Luther, K.H., 1998, *Analytic Solutions to Three-Dimensional Unconfined Groundwater Flow Near Wells,* PhD Dissertation, Indiana University.

Mansur, C.I. and R.I. Kaufman, 1962, Chapter 3 in *Foundation Engineering* Edited by G.A. Leonards, McGraw-Hill Inc., New York, N.Y., 1136 p.

Mahdaviani, M.A., 1976, Steady and unsteady flow towards gravity wells, Journal of the Hydraulics Division, Proceedings of the ASCE, N.Y., 93(HY 6), pp. 135-146.

Marino, M.A., and J.N. Luthin, 1982, Developments in Water Science: Seepage and Groundwater, Elsevier Scinece, New York, N.Y., Vol. 13, 489 p.

McDonald, M.G., and A.W. Harbaugh, 1988, A modular three-dimensional finite-difference ground-water flow model, Techniques of Water-Resources Investigations 06-A1, U.S. Geological Survey, 576 p.

McDonald, M.G., and A.W. Harbaugh, B.R. Orr, D.J. Ackerman, 1991, A method of converting no-flow cells to variable-head cells for the U.S. Geological Survey modular finite-difference ground-water flow model: U.S. Geological Survey Open-file Report 91-536.

McWhorter, D.B., and D.K. Sunada, 1991, *Ground-Water Hydrology and Hydraulics*, Water Resources Publications, Colorado, 290 p.

MS-VMS, 1996, First Fully Integrated MODFLOW-Based Visual Modeling System with Comprehensive Flow and Transport Capability, HydroGeoLogic, Inc., Herndon, VA.

Muskat, M., 1937, *The Flow of Homogeneous Fluids Through Porous Media*, McGraw-Hill Inc., New York, N.Y., 763 p.

Narasimhan, T.N., 1975, *A Unified Numerical Model for Saturated-Unsaturated Flow Groundwater flow*, PhD Dissertation, University of California, Berkeley

Narasimhan, T.N., and P.A. Witherspoon, 1978, Numerical model for saturated-unsaturated flow in deformable porous media, 3, Applications, Water Resources Research, 14(6), pp. 1017-1034.

Neuman, S.P., 1970, Effect of partial penetration on flow in unconfined aquifers considering delayed gravity response, Water Resources Research, 10(2), pp. 303-312.

Neuman, S.P., 1976, *User's guide for FREESURF I*, Department of Hydrology and Water Resources, University of Arizona, Tuscon, AZ, 22p.

Neuman, S.P., and P.A. Witherspoon, 1970, Finite element method of analyzing steady seepage with a free surface, Water Resources Research, 6(3), pp. 889-897.

Neuman, S.P., 1985, Some new procedures for numerical-solution of variably saturated flow problems-comment, Water Resources Research, 21(6), p. 886.

Neuman, S.P., 1973, Saturated-unsaturated seepage by finite-elements, Journal of the Hydraulics Division, Proceedings of the ASCE, N.Y., 99(HY12), pp. 2233-2250.

Nielsen, D.R., M.Th. van Genuchten, and J.W. Biggar, Water-flow and solute transport processes in the unsaturated zone, 1986, Water Resources Research, 22(9), pp. 89S-108S.

Nutting, P.G., 1930, Physical analysis of oil sands, Bulletin of American Association of Petroleum Geology, 14, pp.1337-1349.

Pandy, S., and P.S. Huyakorn, 2000, MODFLOW *Enhancements for Robust, Reliable Simulations of Complex Environmental Flow and Contaminate Transport Situations*, HydroGeoLogic, Inc., Herndon, Virginia (provided by the authors).

Peaceman, D.W., 1978, Interpretation of well-block pressures in numerical reservoir simulation with nonsquare blocks and anisotropic permeability, Society of Petroleum Engineers Journal, 23(3), pp. 531-543.

Peaceman, D.W., 1983, Interpretation of well-block pressures in numerical reservoir simulation, Society of Petroleum Engineers Journal, 18(3), pp. 183-194.

Peaceman, D.W., 1990, Interpretation of well-block pressures in numerical reservoir simulation, Part III. Off centre and multiple wells within a wellblock, Society of Petroleum Engineers Journal, 5(2), pp. 227-232.

Peterson, D.F., 1957, Hydraulics of wells, Transactions. American Society of Civil Engineers, N.Y., 122, pp. 502-517.

Polubarinova-Kochina, P.Ya, 1962, *Theory of Groundwater Movement* (translated from Russian by R.J.M. de Wiest), Princeton University Press, Princeton, N.J.

Powers, J.P., 1992, *Construction Dewatering: New Methods and Applications*, John Wiley and Sons, New York, N.Y., 492 p.

Powrie, W., and M. Preene, 1992, Equivalent well analysis of construction dewatering systems, Géotechnique, 42(4), pp. 635-639.

Powrie, W., and M. Preene, 1994, Time-drawdown behaviour of construction dewatering systems in fine soils, Géotechnique, 44(1), pp. 83-100.

Powrie, W., A.A. Al-Thani, R.P. Beaven, and J.K. White, 2001, Modelling flow to leachate wells in landfills, *Sardinia 2001*, Proceedings of the Eighth International Waste Management and Landfill Symposium, S. Margherita di Pula, Cagliari, Italy; October 1-5, Vol III, pp 615-621.

Preene, M., 1992, *The Design of Pore Pressure Construction Dewatering Systems in fine Soils*, PhD Dissertation, University of London.

Preene, M., T.O.L Roberts, W. Powrie, and M.R. Dyer, 2000, *Groundwater Control: Design and Practice*, CIRIA report no. C515, 204 p.

Prickett, T.A., and C.G. Lonnquist, 1971, Selected digital computer techniques for groundwater resources evaluation, Illinois State Water Survey, Bulletin 55, 63 p.

Reilly, T.E., and A.W. Harbaugh, 1993, Simulation of cylindrical flow to a well using USGS modular finite-difference groundwater-flow model, Ground Water, 31(3), pp. 489-494.

Richards, L.A., 1931, Capillary conduction of liquids through porous mediums, Physics, 1, pp.318-333.

Roberts, T.O.L., 1988, *Seepage in Shallow Unconfined Aquifers: Permeability Limits For Gravity Drainage,* PhD Dissertation, University of London.

Romeu, R.H., and B. Neotinger, 1995, Calculation of inter nodal transmissivites in finite difference models of flow in heterogeneous porous media, Water Resources Research, 3(1), pp. 943-959.

Rowe, K. and P. Nadarajah, 1996, Estimating leachate drawdown due to pumping wells in landfills, Journal of Canadian Geotechnical, 33, pp.1-10.

Rubin, J., 1968, Theoretical analysis of two-dimensional, transient flow of water in unsaturated and partly saturated soils, Proceedings of the American Society of Soil Science, 32, pp. 607-615.

Rushton, K. R., and S.C. Redshaw, 1979, *Seepage and Groundwater Flow*, John Wiley and Sons, New York, N.Y., 339 p.

Schneebeli, G., 1955, Expériences sure la limite de validité de la loi de Darcy et l'apparition de la turbulence dans un écoulement de filtration, La Houille Blanche, 10, pp. 141-149. (see Kresic (1997) page 165).

Shamsai, A., and T. N. Narasimhan, 1991, A numerical investigation of free surface-seepage face relationship under steady state flow conditions, Water Resources Research, 27(3), pp. 409-421.

Sichardt, G., 1928, *Das Fassungsvermögen von Rohrbrunnen und seine Bedeutung für die Grundwasserabsenkung, insbesondere für größere Absenkungstiefen. J. Springer, Berlin.* (see Brauns (1981))

Sisson, J.B. A.H. Ferguson, and M.Th. van Genuchten, 1980, Simple method for predicting drainage from field plots, Soil Science Society of American Journal, 44, 1147-1152.

Somerville, S.H., 1986, *Control of Groundwater for Temporary Works*, CIRIA report no. 113.

Spitz, K., and J. Moreno, 1996, *A Practical Guide to Groundwater and Solute Transport Modeling*, John Wiley and Sons, New York, N.Y., 461 p.

Stone, H.L., 1968, Iterative solution of implicit approximation of multidimensional partial differential equations, SIAM Journal on Numerical Analysis, 5(3), pp. 530-558.

Taylor, G.S., and J.N. Luthin, 1969, Computer methods for transient analysis of water-table aquifers, Water Resources Research, 5(1), pp. 144-152.

Todd, K.D., 1980, *Groundwater Hydrology*, John Wiley and Sons, New York, N.Y., 535 p.

Vajpeyi, D.K., 1998, *Water Resources Management: A Comparative Perspective*, Praeger Publishers, Westport, CT, 173 p.

van Genuchten, M.Th, 1980, A closed-form equation for predicting the hydraulic conductivity of unsaturated soils, Journal of the American Society of Soil Science, 44, pp. 892-898.

van Poollen, H.K., H.C. Bixel and J.R. Jargon, 1970, Individual well pressures in reservoir modeling, Oil and Gas Journal, October 26, pp. 78-80.

Vauclin, M., G. Vachaud and J. Khanji, 1975, Two dimensional numerical analysis of transient water transfer in saturated-unsaturated soils, *Computer Simulation of Water Resources Systems*, Proceedings of the IFIP working conference, Ed. G.C. Vansteenkiste, North-Holland Publishing Company, Amsterdam, and American Elsevier, New York, 229-323.

Vauclin, M., D. Khanji and G. Vachaud, 1979, Experimental and numerical study of a transient, two-dimensional unsaturated-saturated water table recharge problem, Water Resources Research, 15(5), pp. 1089-1101.

Wang, H.F., and M.P. Anderson, 1982, *Introduction to Groundwater Modeling: Finite Difference and Finite Element Methods*, Academic Press, London, 237 p.

Watson, K.K., and S.A. Awadalla, Comparative study of Green Ampt analysis for a falling water table in a homogenous sand profile, Water Resources Research, 21(8), pp. 1157-1164.

Wenzel, L.K., 1932, Specific yield determined from a Thiem's pumping test, Transactions. American Geophysical Union, 13th Annual Meeting. (see Muskat (1937) page 367).

Whisler, F.D., and K.K. Watson, 1968, One-dimensional gravity drainage of uniform columns of porous materials, Journal of Hydrology, 6, pp. 227-296.

Wise, R.W. and T.P. Clement, 1994, Discussion on Maximum water-table drawdown at fully penetrating pumping well, Ground Water, 33(3), pp. 499-501.

White, J.K., 1998, Department of Civil and Environmental Engineering, University of Southampton, Southampton SO17 1BJ, United Kingdom, personal communication.

Woessner, W.W., and M.P. Anderson, M.P., 1998, Advantages and disadvantages of teaching MODFLOW using pre- and post-processors, Proceedings of MODFLOW'98, Volume 1, October 4-8, Golden, Colorado, pp. 473-480.

Wyckoff, R.D., H.G. Botset, and M. Muskat, 1932, Flow of liquids through porous media under the action of gravity, Physics, 2, pp. 90-113.

Yang, S.T., 1949, *Seepage Toward a Well Analyzed by the Relaxation Method*, Doctoral dissertation, Harvard University.

Youngs, E.G., and S. Aggelides, 1976, Drainage to water table analyzed by Green-Ampt approach, Journal of Hydrology, 31, pp. 67-79.

Youngs, E.G., 1966, Exact analysis of certain problems of ground-water flow with free surface conditions, Journal of Hydrology, 4, pp. 277-281.

Zee, C., D.F. Peterson, and R.O. Bock, 1957, Flow into a well by electric and membrane analogy, Transactions. American Society of Civil Engineers, N.Y., 122, pp. 1088-1112.

Zheng, C., and G.D. Bennert, 1995, *Applied Contaminant Transport Modeling: Theory and Practice*, Van Nostrand Reinhold, New York, 440 p.

Appendices

Appendix A

Governing Equation of Groundwater Seepage

A.1 Background

In almost every field of science and engineering the techniques of analysis are based on our understanding of the physical processes. In most cases it is possible to describe these processes mathematically. In the case of groundwater seepage, the basic law of flow is *Darcy's* law and when it is combined with the equation of continuity, the result is a constitutive partial differential equation of flow. The equation describes the conservation of fluid mass during flow through a porous medium. In order to understand how this constitutive partial differential equation can be developed for confined or unconfined aquifers, we need to define both specific storage and storage coefficient. The brief explanation used here is modified from *McWhorter and Sunada* (1993) and for more detailed information the reader is advised to refer to this reference. Other references includes *Anderson and Woessner*, 1992; *Bear,* 1979; *Bear and Verruijt,* 1987; and *de Marsily*, 1986.

A.2 Mass Balance

The differential equation applicable to the flow of groundwater is an expression of the budgetary requirement that mass must be conserved everywhere in the flow domain. The differential equations are developed by combining *Darcy's* equation with the principle of mass balance, which requires consideration of mass inflow, mass outflow,

and change in groundwater storage. The mass balance is derived for a control volume. Figure A.1 shows a control volume in which the mass discharge across any plane of the surface of the volume is the product of the water density ρ and the volume discharge Q. The principle of the conservation of mass means that the difference between the mass flow entering the three faces and the sum of the mass flow exiting the opposite faces is equal to the rate of change of mass contained in the volume.

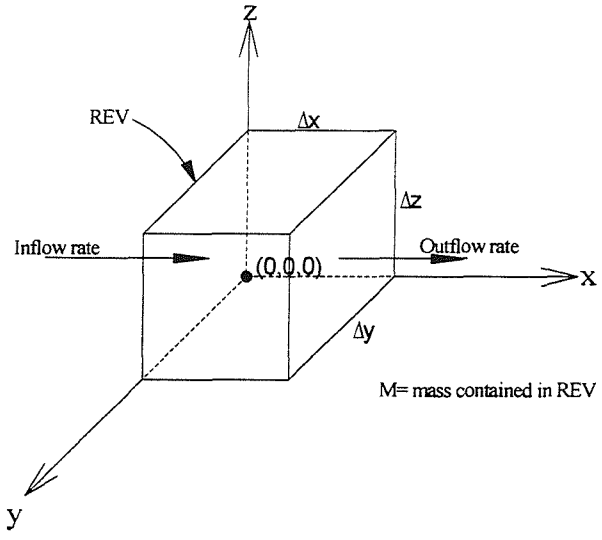

Figure A.1 Control volume for mass balance calculation.

Considering the two planes normal to the x-axis, the difference between the outflow and inflow mass discharge is

$$Outflow\ rate - Inflow\ rate = (\rho Q)_{\Delta x} - (\rho Q)_{0x} \tag{A.1}$$

The same expression maybe written for the y and z directions. Given small dimensions for the control volume, the discharge across the plane at $x=\Delta x$ can be associated with that across the plane at $x=0$ by expansion in a Taylor series.

$$(\rho Q)_{\Delta x} = (\rho Q)_{0x} + \frac{\partial}{\partial x}(\rho Q)\Delta x + 0(\Delta x^2 .....) \tag{A.2}$$

The last term on the right represents terms of order Δx^2, Δx^3 etc. If Δx is small these terms in the Taylor series can be neglected and equation A.2 becomes

$$Outflow\ rate - Inflow\ rate = \frac{\partial}{\partial x}(\rho Q)\Delta x \tag{A.3}$$

The flow Q is computed on the basis of *Darcy's* law and can be expressed as the product of *Darcy* velocity and the area normal to the flow

$$Q = q_x(\Delta y \Delta z) \tag{A.4}$$

Again similar expressions can be written for the y and z directions. Accounting for all planes in the control volume results in the following equation,

$$Outflow\ rate - Inflow\ rate = \left[\frac{\partial}{\partial x}(\rho q_x) + \frac{\partial}{\partial y}(\rho q_y) + \frac{\partial}{\partial z}(\rho q_z)\right]\Delta x \Delta y \Delta z \tag{A.5}$$

Equation A.5 expresses the net rate of mass outflow, which must equal the time rate of change of mass M within the control volume.

$$\left[\frac{\partial}{\partial x}(\rho q_x) + \frac{\partial}{\partial y}(\rho q_y) + \frac{\partial}{\partial z}(\rho q_z)\right]\Delta x \Delta y \Delta z = -\frac{\partial M}{\partial t} \tag{A.6}$$

The negative sign ensures the convention that the net outflow is positive when mass is being drained from storage.

Knowing that the compressibility of water is usually small we may assume that ρ is constant so that, equation A.6 can be rewritten as

$$\rho\left(\frac{\partial q_x}{\partial x} + \frac{\partial q_y}{\partial y} + \frac{\partial q_z}{\partial z}\right)\Delta x \Delta y \Delta z = -\frac{\partial M}{\partial t} \tag{A.7}$$

For flow in a non-homogenous, anisotropic aquifer in which the principal directions of hydraulic conductivity coincide with the coordinate directions x, y, z we can introduce *Darcy's* law into equation A.7 and get

$$\frac{\partial}{\partial x}\left(K_x \frac{\partial h}{\partial x}\right)+\frac{\partial}{\partial y}\left(K_y \frac{\partial h}{\partial y}\right)+\frac{\partial}{\partial z}\left(K_z \frac{\partial h}{\partial z}\right)=\frac{1}{\rho \Delta x \Delta y \Delta z}\frac{\partial M}{\partial t} \qquad \text{(A.8)}$$

since $q_x=-K_x\frac{\partial h}{\partial x}$, $q_y=-K_y\frac{\partial h}{\partial y}$, and $q_z=-K_z\frac{\partial h}{\partial z}$ (see *Darcy's* law in Chapter 2).

A.3 Storativity

The rate of change of mass in an elemental volume has two components. First, there may be a change in mass because of removal (abstraction) or injection (recharge) of flow out of or into the element. Secondly, there may be a change in mass as the result of compression effects following a change in pressure head. The specific storage, S_s, of a saturated aquifer is the volume of water released from storage per unit volume of aquifer under a unit decline in hydraulic head, h, and has a dimension L^{-1}. Thus

$$\frac{1}{\rho \Delta x \Delta y \Delta z}\frac{\partial M}{\partial t}=w+S_s\frac{\partial h}{\partial t} \qquad \text{(A.9)}$$

where w is the volumetric recharge flow per unit volume.

The water that is released from storage by decreasing h is a product of two mechanisms the compaction of the aquifer as a result of increasing effective stress, σ_e, and the expansion of the water as a result of decreasing pressure, p. The nature of these mechanisms indicates that a mass balance approach rather than the volume balance approach is appropriate. The volume balance approach is applicable only when the water is considered to be incompressible, as in the case of an unconfined aquifer.

The mass of water in the saturated element of the aquifer shown in Figure A.1 is

$$M = \rho n \, \Delta x \, \Delta y \Delta z \tag{A.10}$$

where ρ is the fluid density and n is the porosity.

Assuming that the aquifer compresses only in the vertical direction z, the change in mass following the rule of product differentiation, due to both geometric changes and density changes, is given by

$$dM = \{\rho \, d(n\Delta z) + n\Delta z \, d\rho\}\Delta x \Delta y \tag{A.11}$$

The first quantity in equation A.11, $\rho \, d(n\Delta z)$, is the contribution per unit area due to a change in pore volume at constant density. The second quantity $n\Delta z \, d\rho$, is the contribution per unit area due to a change in water density at a constant pore volume, that is the expansion of water. The coefficient of compressibility, α_p, of a pore volume *is* defined as

$$\alpha_p \equiv -\frac{1}{n\Delta z}\frac{d(n\Delta z)}{d\sigma_z} = \frac{1}{n\Delta z}\frac{d(n\Delta z)}{dp} \tag{A.12}$$

The compressibility is therefore the specific change in pore volume per unit change in intergranular stress. From equation A.12

$$d(n\Delta Z) = \alpha_p n\Delta z dp \tag{A.13}$$

Thus the quantity in equation (A.11) $\rho \, d \, (n\Delta z)$ becomes

$$\rho\alpha_p \, n\Delta z \, dp \tag{A.14}$$

It should be noted that in granular materials, the total volume of soil mass reduction due an increase in effective stress occurs almost entirely because of grain rearrangements. In another words, although it is true that individual grains may themselves be compressible, the effect is often considered negligible. Thus, let $dv_T = dv_s$

$+ dv_v$, where dv_T is the change in the total volume, dv_s is the change in volume of solids and dv_v is the change in volume of the water-saturated voids. We are assuming that $dv_s = 0$ and that $dv_T = dv_s$ (*Freeze and Cherry*, 1979).

The coefficient of compressibility of water β can be expressed as

$$\beta = -\frac{1}{V_w}\frac{dV_w}{dp} \tag{A.15}$$

where, V_w is the volume of water, and dV_w is the change in V_w caused by a change in pore pressure dp. Since the mass of water is constant, the density change following a change in volume dV_w is given by,

$$d\rho = -\rho\frac{dV_w}{V_w} \tag{A.16}$$

by combining equation A.15 and equation A.16 we obtain

$$d\rho = \rho\beta dp \tag{A.17}$$

therefore, the change of mass per unit area due to water compressibility $n\Delta z\ d\rho$ becomes

$$dM_2 = n\Delta z\beta\rho dp \tag{A.18}$$

substituting into equation A.11 gives,

$$dM = \{\rho\alpha_p n\Delta z\ dp + n\Delta z\beta\rho dp\}\Delta x\Delta y \tag{A.19}$$

In order to express the changes in units of volume rather than mass, both sides can be divided by ρ and the element volume $\Delta x\ \Delta y\ \Delta z$ to give,

$$\frac{d\bar{V}_w}{\Delta x \Delta y \Delta z} = n(\alpha_p + \beta)\, dp \tag{A.20}$$

where, $d\bar{V}_w$ is the change in water volume in the element. The changes of pressure dp at a point in the aquifer due to a change in the hydraulic head dh is,

$$dp = \rho g\, dh \tag{A.21}$$

Thus from equation A.20 and equation A.21 the specific storage which is the change in volume per unit volume per unit head is obtained,

$$S_s = \frac{dV_w}{(\Delta x \Delta y \Delta z) dh} = \rho g n(\alpha_p + \beta) \tag{A.22}$$

this leads to

$$\frac{\partial}{\partial x}\left(K_x \frac{\partial h}{\partial x}\right) + \frac{\partial}{\partial y}\left(K_y \frac{\partial h}{\partial y}\right) + \frac{\partial}{\partial z}\left(K_z \frac{\partial h}{\partial z}\right) - w = S_s \frac{\partial h}{\partial t} \tag{A.23}$$

or

$$\nabla(K \nabla h) - w = S_s \frac{\partial h}{\partial t} \tag{A.24}$$

where K_x, K_y, and K_z are values of hydraulic conductivity along the x, y, and z coordinate axes; h is the head; w is volumetric recharge flow per unit volume; S_s is the specific storage; x, y, and z are coordinate directions; and t is time. Equation A.24, is a linear partial differential equation that relates time and space distributions of piezometric head, h, in non-homogenous, anisotropic aquifers.

A.4 Comments on 2D Unconfined and Confined Conditions

The transmissivity T of a confined aquifer with a thickness b is

$$T = Kb \tag{A.25}$$

and the storage coefficient, S, which also known as the storativity is

$$S = S_s b \tag{A.26}$$

which can be defined in terms of words as the volume of water an aquifer releases per unit surface area of the aquifer per unit decline in the hydraulic head normal to the surface and has the dimension L^{-1}.

In the case of an unconfined aquifer, transmissivity is defined as shown in equation A.25, but the thickness, b, is now the saturated thickness of the aquifer, which is defined by the level of the water table above the impermeable layer. The term used to describe storage in unconfined aquifer is known as specific yield, S_y. It is defined as the volume of water that an unconfined aquifer would release per unit surface area of the aquifer per unit decline in the water table.

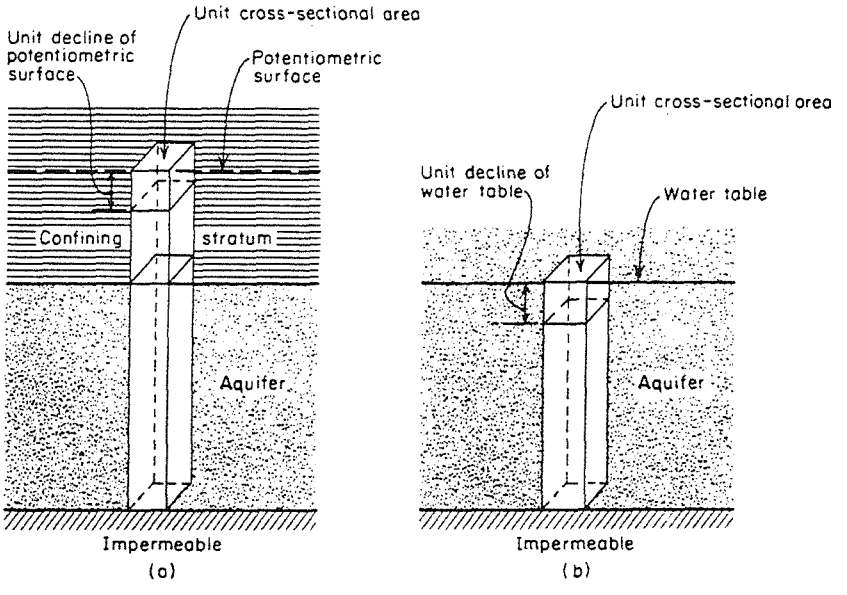

Figure A.2 Schematic representation of the storativity in **(a)** confined and **(b)** unconfined aquifers. (After *Ferris et al.*, 1962.)

A.5 Additional Forms of the Governing Equation

Equation A.24 can be written in different forms according to the aquifer conditions. For homogeneous and anisotropic aquifers,

$$K_x \frac{\partial^2 h}{\partial x^2} + K_y \frac{\partial^2 h}{\partial y^2} + K_z \frac{\partial^2 h}{\partial z^2} = S_s \frac{\partial h}{\partial t} \tag{A.27}$$

For homogeneous and isotropic aquifers where $K_x = K_y = K_z = K$

$$\frac{\partial^2 h}{\partial x^2} + \frac{\partial^2 h}{\partial y^2} + \frac{\partial^2 h}{\partial z^2} = \frac{S_s}{K} \frac{\partial h}{\partial t} \tag{A.28}$$

For steady state conditions equation A.28 becomes

$$\frac{\partial^2 h}{\partial x^2} + \frac{\partial^2 h}{\partial y^2} + \frac{\partial^2 h}{\partial z^2} = 0 \tag{A.29}$$

Equation A.29 is known as the Laplace equation, which describes the flow of groundwater through isotropic, homogenous aquifers under steady state conditions.

A.6 Boussinesq Equation for Deep Unconfined Aquifers

The *Dupuit* assumption of horizontal flow in unconfined aquifers allows the use of a material-balance control volume that extends from the horizontal floor of the aquifer to the water table (Figure A.2b and A.3). A mass balance is assured by volume balance since the changes in water density are unimportant in unconfined aquifers. Following the procedures of the previous section on confined aquifers, the rate of net outflow from the control volume is

$$Net\ \ Flow\ \ Rate\ = \frac{\partial Q_x}{\partial x} \Delta x + \frac{\partial Q_y}{\partial y} \Delta y \tag{A.30}$$

Knowing that $Q = -Kh\frac{dh}{dx}$, equation A.30 can be re-written as

$$\frac{Net\ \ Flow\ \ Rate}{\Delta x \Delta y} = \frac{\partial}{\partial x}(Kh\ \frac{\partial h}{\partial x}) - \frac{\partial}{\partial y}(Kh\ \frac{\partial h}{\partial y}) \qquad (A.31)$$

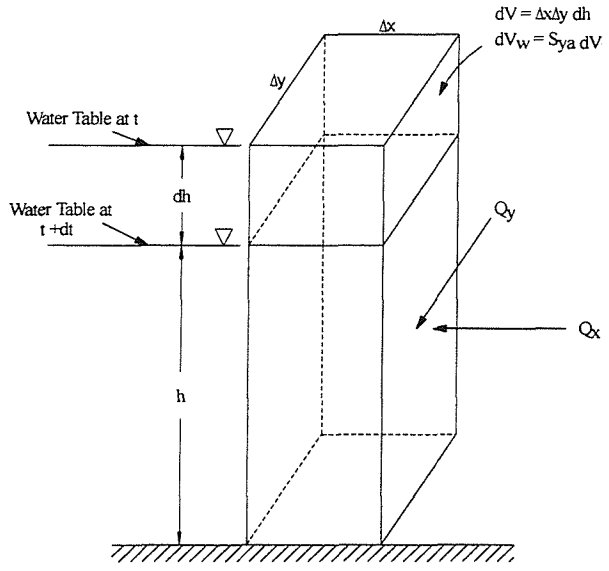

Figure A.3 Control volume in an unconfined aquifer. (After *McWhorter and Sunada*, 1993.)

As before, the rate of outflow must equal the negative time rate of reduction of stored volume. The change in water table combined with a change, *dh*, of water table level follows from the specific yield definition discussed earlier

$$\frac{\partial V_w}{\partial t} = S_{ya}\frac{\partial h}{\partial y}\Delta x \Delta y \qquad (A.32)$$

Combining equation A.31 and A.32 produce

$$\frac{\partial}{\partial x}\left(Kh\ \frac{\partial h}{\partial x}\right) + \frac{\partial}{\partial y}\left(Kh\ \frac{\partial h}{\partial y}\right) = S_{ya}\ \frac{\partial h}{\partial t} \qquad (A.33)$$

This reduces to equation A.33 for a homogenous aquifer

$$\frac{\partial}{\partial x}\left(h\frac{\partial h}{\partial x}\right)+\frac{\partial}{\partial y}\left(h\frac{\partial h}{\partial y}\right)=\frac{S_{ya}}{K}\frac{\partial h}{\partial t} \tag{A.34}$$

Equation A.34 is the non-linear *Boussinesq* equation. Linearization of *Boussinesq* equation is possible when the spatial variation of h remains small compared to h. In this case an average thickness, b, can replace the variably-saturated flow to obtain what is known as the *Linearized Boussinesq* equation.

$$\frac{\partial^2 h}{\partial x^2}+\frac{\partial^2 h}{\partial y^2}=\frac{S_{ya}}{bK}\frac{\partial h}{\partial t} \tag{A.35}$$

Appendix B

MODFLOW

B.1 Background

MODFLOW is a three-dimensional, cell-centered, finite difference, saturated flow model developed by *McDonald and Harbaugh* of the United States Geological Survey. MODFLOW can perform both steady and transient analyses that simulate confined, unconfined, or a combination of confined and unconfined aquifer types. Flow connected with external "stresses", such as wells, areal recharge, evapotranspiration, drains, and streams can also be simulated. The finite-difference equations are solved either using the Strongly Implicit Procedure (SIP) method or the Slice-Successive Overrelaxation (SSOR) method. The popularity of this code is attributed to four factors. First, the code has proved to be a powerful and robust tool for early users who applied the code to a variety of practical problems. Second, the user's guide is very useful and extremely detailed to provide a clear description of how the various codes options are used. Third, the US Geological Survey has been very supportive to the code development and recently more specialized versions of the code have been marketed by several private companies. Finally, the success of the original code has created an extensive array of training courses and a large number of related calculational modules.

B.2 Derivation of the Finite-Difference Equations

In this section, the finite-difference equations for aquifer simulation are developed. The theory here relates specifically to the standard code of MODLFOW. In the finite-difference method, the governing differential equation for groundwater flow is replaced by a finite difference equation that represents the conservation principles of the original differential equation. From equation A.23 we have that the general form of the governing equation is as follows

$$\frac{\partial}{\partial x}\left(K_{xx}\frac{\partial h}{\partial x}\right)+\frac{\partial}{\partial y}\left(K_{yy}\frac{\partial h}{\partial y}\right)+\frac{\partial}{\partial z}\left(K_{zz}\frac{\partial h}{\partial z}\right)-w=S_s\frac{\partial h}{\partial t} \tag{B.1}$$

where K_x, K_y, and K_z are values of hydraulic conductivity along the x, y, and z coordinate axes; h is the head; w is volumetric recharge flow per unit volume; S_s is the specific storage; x, y, and z are coordinate directions; and t is time. In general, S_s, K_x, K_y, and K_z may be functions of space ($S_s = S_s(x, y, z)$, $K_x = K_x(x, y, z)$, etc.) and w may be a function of space and time $w= w(x, y, z, t)$. Equation B.1 describes groundwater flow under non-equilibrium conditions in a heterogeneous and anisotropic medium

The development of the finite-difference flow equation is based on the idea of continuity as previously discussed in sections A.2 and A.3. The continuity equation states that the sum of flows into and out of any cell is equal to the rate of storage change within the cell. Assuming that the density of groundwater is constant, the continuity equation can be expressed mathematically for a cell as

$$\sum Q_i = S_s\frac{\Delta h}{\Delta t}\Delta V \tag{B.2}$$

where Q_i is the flow rate into the cell; S_s is the specific storage; Δh is the change in head over a time interval Δt; and ΔV is the volume of the cell. Both the left hand side and the right hand side of equation B.2 can be expanded, the first in terms of flows

through the six sides of the cell (Figure B.1), and the second in terms of the cell dimensions to give

$$Q_{i,j-1/2,k} + Q_{i,j+1/2,k} + Q_{i-1/2,j,k} + Q_{i+1/2,j,k} + Q_{i,j,k-1/2} + Q_{i,j,k+1/2} + QS_{i,j,k} = Ss_{i,j,k} \frac{\Delta h_{i,j,k}}{\Delta t} \Delta r_j \Delta c_i \Delta v_k \quad \text{(B.3)}$$

where $Q_{i, j-1/2,k}$ is the volumetric fluid discharge through the face between cells i, j, k; and $i, j-1, k$, $QS_{i,j,k}$ is the sum of all other inflows and outflows from the cell; and Δc_i, Δv_k, Δr_j are the dimensions of the cell i, j, k (Figure B.2)

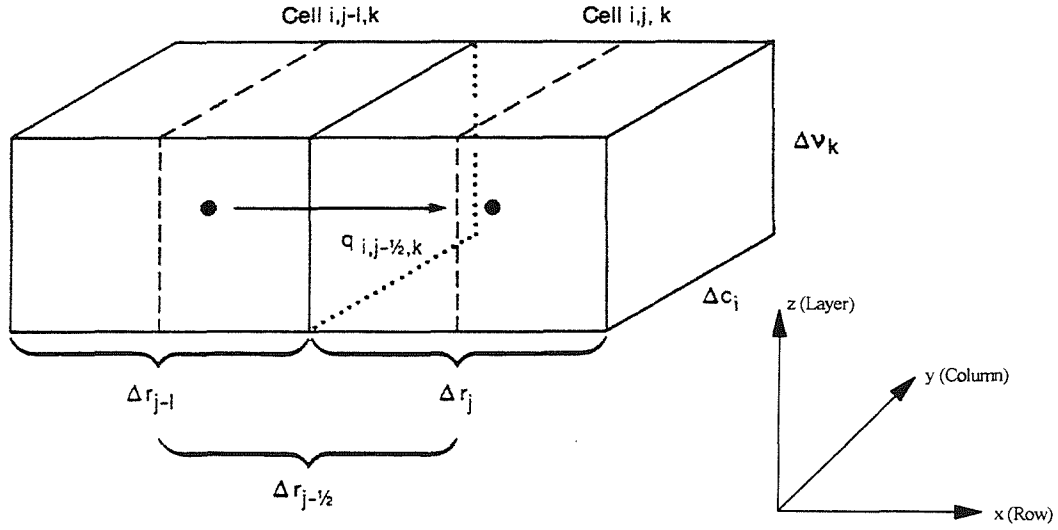

Figure B.1 Cell i, j, and k indices for the six adjacent cells

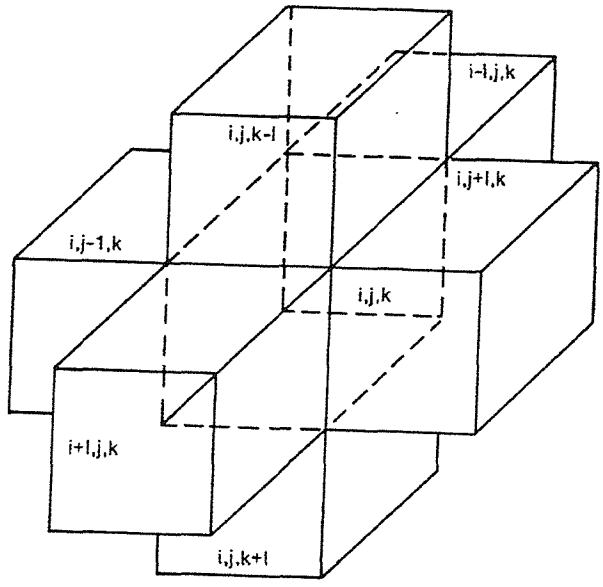

Figure B.2 Flow into cell *i,j*, and *k* from cell *i,j*-1, and *k*. (After *McDonald and Harbaugh*, 1988.)

The inflow through the cell faces can be expressed in terms of hydraulic head using *Darcy's* equation as

$$Q_{i,j-1/2,k} = KR_{i,j-1/2,k}\Delta c_i \Delta v_k \frac{(h_{i,j-1,k} - h_{i,j,k})}{\Delta r_{j-1/2}} \tag{B.4}$$

where $h_{i,j,k}$ is the hydraulic head at node *i, j, k*; $h_{i,j-1,k}$ is the hydraulic head at node *i, j-1, k*; $KR_{i,j-1/2,k}$ is the hydraulic conductivity along the row between nodes *i, j, k* and *i, j-1, k*; $\Delta c_i \Delta v_k$ is the area of the cell face normal to the row direction; and $\Delta r_{j-1/2}$ is the distance between nodes *i, j, k* and *i, j-1, k* (*McDonald and Harbaugh*, 1988). The minus sign was eliminated to simplify the development. The form of this and similar equations for other faces can be simplified by defining a hydraulic conductance term, *CR* where

$$CR_{i,j-1/2,k} = KR_{i,j-1/2,k} \frac{\Delta c_i \Delta v_k}{\Delta r_{j-1/2}} \tag{B.5}$$

Making this substitution, the six inflow equations can be written as

$$Q_{i,j-1/2,k} = CR_{i,j-1/2,k}(h_{i,j-1,k} - h_{i,j,k}) \tag{B.6}$$

$$Q_{i,j+1/2,k} = CR_{i,j+1/2,k}(h_{i,j+1,k} - h_{i,j,k}) \tag{B.7}$$

$$Q_{i-1/2,j,k} = CC_{i-1/2,j,k}(h_{i-1,j,k} - h_{i,j,k}) \tag{B.8}$$

$$Q_{i+1/2,j,k} = CC_{i+1/2,j,k}(h_{i+1,j,k} - h_{i,j,k}) \tag{B.9}$$

$$Q_{i,j,k-1/2} = CV_{i,j,k-1/2}(h_{i,j,k-1} - h_{i,j,k}) \tag{B.10}$$

$$Q_{i,j,k+1/2} = CV_{i,j,k+1/2}(h_{i,j,k+1} - h_{i,j,k}) \tag{B.11}$$

where the hydraulic conductance in the column and layer directions are given by *CC* and *CV*, respectively. Following the notation of *McDonald and Harbaugh* (1988), the combined flows due to a number N of sources or sinks is given as $QS_{i,j,k}$

$$QS_{i,j,k} = P_{i,j,k}\, h_{i,j,k} + Q_{i,j,k} \tag{B.12}$$

where $P_{i,j,k}$ and $Q_{i,j,k}$ represent the sum of constants related to N different inflow or outflow processes like pumping, induced recharge, etc.

The final form of the finite difference equation is written by combining the previous equations

$$CR_{i,j-1/2,k}(h_{i,j-1,k}-h_{i,j,k})+CR_{i,j+1/2,k}(h_{i,j+1,k}-h_{i,j,k})+CC_{i-1/2,j,k}(h_{i-1,j,k}-h_{i,j,k})+$$
$$CC_{i+1/2,j,k}(h_{i+1,j,k}-h_{i,j,k})+CV_{i,j,k-1/2}(h_{i,j,k-1}-h_{i,j,k})+CV_{i,j,k+1/2}(h_{i,j,k+1}-h_{i,j,k}) \quad \text{(B.13)}$$
$$+P_{i,j,k}\ h_{i,j,k}+Q_{i,j,k}=SS_{i,j,k}(\Delta r_j\Delta c_i\Delta v_k)\frac{\Delta h_{i'j'k}}{\Delta t}$$

One final step in the derivation is to replace the $\Delta h/\Delta t$ term on the RHS of equation B.13 by a backward time difference

$$\frac{\Delta h_{i,j,k}}{\Delta t}=\frac{h^m_{i,j,k}-h^{m-1}_{i,j,k}}{t_m-t_{m-1}} \quad \text{(B.14)}$$

where m denotes the present time at which the heads are unknown and m-1 denotes the previous time step. The final step form of the finite difference equation is expressed as

$$CV_{i,j,k-1/2}h^m_{i,j,k-1}+CC_{i-1/2,j,k}h^m_{i-1,j,k}+CR_{i,j-1/2,k}h^m_{i,j-1,k}+(-CV_{i,j,k-1/2}-CC_{i-1/2,j,k}-CR_{i,j-1/2,k}$$
$$-CR_{i,j+1/2,k}-CC_{i+1/2,j,k}-CV_{i,j,k+1/2}+HCOF_{i,j,k})h^m_{i,j,k}+CR_{i,j+1/2,k}h^m_{i,j+1,k}+CC_{i+1/2,j,k}h^m_{i+1,j,k}$$
$$+CV_{i,j,k+1/2}h^m_{i,j,k+1}=RHS_{i,j,k} \quad \text{(B.15)}$$

where

$$HCOF_{i,j,k}=P_{i,j,k}-\frac{SCI_{i,j,k}}{t_m-t_{m-1}} \quad \text{(B.16)}$$

$$RHS_{i,j,k}=-Q_{i,j,k}-\frac{SCI_{i,j,k}\,h^{m-1}_{i,j,k}}{t_m-t_{m-1}} \quad \text{(B.17)}$$

$$SCI_{i,j,k}=Ss_{i,j,k}\Delta r_j\Delta c_i\Delta v_k \quad \text{(B.18)}$$

Writing one equation for each of the cells in the system yields a system of equations

$$[A]\{h\} = \{q\} \tag{B.19}$$

where $[A]$ is the coefficient matrix, $\{h\}$ is the vector of unknown head values, and $\{q\}$ is a vector of constant-head terms.

B.3 Boundary Conditions

Domenico and Schwartz (1990) summarized the boundary conditions described in the MODFLOW documentation as follows, "*the six boundaries of the three-dimensional domain in MODFLOW (that is, top, bottom, and sides) are no-flow boundaries by default. Creating flow across these boundaries requires that a different type of boundary condition be created. For example, one could make one of the side boundaries a constant-head boundary or a flux boundary by adding water to particular nodes along the boundary. There is a place in the Basic Input package to designate specific nodes as fixed head or inactive. A constant-flux boundary may be simulated by simply adding or withdrawing water from boundary nodes as if a well is present. These boundaries are specified with the Basic Input and/or Well package.*

Fluxes into or out of the top and other layers of the model could occur due to the presence of lakes or rivers. In the model region, these features can be represented by constant-head boundaries or variable-flux boundaries using the River Package. Similarly, recharge from precipitation can be added by applying a small flux at all nodes present in recharge areas. It is this ability to adjust the boundary conditions and treat various groups of internal nodes that make numerical models so powerful in representing complex hydrogeologic systems."

B.4 Solving of Finite-Difference Equations

The mathematical solution of the system of equations presented yields the hydraulic head for the given time step. Procedures for solving systems of such algebraic equations maybe categorized broadly as either direct or iterative. The original MODFLOW contained two iterative schemes. The relatively simpler Slice-Successive Overrelaxation (SSOR), and the strongly Implicit Procedure (SIP). The latter procedure involves solving the equations for entire grid simultaneously. In addition, this solution technique is extremely fast and powerful which means that its used more often now in solving systems of linear equations (*McDonald and Harbaugh*, 1988). More recently, *Hill* (1990) implemented a Preconditioned Conjugate Gradient procedure (PCG) for use with MODFLOW. In general, this and similar techniques are extremely fast and robust which are the reasons for the frequent use of the PCG procedure in solving systems of linear equations.

B.5 Modular Program Structure

MODFLOW is built with a modular design that consists of a main program and "packages." Each package is a group of independent subroutines that performs a specific simulation task. The input for each package is stored in a separate input file. Such a structure facilities the integration of new packages to enhance the code's capabilities. Table B.1 lists packages in the basic code and the new packages that were added to the original version along with a brief description of their function (*McDonald and Harbaugh, 1988*)

Table B.1 A summary of the packages contained in MODFLOW (*McDonald and Harbaugh*, 1988).

Package Name	Package Description
Basic (BAS)	Handles those tasks that are part of the model as a whole. Among those tasks are specification of boundaries, determination of time-step length, establishment of initial conditions, calculating a water budget, and printing of results (*.bas)
Block-Centered Flow (BCF)	Required in all model calculations. Reads basic information on the grid spacing, pattern of layering, aquifer type, and hydraulic parameters to

	calculate terms of finite-difference equations that represent flow within porous medium, specifying flow from cell to cell and flow into storage (*.bcf)
Well (WEL)	Location and pumping schedules. The package adds terms representing flow to wells to the finite-difference equations (*.wel)
Recharge (RCH)	This package is designed to simulate the addition of natural recharge from precipitation to the model. Adds terms representing distributed recharge to the finite-difference equations (*.rch)
River (RIV)	This package provides the capability of modelling groundwater, surface water interactions. Accounts for both the size of the stream and the possibility of a discrete low-permeability streamed. Adds terms representing flow to rivers to the finite-difference equations (*.riv)
Drain (DRN)	Similar to the river package except considers only inflow to the drain. The package adds terms representing flow drains to the finite-difference equations (*.drn)
Evapotranspiration (EVT)	Adds terms representing evapotranspiration to the finite-difference equations. Accounts for the effects of plant evapotranspiration and direct evaporation of ground water. Rate varies as a function of the water-table depth (*.evt)
General-Head Boundaries (GHB)	Provides the possibility of variable flow across the model boundaries. The extent of flow depends on the head difference between the cell and some constant head at a source away from the boundary. Adds terms representing general-head boundaries to the finite-difference equations (*.ghb)
Strongly Implicit Procedure (SIP)	Iteratively solves the system of finite-difference equations using the Strongly Implicit Procedure (*.sip)
Slice-Successive Overrelaxation (SOR)	Iteratively solves the system of finite-difference equations using Slice-Successive Overrelaxation (*.sor)
Output Control (OC)	Provides user with the ability to control what calculations are printed as output and at what time steps (*.oc)
Some of the packages that were added to the original version of MODFLOW	
Preconditioned Conjugate Gradient 2 (PCG2)	Alternative matrix solver (*.pcg)
Stream Routing (STR1)	Differs from the river module in that the surface water stage varies based on the surface water flow and the Manning equation (*.str)
Block-Centered Flow 2 (BCF2)	Allows for rewetting of cells that have gone dry (*.bcf)
Block-Centered Flow 3 (BCF3)	A supplement to the BCF2 module, allowing alternative interblock transmissivity formulations (*.bcf)
Horizontal Flow Barrier (HFB1)	Simulation of thin, vertical, low permeability features that impede horizontal flow (*.hfb)
Transient Leakage	Simulates transient leakage and storage changes in confining units of quasi-

(TLK1)	3D models (*.tlk)
General Finite Difference Flow (GFD1)	A substitute for the BCF module, allows user to enter conductance rather than calculating with MODFLOW (*.gfd)
Interbed Storage (IBS1)	Simulates compaction of compressible, fine-grained units within or adjacent to aquifers in response to pumping (*.ibs)
Time-Variant Specified Head Boundary (CHD1)	Allows time varying specified head (*.chd)

Appendix C

Selected Published Papers

1. **The Impact of the Seepage Surface on the Design of Pump-and-Treat Remediation systems for Contaminated Aquifers-Single Well Model.**

Reference: Al-Thani, A.A. and J.K. White, 1999, The impact of the seepage surface on the design of pump-and-treat remediation systems for contaminated aquifers-based on single well, Workshop on Ground Water Pollution, Protection and Remediation, November 7-10, Qatar.

2. **The Impact of the Seepage Surface on the Design of Pump-and-Treat Remediation Systems for Contaminated Aquifers.**

Reference: Al-Thani, A.A. and J.K. White, 2000, The impact of the seepage surface on the design of pump-and-treat remediation systems for contaminated aquifers-based on multiple wells, *Groundwater 2000*, Proceedings of the International Conference on Groundwater Research, June 6-8, Copenhagen-Denmark, A.A. Balkema, Rotterdam.

3. **Modelling flow to leachate wells in landfills**

Reference: Powrie, W., A.A. Al-Thani, R.P. Beaven, and J.K. White, 2001, Modelling flow to leachate wells in landfills, *Sardinia 2001*, Proceedings of the Eighth International Waste Management and Landfill Symposium, S. Margherita di Pula, Cagliari, Italy; October 1-5, Vol III, pp 615-621.

4. **Modelling flow to leachate wells in landfills***

Reference: Submitted for publication to the International Journal of Integrated Waste Management, Science and Technology.

---

* Although this paper has the same title as paper 3 it includes extended results that were not covered in Paper 3.

THE IMPACT OF THE SEEPAGE SURFACE ON THE DESIGN OF PUMP-AND-TREAT REMEDIATION SYSTEMS FOR CONTAMINATED AQUIFERS-SINGLE WELL MODEL.

Abdulla A. Al-Thani
Postgraduate

James K. White
Professor of Civil Engineering

Department of Civil and Environmental Engineering
University of Southampton
Southampton SO17 1BJ

Abstract

The relationship between aquifer geometry, well drawdown and seepage face under steady state conditions of flow has been analyzed for radial flow towards a single well. The groundwater seepage model MODFLOW-SURFACT, which contains the functionality to model seepage surfaces, was used to determine the seepage surface for a number of deep well configurations in unconfined aquifers. The results were first compared with some of the published seepage surface solutions in order to assess the reliability of the MODFLOW-SURFACT solutions. The initial findings indicate that MODFLOW-SURFACT appears to be effective in determining the seepage surface. The study concludes that it should be possible to evaluate the effect of the seepage face in a multiple deep well system in enhancing remediation as the result of exposing a larger region of a contaminated unconfined aquifer to remediating flushing flows

Keywords: Seepage-face, aquifer, contaminated land, landfill engineering, pump-and-treat, MODFLOW-SURFACT.

1. Introduction

The analysis of groundwater flow in unconfined aquifers is complicated by the fact that one boundary is a free surface. When groundwater is pumped from an unconfined aquifer using deep wells, water is derived predominantly from pore-water drainage. This drainage results in a decline in the position of the water table near the pumping wells as time progresses. The vertical surface in a pumped well, which is exposed between the free water surface in the well and the location at which the water-table surface in the unconfined aquifer intersects the well, is referred to as the seepage face or seepage surface. The reason for the

occurrence of the seepage face is that the seepage flow pattern in the neighborhood of a well draining from an unconfined aquifer contains a significant vertical component of seepage velocity when the drawdown in the well is large in relation to the depth of the aquifer.

Arrays of deep wells are used in schemes to remediate contaminated aquifers when using the pump and treat approach. A similar application is found in the field of landfill engineering where there is a requirement to flush residual contaminants out or otherwise inert landfill site. However, it is important that the impact of the seepage surface on the design and evaluation of remediation schemes is fully appreciated. In particular caution should be used in applying a Dupuit-Forchheimer analysis to the design of such systems because flow velocities into a well will be overestimated, as will the depth of cone of depression.

Because of the availability of numerical models, we are now able to investigate flow systems that are otherwise difficult to study experimentally. In this study the groundwater seepage model MODFLOW-SURFACT, which contains the functionality to model seepage surfaces, was used to determine the seepage surface for a number of single deep well configurations in unconfined aquifers. The results were compared with the seepage surface solutions reviewed by Zee et al. (1957) in order to assess the reliability of MODFLOW-SURFACT. The initial findings indicate that MODFLOW-SURFACT solutions are consistent with other experimental and numerical model for determining the seepage surface. This indicates that it should be possible to use MODFLOW-SURFACT to evaluate the effect of the seepage face in a multiple deep well pump and treat system and therefore evaluate the potential for the system enhancement of remediation as the result of exposing a larger region of a contaminated unconfined aquifer to remediating flushing flows.

2. Previous investigations of the seepage face

A number of investigations have been carried out in the past to locate the seepage surface in the immediate vicinity of a gravity well. Table (1) briefly describes these investigations.

Table 1. Summary of previous investigations of the seepage surface

1.	1863	Dupuit	Developed a theory based on a number of simplifying assumptions resulting from the observation that in most groundwater flows the slope of phreatic surface is very small. Dupuit theory does not account for vertical flow components, therefor does not predict a seepage face. The assumptions were (a) equipotential surfaces are vertical (b) flow essentially horizontal. (see Bear (1979))
2.	1928	Sichardt	Identified the possibility of the existence of a limiting gradient and associated seepage face. (see Brauns (1981) and Gefell, Thomas, and Rossello (1944))
3.	1932	Wyckoff, Botset, Muskat	Experimentally studied the steady-state flow of liquids through porous media under the action of gravity.

4.	1937	Muskat	Was the first to show that the discharge estimation from Dupuit formulation is with 1-2% accuracy despite the absence of a seepage face.
5.	1948	Babbitt and Caldwell	Experimentally studied the free surface around, and interface between, gravity wells.
6.	1949	Yang	Analysed seepage toward a well by using the relaxation method. (see Hall (1955) and Taylor and Luthin (1969))
7.	1951	Boulton	Numerically analysed the problem of the free surface near a gravity well by means of the relaxation method. Also, suggested that the deviation from Dupuit discharge is within 1-2%.
8.	1951	Charnii	Was the first to show rigorously that flow rates through a two-dimensional dam with vertical sides are given exactly by Dupuit formulation. (see Polubarinova-Kochina and Ya (1962), Hunt (1970), and Kashef (1986))
9.	1952	Kashef, Toulovkian and Fadum	Simplified numerical method for a flow toward well in semiconfined aquifer.
10.	1953	Hansen	Clarified the nature of unconfined flow to a single and multiple wells using membrane analogy.
11.	1953	Kozeny	Gives a solution for the height of the seepage face based on the assumptions that the maximum possible entrance velocity of water is equal to the permeability. (see Brauns (1981))
12.	1954	Nahrgang	Experimentally studied the free surface around, and interface between, gravity wells. (see Brauns (1981))
13.	1955	Boreli	Analysed the free-surface flow toward partially penetrating wells using the relaxation method. (see Powers (1981))
14.	1955	Hall	Used a sand-filled, wedge-shaped box for examining the radial flow toward a gravity well and wrote an equation for the free surface shape. (see Bouwer (1978))
15.	1957	Peterson	Discussion of the study done by him, Zee, and Bock.
16.	1957	Zee, Peterson and Bock	Collected data from laboratory tests on single wells that were used to investigate the magnitude of the seepage surface.
17.	1962	Leonards	Has Boreli (1955) solution.
18.	1962	Polubarinova-Kochina and Ya	Extended Charnii (1951) proof to derive an analogous theorem for axially symmetric free surface seepage toward a fully penetrating well.
19.	1962 1963 1964	Hantush	Confirmed the validity of flow estimation using Dupuit-Forchheimer even for a significant seepage surface. Also, gives the shape of the free surface.
20.	1964	Heinrich	Explicit form of the approximate analytical solution. (see Brauns (1981))
21.	1964	Kirkham	A theory for the shape of the free water surface about a well in a semiconfined aquifer.
22.	1965	Kashef	The free surface for gravity wells. (see Kashef (1986), which includes the Babbitt and Caldwell (1948) results).
23.	1967	Mahdaviani	Steady and unsteady flow towards gravity wells.
24.	1969	Taylor and Luthin	Presented a method for utilising numerical analysis and computer operations to solve problems of drawdown around a pumped well in an unconfined aquifer. The method takes into account the properties of the unsaturated portion of the aquifer and the contribution of vertical flow. They compared their results with Hall (1955) experimental solution.
25.	1970	Hunt	Flow rates from Dupuit's approximation.
26.	1970	Neuman and Witherspoon	Presented an improved finite element approach to the problem of steady state seepage with a free surface. The study also presents a comparison with Hall (1955) and Taylor and Luthin (1969) solutions.
27.	1973	Todsen	Analysed problems limited to steady state and two-dimensional flows.
28.	1976	Brauns and Zangl	Finite element model to solve two-dimensional or axisymmetrical seepage-

			face with free surface. The model called FREESURF 1. (see Neuman (1976) for FREESURF1 user's guide))
29.	1976	Neuman	User's guide for FREESURF 1.
30.	1979	Bear	Discussed Dupuit assumptions in depth and his book includes Kirkham (1964), Hansen (1953), Boulton (1951) solutions.
31.	1981	Brauns	Studied the drawdown capacity of groundwater wells.
32.	1988	Beljian	Investigated the effects of several possible well situations on the nodal correction in two-dimensional groundwater modelling. His investigation include a well not positioned at the centre of the well block, a rectangular well block with different aspect ratios, an anisotropic medium, and more than one well within the block.
33.	1991	Shamsai and Narasimhan	Numerically investigated the free surface-seepage face relationship under steady state flow conditions.
34.	1992	Preene	Gathered data from arrays of wells indicating that a range of limiting gradient values were possible.
35.	1993	Reilly and Harbaugh	Used MODFLOW to simulate axisymmetric flow to a well and compared the results with Neuman (1974) analytical solution. The study accounts for the large variations in gradient in the vicinity of the well but ignores the seepage face at the well.
36.	1994	Clement, Wise, and Molz	Developed a physically based, two-dimensional, finite-difference algorithm for modelling variably saturated flow. They also compared the performance of the algorithm with Hall (1955).
37.	1994	Gefell, Thomas, and Rossello	Evaluated and confirmed Kozeny's (1953) method of predicating the maximum water-table drawdown using a physical aquifer model to perform controlled steady-state flow tests on a fully penetrating, fully screened pumping well.
38.	1996	Clement, Wise, Molz and Wen	Compared modelling approaches for steady-state unconfined flow.
39.	1999	Anderson	Anderson and Woessner (1992) discussed the models available for solving the seepage face in their book. A personal communication with Anderson concluded that her past trials of using FREESURF to solve for seepage face were unsuccessful.
40.	1999	Townley	By personal communication with the developer of AQUIFEM-N, which is a multi-layered finite-element aquifer flow model for confined and unconfined aquifers, Townley suggested that AQUIFEM-N can be used to solve for seepage face but he did not try the code for that purpose.

The work of Zee et al. (1957) is particularly interesting in that it contains a large quantity of data collected from tests on a single well carried out by a number of authors listed in Table (1). Based on the experimental results and the data from others, which relates h_s to h_w and Q/Kr_w^2, Zee et al. (1957) produced a graphical relationship between these parameters shown in Fig. 1.

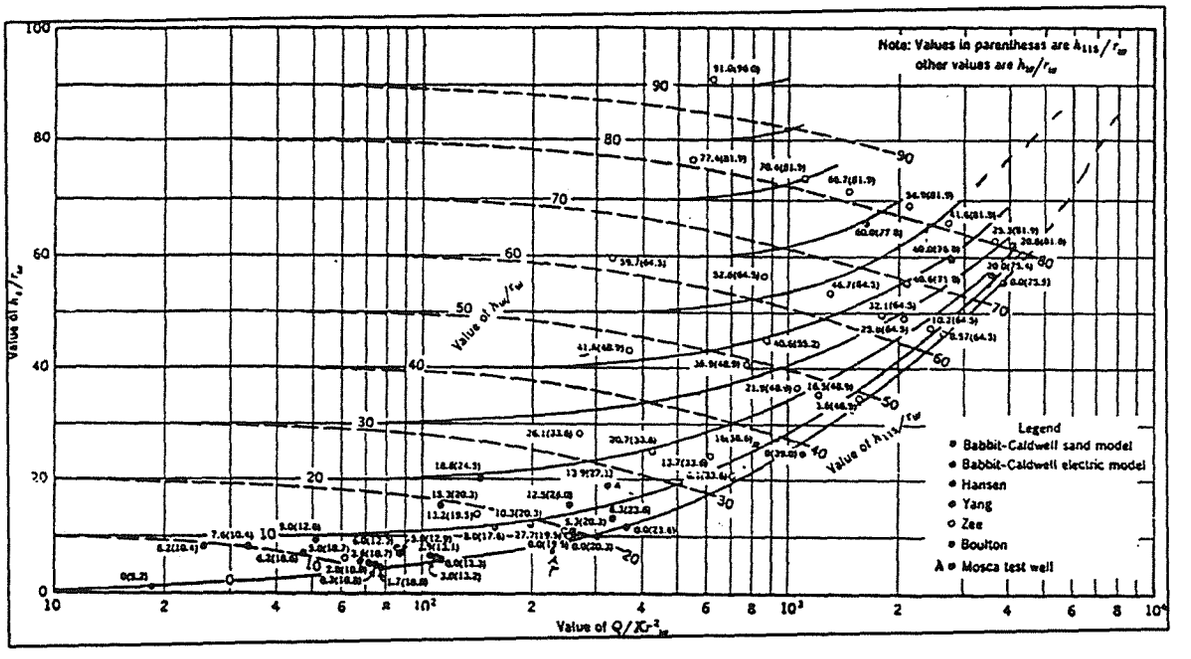

Fig. 1. Relationship of discharge and geometric parameters. (After Zee, Peterson, and Bock, 1957.)

The authors have obtained a best fit algebraic representation of this data. This is,

$$\frac{Q}{Kr_w^2} = 2.5\pi \frac{h_s}{r_w}\left(\frac{h_s}{r_w} - \frac{h_w}{r_w}\right)^{0.53} \tag{1}$$

Where Q is the discharge from the well (L^3/T)
K is the hydraulic conductivity (L/T)
r_w is the radius of the well (L)
h_s is the depth of water outside the well (L)
h_w is the depth of water in the well (L)

and

$$0 < \frac{Q}{Kr_w^2} < 5000 \qquad\qquad 0 < \frac{h_s}{r_w} < 90 \tag{2}$$

3. Numerical investigation using MODFLOW-SURFACT

MODFLOW-SURFACT is a new fully integrated groundwater flow and transport code developed by HydroGeoLogic, Inc., based on the USGS MODFLOW code. MODFLOW has certain limitations in simulating complex field problems and additional computational modules have recently been incorporated to enhance the simulation capabilities and robustness. Three of the many features that have been added are, (1) the ability to readily accommodate conditions of desaturation and resaturation of aquifer systems, (2) the ability to simulate prescribed ponding, recharge, and seepage-face boundary conditions, and (3) the ability to perform axi-symmetric analysis.

The discretization scheme for this application uses twice the well radius as the X and Y (column and row) dimensions of the cell representing the pumping well (the well cell), and then moves outward from the well cell with increasing cell widths starting with a cell width that is a small fraction of the well diameter. The expansion factor, α, is generally given a value not more than 1.5. In addition, by having very small cell widths near the well cell, errors associated with finite differencing of small distance between nodes are small.

With such discretization the MODFLOW-SURFACT model has been used to model the seepage surface for a single well over a range of parameters extending the range of Zee et al. to

$$0 < \frac{Q}{Kr_w^2} < 65000 \qquad 0 < \frac{h_s}{r_w} < 350 \qquad (3)$$

The results are compared in Fig. 2. It can be seen that MODFLOW-SURFACT results are confirmed by the experimental/analytical results assembled by Zee et al. In addition, it appears that equation (1), based on the Zee et al results, may be used to extrapolate over a much greater range of parameters.

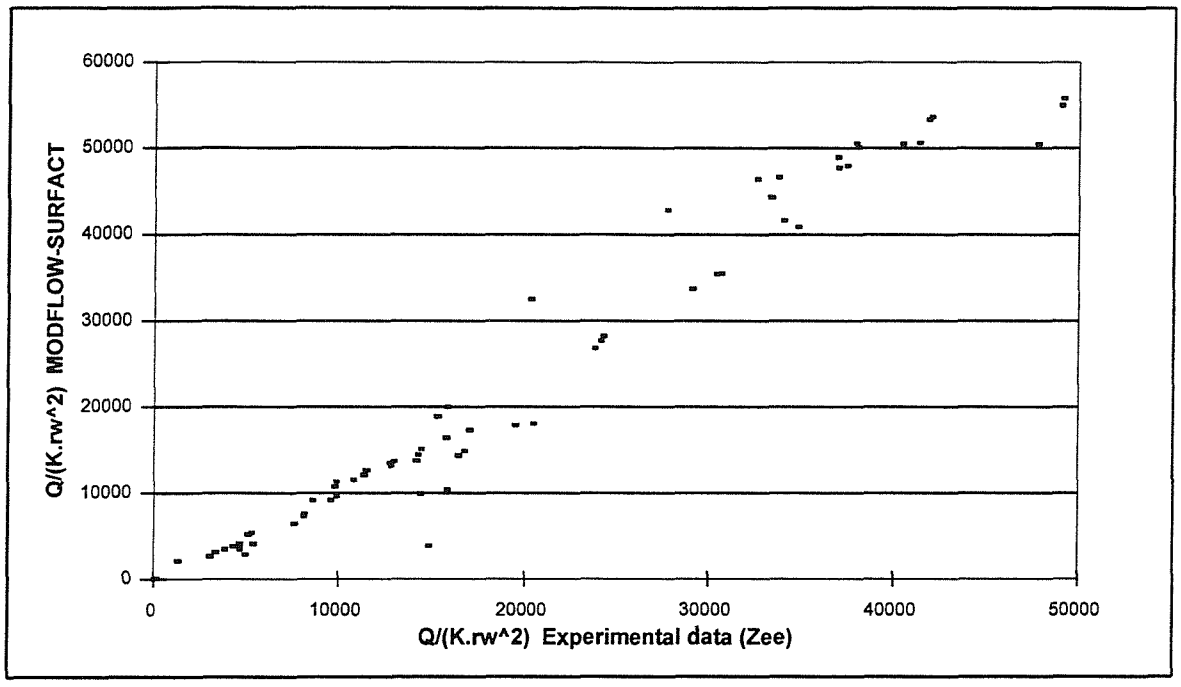

Fig. 2. Comparison between MODFLOW-SURFACT numerical results and Zee et al (1957) experimental results.

The cone of depression predicted by MODFLOW-SURFACT is much smaller than that predicted by Dupuit-Forchheimer model. This difference plays an important role when designing remediation systems for contaminated aquifers using pump-and-treat systems. Seepage faces and associated rises in phreatic surfaces are usually beneficial to pump-and-treat schemes since they expose a larger volume of soil to flushing flows, which will ease the removal of contaminates during clean-up efforts. Furthermore, at higher pumping rates the water level inside a well decreases, but the volume exposed to the flow remain relatively unchanged over a significant variation of drawdowns due to the seepage face effect. This is very important since the remediation wells are usually installed in the most contaminated parts of the site.

Conclusion

The numerical investigation indicates that MODFLOW-SURFACT could be applied with confidence to pump-and-treat analysis. This will involve modelling multiple well arrays in which superposition of drawdown may or may not influence the seepage face and water table surface and therefore the extent of flushing that can be achieved by such well arrays. Studies of this nature will form the next stage of this research.

References:

Babbitt, H.E., D.H. Caldwell, 1948, The free surface around, and interface, gravity wells, University of Illinois Engineering Experiment Station Bulletin, 374, 60 pp..

Bear, J., 1979, *Hydraulics of Groundwater*, McGraw-Hill Inc., New York, N.Y., 569 p.

Beljian, M.S., 1988, Representation of individual wells in two-dimensional groundwater water modeling, Proceedings of Solving Ground Water Problems with models, February 10-12, Denver.

Boreli, M., 1955, Free-surface flow toward partially penetrating wells, Transactions. American Geophysical Union, 36(4) pp. 664-672.

Boulton, N.S., 1951, The flow pattern near a gravity well in a uniform water bearing medium, Journal of Institution of Civil Engineers (London), 36(10), pp. 534-550.

Bouwer, H., 1978, *Groundwater Hydrology*, McGraw-Hill Inc., New York, N.Y., 480 p.

Brauns, J., 1981, Drawdown capacity of groundwater wells, Proceedings of the Xth International Conference of Soil Mechanics of Foundation Engineering, pp. 391-396.

Clement, T.P., R.W. Wise, and F.J. Molz, 1994, A physically based, two dimensional, finite-difference algorithm for modeling variably saturated flow, Journal of Hydrology, 161, pp. 71-90.

Clement, T.P., R.W. Wise, F.J. Molz, and M. Wen, 1996, A comparison of modeling approaches for steady-state unconfined flow, Journal of Hydrology, 181, pp. 189-209.

ESI, 1997, Guide to Using Groundwater Vistas, Environmental Simulations, Inc., Herndon, VA.

Gefell, M.J., G.M. Thomas, and S.J. Rossello, 1994, Maximum water-table drawdown at fully penetrating pumping well, Ground Water, 32(3), pp. 411-419.

Hall, H.P., 1955, An investigation of steady flow toward a gravity well, La Houille Blanche, 10, pp. 8-35.

Hansen, V.E., 1953, Unconfined groundwater flow to multiple wells, Transactions. American Society of Civil Engineers, N.Y., 118, pp. 1098-1130.

Hantush, M.S., 1964, Hydraulics of Wells in V.T. Chow, *Advances in Hydroscience*, Vol. 1, Academic Press Inc., San Diego, California, pp. 281-432.

Harr, M.E., 1991, *Groundwater and Seepage*, Dover Publications Inc., Mineola, N.Y., 315 p.

Hunt, B.W., 1970, Exact flow rates from Dupuit's approximation, Journal of the Hydraulics Division, Proceedings of the ASCE, N.Y., 96(HY 3), pp. 633-641.

Huyakorn, P.S., E.P. Springer, V. Guvanasen, and T.D. Wadsworth, 1986, A three-dimensional finite-element model for simulating water flow in variably saturated porous media, Water Resources Research, 22(13), pp. 1790-1808.

Kashef, A.I., 1965, Exact free surface of gravity wells, Journal of the Hydraulics Division, Proceedings of the ASCE, N.Y., 91(HY 4), pp. 167-184.

Kashef, A.I., 1986, *Groundwater Engineering*, McGraw-Hill Inc., New York, N.Y., 512 p.

Kirkham, D., 1964, Exact theory for the shape of the free surface about a well in a semiconfined aquifer, Journal of Geophysical Research, 69(12), pp. 2537-2549.

Leonards, G.A., 1962, *Foundation Engineering*, McGraw-Hill Inc., New York, N.Y., 1136 p.

Mahdaviani, M.A., 1976, Steady and unsteady flow towards gravity wells, Journal of the Hydraulics Division, Proceedings of the ASCE, N.Y., 93(HY 6), pp. 135-146.

Marino, M.A., and J.N. Luthin, 1982, Developments in Water Science: Seepage and Groundwater, Elsevier Scinece, New York, N.Y., Vol. 13, 489 p.

McDonald, M.G., and A.W. Harbaugh, 1988, A modular three-dimensional finite-difference ground-water flow model, Techniques of Water-Resources Investigations 06-A1, US Geological Survey, 576 p.

McWhorter, D.B., and D.K. Sunada, 1993, *Ground-Water Hydrology and Hydraulics*, Water Resources Publications, Colorado, 290 p.

MS-VMS, 1996, First Fully Integrated MODFLOW-Based Visual Modeling System with Comprehensive Flow and Transport Capability, HydroGeologic , Inc., Herndon, VA.

Muskat, M., 1937, *The Flow of Homogeneous Fluids Through Porous Media*, McGraw-Hill Inc., New York, N.Y., 763 p.

Neuman, S.P., 1970, Effect of partial penetration on flow in unconfined aquifers considering delayed gravity response, Water Resources Research, 10(2), pp. 303-312.

Neuman, S.P., and P.A. Witherspoon, 1970, Finite element method of analyzing steady seepage with a free surface, Water Resources Research, 6(3), pp. 889-897.

Peterson, D.F., 1957, Hydraulics of wells, Transactions. American Society of Civil Engineers, N.Y., 122, pp. 502-517.

Polubarinova-Kochina, P.Ya., 1962, *Theory of Groundwater Movement* (translated from Russian by R.J.M. de Wiest), Princeton University Press, Princeton, N.J.

Powers, J.P., 1992, *Construction Dewatering: New Methods and Applications*, John Wiley and Sons, New York, N.Y., 492 p.

Reilly, T.E., and A.W. Harbaugh, 1993, Simulation of cylindrical flow to a well using USGS modular finite-difference groundwater-flow model, Ground Water, 31(3), pp. 489-494.

Rushton, K. R., and S.C. Redshaw, 1979, *Seepage and Groundwater Flow*, John Wiley and Sons, New York, N.Y., 339 p.

Shamisai, A., and T. N. Narasimhan, 1991, A numerical investigation of free surface-seepage face relationship under steady state flow conditions, Water Resources Research, 27(3), pp. 409-421.

Taylor, G.S., and J.N. Luthin, 1969, Computer methods for transient analysis of water-table aquifers, Water Resources Research, 5(1), pp. 144-152.

Todd, K.D., 1980, *Groundwater Hydrology*, John Wiley and Sons, New York, N.Y., 535 p.

Townley, L.R., 1999, Townley and Associates Pty Ltd., PO Box 425, Claremont WA 6910, Australia, personal communication.

Wyckoff, R.D., H.G. Botset, and M. Muskat, 1932, Flow of liquids through porous media under the action of gravity, Physics, 2, pp. 90-113.

Youngs, E.G., 1966, Exact analysis of certain problems of ground-water flow with free surface conditions, Journal of Hydrology, 4, pp. 277-281.

Zee, C., D.F. Peterson, and R.O. Bock, 1957, Flow into a well by electric and membrane analogy, Transactions. American Society of Civil Engineers, N.Y., 122, pp. 1088-1112.

THE IMPACT OF THE SEEPAGE SURFACE ON THE DESIGN OF PUMP-AND-TREAT REMEDIATION SYSTEMS FOR CONTAMINATED AQUIFERS

A.A. Al-Thani & J.K. White
University of Southampton, Southampton, United Kingdom

Keywords: Seepage-face, aquifer, contaminated land, multiple wells, pump-and-treat, MOFLOW-SURF

ABSTRACT: The relationship between free surface and seepage face under steady state conditions of flow has been analyzed for flow in unconfined aquifers. The groundwater seepage model MOD-FLOW-SURF, which contains the functionality to model seepage surfaces, was used to determine the seepage surface for a single well and arrays of wells. The results were compared with available analytical and published seepage surface solutions and the reliability of the MODFLOW-SURF package has been assessed. Suggestions are also made for modifying conventional analytical solutions in order to account for the seepage face. The relevance of the work to the design of pump and treat remediation systems is noted.

1 INTRODUCTION

In order to design and operate deep well systems in unconfined aquifers, information about the characteristics of the field of induced seepage flows is important. In particular estimating the position of the free surface is often of great importance. In relation to a pumped well, an additional complication is the vertical surface which is exposed between the free water surface in the well and the location at which the water-table surface in the unconfined aquifer intersects the well. This surface is referred to as the seepage face or seepage surface. The reason for the occurrence of the seepage face is that the seepage flow pattern in the neighborhood of a well draining from an unconfined aquifer contains a significant vertical component of seepage velocity when the drawdown in the well is large in relation to the depth of the aquifer.

2 NUMERICAL INVESTIGATION

Because of the availability of numerical models, we are now able to investigate flow systems that are otherwise difficult to study experimentally. In this study the groundwater seepage model MODFLOW-SURF, which contains the functionality to model seepage surfaces, was used to determine the seepage surface for a number of single deep well configurations in unconfined aquifers. The results were compared with the seepage surface solutions reviewed by Zee et al. (1957) in order to assess the reliability of MODFLOW-SURF. The findings indicated that MODFLOW-SURF solutions are consistent with other experimental and numerical models for determining the seepage surface.

It should therefore be possible to use MODFLOW-SURF to accurately evaluate the effect of the seepage face, and three-dimensional effects in general, in circular arrays of multiple deep wells. This will be relevant to the design of pump and treat groundwater remediation systems in that it

will evaluate the potential for the system enhancement as the result of exposing a larger region of a

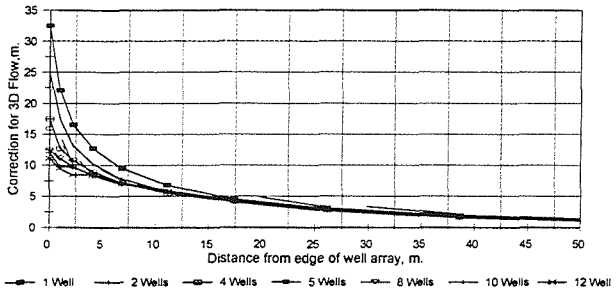

contaminated unconfined aquifer to remediating flushing flows.
– Figure 1. Example of correction to the conventional method of superposition.

3 RESULTS

The cone of depression predicted by MODFLOW-SURF is much smaller than that predicted by the Dupuit-Forchheimer model as the result of the calculation taking accurate account of three-dimensional effects. It was found that the piezometric head at the base of the model aquifer, in the case of a single well, coincided with Dupuit-Forchheimer, as did the flow predictions, provided that the correction for well radius proposed by Beljian (1988), 0.2 Δx, was applied. For multiple wells it was found that the conventional method of superposition, Mansur and Kaufman (1962), gave results which agreed with the model head calculations, again at the aquifer base. However these needed to be elevated by a correction as in the example shown in Figure 1 to match the level of the free surface. This correction plays an important role when designing remediation systems for contaminated aquifers using pump-and-treat systems. Seepage faces and associated rises in phreatic surfaces are usually beneficial to pump-and-treat schemes since they expose a larger volume of soil to flushing flows, which will ease the removal of contaminates during clean-up efforts. Furthermore, at higher pumping rates the water level inside a well decreases, but the volume exposed to the flow remain relatively unchanged over a significant variation of drawdowns due to the seepage face effect. This is very important since the remediation wells are usually installed in the most contaminated parts of the site.

4 CONCLUSIONS

This numerical investigation has indicated that MODFLOW-SURF may be applied with some confidence to unconfined aquifers pumped by multiple deep wells such as those used for pump-and-treat systems. The work indicates that design predictions can be made using simple conventional algebraic models supported by correction schemes derived from numerical studies.

References:

Beljian, M.S. 1988. Representation of individual wells in two-dimensional groundwater water modeling. *Proc. of Solving Ground Water Problems with Models*, Denver, 10-12 February 1988.
Environmental Simulations, Inc. 1997. *Guide to Using Groundwater Vistas.* Herndon: Environmental Sim-

lation, Inc.
HydroGeologic , Inc. 1996. *MS-VMS Software Version 1.2 and Documentation,* Herndon: HydroGeologic , Inc.
Mansur, C.I. & Kaufman, R.I. 1962. Ch. 3 in *Foundation Engineering.* Edited by G. A. Leonards. New York: McGraw-Hill Inc.
Zee, C. Peterson, D.F. & Bock, R.O. 1957. Flow into a well by electric and membrane analogy *Transac tions. American Society of Civil Engineers* (122): 1088-1112.

MODELLING FLOW TO LEACHATE WELLS IN LANDFILLS

W. POWRIE, A.A. AL-THANI, R.P. BEAVEN, J.K. WHITE

Dept' of Civil and Environmental Engineering, University of Southampton, UK

SUMMARY: Vertical wells are frequently used as a means of controlling leachate levels in landfills. They are often the only available dewatering option for both old landfills without any basal leachate collection layer and for newer sites where the installed drainage infrastructure has failed. When the well is pumped, a seepage face develops at the entry into the well so that the drawdown in the surrounding waste will not be as great as might be expected. The numerical groundwater flow model MODFLOW-SURFACT, which contains the functionality to model seepage surfaces, has been used to investigate the transient dewatering of a landfill. The study concludes that the position of the seepage face and information about the characteristics of the induced seepage flow field are important and should not be neglected when designing wells in landfills.

C.1 INTRODUCTION

Landfill operators' experiences of using leachate wells to control leachate levels are varied. It is common for the yield of leachate wells to be relatively small (often <1 m^3/day) and the monitored drawdown around the well to be limited. The low yield of wells can often be related to the low hydraulic conductivity of the surrounding waste and possibly poor well design/badly developed wells. However, it is also possible that the apparent lack of dewatering may in part be explained in terms of the development of a seepage face at the well. Seepage faces are caused by vertical components of flow in the vicinity of a pumped well where the drawdown in the well is a large proportion of the saturated thickness (*Al-Thani and White*, 2000 and p.308 *Bear*, 1979). The purpose of this paper is to report on the possible effects of seepage faces in the dewatering of a landfill by a grid of pumped leachate wells.

C.2 METHOD OF ANALYSIS

Previous studies have considered the effect of seepage faces on pumped leachate wells (*Rowe* and *Nadarajah*, 1996) but results were only presented for steady state conditions. A method of analysis was required that could investigate the transient response to pumping, based on independently measured values of hydraulic conductivity and drainable porosity in a landfill.

MODFLOW-SURFACT is a commercially available fully integrated groundwater flow and transport code based on the USGS' MODFLOW 3d groundwater flow model. The publicly available version of MODFLOW has certain limitations in simulating complex field problems, which make it unsuitable for modelling seepage faces around wells. The enhanced version, which was used for this study, incorporates additional computational modules to improve the simulation capabilities and robustness. Three of the many features that have been added are (1) the ability readily to accommodate conditions of desaturation and resaturation of aquifer systems, (2) the ability to simulate prescribed ponding, recharge, and seepage-face boundary conditions, and (3) the ability to perform axi-symmetric analysis. The reliability of the MODFLOW-SURFACT code has been assessed and found satisfactory in previous work by comparing the predicted results with available analytical and published seepage surface solutions (*Al-Thani and White,* 1999).

C.3 PROBLEM DESCRIPTION

Figure 1 shows a schematic view of a 30 m deep landfill with a 20 m deep saturated zone with a grid of leachate pumping wells at a spacing of 10 m. This spacing was to some extent arbitrary, but probably represents the closest well spacing (at 100 wells per hectare) likely to be installed on most landfills. The wells are assumed to penetrate the landfill fully, and have a fixed radius of 0.15 m. The wells are pumped at rate that maintains fully drawn down conditions inside the well.

A single cell (in plan view) is used to represent the pumped well in this discretization scheme. The dimensions of the cell (x and y co-ordinates) are set to the diameter of the well. The (column and row) dimensions of the cells adjacent to the well are set to a small fraction of the well diameter. Cell dimensions gradually increase with increasing distance from the well. The expansion factor, α, which relates the cell dimensions of any two adjacent cells is generally not more than 1.5. The boundaries to the model were set as no flow boundaries at a distance of 5 metres from the well in the x and y directions. The model was divided vertically into 21 layers as shown in Figure 1. The thickness of Layer 1 was set at 10 m (representing the unsaturated zone) and the remaining layers at 1 m.

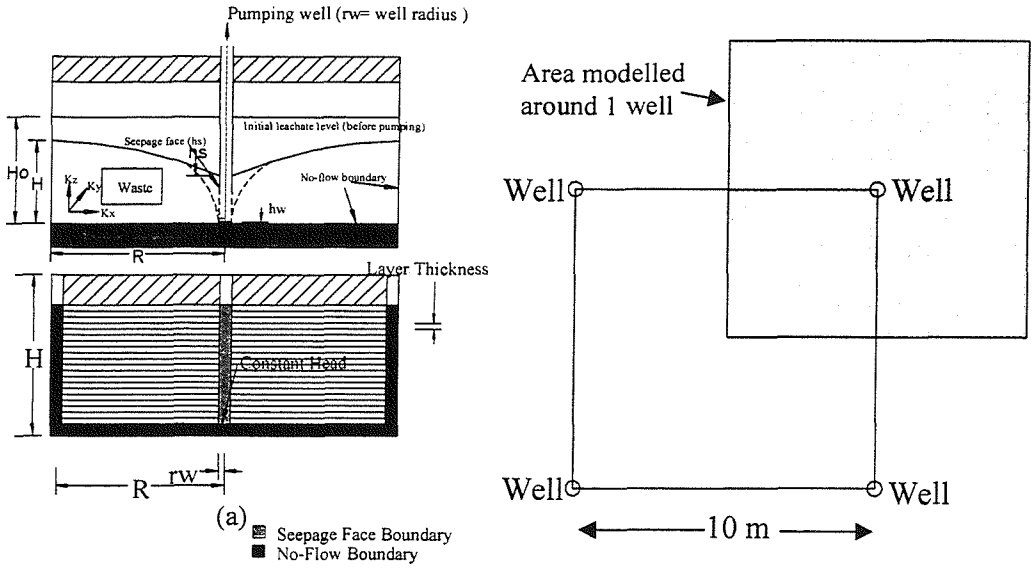

Figure 1 Schematic view of the landfill model **(a)** cross section **(b)** plan view of a grid

Table 1 Best fit and worst case hydraulic conductivities

Depth (m)	Best case K (m/sec)	Worst case K (m/sec)	Depth (m)	Best case K (m/sec)	Worst case K (m/sec)
10.5	3.12×10^{-6}	1.66×10^{-6}	20.5	6.55×10^{-7}	2.54×10^{-7}
11.5	2.57×10^{-6}	1.31×10^{-6}	21.5	5.80×10^{-7}	2.19×10^{-7}
12.5	2.14×10^{-6}	1.05×10^{-6}	22.5	5.16×10^{-7}	1.90×10^{-7}
13.5	1.80×10^{-6}	8.53×10^{-7}	23.5	4.61×10^{-7}	1.66×10^{-7}
14.5	1.52×10^{-6}	7.00×10^{-7}	24.5	4.13×10^{-7}	1.46×10^{-7}
15.5	1.30×10^{-6}	5.79×10^{-7}	25.5	3.72×10^{-7}	1.28×10^{-7}
16.5	1.12×10^{-6}	4.84×10^{-7}	26.5	3.36×10^{-7}	1.14×10^{-7}
17.5	9.72×10^{-7}	4.07×10^{-7}	27.5	3.04×10^{-7}	1.01×10^{-7}
18.5	8.47×10^{-7}	3.46×10^{-7}	28.5	2.76×10^{-7}	8.98×10^{-8}
19.5	7.43×10^{-7}	2.95×10^{-7}	29.5	2.52×10^{-7}	8.03×10^{-8}

The initial saturated leachate level was set at 20 m. A drainable porosity of 5% is used in this study, based on research into the hydrogeological properties of waste (*Hudson et al.*, 1999). The variations in hydraulic conductivity with depth are based on relationships between hydraulic conductivity and effective stress determined experimentally by *Beaven* (2000). Two scenarios using the 'best' fit and 'worst case' fit of the experimental data are used in this study (Table 1). The operation of the well was replicated by applying a combination of a constant head and drains to the cells representing the well. A constant head cell (with a head of zero) was allocated to the cell in the bottom layer of the model (i.e. the well is fully dewatered) and drain cells to each layer above. Drain cells operate by removing water from the model if the head in the model is above the level set for the drain. Each drain cell was allocated a head equivalent to the elevation head of the cell. This has the effect of applying seepage face boundary conditions at the well.

C.4 RESULTS OF NUMERICAL INVESTIGATION

The MODFLOW-SURFACT code was used to solve the described problem for both hydraulic conductivity scenarios in Table 1 over a period of 200 days. Figure 2 shows the location of piezometric head after 50 days, 100 days and 200 days of pumping.

The solid lines represent the elevation of the phreatic surface, i.e. the location at which leachate would be encountered if an observation well was drilled from the surface. These lines are relatively flat. The dashed lines represent the piezometric levels at the base of the site. The leachate levels drop faster in the best scenario case of hydraulic conductivity. This is an expected result, because higher hydraulic conductivity values lead to higher well discharges as shown in Table (2).

The equation for steady state flow to a pumped well in an unconfined aquifer is

$$Q = \frac{\pi K(h_2^2 - h_1^2)}{\ln(r_2 / r_1)} \qquad (1)$$

This equation is based on the *Dupuit-Forchheimer* assumptions that flow is horizontal and uniformly distributed with depth throughout an isotropic formation underlain by an impermeable stratum. The equation neglects the seepage face at the well. However, the applicability of the equation for determining flow to a well has been investigated by *Hantush* (1964) who found that

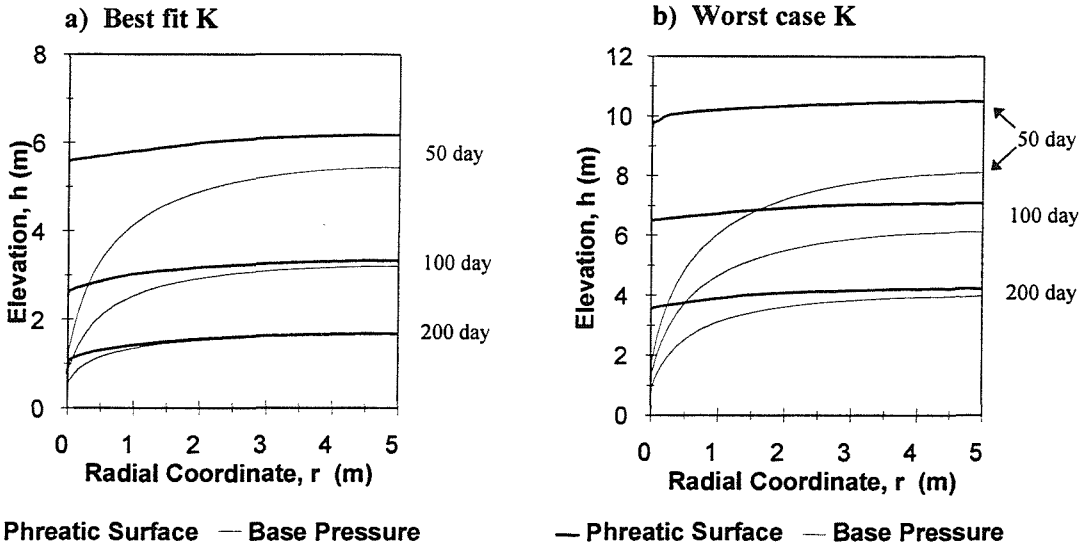

Figure 2 Spatial variation of leachate heads during pumping **(a)** best fit hydraulic conductivity and **(b)** worst case hydraulic conductivity.

equation (1) gives an exact result despite the presence of the seepage face. However,

because it does not take account of the existence of the seepage face, equation (1) does not give an accurate shape curve for the phreatic surface. *Muskat* (1936) and *Wyckoff et al.* (1932), using results from experimental studies, found that it is the piezometric heads along the base, rather than the free surface, that closely follow equation (1). Moreover, the *Dupuit-Forchheimer* assumptions imply that an overall average value for hydraulic conductivity is assumed, hence anisotropy of the hydraulic conductivity as will be found in a solid waste landfill is not taken into account in equation (1).

Equation (1) may be used to define an overall instantaneous effective permeability for a matrix in which the permeability is anisotropic. To do this the results from the numerical analysis were substituted into equation (1) to determine an overall average hydraulic conductivity for each time step. In this case, $h_2 = H$ and $h_1 = 0$. R the radius of influence was based on $\sqrt{A/\pi}$ where A is the plan area of the model. Following *Beljian* (1988), r_w the radius of the well was taken to be the effective well radius equal to 0.2 times the size of the finite element representing the well, in this case 0.06 metres.

Table 2 Discharge values for both scenarios versus time.

Time	Best case K				Worst case K			
	Q	H	h_s,	Mass Bal'	Q	H	h_s,	Mass Bal'
Days	m^3/day	m	m	Error %	m^3/day	m	m	Error %
10	4.389	15.02	14.62	1.74	2.789	15.88	13.24	2.25
50	0.681	6.17	5.57	2.47	0.704	10.49	9.61	3.27
100	0.207	3.33	2.51	3.23	0.326	7.09	6.5	6.37
150	0.095	2.25	1.50	4.21	0.176	5.28	4.51	6.40
200	0.057	1.68	0.77	6.00	0.111	4.23	3.50	7.40
250	-	-	-	-	0.078	3.49	2.50	3.83

Table 3 Calculation of hydraulic conductivity from model results and equation (1).

Q	Model run	H	K	Equivalent infiltration over $100m^2$
m^3/day		m	m/sec	metres/year
4.389	Best fit	15.02	3.26×10^{-7}	16.02
0.681	Best fit	6.17	3.00×10^{-7}	2.49
0.207	Best fit	3.33	3.13×10^{-7}	0.76
0.095	Best fit	2.25	3.14×10^{-7}	0.35
0.057	Best fit	1.68	3.38×10^{-7}	0.21
2.789	Worst case	15.88	1.85×10^{-7}	10.18
0.704	Worst case	10.49	1.07×10^{-7}	2.57
0.326	Worst case	7.09	1.08×10^{-7}	1.19
0.176	Worst case	5.28	1.06×10^{-7}	0.64
0.111	Worst case	4.23	1.04×10^{-7}	0.41
0.078	Worst case	3.49	1.07×10^{-7}	0.28

The results are recorded in Table 3. A comparison of the calculated hydraulic conductivities with Table 1 indicates that it is the hydraulic conductivity in the lower layers that appears to control flow rates. Table 3 also contains a calculation of the

infiltration rate Q/A corresponding to the flow rate Q. These values indicate that the average flow rate could approach typical annual infiltration rates into uncapped landfills in the UK. Where this occurred reductions in leachate levels would be difficult to progress, and may indeed reverse, and an increase in the density of the well array would be require to continue dewatering.

C.5 ANALYTICAL REPRESENTATION

The numerical investigation indicates that the drop of the leachate elevation is almost flat. This observation can be used to develop a simple algebraic representation of the data which may be used to extrapolate the results so that they can be applied to similar systems with different dimensions and hydrogeological parameters.

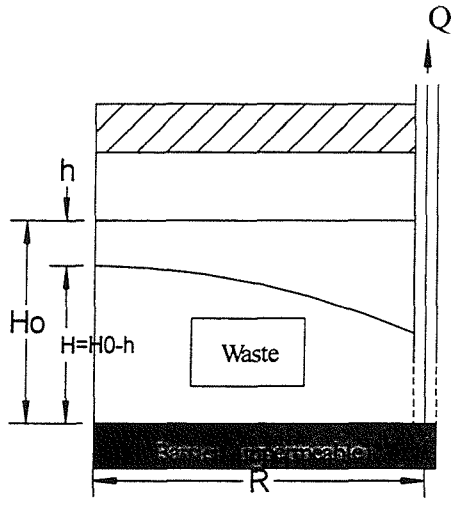

Figure 3 Parameter definition diagram for theoretical representation

Assuming that the piezometric surface is effectively horizontal, the flow Q at any time t may be equated to the rate of change of the drained volume above the surface. This volume is equal to $AS(H_0 - H)$ where A is the plan area and S is porosity (see Figure 3). Thus,

$$Q = -AS\frac{dH}{dt}$$

However Q may be calculated using *Dupuit-Forchheimer* equation so that

$$Q = \frac{\pi K}{\ln\frac{R}{r_w}}H^2 = -AS\frac{dH}{dt}$$

Rearranging and integrating we have,

$$\int_0^t \frac{\pi K}{AS \ln \frac{R}{r_w}} dt = \int_{H_0}^{H} \frac{dH}{H^2}$$

or $$T = \frac{1}{H} - \frac{1}{H_0} \qquad \text{where} \quad T = \frac{\pi K t}{AS \ln \frac{R}{r_w}}$$

The data in Table 2 have been plotted on this basis in Figure 4, and the outcome is

$$\frac{1}{H} - \frac{1}{H_0} = 0.9T \tag{2}$$

when K is taken to be the hydraulic conductivity in the lowest layer.

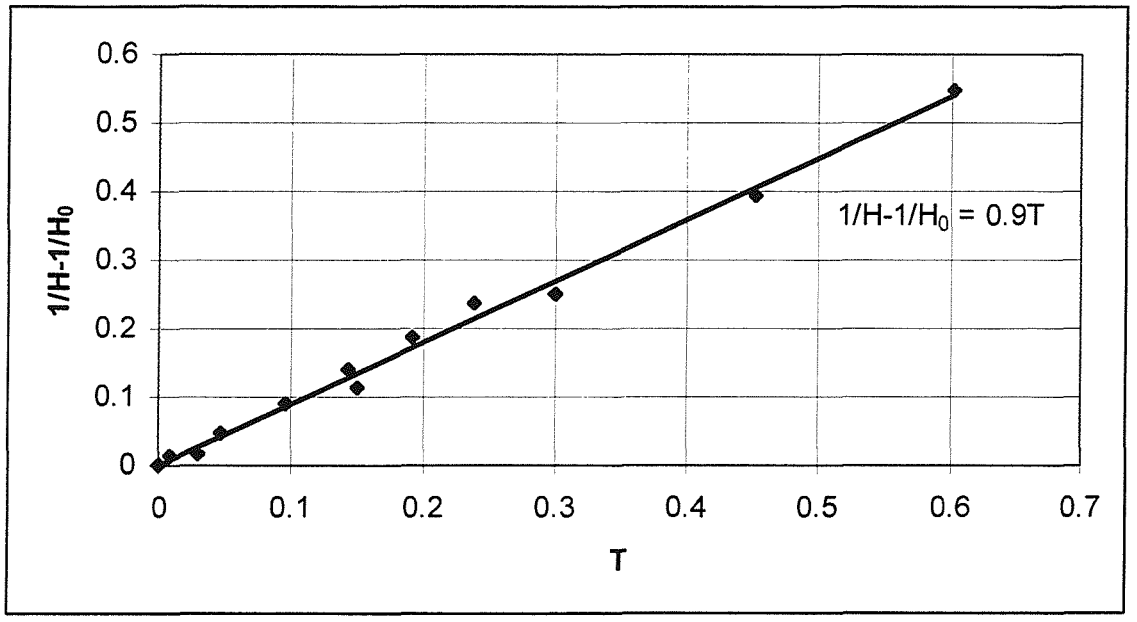

Figure 4 The data in Table 2 plotted to obtain equation (2).

C.6 CONCLUSIONS

The impact of the development of a seepage face at a vertical well has been demonstrated in the context of landfill dewatering. Strong vertical seepage velocities are set up resulting in pore pressures in the upper part of the landfill being higher than at the base producing an almost horizontal phreatic surface. Care therefore needs to be taken when carrying out field investigations to assess the pore pressures on the base of a landfill: only piezometers with a well defined and limited response zone should be used for this purpose. Fully screened observation wells in close proximity to a pumped well will give ambiguous if not meaningless results.

The flow to the well appears to be taking place through the lower layers so that the yield from the well is controlled by the hydraulic conductivity in these layers. For the case of a 30 m deep landfill, the predicted yield from pumped wells becomes very low

when leachate levels are drawn down below approximately 1.5 to 3 m (for a grid of pumped wells at 10 m spacing). Rates of dewatering become slow and could even stop if the pumped rate falls below the equivalent annual rainfall infiltration rate. The data obtained for the case of a model with specific dimensions has been used to calibrate a conventional algebraic model which can be used to extrapolate the results to systems with similar geometry at different scales.

C.7 REFERENCES

Al-Thani, A.A. and J.K. White, 1999, The impact of the seepage surface on the design of pump-and-treat remediation systems for contaminated aquifers-based on single well, Workshop on Ground Water Pollution, Protection and Remediation, November 7-10, Qatar.

Al-Thani, A.A. and J.K. White, 2000, The impact of the seepage surface on the design of pump-and-treat remediation systems for contaminated aquifers-based on multiple wells, Groundwater 2000, Proceedings of the International Conference on Groundwater Research, June 6-8, Copenhagen-Denmark, A.A. Balkema, Rotterdam.

Bear, J., 1979, *Hydraulics of Groundwater*, McGraw-Hill Inc., New York, N.Y., 569 p.

Beaven, R.P., 2000, *The Hydrogeological and Geotechnical Properties of Household Waste in relation to Sustainable Landfilling*, PhD Dissertation, University of London.

Beljian, M.S. 1988. Representation of individual wells in two-dimensional groundwater water modeling. Proceedings of Solving Ground Water Problems with Models, Denver, 10-12 February 1988.

Hantush, M.S., 1964, Hydraulics of Wells in V.T. Chow, *Advances in Hydroscience*, Vol. 1, Academic Press Inc., San Diego, California, pp. 281-432.

Hudson, A.P., R.P. Beaven, and W. Powrie, 1999, Measurement of the hydraulic conductivity of household waste in a large scale compression cell, *Sardinia 99*, Proceedings of the Seventh International Waste Management and Landfill Symposium, S. Margherita di Pula, Cagliari, Italy; October 4-8, Vol III, pp 461-468.

Muskat, M., 1937, *The Flow of Homogeneous Fluids Through Porous Media*, McGraw-Hill Inc., New York, N.Y., 763 p.

Rowe, K. and P. Nadarajah, Estimating leachate drawdown due to pumping wells in landfills, Journal of Canadian Geotechnical, 33, pp.1-10.

Wyckoff, R.D., H.G. Botset, and M. Muskat, 1932, Flow of liquids through porous media under the action of gravity, Physics, 2, pp. 90-113.

MODELLING FLOW TO LEACHATE WELLS IN LANDFILLS

A.A. AL-THANI, R.P. BEAVEN, J.K. WHITE*

University of Southampton, Department of Civil and Environmental Engineering
Highfield
Southampton
SO17 1BJ
United Kingdom

ABSTRACT: Vertical wells are frequently used as a means of controlling leachate levels in landfills. They are often the only available dewatering option for both old landfills without any basal leachate collection layer and for newer sites where the installed drainage infrastructure has failed. When the well is pumped, a seepage face develops at the entry into the well so that the drawdown in the surrounding waste will not be as great as might be expected. The numerical groundwater flow model MODFLOW-SURFACT, which contains the functionality to model seepage surfaces, has been used to investigate the transient dewatering of a landfill. The study concludes that the position of the seepage face and information about the characteristics of the induced seepage flow field are important and should not be neglected when designing wells in landfills.

Keywords: Seepage-face, landfill, wells, flow, leachate, MODFLOW-SURFACT.

---

*Corresponding author: E-mail: J.White@btinternet.com, Tel: +44 (0)23 8059 4651, Fax: +44 (0)23 8067 7519

INTRODUCTION

Landfill operators' experiences of using leachate wells to control leachate levels are varied. It is common for the yield of leachate wells to be relatively small (often <1 m^3/day) and for the monitored drawdown around the well to be limited. The low yield of wells is related to the low hydraulic conductivity of the surrounding waste and may also be due to poor well design or badly developed wells. It is also tempting to attribute the limited drawdown in the waste to a clogged or inefficient well screen and filter pack. However, it is possible that the apparent lack of dewatering may in part be explained in terms of the development of a seepage face at the well. Seepage faces are caused by vertical components of flow in the vicinity of a pumped well where the drawdown in the well is a large proportion of the saturated thickness (*Al-Thani and White*, 2000 and *Bear*, 1979 p308). The purpose of this paper is to report on the possible effects of seepage faces in the dewatering of a landfill by a grid of pumped leachate wells.

METHOD OF ANALYSIS

Previous studies have considered the effect of seepage faces on pumped leachate wells (*Rowe* and *Nadarajah*, 1996) but results were only presented for steady state conditions. A method of analysis was required that could investigate the transient response to pumping, based on independently measured values of hydraulic conductivity and drainable porosity in a landfill.

MODFLOW-SURFACT is a commercially available fully integrated groundwater flow and transport code based on the USGS' MODFLOW 3d groundwater flow model. The standard

publicly available version of MODFLOW has certain limitations in simulating complex field problems, which make it unsuitable for modelling seepage faces around wells. The enhanced version, which was used for this study, incorporates additional computational modules that improve the simulation capabilities and robustness. Three of the many features that have been added are (1) the ability readily to accommodate conditions of desaturation and resaturation of aquifer systems, (2) the ability to simulate prescribed ponding, recharge, and seepage-face boundary conditions, and (3) the ability to perform axi-symmetric analysis. The reliability of the MODFLOW-SURFACT code has been assessed and found satisfactory in previous work by comparing the predicted results with available analytical and published seepage surface solutions (*Al-Thani and White*, 1999).

PROBLEM DESCRIPTION

Figure 1 shows a schematic view of a 30 m deep landfill with a 20 m deep saturated zone with a grid of leachate pumping wells at a spacing of 10 m. This spacing was to some extent arbitrary, but probably represents the closest well spacing (at 100 wells per hectare) likely to be installed on most landfills. The wells are assumed to penetrate the landfill fully, and have a fixed radius of 0.15 m. The wells are pumped at rates that maintain fully drawn down conditions inside the wells.

A single cell (in plan view) is used to represent the pumped well in this discretization scheme. The dimensions of the cell (x and y co-ordinates) are set to the diameter of the well (0.3 m). The (column and row) dimensions of the cells adjacent to the well are set to a small fraction of the well diameter. Cell dimensions gradually increase with increasing

distance from the well. The expansion factor, α, which relates the cell dimensions of any two adjacent cells is generally not more than 1.5. The boundaries to the model were set as no flow boundaries at a distance of 5 metres from the well in the *x* and *y* directions. The model was divided vertically into 21 layers as shown in Figure 1. The thickness of Layer 1 was set at 10 m (representing the unsaturated zone) and the remaining layers at 1 m.

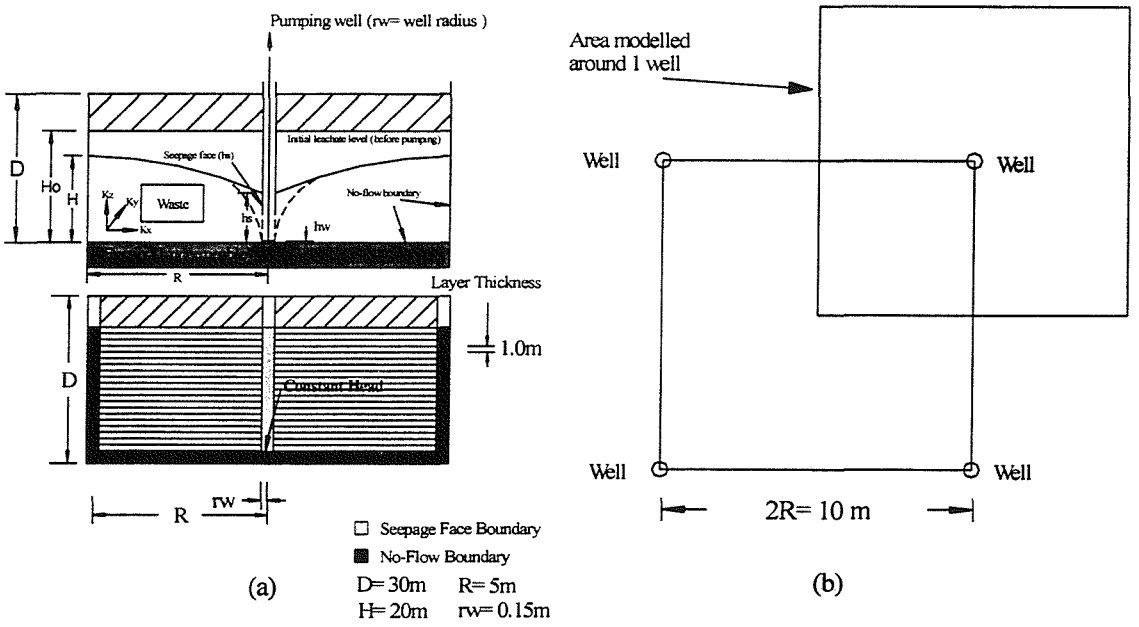

Figure 1 Schematic view of the landfill model **(a)** cross section **(b)** plan view of a grid.

Table 1 Best fit and worst case hydraulic conductivities

Depth (m)	Best fit *K* (m/sec)	Worst case *K* (m/sec)	Depth (m)	Best fit *K* (m/sec)	Worst case *K* (m/sec)
10.5	3.12×10^{-6}	1.66×10^{-6}	20.5	6.55×10^{-7}	2.54×10^{-7}
11.5	2.57×10^{-6}	1.31×10^{-6}	21.5	5.80×10^{-7}	2.19×10^{-7}
12.5	2.14×10^{-6}	1.05×10^{-6}	22.5	5.16×10^{-7}	1.90×10^{-7}
13.5	1.80×10^{-6}	8.53×10^{-7}	23.5	4.61×10^{-7}	1.66×10^{-7}
14.5	1.52×10^{-6}	7.00×10^{-7}	24.5	4.13×10^{-7}	1.46×10^{-7}
15.5	1.30×10^{-6}	5.79×10^{-7}	25.5	3.72×10^{-7}	1.28×10^{-7}
16.5	1.12×10^{-6}	4.84×10^{-7}	26.5	3.36×10^{-7}	1.14×10^{-7}
17.5	9.72×10^{-7}	4.07×10^{-7}	27.5	3.04×10^{-7}	1.01×10^{-7}

18.5	8.47×10^{-7}	3.46×10^{-7}	28.5	2.76×10^{-7}	8.98×10^{-8}
19.5	7.43×10^{-7}	2.95×10^{-7}	29.5	2.52×10^{-7}	8.03×10^{-8}

The initial saturated leachate level was set at 20 m. A drainable porosity of 5% is used in this study, based on research into the hydrogeological properties of waste (*Hudson et al.*, 1999). The variations in hydraulic conductivity with depth are based on relationships between hydraulic conductivity and effective stress determined experimentally by *Powrie and Beaven* (1999) and *Beaven* (2000). Two scenarios using the 'best' fit and 'worst case' fit of the experimental data are used in this study (Table 1).

The operation of the well was replicated by applying a combination of a constant head and drains to the cells representing the well. A constant head cell (with a head of zero) was allocated to the cell in the bottom layer of the model (i.e. the well is fully dewatered) and drain cells to each layer above. Drain cells operate by removing water from the model if the head in the model is above the level set for the drain. Each drain cell was allocated a head equivalent to the elevation head of the cell. This has the effect of applying seepage face boundary conditions at the well.

RESULTS OF NUMERICAL INVESTIGATION

The MODFLOW-SURFACT code was used to solve the described problem for both hydraulic conductivity scenarios in Table 1 over a period of 200 days. Figure 2 shows the location of piezometric head after 50 days, 100 days and 200 days of pumping.

The solid lines represent the elevation of the phreatic surface, i.e. the location at which leachate would be encountered if an observation well was drilled from the surface. These

lines are relatively flat. The dashed lines represent the piezometric levels at the base of the site. The leachate levels drop faster in the best fit scenario of hydraulic conductivity. This is an expected result, because higher hydraulic conductivity values lead to higher well discharges as shown in Table (2).

The equation for steady state flow to a pumped well in an unconfined aquifer is

$$Q = \frac{\pi K (h_2^2 - h_1^2)}{\ln(r_2 / r_1)} \tag{1}$$

This equation is based on the *Dupuit-Forchheimer* assumptions that flow is horizontal and uniformly distributed with depth throughout an isotropic formation underlain by an impermeable stratum. The equation neglects the seepage face at the well (*Bouwer*, 1978 p67)

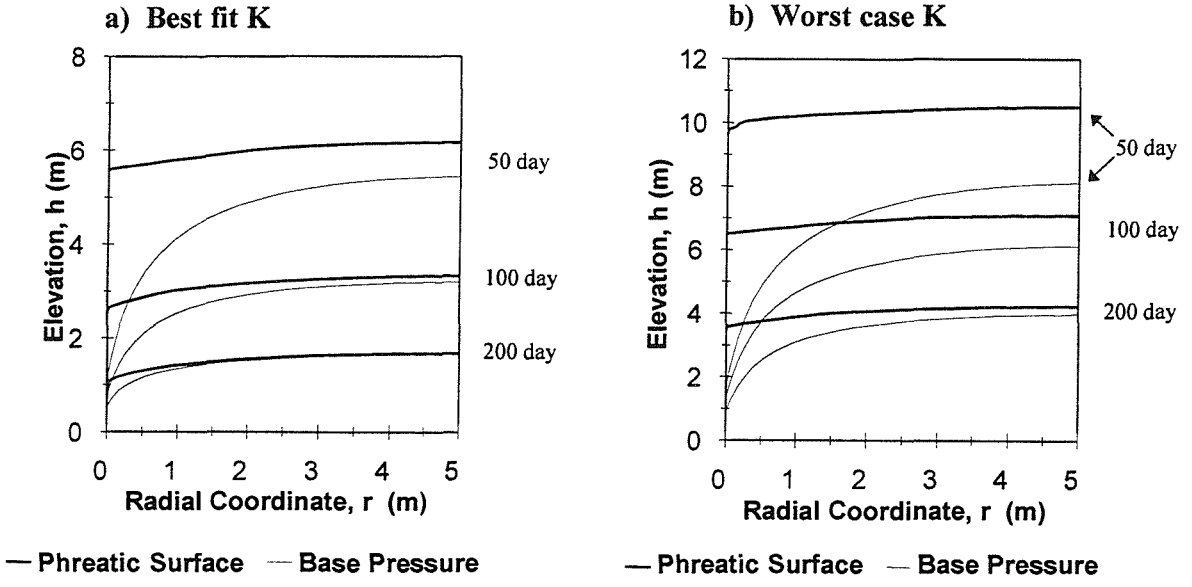

Figure 2 Spatial variation of leachate heads during pumping **(a)** best fit hydraulic conductivity and **(b)** worst case hydraulic conductivity.

However, the applicability of the equation for determining flow to a well has been investigated by *Hantush* (1964) who found that equation (1) gives an exact result despite the presence of the seepage face. However, because it does not take account of the existence of the seepage face, equation (1) does not give an accurate shape curve for the phreatic surface. *Muskat* (1936) and *Wyckoff et al.* (1932), using results from experimental studies, found that it is the piezometric heads along the base, rather than the free surface, that closely follow equation (1). Moreover, the *Dupuit-Forchheimer* assumptions require that an overall average value for hydraulic conductivity is used. Hence variations in hydraulic conductivity with depth, as will be found in a solid waste landfill, are not taken into account in equation (1).

Table 2 Discharge values for both scenarios versus time.

Time	Best fit K				Worst case K			
	Q	H	h_s	Mass Bal' Error	Q	H	h_s	Mass Bal' Error
Days	m^3/day	m	m	%	m^3/day	m	m	%
10	4.389	15.02	14.62	1.74	2.789	15.88	13.24	2.25
50	0.681	6.17	5.57	2.47	0.704	10.49	9.61	3.27
100	0.207	3.33	2.51	3.23	0.326	7.09	6.5	6.37
150	0.095	2.25	1.50	4.21	0.176	5.28	4.51	6.40
200	0.057	1.68	0.77	6.00	0.111	4.23	3.50	7.40
250	-	-	-	-	0.078	3.49	2.50	3.83

Equation (1) may be used to estimate an overall instantaneous effective hydraulic conductivity for a matrix in which the permeability varies with depth. To do this the results from the numerical analysis were substituted into equation (1) to determine an overall

average hydraulic conductivity for each time step. In this case, $h_2 = H$ (=20 m) and $h_1 = 0$. The radius of influence, r_2, was based on $\sqrt{A/\pi}$ where A is the plan area of the model (A= 5×5= 25 m^2) which lead to R= 5.64 m. Following *Beljian* (1988), the radius of the well r_1 was taken to be the effective well radius, which is equal to 0.2 times the size of the element representing the well (i.e. 0.2 x 0.3= 0.06 m). Hence the ratio r_2/r_1 was assumed to be 5.64/0.06 = 94.

The results are recorded in Table 3. A comparison of the calculated hydraulic conductivities with Table 1 indicates that it is the hydraulic conductivity in the lower layers that appears to control flow rates. Table 3 also contains a calculation of the equivalent annual infiltration rate Q/A corresponding to the flow rate Q. These values indicate that the average flow rate could approach typical annual infiltration rates into uncapped landfills in the UK. Where this occurred reductions in leachate levels would be difficult to progress, and may indeed reverse, and an increase in the density of the well array would be require to continue dewatering.

Table 3 Calculation of hydraulic conductivity from model results and equation (1).

Time	Q	Model run	H	K	Equivalent infiltration over 100m^2
Days	m^3/day		m	m/sec	metres/year
10	4.389	Best fit	15.02	3.26 x10^{-7}	16.02
50	0.681	Best fit	6.17	3.00 x10^{-7}	2.49
100	0.207	Best fit	3.33	3.13 x10^{-7}	0.76
150	0.095	Best fit	2.25	3.14 x10^{-7}	0.35
200	0.057	Best fit	1.68	3.38 x10^{-7}	0.21
10	2.789	Worst case	15.88	1.85 x10^{-7}	10.18
50	0.704	Worst case	10.49	1.07 x10^{-7}	2.57
100	0.326	Worst case	7.09	1.08 x10^{-7}	1.19
150	0.176	Worst case	5.28	1.06 x10^{-7}	0.64
200	0.111	Worst case	4.23	1.04 x10^{-7}	0.41

250	0.078	Worst case	3.49	1.07×10^{-7}	0.28

The numerical simulation also provided data on flow rates into the well from each 1 metre thick layer in the model. Figure 3 shows that the maximum flow into the well (Q) generally occurred at the very base of the model, despite this corresponding with the layer with the lowest hydraulic conductivity. The explanation for this is that hydraulic gradients within the seepage face in the waste adjacent to the well are predominantly vertical. This drives leachate downwards towards the base of the model (rather than into the well) until the lower impermeable barrier is reached.

The exception to this is during the early stages of dewatering, before the vertical hydraulic gradients associated with the seepage face have become established and when flow is predominantly horizontal into the well. At this stage there is a closer relationship between the vertical distribution of flow rates into the well and the variation in hydraulic conductivity with depth. This is seen mainly in the simulation using the worst case hydraulic conductivity at times earlier than 20 days. It is also evident within the data set for the best fit hydraulic conductivity model at a time of 5 days. As dewatering progresses more rapidly with the higher hydraulic conductivities, data for times earlier than 5 days for the best fit hydraulic conductivity model would produce similar curves to those produced for worst case hydraulic conductivity model prior to 20 days.

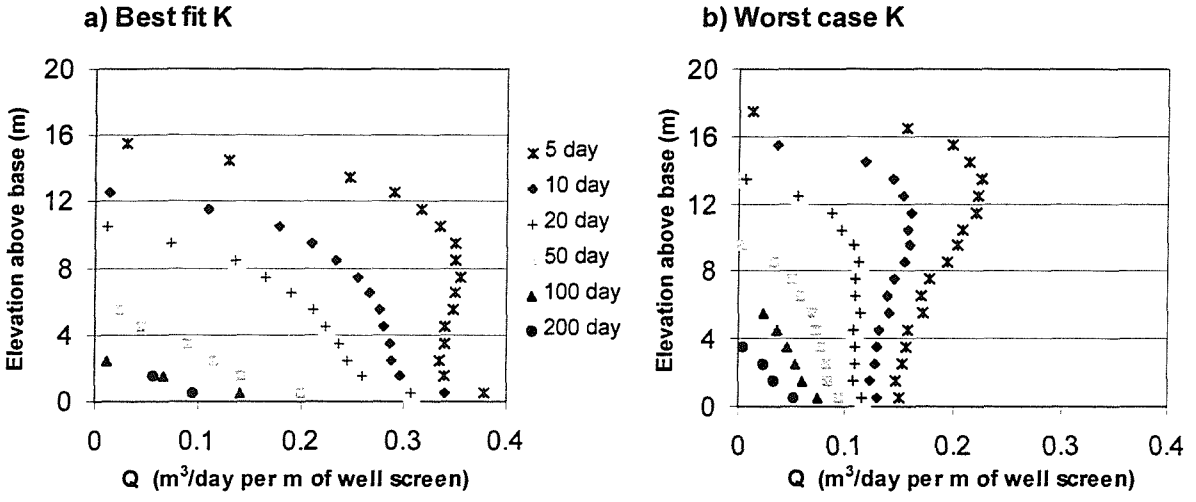

Figure 3 Flow from seepage face into well screen at varying elevations for **(a)** best fit hydraulic conductivity and **(b)** worst case hydraulic conductivity.

ALGEBRIC REPRESENTATION

The numerical investigation indicates that the drop of the leachate elevation is almost flat. This observation can be used to develop a simple algebraic representation of the data which may be used to extrapolate the results so that they can be applied to similar systems with different dimensions and hydrogeological parameters.

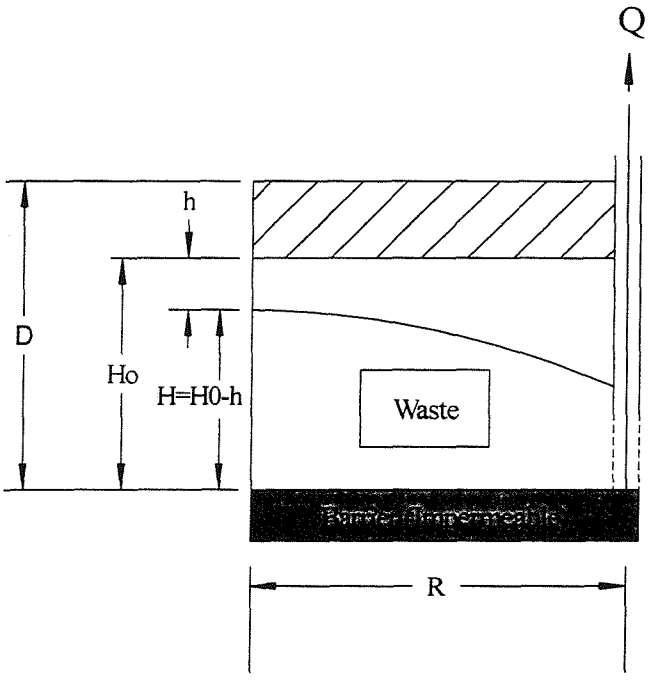

Figure 4 Parameter definition diagram for theoretical representation

Assuming that the piezometric surface is effectively horizontal, the flow Q at any time t may be equated to the rate of change of the drained volume above the surface. This volume is equal to $AS(H_0 - H)$ where A is the plan area and S is porosity (see Figure 4). Thus,

$$Q = -AS\frac{dH}{dt}$$

However Q may be calculated using *Dupuit-Forchheimer* equation so that

$$Q = \frac{\pi K}{\ln\frac{R}{r_w}} H^2 = -AS\frac{dH}{dt}$$

Rearranging and integrating we have,

$$\int_0^t \frac{\pi K}{AS \ln \frac{R}{r_w}} dt = \int_{H_0}^{H} \frac{dH}{H^2}$$

or $$T = \frac{1}{H} - \frac{1}{H_0} \qquad \text{where} \quad T = \frac{\pi K t}{AS \ln \frac{R}{r_w}}$$

The data in Table 2 have been plotted on this basis in Figure 5 with A=100 m^2, S=0.05 and R/r_w=5.64/0.06. The outcome is

$$\frac{1}{H} - \frac{1}{H_0} = 0.9T \tag{2}$$

when K is taken to be the hydraulic conductivity in the lowest layer. The value of 0.9 in equation (2) is effectively a coefficient that calibrates the analytical model to fit the numerical model results. The analytical model does not include any allowance for changes in hydraulic conductivity with depth, and represents time dependency in a very simplified way. It is therefore remarkable that such a simple but useful equation can be derived with only a small modification to the time parameter T.

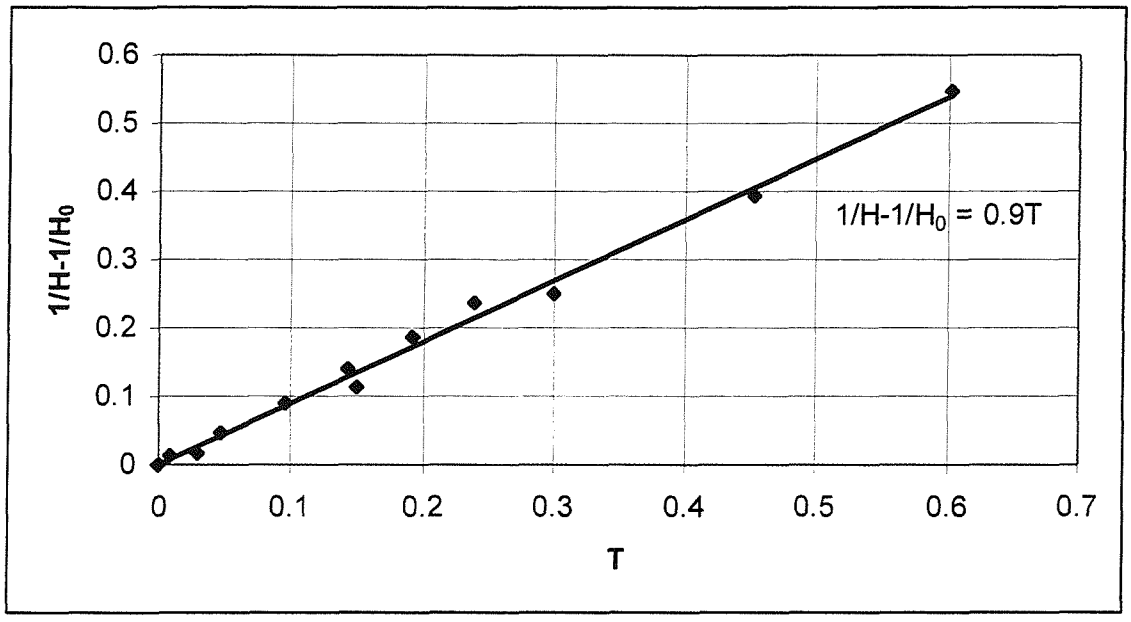

Figure 5 The data in Table 2 plotted to obtain equation (2).

CONCLUSIONS

The impact of the development of a seepage face at a vertical well has been demonstrated in the context of landfill dewatering. Strong vertical seepage velocities are set up resulting in pore pressures in the upper part of the landfill being higher than at the base producing an almost horizontal phreatic surface. Care therefore needs to be taken when carrying out field investigations to assess the pore pressures on the base of a landfill: only piezometers with a well defined and limited response zone should be used for this purpose. Fully screened observation wells in close proximity to a pumped well will give ambiguous if not meaningless results.

When a well is initially pumped, and before seepage faces have developed, hydraulic gradients are predominantly horizontal. Consequently, the vertical distribution of flow rates into the well is related to the vertical variation in hydraulic conductivity with depth. In the

cases analysed, where the hydraulic conductivity of the waste reduces with depth, flow rates into the well are greatest in the upper saturated layers and reduce with depth.

With continuous pumping over time seepage face develops as hydraulic gradients in the immediate vicinity of the well change from being predominantly horizontal to predominantly vertical. The vertical distribution of flow rates into the well also changes and becomes greatest at the base of the well even though this corresponded to the lowest hydraulic conductivity layer in the simulations. The overall yield from the well appears to be controlled by the hydraulic conductivity in these lowest layers. The Dupuit-Forchheimer equation for steady state flow to a pumped well can be used to predict discharge rates with a reasonable degree of accuracy if the hydraulic conductivity at the base of the site is used in the equation.

For the case of a 30 m deep landfill, the predicted yield from pumped wells becomes very low when leachate levels are drawn down below approximately 1.5 to 3 m (for a grid of pumped wells at 10 m spacing). Rates of dewatering become slow and could even stop if the pumped rate falls below the equivalent annual rainfall infiltration rate. The data obtained for the case of a model with specific dimensions has been used to calibrate a conventional algebraic model which can be used to extrapolate the results to systems with similar geometry at different scales.

REFERENCES

Al-Thani, A.A. and J.K. White, 1999, The impact of the seepage surface on the design of pump-and-treat remediation systems for contaminated aquifers-based on single well, Workshop on Ground Water Pollution, Protection and Remediation, November 7-10, Qatar.

Al-Thani, A.A. and J.K. White, 2000, The impact of the seepage surface on the design of pump-and-treat remediation systems for contaminated aquifers-based on multiple wells, Groundwater 2000, Proceedings of the International Conference on Groundwater Research, June 6-8, Copenhagen-Denmark, A.A. Balkema, Rotterdam.

Bear, J., 1979, *Hydraulics of Groundwater*, McGraw-Hill Inc., New York, N.Y., 569 p.

Beaven, R.P., 2000, *The Hydrogeological and Geotechnical Properties of Household Waste in relation to Sustainable Landfilling*, PhD Dissertation, University of London.

Beljian, M.S. 1988. Representation of individual wells in two-dimensional groundwater water modeling. Proceedings of Solving Ground Water Problems with Models, Denver, 10-12 February 1988.

Bouwer, H. (1978) *Groundwater Hydrology* McGraw-Hill ISBN 0-07-006715-5

Hantush, M.S., 1964, Hydraulics of Wells in V.T. Chow, *Advances in Hydroscience*, Vol. 1, Academic Press Inc., San Diego, California, pp. 281-432.

Hudson, A.P., R.P. Beaven, and W. Powrie, 1999, Measurement of the hydraulic conductivity of household waste in a large scale compression cell, *Sardinia 99*, Proceedings of the Seventh International Waste Management and Landfill Symposium, S. Margherita di Pula, Cagliari, Italy; October 4-8, Vol III, pp 461-468.

Muskat, M., 1937, *The Flow of Homogeneous Fluids Through Porous Media*, McGraw-Hill Inc., New York, N.Y., 763 p.

Powrie W. and Beaven R. P., 1999, Hydraulic properties of household waste and implications for liquid flow in landfills. *Proceedings of the Institution of Civil Engineers, Geotechnical Engineering*, October 1999

Rowe, K. and P. Nadarajah, Estimating leachate drawdown due to pumping wells in landfills, Journal of Canadian Geotechnical, 33, pp.1-10.

Wyckoff, R.D., H.G. Botset, and M. Muskat, 1932, Flow of liquids through porous media under the action of gravity, Physics, 2, pp. 90-113.